Universitat Autònoma de Barcelona

Cross-platform biomarker signature of long-term survival with normal allograft function after lung transplantation

Firma de biomarcadores multi-plataforma asociada a la supervivencia a largo plazo con función normal del injerto tras el trasplante pulmonar

Alberto Mendoza Valderrey

UNIVERSITAT AUTÒNOMA DE BARCELONA
Programa de Doctorat en Medicina
Departament de Medicina-Facultat de Medicina

DOCTORAL THESIS

Cross-platform biomarker signature of long-term survival with normal allograft function after lung transplantation

Firma de biomarcadores multi-plataforma asociada a la supervivencia a largo plazo con función normal del injerto tras el trasplante pulmonar

Thesis presented by

Alberto Mendoza Valderrey

to obtain the degree of Doctor

Thesis supervisors

Antonio Román Broto
Susana Gómez Ollés

Thesis tutor

Jaume Joan Ferrer Sancho

Barcelona, April 2020

“Science is built up of facts, as a house is with stones. But a collection of facts is no more a science that a heap of stones in a house”

“La ciencia son hechos; de la misma manera que las casas están hechas de piedras, la ciencia está hecha de hechos; pero un montón de piedras no es una casa y una colección de hechos no es necesariamente ciencia”

Henri Poincare

LIST OF ABBREVIATIONS

A1ATD	Alpha-1-antitrypsin Deficiency
ACR	Acute Cellular Rejection
ADCC	Antibody-dependent Cell-mediated Cytotoxicity
AFOP	Acute Fibrinoid Organizing Pneumonia
AMR	Antibody-mediated Rejection
APC	Antigen Presenting Cell
AR	Acute Rejection
ARAD	Azithromycin Responsive Allograft Dysfunction
AUC	Area Under the ROC Curve
AZA	Azathioprine
BAL	Bronchoalveolar Lavage
BOS	Bronchiolitis Obliterans Syndrome
CCA	Canonical Correlation Analysis
CF	Cystic Fibrosis
CLAD	Chronic Lung Allograft Dysfunction
CMV	Cytomegalovirus
COPD	Chronic Obstructive Pulmonary Disease
CRT	Relative Threshold Cycle Method
CsA	Cyclosporine A
CT	Computed Tomography
CV	Coefficient of Variation
DAD	Diffuse Alveolar Damage
DC	Dendritic cell
DEG	Differentially Expressed Genes
DIABLO	Data Integration Analysis for Biomarker discovery using a Latent component method for Omics studies
DN	Double Negative
DSA	Donor-specific Antibodies
ELISA	Enzyme-Linked Immunosorbent Assay
FC	Fold Change
FDR	False Discovery Rate
FEF_{25-75}	Forced Expiratory Flow between 25% and 75% of FVC
FEV_1	Forced Expiratory Volume in 1 Second
FK	Tacrolimus
FKBP12	FK Binding Protein-12
FVC	Forced Vital Capacity
GERD	Gastroesophageal Reflux Disease
GO	Gene Ontology
HC	Healthy Controls
HLA	Human Leukocyte Antigen
IFN-γ	Interferon-gamma
IL	Interleukin
ILD	Interstitial Lung Diseases
IPAH	Idiopathic Pulmonary Arterial Hypertension
IQR	Interquartile Range
ISHLT	The International Society of Heart and Lung Transplantation
KL-6	Krebs von den Lungen-6
LAM	Lymphangioleiomyomatosis
LASSO	Least Absolute Shrinkage and Selection Operator

LT	Lung Transplantation
LTS	Long-term Survivors
MDR1	Multidrug Resistance Gene
MFI	Mean Fluorescence Intensity
MHC	Major Histocompatibility Complex
miRNA	MicroRNA
MMF	Mycophenolate Mofetil
mTOR	Mammalian Target of Rapamycin
NDSA	Serum non-donor-specific Antibodies
NFAT	Nuclear Factor of Activated T-cells
NF-κB	Nuclear Factor κ-B
NK	Natural Killer
NKT	Natural Killer T cells
NPV	Negative Predictive Value
OB	Obliterative Bronchiolitis
OCATT	Organització Catalana de Transplantaments
ONT	Organización Nacional de Trasplantes
PBMC	Peripheral Blood Mononuclear Cells
PCA	Principal Component Analysis
PCoA	Principal Coordinate Analysis
pDC	Plasmacytoid Dendritic Cell
PGD	Primary Graft Dysfunction
PLS	Partial Least Squares
PPV	Positive Predictive Value
RAS	Restrictive Allograft Syndrome
RMA	Robust Multiarray Average
ROC	Receiver Operating Characteristics
rRNA	ribosomal RNA
RT-qPCR	Real Time PCR
SAB	Single Antigen Beads
SD	Standard Deviation
sGCCA	sparse Generalized Canonical Correlation Analysis
SOT	Solid Organ Transplant
TCR	T cell Receptor
TLC	Total Lung Capacity
TLDA	Taqman Low-density Array
TNF-α	Tumour Necrosis Factor-α
Treg	Regulatory T
UAT	High Technology Unit
UEB	Statistics and Bioinformatics Unit
VHIR	Vall d'Hebron Research Institut

TABLE OF CONTENTS

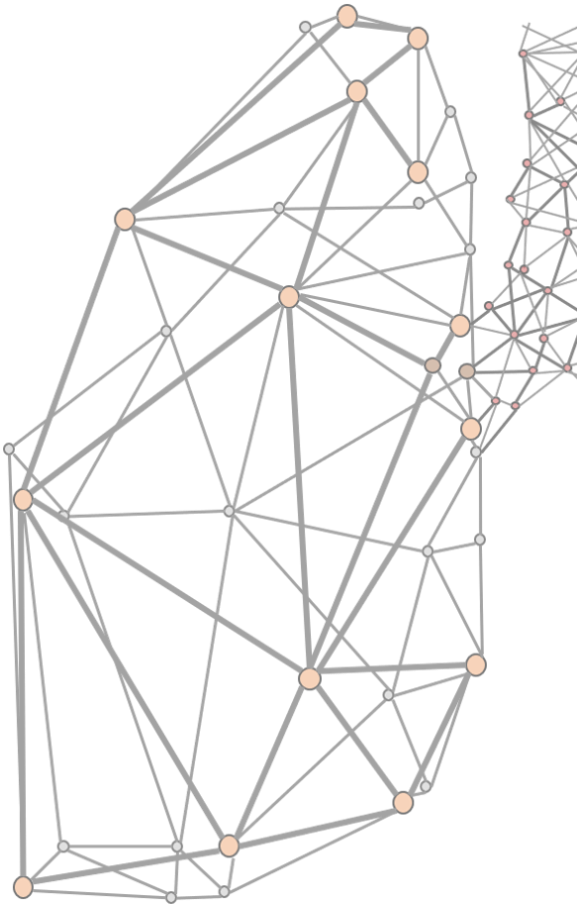

ABSTRACT

Lung transplantation (LT) is an established treatment for end-stage respiratory diseases. Short-term survival has progressively improved due to advancements in surgical techniques, donor preservation, immunosuppressive agents and perioperative management. However, the development of chronic lung allograft dysfunction (CLAD) is the main limiting factor of long-term success after LT, with an approximate ten-year survival rate of 34.3%.

The lifelong immunosuppression of solid organ transplant patients leads to severe complications, such as nephrotoxicity, infectious diseases, malignancies, and metabolic disorders, which poorly affect their long-term survival. For this reason, one of the main goals in organ transplantation is achieving an alloantigen-specific unresponsiveness state in the sustained absence of toxic immunosuppressive therapies. In most cases, immunosuppression withdrawal leads to transplant rejection. However, a small group of transplant patients maintains long-term stable graft function despite interrupted treatment (operational tolerance state). This phenomenon is infrequent and varies according to the type of allograft; excluding kidney and liver transplant fields, there are only anecdotal cases in lung, heart and intestine transplantation. Due to the lack of operationally tolerant lung transplant recipients, long-term survivors with normal allograft function (LTS) after LT are the closest group to “operational tolerance” of kidney or liver transplant patients.

Identifying biomarkers of operational tolerance would serve to accurately identify candidate patients for minimization and potential withdrawal of immunosuppression. Furthermore, these potential tolerance biomarkers could provide knowledge of the underlying biological mechanism of tolerance for new tolerogenic therapies. It has been observed that tolerance fingerprints from kidney and liver transplant recipients differ, suggesting that the underlying mechanisms of operational tolerance, not fully elucidated, are organ-specific and consequently, potential renal and liver tolerance biomarkers cannot be extrapolated to lung.

Since no extensive studies examining this LT state have been published, the main objective of this thesis was to screen the greatest number of clinical and immunological parameters to identify potential biomarkers across different platforms in order to provide a better understanding of the biological mechanisms underlying LTS with normal allograft function after LT in comparison with CLAD patients.

The microbiome of the upper respiratory tract and the full transcriptomic expression profile and extensive cell immunophenotyping of peripheral blood samples were studied to assess the particular characteristics of LTS patients. The results derived from bioinformatics analyses of gene and miRNA expression provided a better understanding of the mechanisms involved in long-term survival. Moreover, they proved to be highly accurate in the classification of LT patients by employing gene and multi-biomarker expression profiling using different transcriptional platforms, including microarrays and RT-qPCR arrays.

The findings obtained demonstrated the usefulness of global transcriptome profile and peripheral blood samples to differentiate between LTS and CLAD patients and to identify some of the potential mechanisms responsible for graft acceptance.

Overall, the studies included in this thesis shed light on the biology underlying graft acceptance after LT, suggesting a complex interaction of several immunological mechanisms and opening up new perspectives for future research in LT immunology.

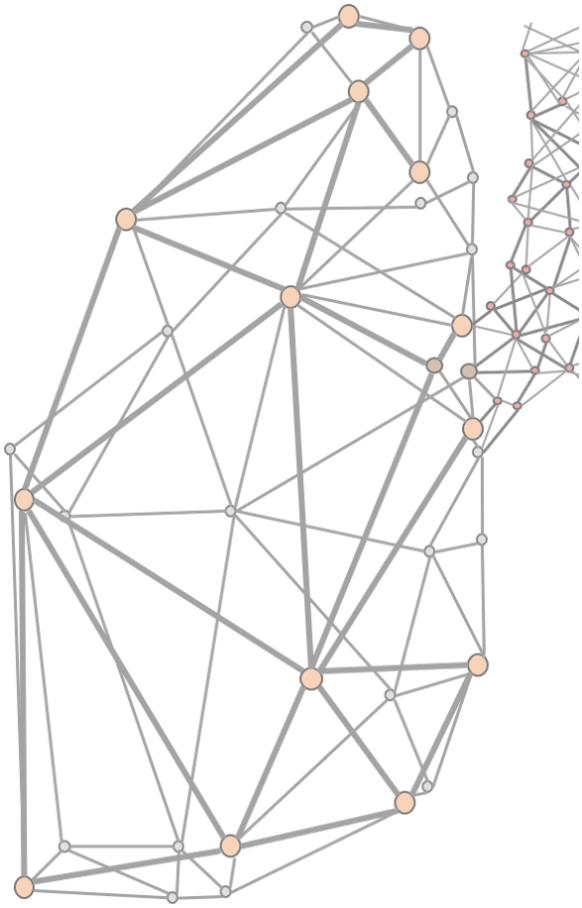

RESUMEN

El trasplante pulmonar (TP) es el tratamiento de elección en enfermedades respiratorias terminales. La supervivencia a corto plazo tras el mismo ha ido aumentando progresivamente debido a las mejoras en las técnicas quirúrgicas, la preservación de órganos, las terapias inmunosupresoras y el manejo perioperatorio. Sin embargo, el desarrollo de la disfunción crónica del injerto pulmonar (DCIP) representa el principal factor limitante para alcanzar la supervivencia a largo plazo tras el TP, siendo la tasa de supervivencia a diez años aproximadamente de un 34.3%.

El tratamiento inmunosupresor de por vida en los pacientes trasplantados de órgano sólido conlleva una serie de complicaciones, como pueden ser la nefrotoxicidad, infecciones, aparición de cáncer, así como desórdenes metabólicos, que influyen negativamente en su supervivencia a largo plazo. Es por ello, que uno de los principales objetivos en el trasplante de órganos es conseguir la falta de respuesta inmunológica del receptor frente al injerto en ausencia de terapias inmunosupresoras sostenidas. En la mayoría de los casos, la retirada de la inmunosupresión conlleva el rechazo del injerto. Sin embargo, se ha observado que un pequeño grupo de pacientes mantiene una buena función del injerto a largo plazo a pesar de la interrupción del tratamiento (fenómeno conocido como tolerancia operacional). Este estado es infrecuente y su aparición varía en función del tipo de órgano, observándose únicamente casos en pacientes trasplantados renales y de hígado. En otros trasplantes de órgano sólido (pulmón, corazón o intestino) solo se han reportado casos anecdóticos de este fenómeno. Dada la falta de pacientes trasplantados pulmonares con tolerancia operacional, los supervivientes a largo plazo (SLP) con una buena función del injerto tras el TP son el grupo que más se asemeja a los tolerantes operacionales tras el trasplante de riñón o de hígado.

La identificación de biomarcadores de tolerancia operacional permitiría la precisa selección de aquellos pacientes candidatos a la minimización y potencial retirada del tratamiento inmunosupresor. Además, estos potenciales biomarcadores podrían proporcionar conocimiento acerca de los mecanismos biológicos que subyacen a la tolerancia y podrían usarse en el desarrollo de nuevas terapias tolerogénicas. Se ha observado que las firmas de tolerancia en riñón e hígado difieren, sugiriendo que los mecanismos responsables de la tolerancia operacional, no completamente dilucidados, son órgano-específicos y que, por lo tanto, los potenciales biomarcadores de tolerancia de riñón e hígado no pueden extrapolarse al caso del pulmón.

Dado los escasos estudios publicados sobre la supervivencia a largo plazo con buena función del injerto tras el TP, el objetivo de esta tesis es analizar el mayor número de parámetros clínicos e inmunológicos a través de diferentes plataformas para la identificación de potenciales biomarcadores, y así, proporcionar nuevo conocimiento sobre los mecanismos biológicos responsables de la supervivencia a largo plazo con buena función del injerto en comparación con pacientes con DCIP.

El microbioma de las vías respiratorias altas y el completo perfil transcriptómico e inmunofenotipado en sangre periférica fue analizado para evaluar las características de los pacientes SLP. Los resultados derivados de los análisis bioinformáticos correspondientes a la expresión génica y de microRNAs proporcionaron nuevos datos referentes a los mecanismos implicados en la supervivencia a largo plazo. Además, se consiguió clasificar a los pacientes

trasplantados pulmonares con alta precisión empleándose para ello perfiles de expresión génica y de expresión combinada de varios biomarcadores, haciendo uso de diferentes plataformas transcriptómicas (microarrays y PCR a tiempo real).

Los hallazgos obtenidos han demostrado la utilidad del uso del perfil transcriptómico y de las muestras de sangre periférica para discriminar a los pacientes SLP y con DCIP y para identificar potenciales mecanismos responsables de la aceptación del injerto a largo plazo.

En conclusión, los estudios incluidos en la presente tesis proporcionan nuevos conocimientos sobre los mecanismos subyacentes a la aceptación del injerto tras el TP, sugiriendo una compleja interacción entre varios mecanismos inmunológicos y proporcionando nuevas perspectivas para futuras investigaciones en la inmunología del TP.

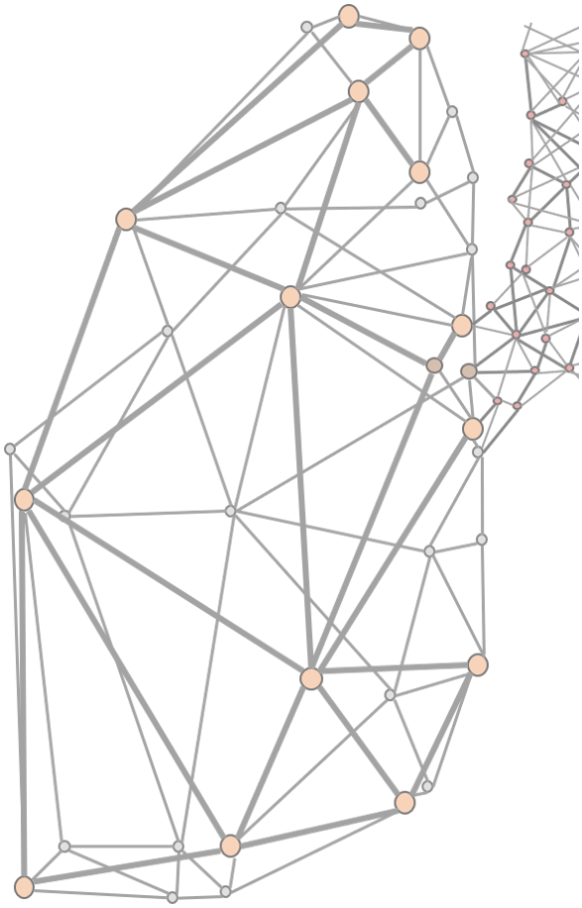

1
INTRODUCTION

1.1 HISTORY OF LUNG TRANSPLANTATION

The history of Lung Transplantation (LT) began in The Soviet Union in 1946 with animal experimentation when Demikhov performed the first cardiopulmonary transplant in a dog. One year later he also performed the first unilateral LT, both without success[1].

After this experimental stage with dogs involving more than 400 re-implantation and homo-transplantation experiments[2,3], the first human unilateral LT was conducted in 1963 at the University of Mississippi Medical Center by Hardy[4] and his team in a patient with left lung bronchial carcinoma. The patient died on the 18th post-operative day as a result of renal failure and malnutrition.

From 1963 to 1980, only 38 LT were performed, using corticoids and azathioprine (AZA) as the main immunosuppressive treatment and with a median survival of 8.5 days[5,6], although two patients survived six[7] and ten[8] months, respectively. The main causes of death were infection and dehiscence of the bronchial anastomosis[6].

The discovery of cyclosporine A (CsA) revolutionized transplant medicine. It was initially discovered in the microbiology laboratory of Sandoz (Basel) in 1970 when a group of researchers were examining cultures of microorganisms from soil samples from Hardanger, in Norway. They isolated the ascomycete fungus *Tolypocladium inflatum*, which produced a polypeptide that would later be called CsA.

In 1976, Borel and colleagues discovered its immunosuppressive effect[9] and in 1981, it was confirmed that CsA prevented rejection in recipients of cadaveric renal transplant[10].

The introduction of CsA entailed a change in immunosuppression regimens and served to enhance survival in organ transplantation[10,11]. In the LT field, CsA served to reduce the dose of corticoids and, consequently, the dehiscence of the bronchial suture[12].

In the 1980s, improvements in immunosuppression and surgical techniques led to renewed interest in LT. In 1983, Cooper and co-workers from The Toronto Lung Transplant Group performed their second attempt at LT, achieving the first successful unilateral LT with long-term survival[13]. The patient died of renal failure more than seven years later.

Later, in 1987, Cooper published the results of five unilateral LT, four of them with long-term survival[14] and two years later Pearson's team described 16 unilateral LT with only six deaths among their patients[15].

Feasibility of bilateral LT was experimentally demonstrated in dogs[16], and it was subsequently performed in a patient with end-stage emphysema in 1986 at the Toronto General Hospital[17]. After replacing the *en bloc* double-lung operation with the bilateral sequential technique[18], in 1991 the St. Louis team published the results of 28 bilateral LT, and showed that bilateral sequential LT can be performed with a minimum of early mortality and morbidity, being comparable to unilateral LT[19].

In the 1990s, LT was established as a therapeutic option for end-stage respiratory diseases and according to the International Society of Heart and Lung Transplantation (ISHLT) Registry data, the number of LT since then has progressively increased.

After more than 37 years of experience and more than 69,200 procedures performed worldwide, LT has evolved considerably. Currently, the most frequent procedure performed is bilateral LT with more than 3,500 patients per year, followed by unilateral LT with 700-900 annual operations[20] (Figure 1).

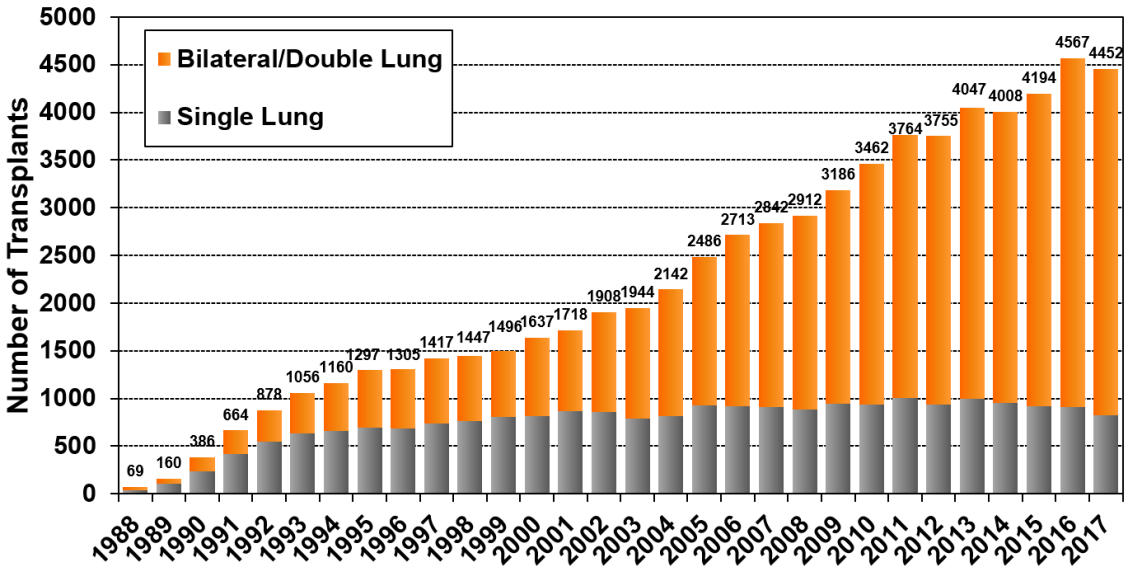

Figure 1. International evolution of the number of adult lung transplants reported to the ISHLT Registry by year and procedure type (1988-2017 period)[20].

1.2 LUNG TRANSPLANTATION IN SPAIN

Spanish LT programmes started in the beginning of the 1990s. The first successful LT was performed at the Hospital Universitario Vall d'Hebron in 1990[21] and after that, other Spanish LT programmes started their activity: Hospital Universitario Puerta de Hierro (Madrid) in 1991, Hospital Universitario de La Fe (Valencia) in 1992, Hospital Universitario Reina Sofía (Córdoba) in 1993, Hospital Universitario Marqués de Valdecilla (Santander) in 1997, Hospital Universitario de A Coruña (La Coruña) in 1999 and Hospital Universitario 12 de Octubre (Madrid) in 2008.

Currently, more than 1,133 LT have been performed in Spain and the annual activity presents a continuous increase; in 2018 a total of 369 LT were performed[22] (Figure 2), and the Catalan LT programme led the state's activity[23] (Figure 3).

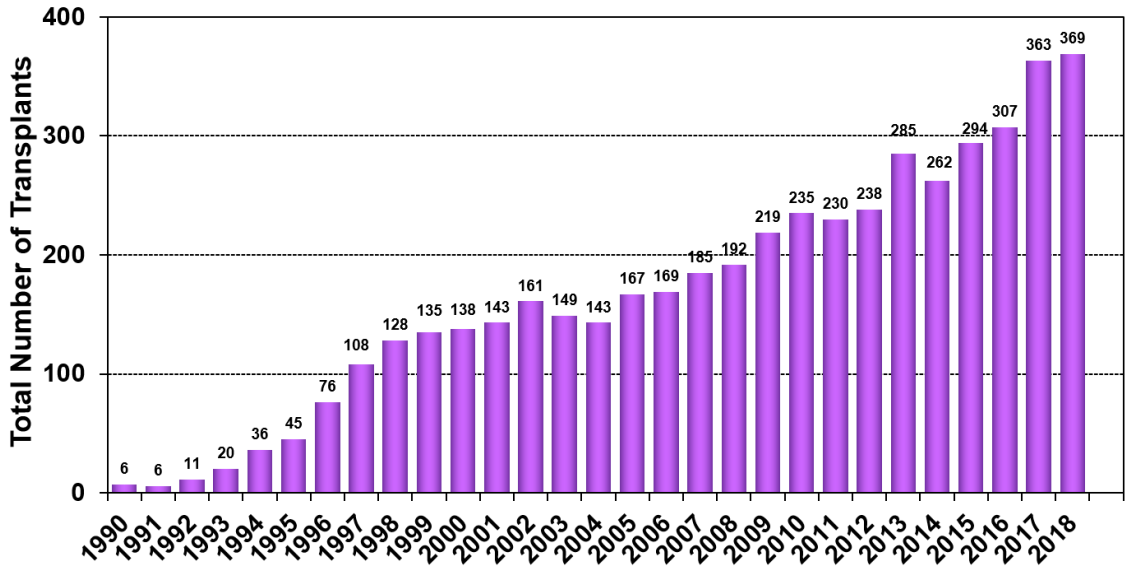

Figure 2. Evolution of the number of lung transplants in Spain reported to the Organización Nacional de Trasplantes (ONT) by year (1990-2018 period)[22].

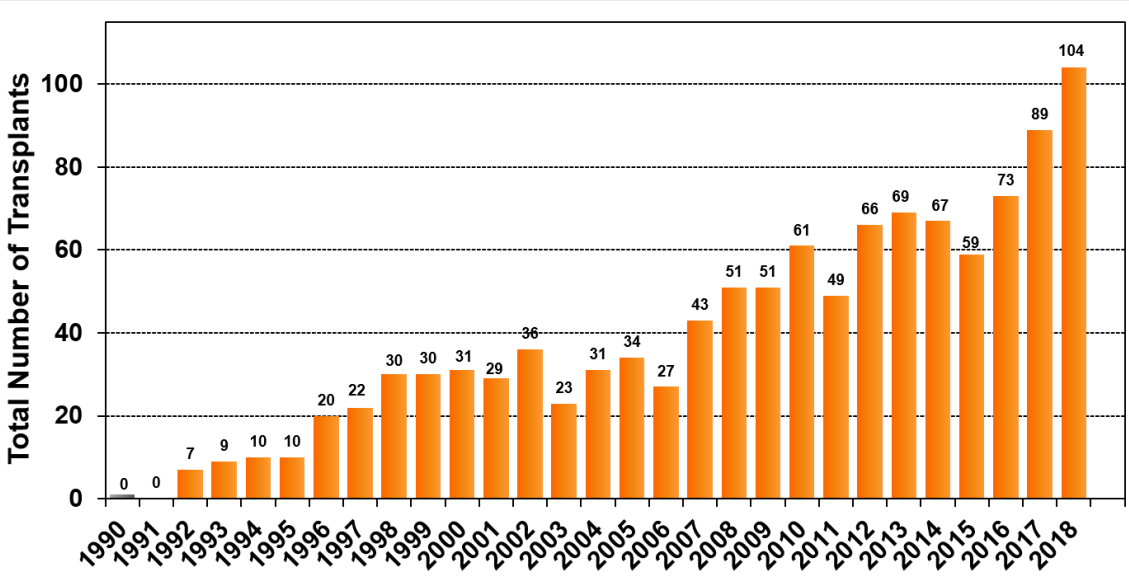

Figure 3. Evolution of the number of lung transplants in Catalonia reported to the Organització Catalana de Transplantaments (OCATT) by year (1990-2018 period)[23].

1.3 INDICATIONS FOR LUNG TRANSPLANTATION

Lung transplantation is a well-established treatment option for patients with end-stage congenital or acquired lung disease when all conservative treatment options have been exhausted[24]. The main indications for LT are interstitial lung diseases (ILD) (32.4%), chronic obstructive pulmonary disease (COPD) (26.1%), cystic fibrosis (CF) (13.1%), alpha-1-antitrypsin deficiency (A1ATD) (2.7%), re-transplant (3.8%) and idiopathic pulmonary arterial hypertension (IPAH) (2,9%)[20].

Over the years, most recipients who suffered CF or IPAH underwent bilateral LT, whereas a marked change from unilateral to bilateral transplantation occurred for COPD, A1ATD and ILD recipients. Since the mid-1990s, the number of procedures has increased in parallel with the persistent growth in the number of bilateral LT, whereas the number of unilateral LT performed annually during this time has remained relatively stable[25] (Figure 1).

The choice of one technique or another depends on the pathology, age and presence or not of colonization in the recipient, pulmonary hypertension, the expected symptoms derived from the residual native lung and the preferences of each transplanting center. Currently, most common indications for LT undergo bilateral procedures.

1.4 SHORT-TERM COMPLICATIONS AFTER LUNG TRANSPLANTATION

1.4.1 EARLY POST-OPERATIVE COMPLICATIONS

The mortality associated with airway complications following surgery remains between 2% and 4%[26]. Common airway complications after LT include those related to suturing. The LT surgical procedure includes three anastomoses: bronchial, pulmonary arteries and left atrium, with the bronchial anastomosis being the most vulnerable and the one with the highest number of complications[27]. These complications can occur within the first month post-transplant, as in the case of anastomotic infections, necrosis and bronchial dehiscence, or later, for example, the development of excess granulation tissue, anastomotic stenosis, bronchomalacia and airway fistulas[26].

Regarding vascular suture, pulmonary arterial and venous anastomosis complications are less frequent but have a dire prognosis. Vascular complications include stenosis[28], vascular bending, arterial torsion and the development of pulmonary vein thrombosis which can lead to peripheral embolism, stroke and pulmonary venous obstruction[29].

Another relevant surgical complication is phrenic nerve injury[30]. It is reported that diaphragmatic paralysis due to phrenic nerve injury incidence after LT is around 1-17%[31]. This complication is associated with prolonged post-operative mechanical ventilation, and consequently, with a longer hospital stay. However, diaphragmatic paralysis is not necessarily associated with a more complicated post-operative course or with a long-term impact on patient survival[31].

Other less common complications after LT include pleural alterations such as the development of bronchopleural fistula, pleural effusion, pneumothorax, hemothorax and chylothorax[32].

1.4.2 PRIMARY GRAFT DYSFUNCTION

Primary graft dysfunction (PGD), which typically develops within 72 hours of LT, is a multifactorial acute lung injury form the pathophysiology of which is not well known. It occurs as a result of events inherent in the LT procedure including brain death in the donor, pulmonary ischemia, cooling and graft preservation and the transplant and reperfusion in the recipient[33].

PGD is a leading cause of early morbidity and mortality and affects from 10 to 25% of all LT[33]. In addition, this acute alteration has an impact on the long-term graft survival increasing the risk of the development of bronchiolitis obliterans syndrome (BOS)[33–35].

PGD is characterized by interstitial and alveolar edema which causes impaired oxygenation, diffuse pulmonary radiographic opacities and decreased lung compliance due to diffuse alveolar damage (DAD)[33].

1.4.3 ACUTE CELLULAR REJECTION

Acute rejection (AR) is one of the most common complications after LT with an incidence of approximately 27% within the first post-transplant year[20]. It is the most important risk factor for the development of BOS[36–38].

AR can be presented in two different forms: acute cellular rejection and antibody mediated rejection (*see section 1.4.4. Antibody mediated rejection*)

Acute cellular rejection (ACR) is the main way AR manifest after LT. This alloimmune response is predominantly driven by the recipient T cell's recognition of foreign major histocompatibility complex (MHC) molecules [Human Leucocyte Antigen (HLA) in humans] by donor antigen presenting cells (APCs), or processed self-peptides of the graft through recipient APCs, inducing a subsequent immune response against the grafted organ[39,40]. This rejection type is blocked by current immunosuppressive strategies.

Bronchoscopic transbronchial biopsy remains the gold standard for the diagnosis of ACR[41]. Histologically, ACR is characterized by perivascular and/or peribronchiolar mononuclear cell infiltrates in lung tissue which can be associated or not with a concomitant lymphocytic bronchiolitis[42].

The main factors that can contribute to the development of ACR include those related to the HLA mismatching between donor and recipient, immunosuppression therapy, infections[43] and those dependent on donor or recipient characteristics such as age[20], pre-transplant vitamin D deficiency[44] and genetic variations in: interleukin (IL)-10 gene[45], in human multidrug resistance gene (MDR1)[46] and in innate pattern recognition receptors[47,48].

1.4.4 ANTIBODY MEDIATED REJECTION

Another less common immunological complication than ACR is the antibody-mediated rejection (AMR), or humoral rejection, which is mediated by anti-HLA and non-anti HLA antibodies against the donor graft, known as donor-specific antibodies (DSA), produced by B cells and plasma cells.

A correlation between the presence of circulating anti-HLA antibodies and the development of BOS has been demonstrated in several studies. These anti-HLA antibodies can be pre-existing[49] or formed post-LT via de novo synthesis[50]. Furthermore, other studies suggest that non-HLA antibodies might play a role in BOS pathogenesis in the absence of anti-HLA antibodies[51].

AMR has been classified into three categories based on clinical and histological features: hyperacute, acute and chronic AMR[52].

Hyperacute AMR is a fulminant form of AMR that occurs intraoperatively or within 24 hours of surgery due to pre-existing DSA, and that causes a very serious immune response[53]. The advent of solid-phase HLA antibody techniques has improved the sensitivity and specificity of antibody detection before transplantation[54]. This has led to the use of a virtual cross-match to accept potential donors for an allosensitized recipient and consequently, the incidence of hyperacute AMR has decreased significantly[55,52].

Acute AMR can occur at any time after the immediate post-operative period (often mimicking ACR) and chronic AMR manifests as an occult cause of chronic lung allograft dysfunction (CLAD)[56,57].

Acute AMR has been widely accepted as a significant cause of graft failure in other solid organ transplants (SOT), including kidney and heart transplantation[58,59]; and chronic AMR is well characterized in kidney transplantation[60].

In the LT field, it is accepted that AMR exists in its acute form[61], but the existence of its chronic form is more controversial[62,43]. No standardized diagnostic criteria exist for AMR, so a multidisciplinary approach for patients suspected of having AMR is recommended. Key diagnostic criteria include clinical evidence of graft dysfunction, the presence of circulating DSA (pre-existing or de novo) and histological tissue injury with evidence of complement deposition in allograft biopsies (positive C4d staining) [56,57,63].

AMR histopathologic features include vasculitis, intra-alveolar haemorrhage, DAD, vascular thrombosis, neutrophilic margination, neutrophil capillaritis and arteritis, as well as the deposition of complement-fixing DSA in the graft.

Recent studies suggest that capillary complement deposition through the detection of complement components C1p, C3d, C4d and C5b-9, along with immunoglobulin, is the most appropriate way to diagnose AMR[64,65] . However, other studies have shown that C3d/C4d deposition can also be observed in other different AMR conditions, such as PGD and airway infections[66].

1.5 LONG-TERM COMPLICATIONS AFTER LUNG TRANSPLANTATION

1.5.1 INFECTIONS

Although the main obstacle to the long-term success of LT is the development of CLAD, which occurs in up to two-thirds of patients, infectious complications remain one of the chief causes of morbidity and mortality at all time points after LT[67]. Infections are the main cause of mortality during the early post-operative period and during the first post-transplant year[68]. This is because the pulmonary allograft is the most common site of infection[69]. This susceptibility is determined by the interrelation of different factors such as the continuous and direct exposure of the allograft to microbes; the denervation of the allograft with subsequent impaired cough reflex and abnormal mucociliary clearance; impaired lymphatic drainage; complications associated with the anastomosis site; transmission or infection from the donor lungs; infection from the native lung in single LT and the immunosuppression involved in transplantation[70]. At the same time, many of the infection episodes have been recognized as risk factors for the further development of CLAD[71].

The category of these infections is affected by time; nosocomial infections are frequent in the first post-operative month. From one to six months after transplantation, opportunistic agents as well as activation of latent infection are common. Six months after LT, the main infections are due to community-acquired pathogens[72,73].

The relationship between pathogens and the host is currently being studied. In recent years, different studies have analysed the role of the graft microbiome *("the full collection of microbes that naturally exist in the lung")*[74] in the development of chronic rejection by providing new information about the relationship between infection and CLAD[75–77].

In 2012, a study from the University of Pennsylvania[78] demonstrated that lung microbiome from LT recipients was significantly different from healthy controls. They observed that the richness and diversity of microbial communities were reduced in transplant subjects compared with control subjects.

These results were also reproduced one year later by Dickson and colleagues[79] who also found that lung microbiome was significantly different between BOS and lung transplant stable patients. Accordingly, Willner and colleagues[80], from the University of Queensland, also demonstrated a different lung microbiome between transplant recipients with and without BOS.

Furthermore, they observed that there was an association between the decrease in microbial community composition and the development of BOS, and that reestablishment of pretransplant microbiome in the allograft was protective and reduced the risk of chronic rejection[80].

In conclusion, infection episodes have a double impact on graft survival; on the one hand, they have implicit morbidity and mortality, and on the other hand, they make patients predisposed to the development of BOS. Exploring the involvement of the microbiome in long-term survival after LT will be an objective of this thesis.

1.5.2 CHRONIC LUNG ALLOGRAFT DYSFUNCTION

1.5.2.1 CHRONIC LUNG ALLOGRAFT DYSFUNCTION CONCEPT

Chronic rejection was originally described in 1969 by Derom *et al* as a progressive loss of pulmonary function that finally causes graft loss[8,81].

Historically, the concept of chronic allograft dysfunction was based on the presence of histopathological lesions of obliterative bronchiolitis (OB), a hallmark of chronic rejection, which was characterized by small airway fibrosis and luminal obliteration[82] and its clinical correlation was defined as BOS[83].

In 1993, Cooper *et al* introduced the first definition of BOS as the main manifestation of chronic rejection. It was defined as *a persistent (three weeks or more) decline in forced expiratory volume in 1 second (FEV_1) of ≥ 20%, from a defined baseline, obtained by averaging the two best post-operative FEV_1 values* taken at least three weeks apart *and after the exclusion of other known pulmonary and extrapulmonary confounding causes of FEV_1 decline* such as acute rejection, infection or bronchial suture problems[83,84]. However, not all patients who initiate a BOS process follow the same clinical pattern.

The acronym CLAD was first introduced in lung transplant literature in 2010 by Granville[85] as an umbrella term to describe the clinical manifestations of several pathologic processes that lead to a significant and persistent deterioration in lung function over a specific period of time.

The term CLAD includes the two different clinical manifestations of chronic rejection: obstructive CLAD (BOS), restrictive CLAD (RAS, restrictive allograft syndrome), in addition to dysfunction due to causes not related to chronic rejection[86]

The lack of consensus regarding the definition of CLAD has been problematic, as it is an overarching term for heterogeneous conditions which cause persistent lack of normal function of the transplanted allografts[87]. Some authors have used the term CLAD as a synonym for BOS, or a combination of BOS and RAS, whereas others propose using CLAD for every possible post-transplant decline in FEV_1[87].

As a consequence, in 2019, the ISHLT Pulmonary Council created a robust description of the term CLAD, which was defined as a *substantial and persistent decline of >20% in measured FEV_1 value from the reference (baseline) value defined as the mean of the two best post-operative FEV_1 measurements taken at least three weeks apart*.

CLAD can be presented either as a predominantly obstructive ventilatory pattern, a restrictive pattern, or a mixed obstructive and restrictive pattern that cannot be explained by other potentially reversible complications[84].

Approximately 70% of CLAD is attributable to BOS, 30% to RAS and only a reduced number to non-rejection related causes such as muscular dysfunction, chronic colonization, thoracic cage problems or gastroesophageal reflux disease (GERD)[88,86]. Overall, CLAD is the most important cause of death after the first year post transplant, presenting an approximate prevalence of 50% at five years and 76% at ten years[20]. Both chronic rejection phenotypes, BOS and RAS,

present different courses and prognoses[89,90]. Physiologically, based on pulmonary function tests, BOS is characterized by a persistent obstruction [91] whereas RAS is defined by a persistent restriction[89,92].

1.5.2.2 PATHOPHYSIOLOGY OF CHRONIC REJECTION PHENOTYPES

The pathogenesis of both BOS and RAS has not been clearly elucidated. Historically, in 1993 BOS was considered the equivalent to chronic rejection[83]. The appearance of a new chronic rejection phenotype 18 years later supported the idea that the pathophysiology of these processes was more complex and less uniform than was initially thought.

BOS is postulated to be the end result of multiple immunological factors (HLA mismatch[93], the number and severity of ACR episodes[94], lymphocytic bronchiolitis[95], self-antigen exposure[96,97], persistent elevated bronchoalveolar lavage (BAL) neutrophilia and IL-8[98] and donor specific antibodies, including anti-HLA antibodies[50,99] and non HLA-antibodies[51]) and non-immune mechanisms (recipient age[100], ischemia-reperfusion injury[101], PGD[35], GERD[102,103], cytomegalovirus (CMV)[104,105] and other respiratory viral infections[73,106,107] and graft colonization [108,109,76]) that lead to chronic inflammation and lung injury. Recently, other risk factors have been included in the list such as traffic-related air pollution exposure, which could represent up to 25% of BOS events[110,111].

It has been speculated that all these alloimmune and non-alloimmune risk factors lead to the activation of both innate and acquired immunity[112–114]. BOS is hallmarked by excessive fibrosis, extracellular matrix deposition, bronchial epithelial cell loss, and scar tissue formation which all result in small airway obliteration and finally in lung function loss[113,115] (Figure 4).

As described above, neutrophils are recognized as major players in BOS pathogenesis. Activated neutrophils have a remarkable potential to cause damage to lung tissue given their ability to release large amounts of reactive oxygen species and matrix metalloproteinases that produce further airway injury[116,117].

RAS pathogenesis is much less well known than BOS. Histologically, RAS is characterized by tissue damage and fibrotic lesions in the periphery of the lungs (alveolar interstitium, visceral pleura and in the interlobular septa)[89,118]. In the case of BOS, as mentioned before, the fibrotic lesions are more likely to occur in the bronchioles[113,118] with relatively intact peripheral lung tissue[89].

Anatomopathological lesions of both BOS and RAS are clearly different. However, both types of lesions may coexist[119], with OB being a common denominator. Overall, risk factors are similar between them[120], suggesting that common physio-pathological mechanisms are shared between both syndromes[118].

Among the exclusive risk factors contributing to RAS, elevated BAL and blood eosinophilia[121] and higher serum levels of Krebs von den Lungen-6 (KL-6) protein compared with BOS patients[122] are included.

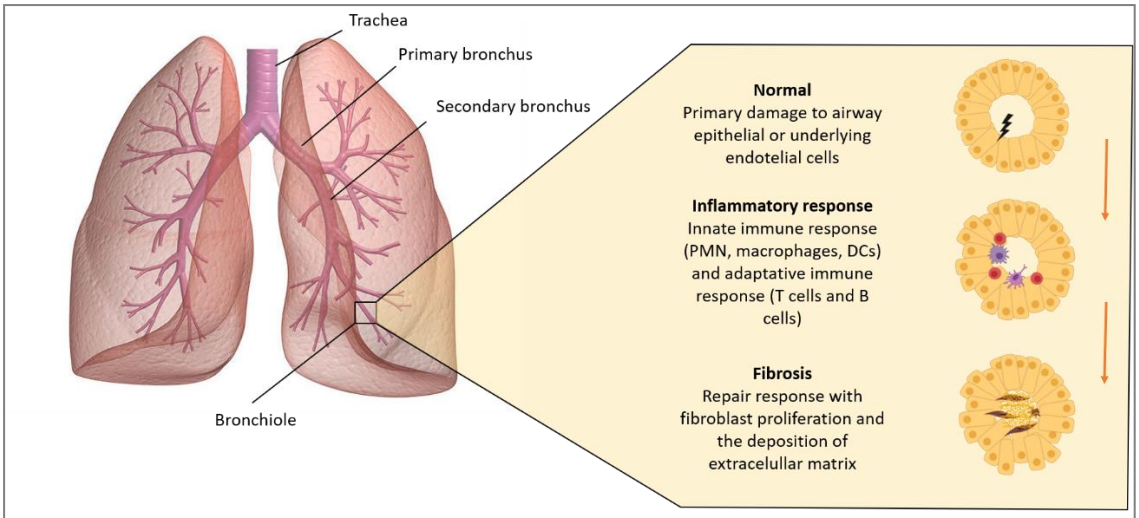

Figure 4. Primary damage to the airway epithelium or underlying endothelial cells leads to the activation of the innate and adaptive immune system and a consequent inflammatory response. Epithelium or endothelium activation results in the secretion of proinflammatory cytokines [i.e. interleukin (IL) 2, IL-6, tumour necrosis factor-α (TNF-α)], and chemokines (i.e. IL-8, RANTES, MCP-1) that trigger a massive influx of polymorphonuclear leucocytes (PMNs), macrophages, dendritic cells (DCs), T and B cells. This process also leads to the attraction and accumulation of activated neutrophils which promote an additional production of cytokines and chemokines that amplify cell recruitment. Injury to the airway epithelium and subepithelial structures of small airways lead to excessive fibroproliferation due to ineffective epithelial regeneration and aberrant tissue repair mechanisms, the secretion of profibrotic cytokines, and extracellular matrix deposition, which finally results in fibrotic plugging of the small airways, presenting the typical OB lesions. (adapted from Boehler A., and Estenne M. Eur Respir J, 2003 and Budding K., 2016)[113,123]. RANTES: regulated on activation, normal T cell expressed and secreted; MCP-1: Monocyte chemoattractant protein-1.

1.5.2.3 CHRONIC LUNG ALLOGRAFT DYSFUNCTION PHENOTYPES

1.5.2.3.1 Bronchiolitis Obliterans Syndrome

BOS diagnosis is rare within the first year after LT with an incidence of 10% per year and a prevalence of 50% after five years[20]. As discussed above, BOS is characterized by an obstructive and persistent pulmonary function decline[83,124] with a heterogeneous clinical course; from an insidious onset and gradual decline in pulmonary function over months to years to abrupt onset with severe decline in pulmonary function over a few weeks[125].

The diagnosis and severity of BOS was initially divided into four grades, only based on FEV_1 decline, compared to the baseline post-transplant FEV_1[83,124]. In a first revision of the BOS definition, a fifth category was added as an early class for BOS or a potential BOS stage (BOS 0-p) in which only a reduction in the forced expiratory flow between 25% and 75% of forced vital capacity (FEF_{25-75}) was modified[126].

Nowadays, classical BOS staging has been replaced by a CLAD staging (from CLAD 0 to 4), which is more appropriate due to the establishment of different allograft dysfunction phenotypes[84] (Table 1).

Table 1. CLAD classification[84]. CLAD: chronic lung allograft dysfunction; FEV_1: forced expiratory volume in 1 second.

Stage	Spirometry
CLAD 0	Current FEV_1 >80% FEV_1 baseline
CLAD 1	Current FEV_1 >65-80% FEV_1 baseline
CLAD 2	Current FEV_1 >50-65% FEV_1 baseline
CLAD 3	Current FEV_1 >35-50% FEV_1 baseline
CLAD 4	Current FEV_1≤ 35% FEV_1 baseline

The diagnosis of BOS is defined by clinical and physiological criteria and requires the careful exclusion of other post-transplant complications that cause a persistent decline in FEV_1.

Transbronchial biopsies are not necessary to diagnose BOS[126], although they may be indicated to exclude alternative diagnoses. Accordingly, it has been described that early-onset DAD (within 3 months of LT) has been associated with BOS[127,121].

Radiology could also be helpful for BOS diagnosis. Imaging by computed tomography (CT) scan shows two main abnormalities during the clinical course of BOS: air trapping on expiratory thoracic CT scans[128] and the presence of bronchiectasis and large bronchi injury.

The combination of all these findings may help to exclude other causes of loss of allograft function. The use of micro-CT might help to determine precisely the site of airway obstruction and could refine the radiological diagnosis of BOS[129].

The treatment options for BOS have shown limited efficacy. Sustained treatment with high-dose corticosteroids is not recommended given its association with numerous and frequent harmful side effects and as it has not been demonstrated to improve BOS[84,130].

On the other hand, maintenance azithromycin therapy in the treatment of BOS has shown beneficial effects in some groups of patients[131]. It has been described that approximately 40% of neutrophilic and non-neutrophilic BOS patients respond to azithromycin, increasing by ≥ 10% in FEV_1 values from baseline[132–137]. The clinical condition of the responders to azithromycin (defined as FEV_1 increase of ≥ 10% after a 2-3 month treatment) is called azithromycin responsive allograft dysfunction (ARAD) and due to its reversible nature is currently classified as a separate entity to CLAD[138,87].

Adjustments in BOS immunosuppressive therapy, including the increase in calcineurin inhibitor doses, the switch from CsA to tacrolimus (FK), the conversion of AZA to mycophenolate mofetil (MMF)[125,139] and the introduction of new treatments such as montelukast[84], cyclophosphamide and methotrexate[139] are potential therapeutic options. Other more aggressive therapeutic choices for BOS cover total lymphoid irradiation[140] or extracorporeal photopheresis[141].

Most of these treatment options are reportedly beneficial in a variable percentage of the patients. However, these results may be unreliable as the current studies related to the treatment of BOS are retrospective and mostly performed in a single-center[139]. Re-transplantation for carefully selected BOS patients remains the ultimate treatment option as it is the only procedure that has been proven to have an impact on survival[130] .

1.5.2.3.2 Restrictive Allograft Syndrome

Restrictive Allograft Syndrome (RAS) was first described as a novel form of CLAD in 2011 by Sato and colleagues from the Toronto Lung Transplant Program[89]. Compared with BOS, this chronic rejection phenotype presents a faster clinical course and shows poorer survival[89] (*see section 1.7 Survival after lung transplantation*). Preliminary studies suggest that one out of four CLAD patients will develop RAS[124].

In the last consensus report from the Pulmonary Council of the ISHLT, RAS was defined physiologically by[121,84]:

(1) *A persistent ≥20% decline in FEV_1 compared with the reference or baseline value, which is computed as the mean of the best two post-operative FEV_1 measurements taken at least three weeks apart.*

(2) *A concomitant decline in total lung capacity (TLC) to ≥10% compared with the reference or baseline value, defined as the average of the two measurements obtained at the same time as or very near to the best two post-operative FEV_1 measurements.*

(3) *The presence of persistent opacities on chest imaging (chest X-ray and/or CT).*

A problem with this definition is its applicability in unilateral LT[88]. For this reason, the introduction of the FEV_1/Forced vital capacity (FVC) ratio (FEV_1%), also known as the Tiffeneau-Pinelli index, has been proposed as a restriction indicator that could be useful for unilateral LT cases[124].

Histopathological RAS characteristics are non-specific. These findings include: DAD lesions[127], different degrees of interstitial fibrosis and development of pleuroparenchymal fibroelastosis[119]. It has even been described that late new-onset DAD (>3 months after LT) increases the risk of the development of RAS[127,142,121]. The presence of acute fibrinoid organizing pneumonia (AFOP)[143] lesions on transbronchial biopsies has also been associated with the development of the RAS phenotype[144,145]. Both histological diagnoses are mutually exclusive[143].

The AFOP entity is characterized by a radiological pattern of ground-glass opacities with interlobular septal thickening[86]. Histopathologically, it is characterized by the intra-alveolar deposition of fibrin with no interstitial infiltrate or fibrosis[143]. AFOP shows clear clinical similarities with RAS, suggesting a likely extensive overlap between both entities[88]. Further investigation is needed to assess whether AFOP may be an early or acute manifestation of RAS[86].

From a radiological point of view, RAS patients show alterations of interstitial lung disease[89]. The RAS phenotype is not homogenous, as two subgroups of RAS patients have been identified: slow progression and fast progression[146]. The slow-progressing RAS group is characterized by a stair-step progression pattern. In the early stages of RAS, central and peripheral ground glass are the most notable features on CT, whereas in the later stages, the most commonly observed features are (traction-) bronchiectasis, central and peripheral consolidation, pleural thickening, volume loss and hilus retraction[147], with most patients

showing an upper lobe-dominant fibrotic pattern[121]. According to the last consensus report from the ISHLT Pulmonary Council, the presence of pleural thickening and volume loss in the upper lobes is associated with survival [121].

The slow progressing group shows a significant overlap with pleuroparenchymal fibroelastosis, whereas the fast progressing group shows a possible overlap with previously described AFOP[146].

An additional problem is the coexistence of both BOS and RAS characteristic lesions in some patients who develop a combined syndrome[87]. Moreover, it has also been described that some patients who initiate a BOS process incorporate RAS characteristic lesions during their clinical course, thus producing the conversion from obstructive BOS to the RAS phenotype[87]. Patients may also first develop RAS, later clear their opacities, and end up with classical BOS physiology[87], although it has not been observed a switch from a clearly RAS phenotype to a BOS phenotype in any of the Vall d'Hebron patient series.

As the description of the RAS phenotype is relatively new, there are no formal clinical practice guidelines for RAS, and management is rather experimental[84]. Generally, physicians have used the same therapeutic interventions as those indicated for BOS[121,84].

1.6 LUNG TRANSPLANTATION TREATMENT AND MANAGEMENT

1.6.1 IMMUNOSUPPRESIVE DRUG THERAPY

Currently a SOT cannot be successfully carried out without using immunosuppressive drugs. Immunosuppression is used to prevent acute and chronic rejection and to treat rejection once established.

There are four main groups of drugs used as maintenance therapy after transplantation: calcineurin inhibitors (CsA and FK), mammalian target of rapamycin (mTOR) inhibitors (sirolimus, also known as rapamycin and everolimus), antiproliferative agents (AZA and (MMF) and corticosteroids.

Whereas different centers adopt different immunosuppresive strategies, the most accepted protocols after LT are based on a triple therapy that comprises a combination of a calcineurin inhibitor (CsA or FK), an antiproliferative agent (AZA or MMF) or an m-TOR inhibitor (sirolimus or everolimus) and corticosteroids.

The combination of drugs targeting the immune response at different levels, makes them more effective, and each immunosuppressant dose can be reduced, decreasing their individual toxicity.

CALCINEURIN INHIBITORS

Despite chemical structure differences between CsA and FK, both have similar mechanisms of action. After entering the cell, they are complexed with an immunophilin; CsA binds to cyclophilin while FK acts through immunophilin FK binding protein-12 (FKBP12). The drug-immunophilin complex inhibits the phosphatase activity of the calcineurin, preventing the dephosphorylation of the nuclear factor of activated T-cells (NFAT), and avoiding its translocation into the nucleus. Subsequently, this turns into the down-regulation of cytokine genes and other immune mediators regulated by the NFAT transcription factor, such as IL-2. As a result, T-cell activation is blocked and thereby, immune response propagation is decreased[148].

ANTIPROLIFERATIVE AGENTS

AZA and MMF are antimetabolites that specifically exert their antiproliferative effect inhibiting *de novo* nucleotide synthesis in lymphocytes, as these cells lack the alternative salvage pathway, in which nucleotides are synthesized from intermediates.

AZA is one of the earliest immunosuppressive drugs used after organ transplantation. It is metabolized to its active component 6-mercaptopurine, a purine antagonist which inhibits DNA, RNA, and protein synthesis, blocking lymphocyte proliferation[149].

On the other hand, the mechanism of action of MMF is based on the capacity of its active component mycophenolic acid to inhibit inosine monophosphate dehydrogenase, the enzyme that controls the production of guanosine nucleotides required for DNA synthesis, thus blocking the proliferation and clonal expansion of T and B lymphocytes[150].

mTOR INHIBITORS

The main mechanism of action of these agents is the inhibition of the protein serine/threonine kinase mTOR, which is a key regulator of cell growth, proliferation and metabolism.

After entering the cell, sirolimus and everolimus bind to FKBP12 and the resulting complex binds to mTOR inhibiting its kinase activity with subsequent suppression of T-cell proliferation[151].

CORTICOSTEROIDS

The mechanism by which corticosteroids exert their immunosuppressive effects remains poorly understood. Nevertheless, it is known that after entering the cell, corticosteroids bind to its cytoplasmic receptors and this steroid-receptor complex translocates into the nucleus, binding to a number of DNA sites and inhibiting the transcription of cytokine genes[152].

Corticosteroids also act by inhibiting the translocation to the nucleus of nuclear factor κ-β (NF-κβ), preventing the transcription of several inflammatory genes and thus blocking the activation of the immune system[153].

1.6.2 ANTI-MICROBIAL THERAPY

Solid organ transplant (SOT) recipients have an elevated risk of acquiring infections, that is the reason why broad-spectrum antimicrobials are given prophylactically post-transplant. The regimens used varies by SOT and anti-microbial LT prophylaxis is carried out by a triple therapy including antibacterial, antifungal and antiviral drugs.

Antiviral prophylaxis with either intravenous ganciclovir or oral valganciclovir reduced significantly the risk for cytomegalovirus infection, one of the most important pathogens after LT. Different antifungal prophylactic regimens have been reported, being aerosolized Amphotericin B alone or in combination with itraconazole the most used drugs. One of the most successful antimicrobial prophylaxes is probably the administration of cotrimoxazole for the prevention of *Pneumocystis jirovecci* infection.

As regards azithromycin, as previously mentioned, it is used as immunomodulatory therapy in BOS treatment and in the prevention of BOS or ARAD conditions.

1.7 SURVIVAL AFTER LUNG TRANSPLANTATION

Short-term survival has progressively improved due to advancements in surgical techniques, donor preservation, immunosuppressive agents and perioperative management. Around 85% of patients who undergo a LT are still alive one year after the intervention[20]. However, long-term survival after LT remains reduced; with 6.7 years being the median survival after transplantation[20], as shown in Figure 5.

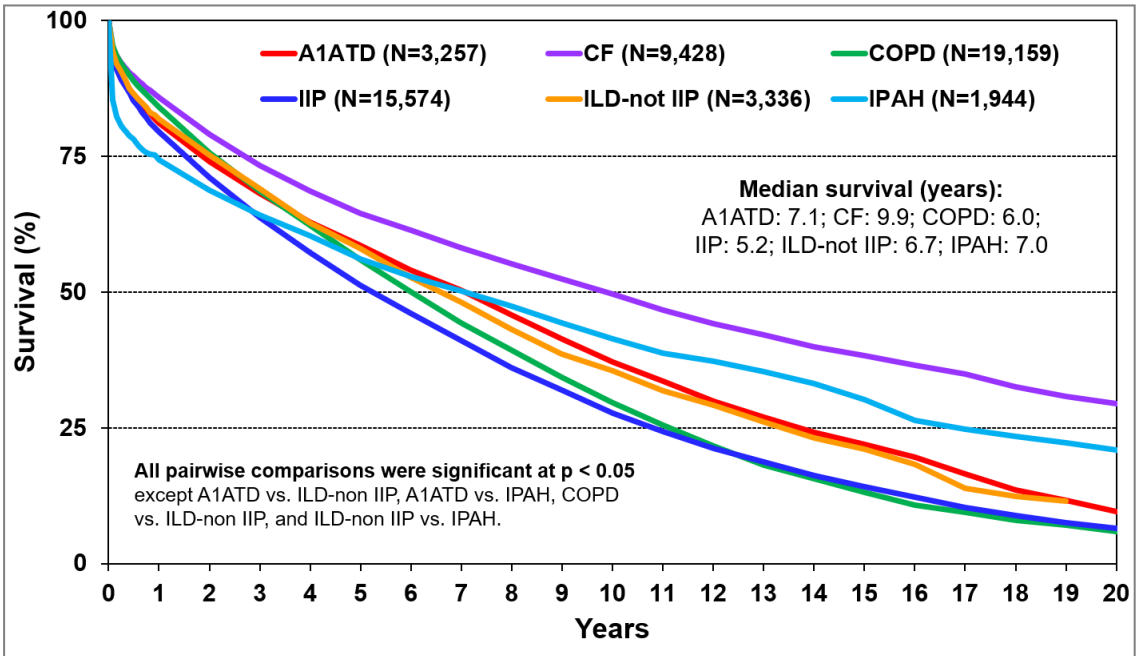

Figure 5. Kaplan-Meier survival analysis for adult lung transplant recipients reported to the ISHLT Registry by indication for transplantation (1992- June 2017 period)[20]. A1ATD: α–1-anti-trypsin deficiency; CF: cystic fibrosis; COPD: Chronic obstructive pulmonary disease; IIP: idiopathic interstitial pneumonia; ILD: interstitial lung disease; IPAH: idiopathic pulmonary arterial hypertension.

CLAD represents the main limiting factor of long-term success after LT; with approximate five- and ten-year survival rates of 56% and 34.3%, respectively[20]. Thereby, long-term survival remains far below other SOT such as kidney (86.2%)[154], liver (61%)[155], heart (56%)[156], pancreas (80%)[157] and intestine (43%)[158].

Unadjusted Kaplan-Meier survival analyses have demonstrated that bilateral LT, women recipients and CF patients who underwent LT, present higher survival than all other groups[20].

The survival of RAS patients after CLAD onset was significantly shorter than BOS; their mean survival post-diagnosis was only 1.5 years, compared to four years with BOS[89].

BOS survival is influenced by several factors such as timing of disease onset, BOS progression[159], and the initial BOS grade at diagnosis[160]. Patients who developed BOS early after transplantation showed a poorer prognosis than late-onset BOS (> three years), whose prognosis was almost comparable with that of patients free of CLAD[91]. On the other hand, high-grade (grades two or three from the old BOS classification[126]) onset BOS was associated with significantly increased mortality compared with grade one (from the old BOS classification[126]) onset[160,91].

Considering incidence estimates of BOS and Kaplan-Meier estimates of freedom from BOS exclude death, a recent study focused on the composite outcome of death or BOS (BOS-free survival) provided a more robust estimate than either of its components. The study concluded that the median BOS-free survival of unilateral and bilateral LT was 3.16 and 3.58 years respectively[161].

1.8 TOLERANCE AFTER TRANSPLANTATION

Current immunosuppressive agents are not alloreactive cell selective and exert an extended non-specific effect on the immune system. Consequently, lifelong immunosuppression therapy in SOT is associated with nephrotoxicity[162,163] and considerable other side effects, including higher rates of infections[72], malignancies[164], hypertension, new onset diabetes after transplant and hyperlipidemia due to the metabolic effects of steroids, calcineurin inhibitors and sirolimus[165], besides interaction with other medications, that considerably contribute to morbidity and mortality among transplant recipients.

One of the highly desirable goals of current transplantation research is to achieve the phenomenon known as “tolerance”[166], defined as the stable maintenance of good allograft function in the sustained absence of toxic immunosuppressive therapies.

The term transplantation tolerance was first introduced by Billingham *et al*[167] in 1953, with the report of a murine model that developed donor-specific unresponsiveness. This phenomenon has been widely reported in numerous animal models[168,169].

In the clinical arena, the best proof that tolerance is certainly achievable is the existence of a small group of transplant patients who, after having discontinued immunosuppressive therapy, either through physician-led voluntary weaning or attributable to non-adherence, did not suffer from graft rejection. The clinical state that develops in these patients is known as

"operational tolerance", in which there is long-term allograft survival in the absence of immunosuppression[170]. Operational tolerance is infrequent and its incidence varies by allograft type; up to 20% of liver transplant recipients show spontaneous operational tolerance[171,172], although this phenomenon has rarely been reported in renal transplantation[173–175]

Excluding liver and kidney cases, there are only anecdotal cases of operational tolerance in other SOT such as lung[176], heart[177] and intestine[178]. The underlying mechanisms responsible for the establishment of operational tolerance have not been fully elucidated.

1.8.1 TOLERANCE BIOMARKERS

A biomarker has been defined as "*a characteristic that is objectively measured and evaluated as an indicator of normal biologic processes, or pharmacologic responses to a therapeutic intervention*" by The Biomarkers Definitions Working Group [179].

Identifying operational tolerance biomarkers would facilitate an accurate identification of candidate patients for minimization and potential withdrawal of immunosuppression. Furthermore, the potential tolerance biomarkers identified could provide knowledge of the underlying biological mechanism of tolerance for new tolerogenic therapies.

In recent years, great efforts have been made in the identification of non-invasive biomarkers of operational tolerance in kidney and liver transplantation. Although peripheral blood probably does not reflect all the molecular mechanisms responsible for maintaining tolerance which are occurring in the allograft, the use of non-invasive blood monitoring has clear clinical advantages, facilitating the methodological standardization methods and increasing the attempts at obtaining clinically applicable results. Furthermore, this type of sample has been widely validated for diagnostic purposes in transplantation studies employing both immunophenotyping and gene expression profiling[180–182].

These studies reported that kidney and liver tolerant recipients differed in blood gene expression and immunophenotypic patterns from those of non-tolerant recipients and healthy individuals. A list of biomarkers that are suggested to have a role in organ tolerance is detailed in Table 2.

In the kidney transplant field, a number of phenotypic and transcriptomic studies have facilitated the identification of a B-cell-related signature that predominates in peripheral blood from tolerant patients[183–187](Table 2). However, none of these studies had assessed the confounding effect of pharmacological immunosuppressive therapy. In this way, Rebollo-Mesa[188] and co-workers demonstrated that the percentage of transitional B cells within the naïve B cell population in peripheral blood, previously described as a feature of tolerant recipients, was significantly affected by immunosuppressive drugs.

In contrast, in the liver transplant field, blood samples from tolerant recipients showed increases in the percentage of $\gamma\delta$ T cells (specifically Vδ1$\gamma\delta$ T cells)[189,190], the ratio of plasmacytoid to myeloid DCs[191] and in innate immunity-related transcripts[185,192,193] (Table 2).

Table 2. Summary of potential tolerance biomarkers in renal and liver recipients from selected clinical studies.

Clinical study	Transplanted organ	Sample	Methodology	Cells	Genes
Louis *et al*[181], 2006	Kidney	Blood	Flow cytometry, qPCR	↑ $CD4^+$ $CD25^{high}$ T cells	*FOXP3*
Sagoo *et al*[183], 2010	Kidney	Blood	Flow cytometry, microarray, qPCR	↑ B cells, NK cells	*CD79B, TCL1A, HS3ST1, SH2D1B, MS4A1, TLR5, FCRL1, PNOC, SLC8A1, FCRL2*
Newell *et al*[184], 2010	Kidney	Blood	Flow cytometry, microarray, qPCR	↑ Total B cells, naïve B cells and transitional B cells	*IGKV1D-13, IGKV4-1, IGLL1*
Lozano *et al*[185], 2010	Kidney	Blood	Flow cytometry, microarray, qPCR	↑ Total B cells, memory B cells and activated B cells	B-cell-related genes
Moreso *et al*[186], 2014	Kidney	Blood	Flow cytometry, qPCR	-	*IGKV1D-13, IGKV4-1*
Baron *et al*[187], 2015	Kidney	Blood	Meta-analysis	↑ Total B cells, CD4 T cells	B-cell-related genes
Rebollo-Mesa *et al*[188], 2016	Kidney	Blood	ElasticNet qPCR	-	*ATXN3, BCL2A1, EEF1A1, GEMIN7, IGLC1, MS4A4A, NFκBIA, RAB40C, TNFAIP3*
Mazariegos *et al*[191], 2003	Liver	Blood	Flow cytometry	↑Plasmacytoid DCs	-
Li *et al*[189],2004	Liver	Blood	Flow cytometry	↑ $CD4^+$ $CD25^{high}$ T cells, B cells Vδ1/Vδ2 γδ T cells ratio ↓ NK and NKT cells	-
Martinez-Llordela *et al*[190], 2007	Liver	Blood	Flow cytometry, microarray, qPCR	↑ $CD4^+$ $CD25^+$ T cells, $V\gamma1^+$ γδ T cells	*CD94, IL1, IL23, ICAM1, TNF-α,*
Martinez-Llordela *et al*[192], 2008	Liver	Blood	Microarray, qPCR	-	*KLRF1, SLAMF7, NKG7, ILR2B, KLRB1, FANCG, GNPTAB, CLIC3, PSMD14, ALG8, CX3CR1, RGS3*
Pons *et al*[182], 2008	Liver	Blood	Flow cytometry, qPCR	↑ $CD4^+$ $CD25^{high}$ T cells	*FOXP3*
Lozano *et al*[185], 2010	Liver	Blood	Flow cytometry, microarray, qPCR	-	NK-related genes
Li *et al*[193], 2012	Liver	Blood	microarray, qPCR	-	*SENP6, FEM1C, ERBB2, AKR1C3, MAN1A1, UBAC2, GRP68, NFKB1, MAFG, BTG3, ASPH, PTBP2, PDE4DIP*

Kidney and liver tolerant recipients exhibit different blood expression and immunophenotypic patterns and, as can be observed in Table 2, there is a minimal overlap between the kidney and liver tolerance fingerprints. These differences indicate that the mechanism underlying operational tolerance in kidney transplantation is different to those in liver recipients[194].

The major common methodological limitation to all previous studies is the small number of operationally tolerant transplant recipients. This sample size constraint constitutes a serious obstacle in reaching acceptable statistical power to perform relevant analyses in the search for tolerance biomarkers.

In the LT field, there are no true operationally tolerant recipients, being long-term survivors with normal allograft function (LTS) after LT the closest group to “operational tolerance” of other solid organ allografts. Patients who survive more than ten years after LT and have normal pulmonary function test values constitute a special LT population for research studies.

There is limited evidence in long-term survival after LT and very little knowledge has been reported above ten years after LT considering graft condition. In this scenario, few studies conducted in isolated series of patients form single centers have published inconsistent data[195–198].

In connection with this, some studies have focused on specific mechanisms or particular pathways to explain long-term survival, but no studies have pointed to a global sight for LT.

The aim of the present work is to define a multiparameter “fingerprint” of LTS, using for comparison age, sex and underlying disease matched CLAD individuals.

2

HYPOTHESIS AND OBJECTIVES

HYPOTHESIS

Several studies performed in kidney and liver transplantation have revealed different tolerance fingerprints, suggesting an organ-specific mechanism for operational tolerance. Consequently, potential renal and liver tolerance biomarkers cannot be extrapolated to lung.

Due to the lack of operationally tolerant lung transplant recipients, long-term survivors with normal allograft function after lung transplantation are the closest to operational tolerance kidney or liver transplant patients.

Overall, the working hypothesis of the present thesis included the following: long-term survival with normal allograft function after lung transplantation signature differs from kidney and liver tolerance fingerprints.

MAIN OBJECTIVE

The final goal of this study is to identify potential biomarkers across different platforms in order to provide a better understanding of the biological mechanisms underlying long-term survival with normal allograft function after lung transplantation in comparison with chronic lung allograft dysfunction patients.

SPECIFIC OBJECTIVES

1- To define the clinical characteristics of long-term survivors with normal allograft function.

2- To determine genetic expression patterns (mRNA and microRNA) and perform an integrative analysis of both expression profiles. To build classification mRNA and miRNA models to differentiate between long-term survivors with normal allograft function and chronic lung allograft dysfunction patients.

3- To compare the composition of the different peripheral blood leucocyte subpopulations, donor-specific antibodies and serum proteins between long-term survivors with normal allograft function and chronic lung allograft dysfunction patients.

4- To identify the differences in the upper respiratory tract bacterial microbiome between long-term survivors with normal allograft function and chronic lung allograft dysfunction patients.

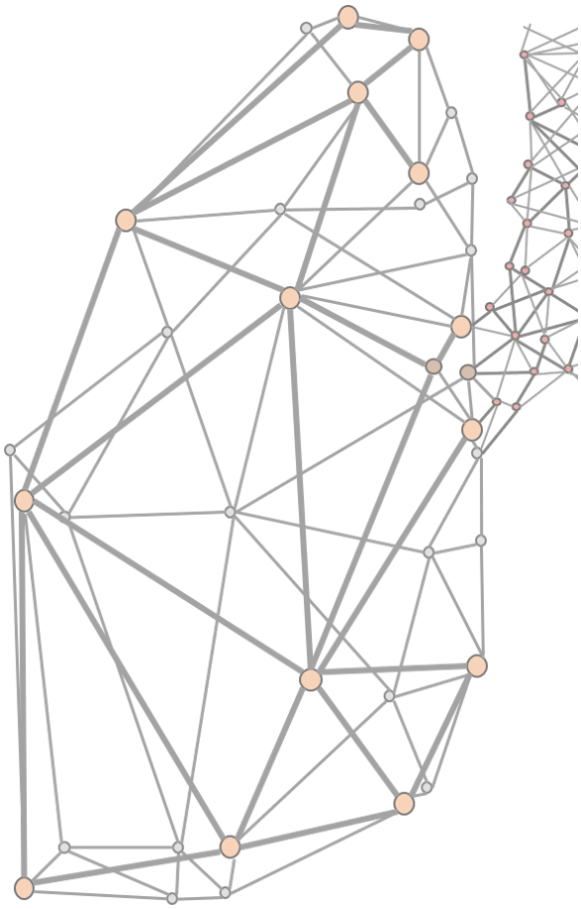

3
METHODS AND RESULTS

THESIS OUTLINE

In order to achieve the main and specific goals, the present thesis comprises five separate sections, detailed as following:

Part I *(Section 3.1)*. Definition of the clinical characteristics of long-term survivors with normal allograft function.

Part II *(Section 3.2)*. Transcriptomic analyses: gene expression and gene regulation analyses, construction of transcriptomic models to discriminate LTS and CLAD patients and integrative analyses studies.

Part III *(Section 3.3)*. Immunophenotype and molecular characterization: cell subpopulations, anti-HLA antibody detection and serum protein determination.

Part IV *(Section 3.4)*. Multi-platform biomarker analysis: construction of a highly correlated multi-biomarker signature to discriminate LTS and CLAD patients including data from part I, II and III.

Part V *(Section 3.5)*. Identification of the upper respiratory tract bacterial microbiome composition.

In summary, several platforms have been used to assess clinical factors, genetic expression, leucocyte subpopulations profile, molecular biomarkers and microbiome composition in order to define a specific long-term survival signature as shown in Figure 6.

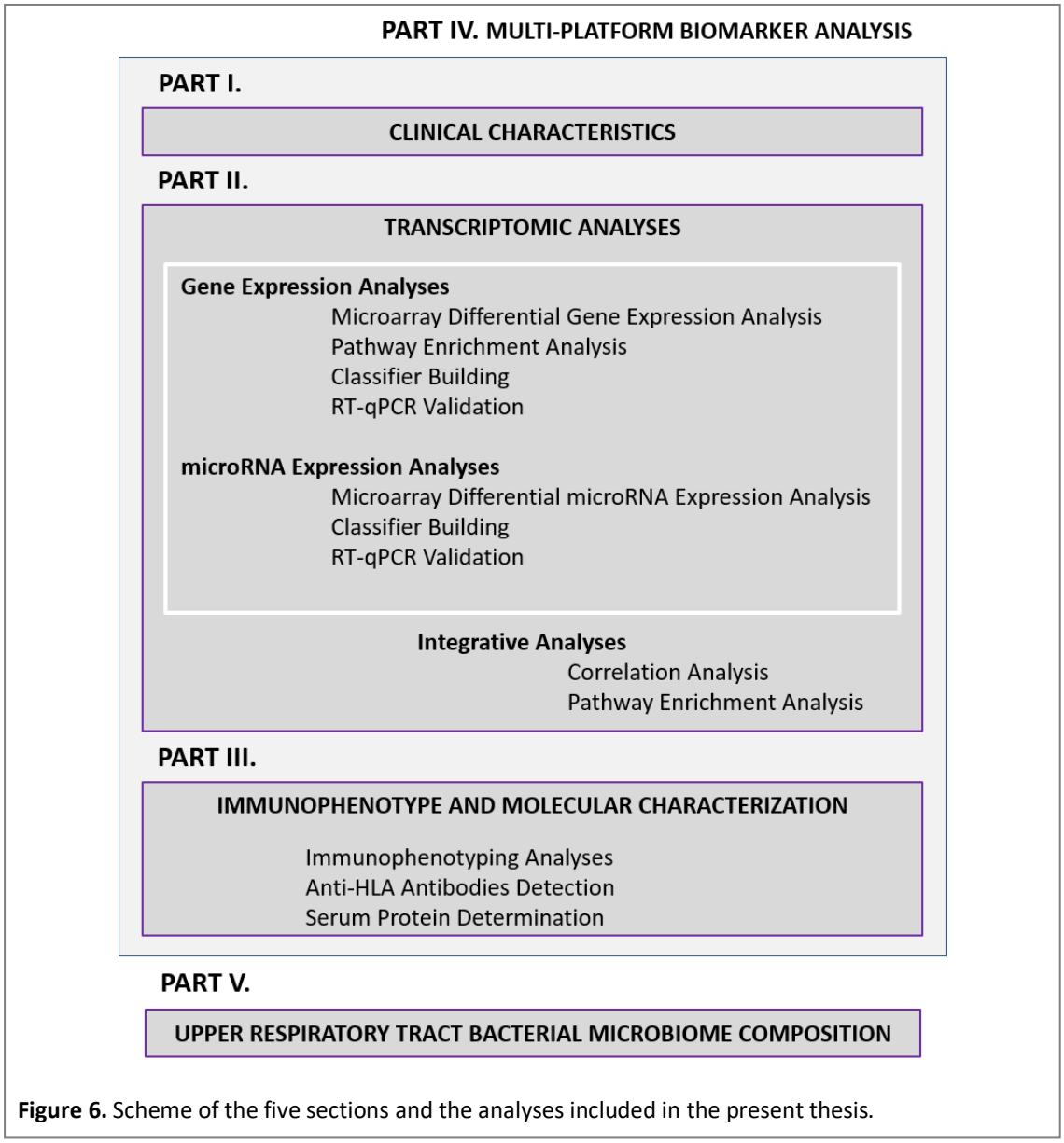

Figure 6. Scheme of the five sections and the analyses included in the present thesis.

3.1 PART I. CLINICAL CHARACTERISTICS OF LONG-TERM SURVIVORS WITH NORMAL ALLOGRAFT FUNCTION

3.1.1 PATIENTS AND METHODS

3.1.1.1 STUDY DESIGN

This doctoral thesis is based on a cross-sectional multi-center case-control study. A total of 62 patients undergoing bilateral LT were included: 31 long-term survivors with normal allograft function (LTS; cases) and 31 CLAD patients (controls). The study was approved by the local ethics committees and all patient samples were collected with written informed consent.

Cases were identified in five Spanish centers[1] with more than 10 years of experience in LT. Cases were defined as LT patients, 10-year survivors, alive at the time of the study, with stable and normal lung function (FEV_1 ≥ 90% of the best FEV_1 and corrected FEF_{25-75} > 75%) and no CLAD.

Control group was composed by LT patients with CLAD, defined as a persistent FEV_1 decline > 20% of the best post-operative value for 6 months and without other explanation. All of them came from the same centers (Hospital Universitario Vall d'Hebron). Controls were matched by age, gender and underlying disease in order to achieve homogeneous groups.

3.1.1.2 PATIENTS DATA AND SAMPLE COLLECTION

All clinical histories were retrospectively reviewed by the same clinician to avoid center bias. The clinical variables recorded for each individual of the study are detailed in *Supplementary Information section.*

All patients were visited at the Hospital Universitario Vall d'Hebron. During their medical visit, peripheral blood samples obtained by venous puncture were collected in: EDTA-anti-coagulant coated Vacutainer™ tubes (BD Biosciences), heparin Vacutainer™ tubes (BD Biosciences), Serum-Separator Vacutainer™ (BD Biosciences) tubes and Tempus™ Blood RNA tubes (Life Technologies). In addition, nasopharyngeal swabs were also collected.

One part of fresh peripheral blood samples in EDTA and heparin tubes were used for immunophenotyping analysis. Serum and plasma aliquots were obtained from the rest of peripheral blood samples in EDTA tubes and Serum-Separator tubes and were stored at -80º C until further analysis. Tempus™ Blood RNA tubes and nasopharyngeal swabs were also stored at -80º C.

[1] Hospital Universitario Puerta de Hierro (Madrid), Hospital Universitario de La Fe (Valencia), Hospital Universitario Reina Sofía (Córdoba), Hospital Universitario Marqués de Valdecilla (Santander), and Hospital Universitario Vall d'Hebron (Barcelona).

3.1.1.3 STATISTICAL ANALYSES

Comparisons between the two groups were performed employing nonparametric Mann-Whitney test for quantitative variables and Chi-square or Fisher's exact tests for categorical variables. Variables compared using Mann-Whitney test were presented as medians with interquartile ranges (IQR) whereas categorical variables were presented as frequencies with percentages. For comorbidity, immunological and infectious events two different calculations were conducted, as a number of events to a define time point and as an incidence rate, in order to correct for differences in the length of the follow-up period.

3.1.2 CLINICAL RESULTS

Initial clinical characteristics of patients are summarized in Table 3. There were no significant differences in basal characteristics and immediate postoperative follow-up between the 2 groups except for diabetes mellitus after LT and days in the waiting list, which were more frequent in the CLAD group.

Table 3. Demographics and transplant characteristics of LTS and CLAD subjects. Comparisons between the two groups were performed employing nonparametric Mann-Whitney test for quantitative variables and Chi-square or Fisher's exact tests for categorical variables. Variables compared using Mann-Whitney test are presented as medians with interquartile ranges (IQR) whereas categorical variables are presented as frequencies with percentages.

	LTS (n=31)	**CLAD (n=31)**	**p-value**
Age, median (IQR)	31.0 (23.1; 46.5)	41.5 (22.7; 51.8)	0.371
Gender (males), n (%)	14 (45.2)	15 (48.4)	1.00
Diagnosis, n (%)			0.857
ILD	4 (12.9)	4 (12.9)	
COPD	4 (12.9)	8 (25.8)	
CF	14 (45.2)	13 (41.9)	
Non-CF bronchiectasis	2 (6.45)	2 (6.45)	
Pulmonary arterial hypertension	1 (3.23)	1 (3.23)	
Langerhans cell histiocytosis	1 (3.23)	1 (3.23)	
Lymphangioleiomyomatosis (LAM)	5 (16.1)	2 (6.45)	
Recipient characteristics			
Pre LT FVC (%), median (IQR)	46 (32.5; 54.5)	41 (28.5; 47.5)	0.202
Pre LT FEV_1 (%), median (IQR)	26 (22.0; 35.0)	25 (17.5; 29.5)	0.307
Pre LT O2 treatment, n (%)	26 (83.9)	24 (80)	0.952
Pre LT diabetes mellitus, n (%)	5 (16.1)	15 (48.4)	**0.014**
Days Waiting List, median (IQR)	138 (56.2; 248)	256 (200; 541)	**0.011**
Years after LT, median (IQR)	15.3 (12.4; 17.1)	6.9 (4.95; 10.7)	**<0.001**
Extracorporeal circulation, n (%)	9 (30)	7 (23.3)	0.772
Primary graft dysfunction (positive), n (%)	2 (6.67)	3 (10.0)	1.00
Days in the ICU, median (IQR)	8 (5.0; 17.0)	13 (5.75; 32.75)	0.213
Days on mechanical ventilation, median	2 (1.0; 11.50)	3 (2.0; 30.0)	0.181
Days of hospitalization, median (IQR)	8 (5.25; 18.2)	13 (6.0; 32.0)	0.291
CMV serology (positive), n (%)	22 (71.0)	21 (70.0)	1.00

In Table 4 long-term follow-up variables after LT are shown. LTS patients showed a lower comorbidity rate, due to fewer incidence of diabetes mellitus and psychiatric disorders. Besides, LTS patients showed a lower incidence of infectious events and their best lung function test was better, although it took longer to achieve it. However, no differences in immunological events were observed. LTS patients also showed a lower rate of use of antimicrobial prophylactic therapies.

CLAD patients were evenly treated with cotrimoxazole, azithromycin and inhaled amphotericin B with few exceptions whereas some LTS patients did not receive them due to specific center-related protocols.

Differences in immunosuppressive treatment were also observed between both groups. Whereas LTS patients were treated more frequently with antimetabolites, CLAD patients were more frequently treated with mTOR inhibitors. All LTS patients received standard immunosuppression treatment (CsA or FK, MMF or AZA and corticosteroids), except 4 of them who were treated with mTOR inhibitors due to renal impairment (n=2), LAM as underlying disease and recurrent infections (3 in combination with calcineurin inhibitors and one in combination with MMF). In the CLAD group, 23 patients received mTOR inhibitors combined with calcineurin inhibitors. High variability in immunosuppression was observed equally in both groups (Table 4).

Table 4. Follow-up variables of LTS and CLAD subjects. Comparisons between the two groups were performed employing nonparametric Mann-Whitney test for quantitative variables and Chi-square or Fisher's exact tests for categorical variables. Variables compared using Mann-Whitney test are presented as medians with interquartile ranges (IQR) whereas categorical variables are presented as frequencies with percentages.

	LTS (n=31)	CLAD (n=31)	p-value
Comorbidities			
Comorbidity events at 5th yr, median (IQR)	2 (1.0; 3.0)	4 (2.0; 5.0)	**0.0012**
Comorbidity rate, median per year (IQR)	0.24 (0.16; 0.30)	0.63 (0.34; 0.92)	**1.1e-06**
Arterial hypertension*, n (%)*	15 (48.4)	16 (51.6)	1.00
Diabetes mellitus*, n (%)*	5 (16.13)	15 (48.39)	**0.014**
Dyslipidemia*, n (%)*	12 (38.71)	19 (61.29)	0.128
Renal dysfunction, *n (%)*	15 (48.39)	21 (67.74)	0.198
Obesity, *n (%)*	1 (3.23)	5 (16.13)	0.195
Anaemia, *n (%)*	4 (12.90)	11 (35.48)	0.075
Osteoporosis, *n (%)*	9 (29.03)	11 (35.48)	0.492
Psychiatric disorders, *n (%)*	2 (6.67)	11 (35.5)	**0.015**
GERD	5 (16.13)	10 (32.26)	0.236
Infectious events			
Infection episodes at 3rd yr, median (IQR)[1]	2 (1.0; 5.0)	4 (3.0; 7.0)	**0.0105**
Infection rate, median per year (IQR)	0.54 (0.29; 0.73)	1.50 (1.0; 2.22)	**5.1e-09**
Mild infections rate, median per year (IQR)[2]	0.54 (0.29; 0.73)	1.50 (1.00; 2.22)	**6e-09**
Immunological events			
Immunological events at 1st yr, median (IQR)[3]	1 (0.0; 1.0)	0 (0.0; 1.0)	0.666
Immunological events at 3rd yr, median (IQR)[3]	1 (0.0; 1.0)	1 (0.0; 1.0)	0.988
Immunological events rate, median per year	0.05 (0.0; 0.08)	0.07 (0.0; 0.15)	0.073
Laboratory tests			
Hb (g/dL) at 5thyr, median (IQR)	12.6 (11.9;13.9)	12.7 (12.2; 13.6)	0.485
WBC (x10E9/L) at 5th yr, median (IQR)	7.9 (6.8; 9.6)	6.8 (5.5; 8.1)	0.054
Creatine (mg/dL) at 5th yr, median (IQR)	1.30 (0.88; 1.30)	1.20 (0.93; 1.48)	0.171
Cholesterol (mg/dL) at 5th yr, median (IQR)	198 (145; 223)	193 (180; 218)	0.760
Lung Function tests (first after LT), *median (IQR)*			
FEV_1 (L)	1.84 (1.55; 2.55)	1.81 (1.44; 2.24)	0.477
FEV_1 (%)	60.0 (49.5; 71.0)	61.0 (46.0; 69.0)	0.652
FVC (L)	2.03 (1.73; 2.82)	2.22 (1.775; 2.67)	0.972
FVC (%)	57.0 (44.5; 70.0)	56.0 (45.0; 67.0)	0.636
FEV_1%	94.0 (83.0; 96.0)	85.0 (78.2; 93.0)	0.059
TLC (%)	76.0 (70.0; 83.0)	88 (79.5; 91.2)	0.537
DLCO (%)	51.0 (44.0; 58.0)	47.0 (39.0; 52.0)	0.593
Lung Function tests (best after LT), *median (IQR)*			
FEV_1 (L)	3.41 (2.76; 4.22)	2.44 (2.16; 3.13)	**<0.001**
FEV_1 (%)	103 (95.0; 110)	83.0 (75.0; 93.0)	**<0.001**
FVC (L)	3.55 (3.03; 4.42)	3.02 (2.7; 3.71)	**0.023**
FVC (%)	91.0 (88.5; 104)	79.0 (72.0; 93.0)	**0.002**
FEV_1%	90.5 (82.0; 96.0)	85.0 (72.0; 91.0)	**0.011**
TLC (%)	96.5 (85.8; 109)	96.0 (86.0; 97.0)	0.555
DLCO (%)	78.5 (69.0; 86.5)	58.0 (51.0; 72.0)	**0.015**

	LTS (n=31)	CLAD (n=31)	p-value
Time to best lung function tests, *median (IQR)*	2.15 (1.54;4.01)	1.19 (0.68; 1.83)	**0.001**
Treatment			
Cotrimoxazole, n (%)	18 (58.06)	29 (93.55)	**0.003**
Azithromycin, n (%)	20 (64.52)	31 (100)	**0.001**
Inhaled amphotericin B, n (%)	18 (58.06)	27 (87.09)	**0.023**
Immunosuppressive therapy			
Calcineurin inhibitors, n (%)	31 (100)	31 (100)	1.00
Antimetabolites, n (%)	26 (83.87)	7 (22.58)	**<0.001**
mTOR inhibitors, n (%)	4 (12.90)	23 (74.19)	**<0.001**
Corticosteroids, n (%)	28 (90.32)	30 (96.77)	0.612
High variability in immunosuppression levels[4], n (%)	10 (32.26)	14 (45.16)	0.297

[1] Infection episodes were defined as bronchitis, pneumonia, viral respiratory infections or CMV infections.
[2] Mild infection episodes were defined as any respiratory infection excluding pneumonia, sepsis and bacteraemia.
[3] CLAD events, both BOS and RAS, have not been taken into consideration.
[4] Defined as CsA levels under 100ng/ml or FK levels under 5ng/ml more than 3 times during follow-up.

Considering each comorbid condition as a separate event, CLAD patients had more events at 5 and 10 years post-LT than LTS patients whereas no significant differences were observed at the first year post- LT (Figure 7).

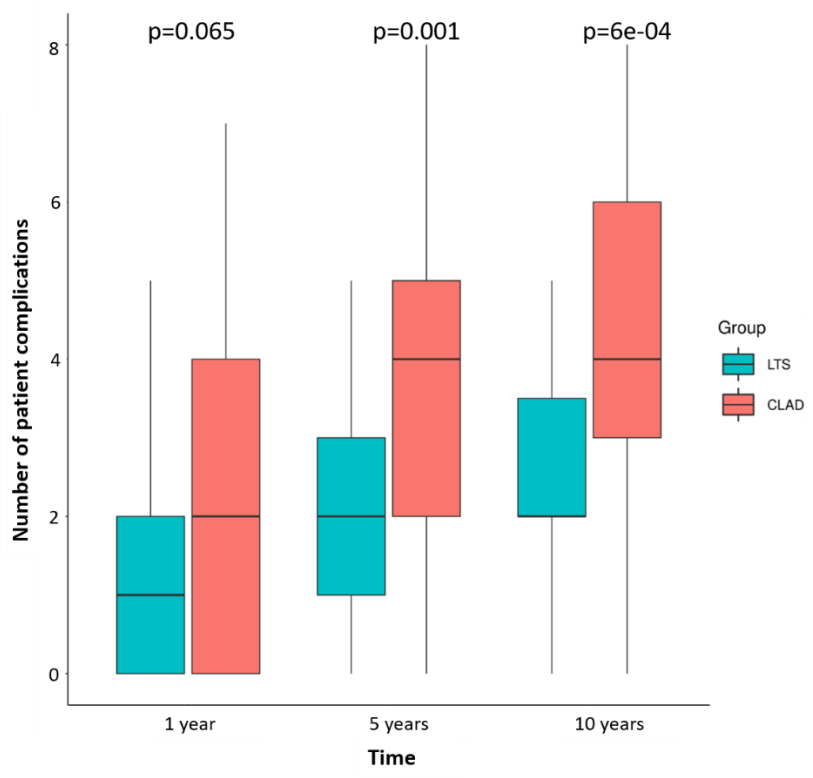

Figure 7. Comorbidity events at 1st year, 5th year and 10th year in LTS (blue) and CLAD (red) patients.

As shown in Table 4, infectious events were more frequent in the CLAD group at three years [2 (1.0; 5.0) episodes in LTS vs 4 (3.0; 7.0) episodes in CLAD, p=0.01] and the infection rate was also higher [0.54 (0.29: 0.73) in LTS vs 1.50 (1.0; 2.22) in CLAD, p=5.1e-09], mainly due to a higher rate of mild infections [0.54 (0.29: 0.73) in LTS vs 1.50 (1.0; 2.22) in CLAD, p=6e-09], defined as a respiratory infection after excluding pneumonia, sepsis and bacteraemia This higher rate of infections in the CLAD groups were observed graphically in Figure 8, where all the infection events for each patient were represented in a timeline.

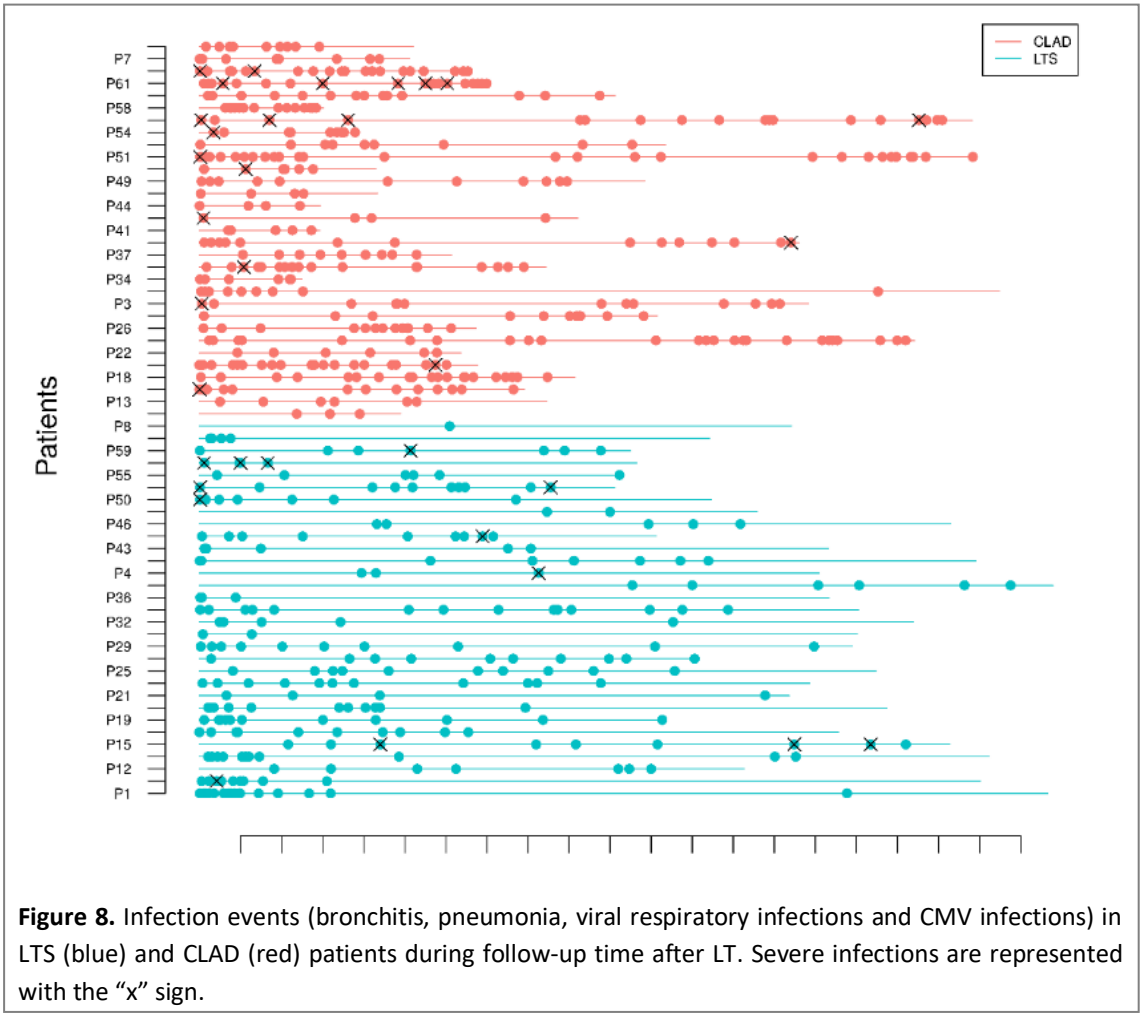

Figure 8. Infection events (bronchitis, pneumonia, viral respiratory infections and CMV infections) in LTS (blue) and CLAD (red) patients during follow-up time after LT. Severe infections are represented with the "x" sign.

Best pulmonary function tests differed significantly between the LTS and CLAD group with the better values in LTS group, although no significant differences were found in lung function tests neither before LT nor first spirometry after LT (Table 4 and Figure 9).

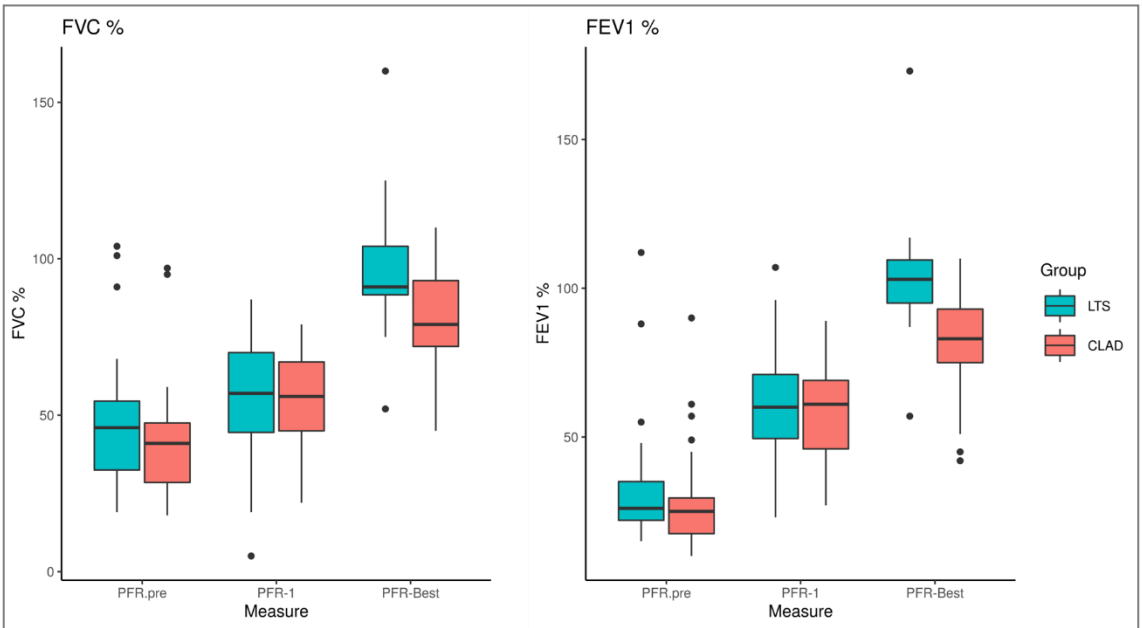

Figure 9. FVC and FEV_1 values before LT (PFR pre), first time after LT (PFR -1) and best value after LT (PFR-Best) in LTS (blue) and CLAD (red) patients. P-values are detailed in Table 4**.**

The characteristics of CLAD group are detailed in Table 5. Briefly, the vast majority (83.87%) of CLAD patients showed a BOS phenotype and all CLAD grades were equally distributed, except grade 0, with no patients.

Table 5. Characteristics of CLAD subjects. Quantitative variables are presented as medians with interquartile ranges (IQR) whereas categorical variables are presented as frequencies with percentages.

	Total (n=31)
Years from LT to diagnosis of CLAD, median (IQR)	3.32 (2.24;5.71)
Years from diagnosis of CLAD	3.05 (1.83; 5.87)
CLAD phenotype	
BOS, *n (%)*	26 (83.87)
Combined, *n (%)*	2 (6.45)
RAS, *n (%)*	3 (9.68)
ISHLT CLAD grade	
CLAD-0, *n (%)*	0 (0.0)
CLAD-1, *n (%)*	7 (22.58)
CLAD-2, *n (%)*	8 (25.81)
CLAD-3, *n (%)*	8 (25.81)
CLAD-4, *n (%)*	8 (25.81)

3.2 PART II. TRANSCRIPTOMIC ANALYSES

TRANSCRIPTOMIC ANALYSES WORKFLOW

The transcriptomic analyses performed can be grouped into the three following blocks: gene expression analysis studies, miRNA expression analysis studies and integrative analysis studies. The workflow of the transcriptomic analyses is shown in Figure 10.

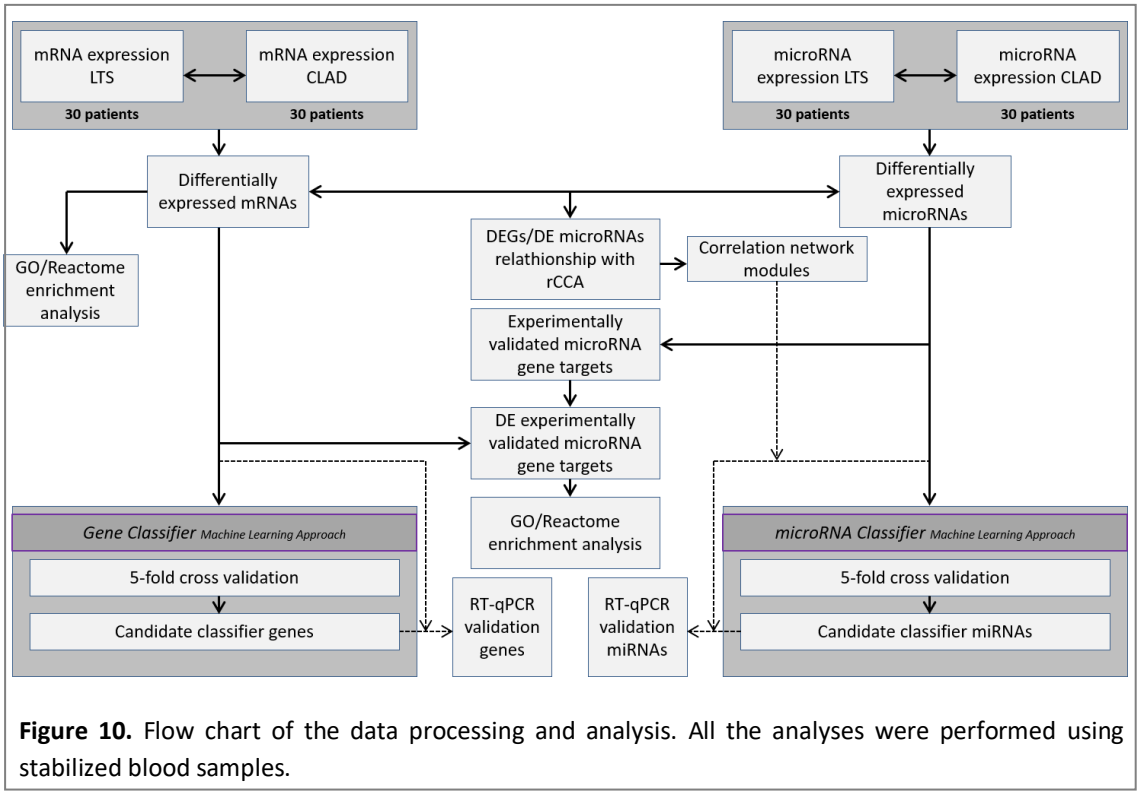

Figure 10. Flow chart of the data processing and analysis. All the analyses were performed using stabilized blood samples.

Gene expression analysis block is composed by the following sub-studies: microarray differential gene expression analysis, pathway enrichment analysis, gene classification model building and RT-qPCR validation of microarray expression data.

miRNA expression analysis block is composed by the following sub-studies: microarray differential microRNA (miRNA) expression analysis, mature miRNA classification model building and RT-qPCR validation of microarray expression data.

Integrative analysis block is composed by the following sub-studies: correlation analysis of the differentially expressed genes and differentially expressed miRNA expression values and the pathway enrichment analysis of the differentially expressed experimentally validated miRNA gene targets.

3.2.1 TRANSCRIPTOMIC MATERIAL AND METHODS

3.2.1.1 GENE EXPRESSION ANALYSES BLOCK

3.2.1.1.1 Total RNA Extraction

Total RNA was extracted from thawed whole blood stored in Tempus™ Blood RNA tubes (Life Technologies) at -80°C using a magnetic bead method (MagMAX™ for Stabilized Blood Tubes RNA Isolation Kit, compatible with Tempus™ Blood RNA Tubes; Thermo Fisher Scientific) following the manufacturer's guidelines. RNA was stored at -80ºC until further analysis.

The quality and integrity of extracted RNA was assessed using the Agilent RNA 600 Nano Kit on the Agilent 2100 Bioanalyzer (Agilent Technologies, Palo Alto, CA, USA).

Two samples (1 LTS and 1 CLAD) were missing, so gene and miRNA expression were analysed by microarrays and RT-qPCR from 60 extracted total RNA samples (30 samples from LTS group and 30 samples from CLAD group).

3.2.1.1.2 Microarray Analysis

Microarrays service was carried out at High Technology Unit (UAT) at Vall d'Hebron Research Institut (VHIR), Barcelona (Spain). Affymetrix microarray platform and the Genechip Human Clariom D array cartridges (Affymetrix UK Ltd., High Wycombe, United Kingdom) were used for this experiment. This array analyses gene expression patterns on a whole-genome scale on a single array with probes covering many exons on the target genomes, and thus permitting an accurate expression summarization at gene level. Clariom D arrays contain >6,765,500 total probes for >134,700 genes[199].

Starting material was 10 ng of total RNA for each sample. Quality of isolated RNA was first measured by Bioanalyzer Assay (Agilent). Briefly, sense ssDNA suitable for labelling was generated from total RNA with the GeneChip WT Pico Reagent Kit from Affymetrix (Thermofisher - Affymetrix, UK) according to the manufacturer's instructions. Sense ssDNA was fragmented, labelled and hybridized to the arrays with the GeneChip WT Pico Terminal Labeling and Hybridization Kit from the same manufacturer.

3.2.1.1.3 Statistical and Bioinformatics Methodology

All the statistical analyses were performed using R software version 3.4.4 (Copyright© 2018 The R Foundation for Statistical Computing) and the libraries developed for the microarray analysis in the Bioconductor Project[200]. Bioinformatic analyses were performed at the Statistics and Bioinformatics Unit (UEB) from the Vall d'Hebron Research Institute (VHIR).

3.2.1.1.3.1 Microarray Quality Control

Different types of quality controls were performed before and after array normalization in the analysis to check if all the arrays were suitable for the normalization process, and check if normalized data were appropriated for differential expression analysis.

Different approaches to examine the quality of the arrays were conducted: Principal Component Analysis (PCA), heatmap depicting the distances between arrays and hierarchical clustering. After performing the different outlier-detection approaches, they were compared in order to decide whether an array should be removed.

3.2.1.1.3.2 Microarray Data Pre-processing: Normalization and Filtering

In order to make data comparable and remove technical biases, the arrays were pre-processed using the RMA (Robust Multiarray Average) normalization algorithm.[200,201] After data were normalised, some quality controls were performed again. In addition, the exon level values were averaged to yield one expression value per gen.

In order to increase statistical power and reduce unnecessary noise, genes considered non-expressed or un-differentially expressed were removed. To assure that any gene differentially expressed was removed, the standard deviations (SD) of all genes in the array were calculated, ordered and plotted (Figure 11).

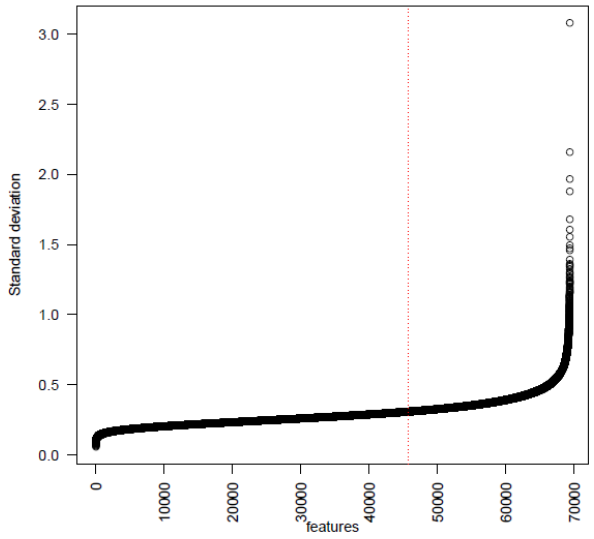

Figure 11. Standard deviation of all probesets in the array. Red line marks 80% of the total probesets.

All the genes with a SD below the 66 percentile were removed. Moreover, those genes without a valid Entrez Gene ID were also removed. These filters were applied to all samples, setting a list of 8239 genes for further statistical analysis.

3.2.1.1.3.3 Differential Gene Expression Analysis

After the dataset was cleaned (filtered, normalized and without outliers), the next step was to perform the differential gene expression analysis. The analysis to select differentially expressed genes (DEG) was based on adjusting a linear model with empirical Bayes moderation of the variance[202].

The comparison between LTS vs CLAD patients yielded a list of genes sorted from most to least differentially expressed. Benjamini & Hocherg method[203] (False Discovery Rate, FDR) was applied for multiple testing corrections.

A heatmap using DEG with a raw p-value below 0.05 and absolute logarithmic FC above 0.5 (112 genes included) was plotted to visualize the expression profiles between the two experimental conditions in order to find common patterns of regulation. In the same way, a volcano plot was used to represent the biological fold change (FC) and the statistical differences between both groups. A FC greater than 1 (in absolute terms) and a raw p-value lower than 0.01 were defined as the minimum to consider potential significance for discrimination between both groups.

3.2.1.1.3.4 Pathway Enrichment Analysis

DEG identified were subjected to pathway enrichment analysis, in order to understand their biological implications. The analyses were performed over two annotation databases: the Gene Ontology (GO) and the Reactome Pathway Knowledge base[204].

The goal of these analyses was to perform one of the available statistical tests to determine whether a given *Gene Set* (a particular category of the GO/Reactome) was over-represented in the list of selected genes (the sample) with respect to a reference set (the population) from where it had been selected. The reference set taken in these analyses was the whole genes that were included in the array used.

Genes with a raw p-value below 0.05 and absolute log FC above 0.4 were only included in GO analysis and Reactome analysis (236 genes). Genes with up- or down-regulation were considered in the same list. GO and Reactome terms were considered enriched when the raw p-value was below 0.05. Dot plots of the first enriched pathways and an enrichment map of the top enriched GO pathways grouped by similarity were performed.

3.2.1.1.3.5 Gene Classification Model Building

The objective of this section was to build models with different sets of genes that allow the classification of the LT population into LTS and CLAD patients. Since the genes which best classified both groups of patients might not be the top ranked DEG[205–207], classification models were built.

Firstly, the fundamentals of supervised and unsupervised analyses should be noted. The supervised methodology classifies the observations regarding the state of the individuals (LTS or CLAD patients in this study), while the unsupervised algorithms try to establish the existence of classes or clusters throughout the distance calculated between observations (e.g PCA or hierarchical clustering).

This part of the work was focused on supervised methods, since they allow building classifiers[208]. A classifier or classification algorithm is a mathematical function that allows predicting the class of a new sample. In recent years, there has been a large number of studies that describe the use of machine learning techniques to develop models for diagnosis, prognosis and patient classification[209,210].

Machine learning can be defined as a computational system that learns patterns from training data to be able to classify unknown cases[211]. Training set and test set are two important concepts that will also be mentioned throughout this section. In Figure 12 the pipeline of the machine learning process used for classification model building is shown.

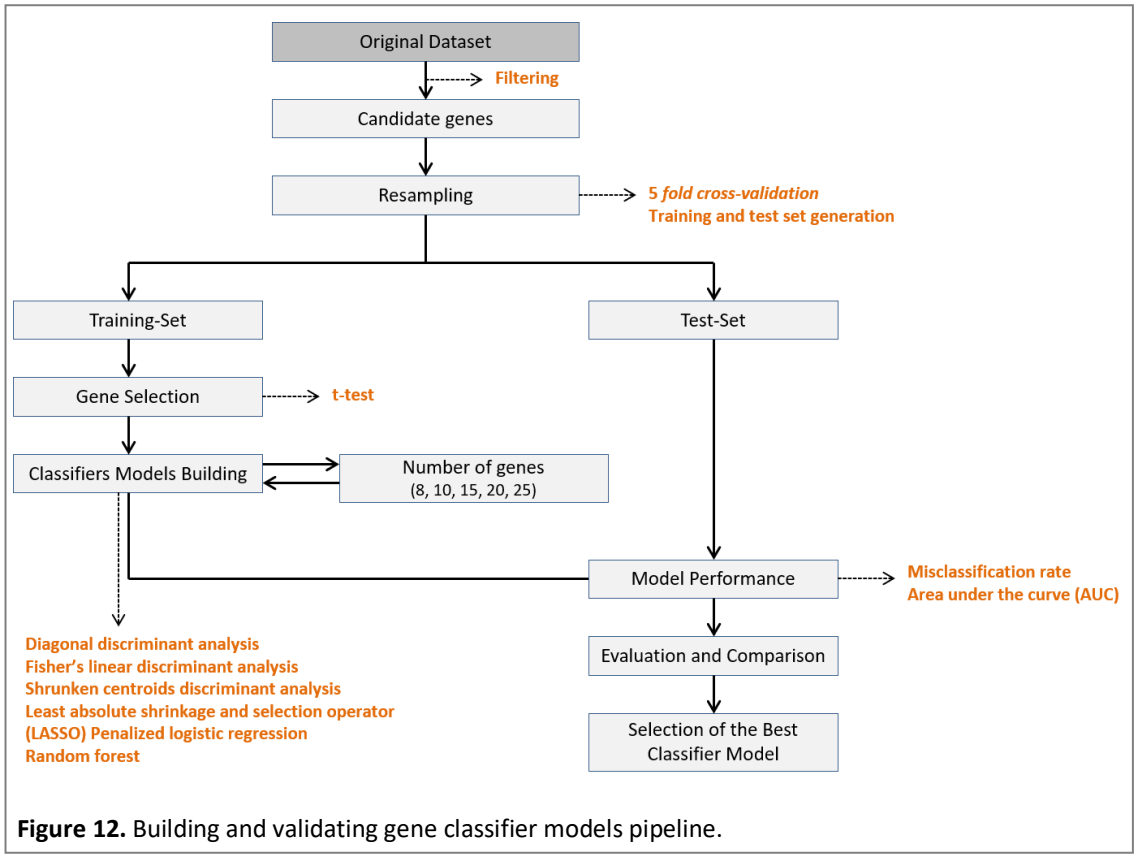

Figure 12. Building and validating gene classifier models pipeline.

To build and validate the gene classification models, 5-fold cross-validation resampling strategy was used. In 5-fold cross-validation method the training and testing sets were created by splitting the original data into five equally size subsets (five folds; 12 patients per subset in this case). In each learning-test iteration, the model was built using 4 folds, and was tested on the remaining partition[212]: four of the subsets (training set, composed by 48 patients) were used for training the classification models. The fifth subset (test set, composed by 12 patients) was used as an independent subset for evaluating the performance of the trained classifier. The process was repeated 5 times until all the subsets were used as a test set (Figure 13).

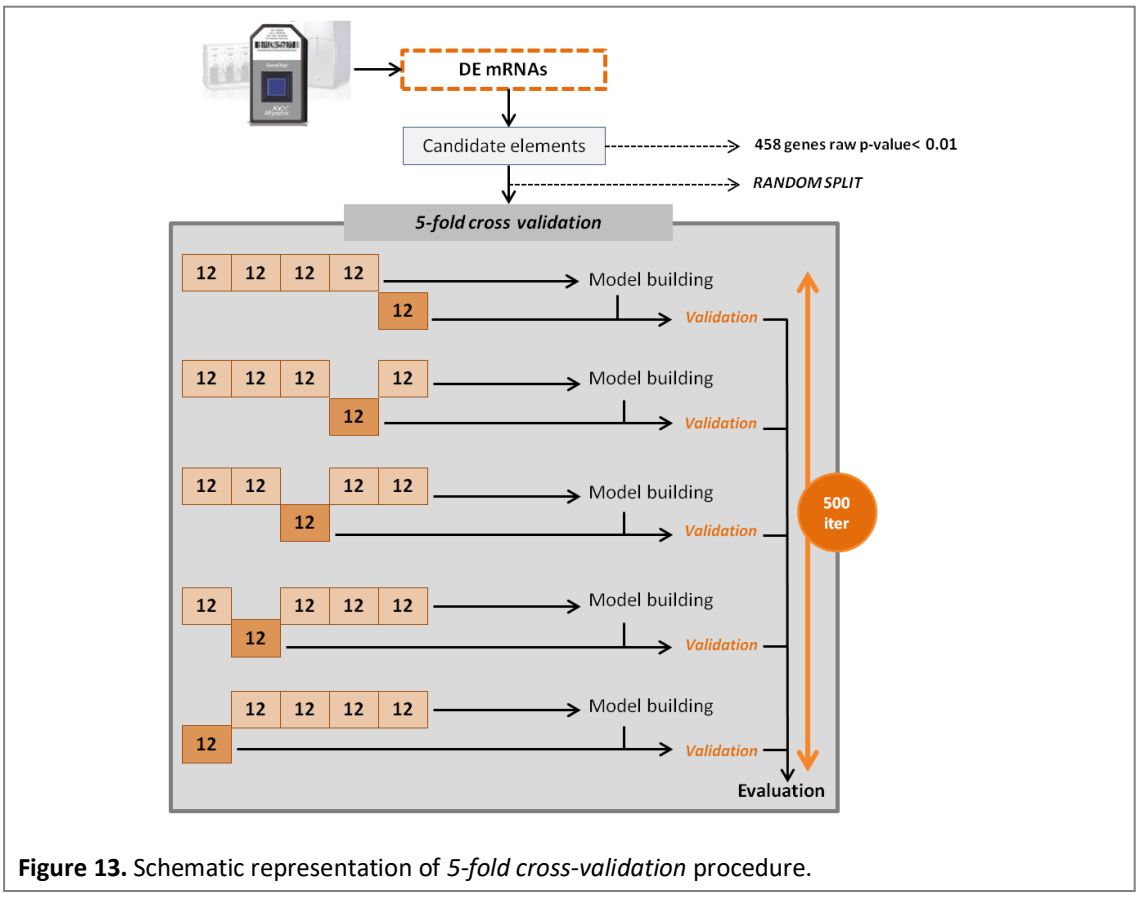

Figure 13. Schematic representation of *5-fold cross-validation* procedure.

The overall prediction performance in each iteration was estimated as the average of the performance values obtained from the 5 test folds. Given the limited sample size of the training set and to get more robust classifiers, the 5-fold cross validation process was performed 500 times (500 iterations) and the average classification accuracy was estimated.

Within each iteration, the classifier parameters (genes in this case) were selected by comparing expression means between LTS and CLAD patients (t-test comparison). Only the genes with a raw p-value below 0.01 in the differential gene expression analysis of the 8239 initial filtered genes were candidate parameters to be part of the classifier (458 genes). Six different supervised classification algorithms, of distinct statistical nature, were used: diagonal discriminant analysis, fisher's linear discriminant analysis, shrunken centroids discriminant analysis, least absolute shrinkage and selection operator (LASSO), penalized logistic regression and random forest. The reason for building classifiers using different methods is consistent with the "No-Free-Lunch theorem", that states that "there is no universal model that works best for every problem"[213]. Furthermore, the number of genes to be used as biomarkers was

also optimized by building the classification models with different number of parameters: 8, 10, 15, 20 and 25 genes.

All the steps involved in the statistical process for biomarker discovery (building and validation classifiers) have been carried out using the *CMA* R package[214].

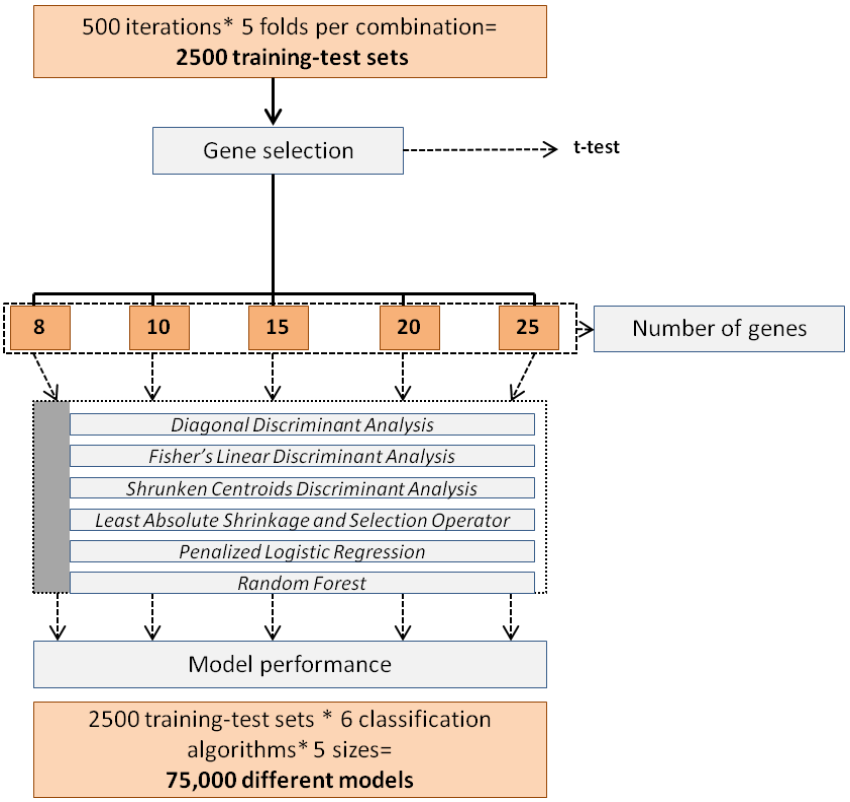

Figure 14. Schematic representation of the different mRNA classification models building.

The overall process resulted in 75,000 classification models: for each 5-fold, 5 subsets were generated, thus 5 x 500 iterations resulted in 2500 training-test sets. In each training-test the selection of the genes was carried out and six different classification algorithms were tested in conjunction with 5 different classifier gene sets. Therefore, 6 classification algorithms x 5 different classifier gene sets x 2500 training-test sets resulted in75,000 different models (Figure 14).

The combinations of the different classification algorithms with the different gene sets were evaluated as an average of the performance of them in each iteration (an average of the performance of the 2500 training-test sets). Thereby, the final result of the computational process was the performance average of 30 classification models.

For visualizing and comparing classifiers based on their performance, receiver operating characteristics (ROC) graphs were used[215].The area under the ROC curve (AUC) values were calculated to compare the different classification models and to summarize their classification accuracy. A higher AUC value corresponds to a better classification. Furthermore, misclassification rate was also evaluated in order to conclude which combination had the best discriminatory ability.

3.2.1.1.3.6 Validation of Microarray Gene Expression Data by RT-qPCR

TaqMan low-density arrays (TLDAs) were employed to confirm the microarray hybridization results as an independent technique. More specifically, the expression pattern of 21 target genes, previously identified by microarrays were measured by RT-qPCR employing the 7900 HT Fast Real-Time PCR System with 384-well block module (Applied Biosystems™, Foster City, CA, USA) using this microfluidic card technology on the same set of samples used for microarray experiments. Thermal cycling conditions were as follow 50°C for 2 min, 94.5°C for 10 min followed by 40 cycles of 97°C for 30 sec and 59.7 °C for 60 sec.

Besides these 21 genes, also two housekeeping genes were included in the cards. In order to select the housekeeping genes, the coefficient of variation (CV) of all genes in the microarrays was calculated to determine which reference genes were most stably expressed across the evaluated samples. In addition, gene intensity was also considered. Hence, *GAPDH* (high intensity) and *TUBGCP4* (medium intensity) were selected and all samples were normalized over them.

Customised 384-well TLDAs cards were produced by Applied Biosystems™ (Foster City, CA, USA) using information for optimized gene probes provided by Applied Biosystems™ Transcriptome Analysis Console Software ver.4.0. Twenty-four TaqMan assays (21 targets, 2 endogenous controls and 1 manufacturing control) were plated in duplicate for each sample with eight samples per TLDA card. One of the samples was used as an internal control for every TLDA in order to evaluate inter-assay variation.

Total RNA samples were reverse transcribed into cDNA using the SuperScript™ IV VILO™ Master Mix cDNA Synthesis Kit (Invitrogen) according to manufacturer's instructions. 500 ng of total extracted RNA were used as starting material for each sample. Pre-designed hydrolysis probe-based TaqMan Gene Expression Assays and Taqman Universal Master Mix II, no UNG (Thermo Fisher Scientific) were used.

Prior to the analysis, the shape of all the amplification curves was checked in order to eliminate outlier amplifications. A quality control was also carried out to determine if there was any sample or gene that should be eliminated from the study in order to improve its final quality.

Gene expression values were calculated by the relative threshold cycle (C_{RT}) method. The relative threshold cycle C_{RT} indicates the cycle number taken to reach an automatically determined threshold of quantification. C_{RT} values were determined using the Relative Quantification module of Thermo Fisher Cloud Software (Thermo Fisher Scientific).

To quantify the levels of mRNA, the expression of the target genes were normalized to the geometric mean of the 2 selected housekeeping genes[216] and the results were presented as relative expression of the cDNA from the LTS samples versus the CLAD samples according to the $2^{-\Delta\Delta Cq}$ method[217]. Results were analysed employing standard 2-class unpaired t test.

Finally, the microarray and RT-qPCR gene linear FC values were analysed in order to assess the degree of correlation between both technologies. A data transformation (-1/linear FC) was applied to the genes whose linear FC was under 1 in order to compare the data of both technologies.

3.2.1.2 microRNA EXPRESSION ANALYSES BLOCK

3.2.1.2.1 Microarray Analysis

Microarrays service was carried out at High Technology Unit (UAT) at Vall d'Hebron Research Institut (VHIR), Barcelona (Spain). Affymetrix microarray platform and the Genechip miRNA array cartridges 4.0 (Affymetrix UK Ltd., High Wycombe, United Kingdom) were used for this experiment. This arrays contain 41404 probes from 203 different organisms, of which 6631 miRNA probe sets correspond to *Homo sapiens* [218]

Starting material was 250 ng of total RNA for each sample. miRNA in the sample was labelled using Flash Tag Biotin HSR RNA Labelling kit (Thermofisher - Affymetrix, UK) following the manufacturer's instructions.

3.2.1.2.2 Statistical and Bioinformatics Methodology

The miRNA data were analysed using the same pipeline as detailed in the gene section. The specific aspects of the miRNA analysis are detailed below. Bioinformatic analyses were performed at the Statistics and Bioinformatics Unit (UEB) from the Vall d'Hebron Research Institute (VHIR).

3.2.1.2.2.1 Microarray Quality Control

As in the case of gene expression analysis, different types of quality controls were performed before and after array normalization in the analysis to check if all the arrays were suitable for normalization process, and check if normalized data were appropriated for differential expression analysis.

Different approaches to assess the quality of the arrays were conducted: PCA, heatmap depicting the distances between arrays and hierarchical clustering. After performing the different outlier-detection approaches, they were compared in order to decide whether an array should be removed.

3.2.1.2.2.2 Microarray Data Pre-processing: Normalization and Filtering

In order to make data comparable and remove technical biases, the arrays were pre-processed using the RMA normalization algorithm.[200,201]. After the data were normalised, some quality controls were performed again.

In order to increase statistical power and reduce unnecessary noise, miRNAs probes from species different from *Homo sapiens* were removed.

3.2.1.2.2.3 Differential microRNA Expression Analysis

After the dataset was cleaned (filtered, normalized and without outliers) the next step was to perform the differential miRNA expression analysis. The analysis to select differentially expressed miRNAs was based on adjusting a linear model with empirical Bayes moderation of the variance.[202] The comparison between LTS vs CLAD patients yielded a list of miRNAs sorted from most to least differentially expressed. Benjamini & Hocherg method[203] was applied for multiple testing corrections.

A volcano plot was used to represent the biological FC and the statistical differences between both groups. A FC, greater than 0.75 (in absolute terms) and a raw p-value lower than 0.01 were defined as the minimum to consider potential significance for discrimination between both groups.

In the same way, two heatmaps using differentially mature miRNAs with a raw p-value below 0.01 were plotted to visualize the expression profiles between the two experimental conditions in order to find common patterns of regulation; the former based on hierarchical clustering and the latter relying on supervised clustering of the 2 experimental groups.

3.2.1.2.2.4 Identification of microRNA Gene Targets

Since miRNAs regulate gene expression by binding to their target mRNAs and repressing the protein translation[219], miRNA target sites have been catalogued in databases based on experimental validation and computational prediction using a variety of algorithms.

M*ultiMiR* R package was used for the identification of miRNA gene targets[220].This package enables retrieval of miRNA-target interactions from 14 different databases MiRNA targets will be used in the pathway enrichment analysis of the differentially expressed experimentally validated miRNA gene targets (*included in the Integrative Analysis Block section*).

3.2.1.2.2.5 microRNA Classification Model Building

The pipeline of the machine learning process used for miRNA classification model building was the same as the one described in gene expression analysis block (Figure 12). The classification models were built and validated using 5-fold cross-validation strategy (Figure 13).

The only difference regarding the gene classification model building was the number of supervised classification algorithms performed; in this case, five algorithms, instead of six were used (Figure 15). In order to build the miRNA classification models, from the initial 6631 miRNAs that corresponds to *Homo sapiens*, only the mature miRNAs with a raw p-value below 0.01 were postulated as candidates to be part of the classifier.

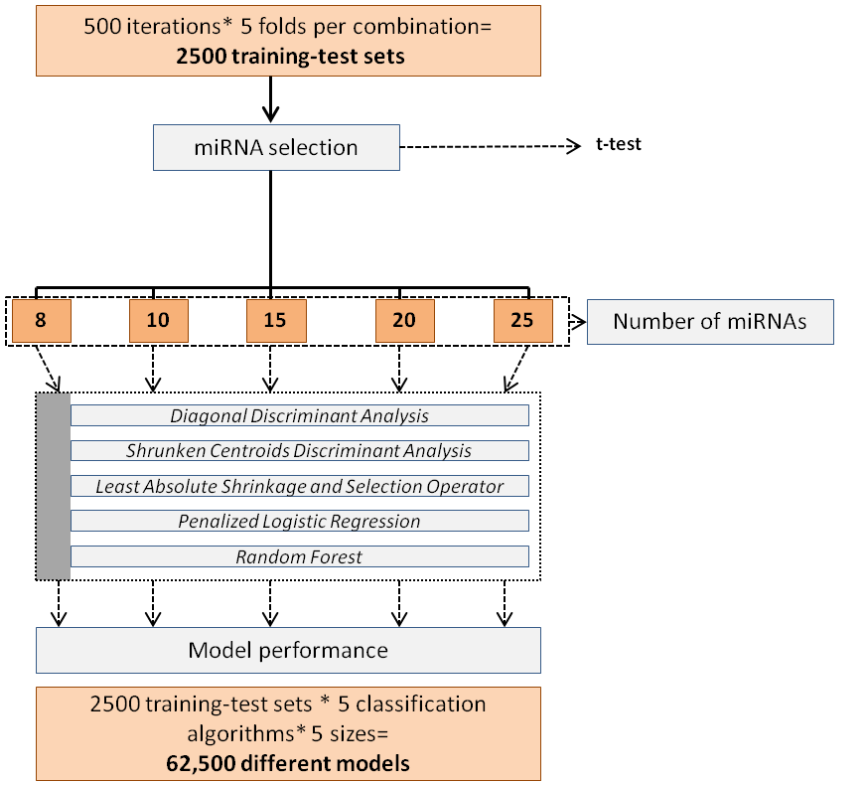

Figure 15. Schematic representation of the different miRNA classification models building.

The overall process resulted in 62,500 classification models: for each 5-fold, 5 subsets were generated, thus 5 x 500 iterations resulted in 2500 training-test sets. In each training-test the selection of the miRNAs was carried out and five different classification algorithms were tested in conjunction with 5 different classifier miRNA sets. Therefore, 5 classification algorithms x 5 different classifier miRNA sets x 2500 training-test sets resulted in 62,500 different models (Figure 15).

The combinations of the different classification algorithms with the different miRNAs sets were evaluated as an average of the performance of them in each iteration (an average of the performance of the 2500 training-test sets). Thereby, the final result of the computational process was the performance average of 25 classification models.

As in the case of gene section, for visualizing and comparing classifiers based on their performance, ROC graphs were used[215]. The AUC values were calculated to compare the different classification models and to summarize their classification accuracy. A higher AUC value corresponds to a better classification. Furthermore, misclassification rate was also evaluated in order to conclude which combination had the best discriminatory ability.

3.2.1.2.2.6 Validation of Microarray microRNA Expression Data by RT-qPCR

Taqman low-density arrays (TLDAs) were employed to confirm the microarray hybridization results as an independent technique. More specifically, the expression pattern of 21 target mature miRNAs previously identified by microarrays were measured by RT-qPCR employing the 7900 HT Fast Real-Time PCR System with 384-well block module (Applied Biosystems™, Foster City, CA, USA) using this microfluidic card technology on the same set of samples used

for microarray experiments. In this case, thermal cycling conditions were as follow 92°C for 10 min followed by 40 cycles of 95°C for 1 sec and 60 °C for 20 sec.

Besides these 21 miRNAs, also two housekeeping miRNAs were included in the cards. In order to select the housekeeping miRNAs, the CV of all miRNAs in the microarrays was calculated to determine which reference mature miRNAs were most stably expressed across the evaluated samples. In addition, miRNA intensity was also considered. Hence, hsa-miR-106b-3p (high intensity) and hsa-miR-877-5p (medium intensity) were selected and all samples were normalized over them.

Customised 384-well TLDAs cards were produced by Applied Biosystems™ (Foster City, CA, USA) using information provided for mature miRNA probes. Twenty-four TaqMan assays (21 targets, 2 endogenous controls and 1 manufacturing control) were plated in duplicate for each sample with eight samples per TLDA card. One of the samples was used as an internal control for every TLDA in order to evaluate inter-assay variation.

2 μl of total extracted RNA of each sample was reverse transcribed into cDNA using an adapter-based *Taqman® Advanced miRNA cDNA Synthesis Kit* (Thermo Fisher Scientific) with preamplification step according to the manufacturer's protocol. Predesigned hydrolysis probe-based TaqMan Advanced miRNA Assays and Taqman Fast Advanced Master Mix (Thermo Fisher Scientific) were used.

Prior to the analysis, the shape of all the amplification curves was checked in order to eliminate outlier amplifications. A quality control was also carried out to determine if there was any sample or miRNA that should be eliminated from the study in order to improve its final quality.

miRNA expression values were calculated by the relative threshold cycle (C_{RT}) method. The relative threshold cycle C_{RT} indicates the cycle number taken to reach an automatically determined threshold of quantification. C_{RT} values were determined using the Relative Quantification module of Thermo Fisher Cloud Software (Thermo Fisher Scientific).

To quantify the levels of miRNA, the expression of the target mature miRNAs were normalized to the geometric mean of the 2 selected housekeeping mature miRNAs[216] and the results were presented as relative expression of the cDNA from the LTS samples versus the CLAD samples according to the $2^{-\Delta\Delta Cq}$ method[217]. Results were analysed employing standard 2-class unpaired t test.

Finally, the microarray and RT-qPCR miRNA linear FC values were analysed in order to assess the degree of correlation between both technologies. A data transformation (-1/linear FC) was applied to the miRNAs whose linear FC was under 1 in order to compare the data of both technologies.

3.2.1.3 INTEGRATIVE ANALYSES BLOCK

After obtaining the results of the gene and miRNA blocks separately, both expression profiles were simultaneously analysed to move a step forward in the biological interpretation of the combined results.

The analyses were performed following two different integrative approaches:

- Correlation analysis of DEG and differentially expressed mature miRNA expression values.
- Analysis of biological significance of the differentially expressed experimentally validated miRNA gene targets.

3.2.1.3.1 Statistical and Bioinformatics Methodology

Bioinformatic analyses were performed at the Statistics and Bioinformatics Unit (UEB) from the Vall d'Hebron Research Institute (VHIR).

3.2.1.3.1.1 Correlation Analysis of DEG and Differentially Expressed microRNA Expression Values

The main objective of this sub-study was to assembly DEG and differentially expressed miRNAs expression values by integrative analysis in order to find correlated elements between them. The analyses were performed using the *mixOmics* R package[221].

Data Pre-processing: Filtering

The gene and miRNA data sets were both properly filtered using the same statistically criteria in order to just select the most significative features. The elements with a raw p-value below 0.01 were only included in the analysis: 458 genes and 36 mature miRNAs.

Since the miRNA data set has one less sample that was discarded during the quality control analyses in the miRNA expression analysis block, this sample was removed from the gene data set too for further correlation analyses.

Canonical Correlation Analysis

The correlation structure between the paired genetic data sets (mRNA and miRNA) was performed based on regularized Canonical Correlation Analysis[2] (rCCA), due to the amount of variables in the mRNA data set (genes) was higher than the number of experimental units (patients).

[2] Canonical Correlation Analysis (CCA) is a multivariate exploratory approach to highlight correlations between two sets of quantitative variables acquired on the same experimental units. CCA seeks for linear combinations of the variables to reduce the dimensions of the data sets trying to maximize the correlation between the two variables (the canonical correlation)[309].

The correlations between genes and miRNAs were graphically displayed with a Clustered Image Map. A relevance network showing the connections between genes and miRNAs applying a rCCA correlation value threshold of 0.5 was also plotted.

3.2.1.3.1.2 Pathway Enrichment Analysis of the Differentially Expressed Experimentally Validated microRNA Gene Targets

The goal of this part was to perform a biological significance analysis of the genes targeted by differentially expressed miRNAs that were also found differentially expressed in the gene expression analysis (Figure 10) in order to understand their biological implications. As in the previous case, only elements with a raw p-value below 0.01 were included in the analysis: 458 genes and 36 mature miRNAs.

Gene targets for the 36 mature miRNAs were retrieved using multiMiR Bioconductor's package.[220] The resulting validated gene targets were intersected with the top 458 DEG to find the subset of differentially expressed validated gene targets. Finally, an enrichment analysis was performed for this subset of genes across GO and Reactome databases. The reference set taken in these analyses was the whole human genes annotated. GO and Reactome terms were considered enriched under a p-value below 0.05.

An enrichment analysis for the miRNA with the highest number of validated differentially expressed gene targets was also performed across GO database.

3.2.2 TRANSCRIPTOMIC RESULTS

3.2.2.1 GENE EXPRESSION ANALYSES BLOCK

3.2.2.1.1 Differential Gene Expression Analysis

None of the samples were discarded in quality control analyses; therefore, the 60 samples were used for the differential expression analysis. After non-specific filtering, 8239 genes were included in the analysis.

Gene expression analysis revealed 458 DEG (raw p-value below 0.01) between LTS and CLAD subjects. Among them, 201 genes were up-regulated and 257 genes were down-regulated in LTS compared to CLAD individuals. A complete list with the top 50 DEG is provided in *Supplementary Information section.*

A heatmap comparing LTS and CLAD patients using DEG with a raw p-value below 0.05 and absolute logarithmic FC above 0.5 was performed, giving a total of 112 genes included. Hierarchical clustering showed a relative good classification of samples (columns), except for a few samples of both groups, which were classified within the other group. Despite this fact, the heatmap showed a clear different expression profile between samples of LTS and CLAD condition (Figure 16).

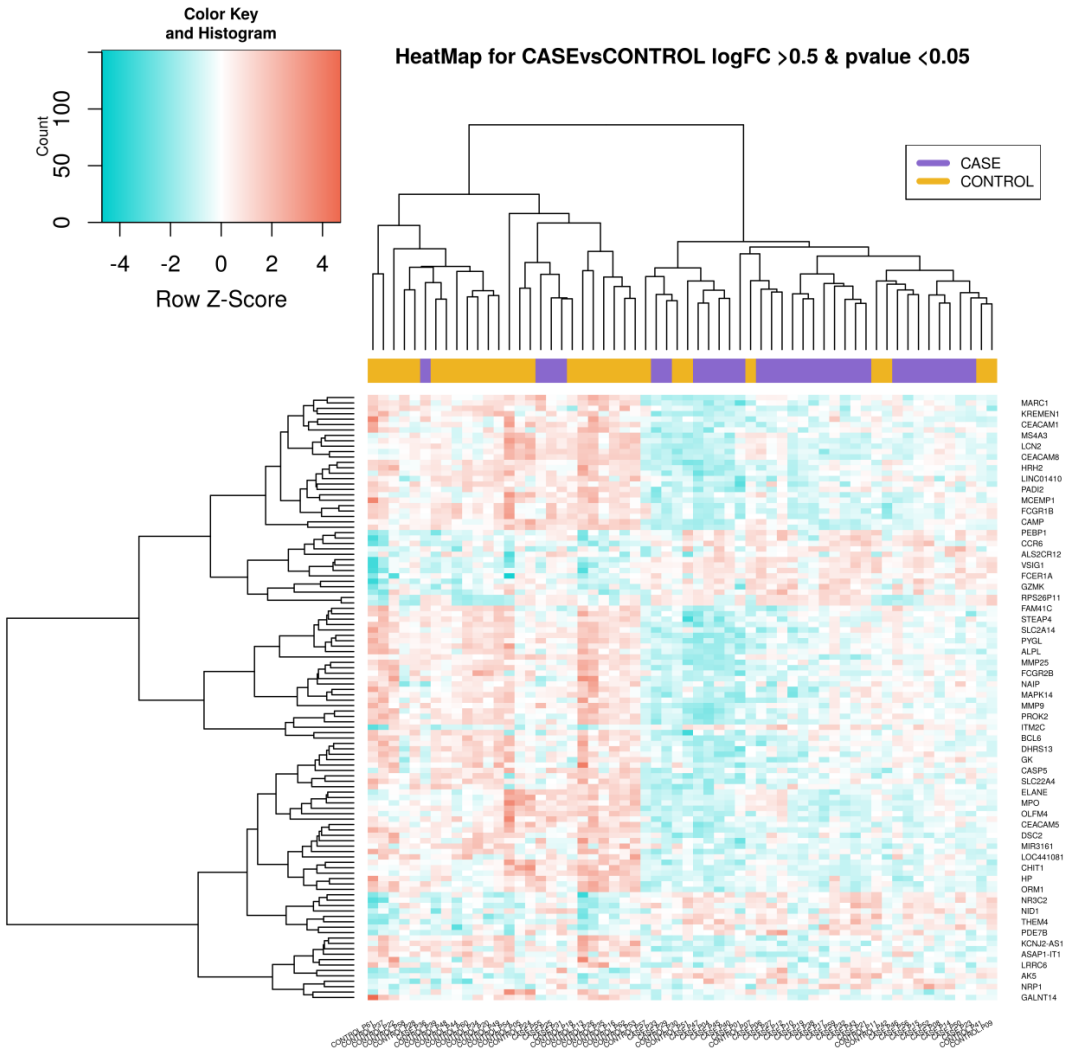

Figure 16. Hierarchical clustering of the two experimental groups based on their gene expression profiles. Each column represents a patient, being purple LTS group and yellow CLAD group, whereas each row represents a gene. For each gene, red indicates up-regulated expression, and blue indicates down-regulated expression.

A volcano plot showing DEG with a raw p-value below 0.01 and absolute logarithmic FC above 1 was performed (Figure 17). In LTS group, most up-regulated DEG correspond to *RPS26*, *RPS26P11* and *JCHAIN*, whereas the most down-regulated DEG were *MMP8, LTF, OLFM4, TCN1, OLR1, CAMP, FCGR1B* and *ANKRD22*.

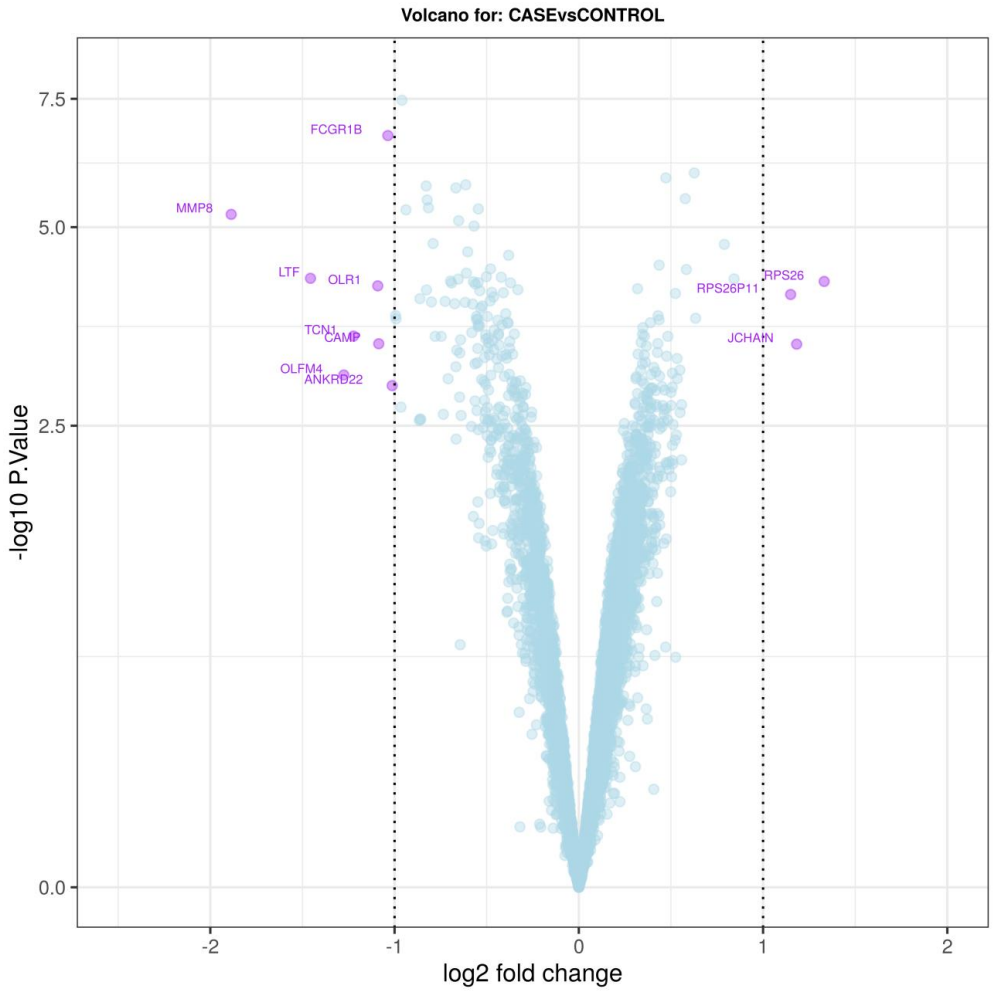

Figure 17. Volcano plot of DEG between LTS compared to CLAD patients. Each dot of the graph corresponds to a gene. The fold difference in expression between LTS and CLAD patients is graphed on the x axis (logarithm of the base 2-fold changes), giving an idea of the magnitude of the change. The p-value for each gene is graphed on the y axis (negative logarithm to the base 10 of the t-test p-values). The vertical dashed lines correspond to logarithmic fold difference of -1.0 and 1.0. The purple dots represent up and down-regulated DEG whose p-value is below 0.01 and absolute logarithmic2 fold change is above 1. The blue dots denote genes that do not fit that criteria of DEG.

3.2.2.1.2 Pathway Enrichment Analysis

Analyses of biological significance were done including those genes with a raw p-value below 0.05 and absolute log FC value above 0.4 (236 genes included).

The most significant GO biological process terms enriched in the gene list were related to neutrophil mediated processes (Table 6). Similarly, pathways significantly enriched in this gene list using Reactome database were related to innate immunity (Table 7).

Graphically, these results were represented in dot plots of the top enriched pathways (Figure 18). An enrichment map of the top enriched GO pathways grouped by similarity is shown in Figure 19.

Table 6. Pathway enrichment analysis representing top 10 GO enriched biological processes among DEG between LTS and CLAD patients. Enriched terms are ranked based on the FDR value.

Term	ID	Gene ratio	p-value	FDR
Neutrophil activation	GO:0042119	46/199	6.54E-28	1.88E-24
Granulocyte activation	GO:0036230	46/199	1.16E-27	1.88E-24
Neutrophil degranulation	GO:0043312	45/199	2.21E-27	2.39E-24
Neutrophil activation involved in immune response	GO:0002283	45/199	2.95E-27	2.39E-24
Neutrophil mediated immunity	GO:0002446	45/199	8.34E-27	5.20E-24
Leucocyte degranulation	GO:0043299	46/199	9.64E-27	5.20E-24
Myeloid cell activation involved in immune response	GO:0002275	46/199	2.14E-26	9.89E-24
Leucocyte migration	GO:0050900	24/199	3.54E-10	1.44E-07
Immune response-regulating cell surface receptor signalling pathway	GO:0002768	20/199	5.74E-09	2.07E-06
Immune response-regulating signalling pathway	GO:0002764	24/199	6.96E-09	2.25E-06

Table 7. Pathway enrichment analysis representing top 10 Reactome enriched pathways among DEG between LTS and CLAD patients. Enriched terms are ranked based on the FDR value.

Description	ID	Gene ratio	p-value	FDR
Neutrophil degranulation	R-HSA-6798695	43/146	4.29E-24	2.44E-21
Antimicrobial peptides	R-HSA-6803157	9/146	7.52E-08	2.14E-05
Role of phospholipids in phagocytosis	R-HSA-2029485	6/146	1.24E-06	2.35E-04
Cell surface interactions at the vascular wall	R-HSA-202733	10/146	1.77E-05	2.52E-03
FCGR activation	R-HSA-2029481	4/146	2.36E-05	2.69E-03
Fibronectin matrix formation	R-HSA-1566977	3/146	6.78E-05	6.44E-03
Activation of Matrix Metalloproteinases	R-HSA-1592389	5/146	9.63E-05	7.85E-03
CD28 dependent PI3K/Akt signalling	R-HSA-389357	4/146	2.10E-04	1.50E-02
Class A/1 (Rhodopsin-like receptors)	R-HSA-373076	14/146	2.74E-04	1.74E-02
Costimulation by the CD28 family	R-HSA-388841	6/146	4.93E-04	2.81E-02

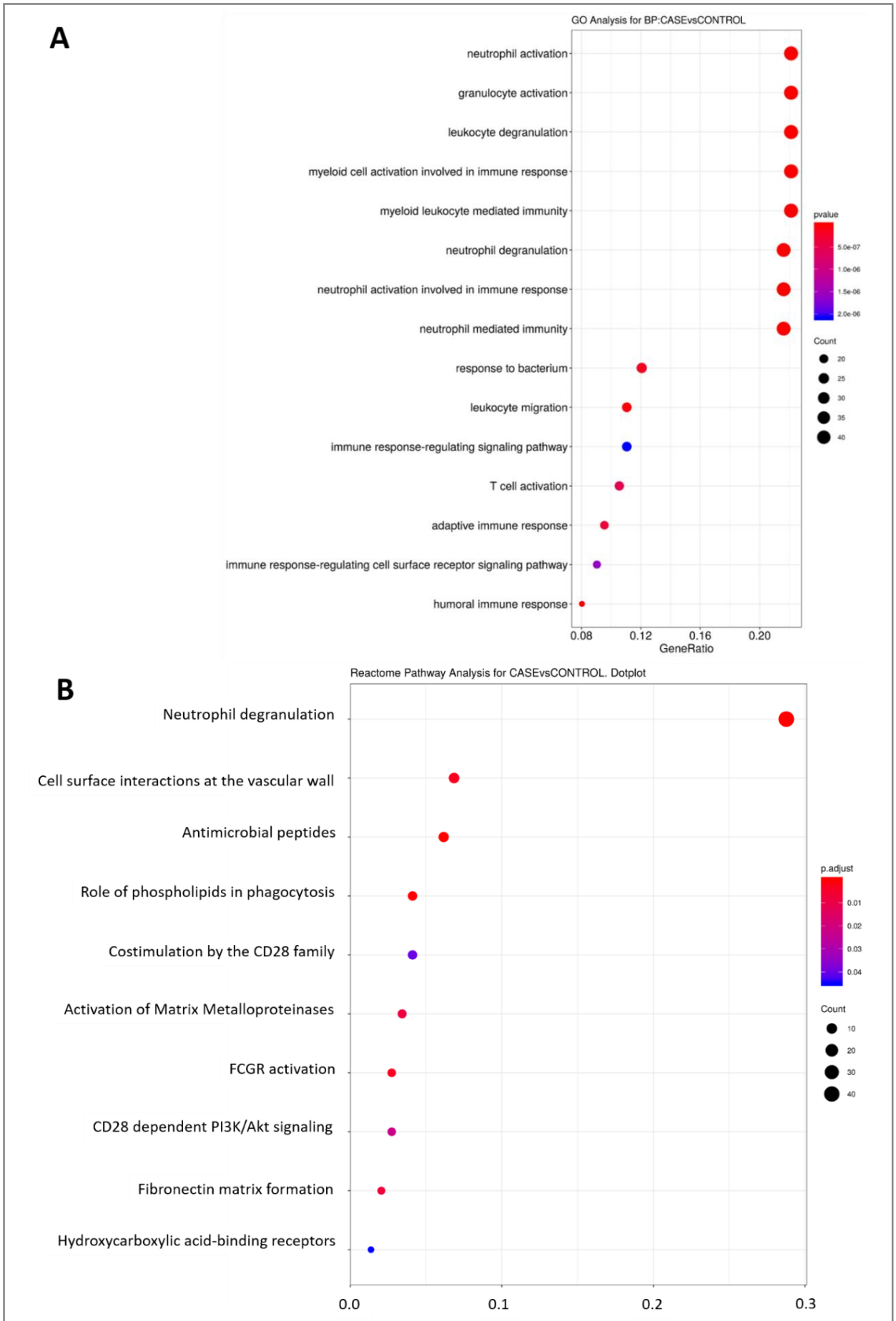

Figure 18. Dot plots of the fifteen and ten statistically significant top enriched pathways using the GO (A) and Reactome (B) databases. The color of circles depends on the p-value and the size depends on the number of genes included in the pathway. Gene ratio is the ratio between the genes in the data that belong to that pathway and the total number of genes in the pathway.

Multiple GO pathway clusters can be identified, highlighting those related to the immune response and neutrophils (Figure 19).

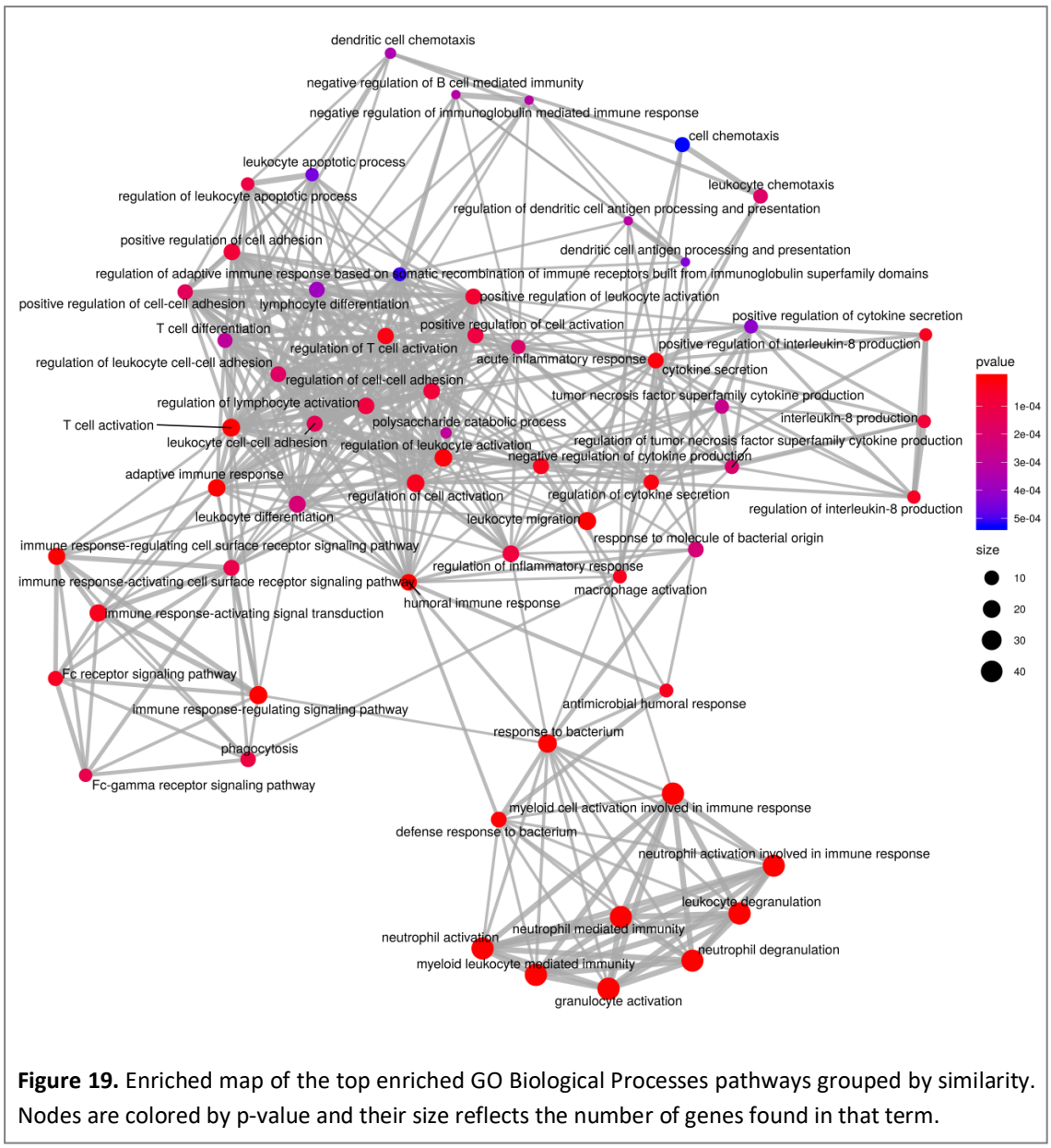

Figure 19. Enriched map of the top enriched GO Biological Processes pathways grouped by similarity. Nodes are colored by p-value and their size reflects the number of genes found in that term.

3.2.2.1.3 Gene Classification Model Building

The classification capacity combining different classifier gene sets with different classification methods is displayed in Table 8. The best discriminatory power was provided by the combination of the LASSO classifier algorithm using 25 genes (AUC of 0.87, misclassification value of 0.21) (Figure 20). The 25 genes included in the classifier model are detailed in Table 9. Actually, the combination of the LASSO algorithm using smaller set of genes (20 or 15 genes) provided similar performances.

The performances of all the models obtained are acceptable, since the misclassification rate is below the 26% and AUC values are over the 80% for all the combinations.

Table 8. Performance of the 30 gene classification models derived from the combination of the different classifier gene sets with the 6 classification algorithms to discriminate LTS and CLAD patients. The best classification model is marked in bold. SN: sensitivity, SP: specificity, AUC: area under the curve.

Number of genes	Classification algorithms	Misclassification	SN	SP	AUC
8	Diagonal Discriminant Analysis	0.25	0.71	0.79	0.82
	Penalized Logistic Regression	0.24	0.77	0.77	0.84
	Random Forest	0.26	0.74	0.75	0.82
	Fisher's Linear Discriminant Analysis	0.23	0.76	0.78	0.84
	Lasso	0.25	0.76	0.75	0.82
	Shrunken Centroids Discriminant Analysis	0.25	0.71	0.79	0.82
10	Diagonal Discriminant Analysis	0.25	0.70	0.80	0.82
	Penalized Logistic Regression	0.23	0.78	0.78	0.85
	Random Forest	0.26	0.74	0.76	0.82
	Fisher's Linear Discriminant Analysis	0.23	0.76	0.79	0.85
	Lasso	0.24	0.78	0.75	0.84
	Shrunken Centroids Discriminant Analysis	0.25	0.71	0.80	0.82
15	Diagonal Discriminant Analysis	0.25	0.70	0.81	0.81
	Penalized Logistic Regression	0.22	0.78	0.79	0.86
	Random Forest	0.26	0.73	0.77	0.83
	Fisher's Linear Discriminant Analysis	0.22	0.77	0.80	0.86
	Lasso	0.22	0.79	0.78	0.86
	Shrunken Centroids Discriminant Analysis	0.25	0.70	0.81	0.81
20	Diagonal Discriminant Analysis	0.25	0.69	0.82	0.81
	Penalized Logistic Regression	0.23	0.77	0.77	0.84
	Random Forest	0.25	0.73	0.77	0.83
	Fisher's Linear Discriminant Analysis	0.24	0.76	0.78	0.84
	Lasso	0.21	0.79	0.79	0.87
	Shrunken Centroids Discriminant Analysis	0.25	0.69	0.82	0.81
25	Diagonal Discriminant Analysis	0.25	0.69	0.82	0.81
	Penalized Logistic Regression	0.26	0.74	0.74	0.82
	Random Forest	0.25	0.73	0.78	0.83
	Fisher's Linear Discriminant Analysis	0.26	0.73	0.75	0.81
	Lasso	**0.21**	**0.79**	**0.80**	**0.87**
	Shrunken Centroids Discriminant Analysis	0.25	0.69	0.82	0.81

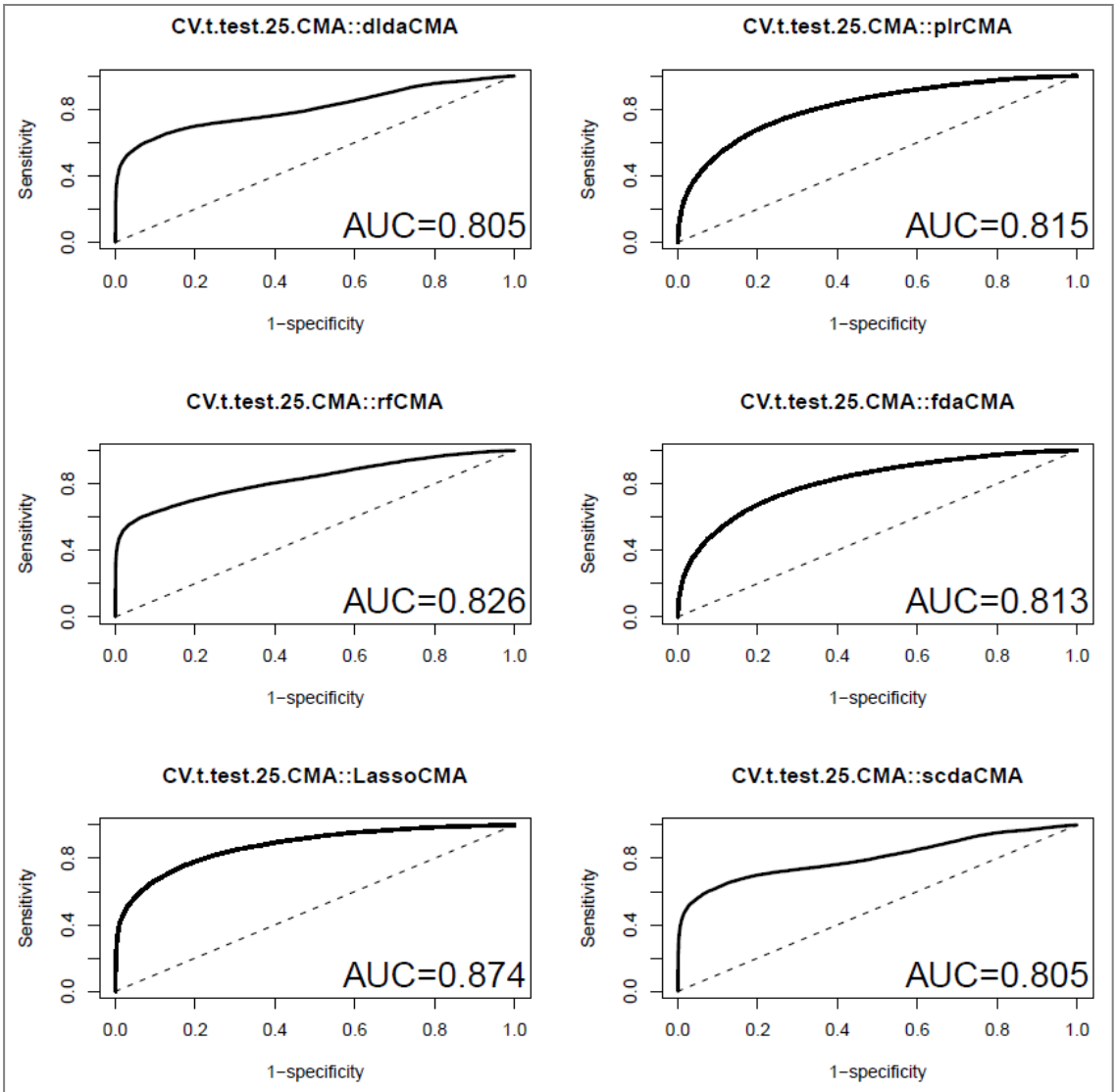

Figure 20. ROC curves showing the accuracy of the gene classification models derived from the combination of the 25 classifier genes with the 6 classification algorithms. dlda: Diagonal Discriminant Analysis; plr: Penalized Logistic Regression; rf: Random Forest; fda: Fisher's Linear Discriminant Analysis; Lasso: least absolute shrinkage and selection operator; scda: Shrunken Centroids Discriminant Analysis.

As can be observed in Table 8 and Figure 20 above, the measures obtained from the 6 different classification methods within each different classifier gene set are homogeneous. This means that the gene classification models are robust, as their performances are not conditioned by the classification algorithm used.

Table 9. List of the 25 genes finally used for building the gene classification models. Genes chosen for subsequent RT-qPCR validation are identified with an *.

Classification rank	Gene symbol	Entrez gene-ID	Gene-name	Linear FC LTS vs CLAD	FDR
1	**ANXA3*	306	Annexin A3	0.514	0.0003
2	**FCGR1B*	2210	Fc fragment of IgG receptor Ib	0.488	0.0008
3	**TNFRSF21*	27242	TNF receptor superfamily member 21	1.387	0.0025
4	**NRP1*	8829	Neuropilin 1	1.493	0.0032
5	**LILRA4*	23547	Leucocyte immunoglobulin like receptor A4	1.544	0.0025
6	**SLC22A4*	6583	Solute carrier family 22 member 4	0.674	0.0053
7	**HCK*	3055	HCK proto-oncogene, Src family tyrosine kinase	0.773	0.0169
8	*FCGR1CP*	100132417	Fc fragment of IgG receptor Ic, pseudogene	0.568	0.0035
9	*MGAM2*	93432	maltase-glucoamylase 2 (putative)	0.522	0.0035
10	**KCNJ15*	3772	Potassium voltage-gated channel subfamily J member 15	0.565	0.0032
11	**PNPLA2*	57104	Patatin like phospholipase domain containing 2	0.768	0.012
12	**CA4*	762	Carbonic anhydrase 4	0.739	0.0336
13	**ACSL1*	2180	Acyl-CoA synthetase long chain family member 1	0.563	0.0025
14	*TGM2*	7052	transglutaminase 2	0.795	0.0184
15	**MMP8*	4317	Matrix metallopeptidase 8	0.27	0.0039
16	**FCGR2A*	2212	Fc fragment of IgG receptor IIa	0.747	0.0169
17	**DHRS13*	147015	Dehydrogenase/reductase 13	0.685	0.0035
18	*ZNF438*	220929	zinc finger protein 438	0.785	0.0336
19	**LRRC6*	23639	Leucine rich repeat containing 6	0.63	0.0025
20	**BCL6*	604	B cell CLL/lymphoma 6	0.636	0.0046
21	*SH3BP4*	23677	SH3 domain binding protein 4	1.247	0.0184
22	*KCNJ2-AS1*	400617	KCNJ2 antisense RNA 1	0.654	0.0025
23	**TLR5*	7100	Toll like receptor 5	0.717	0.0168
24	**PROK2*	60675	Prokineticin 2	0.658	0.0112
25	*WNK1*	65125	WNK lysine deficient protein kinase 1	0.761	0.0435

3.2.2.1.4 Validation of Microarray Gene Expression Data by RT-qPCR

RT-qPCR analyses employing TLDAs were performed on the same set of samples used for microarray experiments to confirm the expression results of a selected target gene list.

Selected target genes for RT-qPCR experiments included 18 genes that were part of the gene classifier (identified with an * in Table 9), most of them also in the top table of DEG (*see Table S-1 in Supplementary Information section)*, and 3 genes (Table 10) which had the highest FC of the 8239 genes included in the differential gene expression analysis. Thus, 21 target genes were analysed by RT-qPCR plus 2 housekeeping genes.

Table 10. List of the three genes with the highest microarray FC that did not form part of the classifiers included in the RT-qPCR analyses.

Gene top table rank	Gene Symbol	Entrez gene ID	Gene name	Linear FC LTS vs. CLAD	FDR
129	*OLFM4*	10562	Olfactomedin 4	0.413	0.0612
26	*LTF*	4057	Lactotransferrin	0.364	0.0169
82	*TCN1*	6947	Transcobalamin 1	0.428	0.0336

None of the samples were discarded in RT-qPCR quality control analyses; therefore the 60 samples were used for the differential expression analysis. The analysis of the control sample included in every TLDA showed very low inter-assay variability (CV of 0.75%).

The RT-qPCR results for 20 of the 21 genes were consistent with the trend observed in the microarray analysis: up-regulation of *TNFRSF21, LILRA4, NRP1* and down-regulation of *ANXA3*, *MMP8, FCGR1B, LTF, TCN1, OLFM4, ACSL1, KCNJ15, LRRC6, BCL6, SLC22A4, HCK, DHRS13, FCGR2A, CA4, PROK2* and *PNPLA2* were confirmed by RT-qPCR analysis *TLR5* gene was differentially expressed when assessed by microarrays but not by RT-qPCR. Hence, RT-qPCR confirmed the differential expression of 95% of the genes selected by microarrays (Table 11 and Figure 21).

Table 11. List of the genes validated using RT-qPCR ranked by FDR value.

Gene Symbol	Taqman mRNA Assay name	$\Delta\Delta C_{RT}$	Linear FC	p-value	FDR
TNFRSF21	Hs00377837_m1	-1.798	3.478	0.0000	0
LILRA4	Hs01110096_g1	-2.081	4.231	0.0000	0
NRP1	Hs01546498_m1	-1.382	2.606	0.0000	1E-05
ANXA3	Hs00971415_m1	1.299	0.406	0.0000	4E-05
MMP8	Hs01029057_m1	2.204	0.217	0.0001	0.0003
FCGR1B	Hs02387778_mH	0.709	0.612	0.0001	0.0004
LTF	Hs00914337_m1	1.894	0.269	0.0003	0.0007
TCN1	Hs01055538_m1	1.331	0.397	0.0003	0.0008
OLFM4	Hs00197437_m1	2.169	0.222	0.0009	0.0022
ACSL1	Hs00960569_m1	0.732	0.602	0.0011	0.0022
KCNJ15	Hs00158427_m1	0.804	0.573	0.0011	0.0022
LRRC6	Hs00917166_m1	0.815	0.568	0.0015	0.0026
BCL6	Hs01115888_m1	0.641	0.641	0.0025	0.0039
SLC22A4	Hs01548716_m1	0.705	0.613	0.0027	0.0041
HCK	Hs01067405_m1	0.314	0.804	0.0043	0.0060
DHRS13	Hs00376268_m1	0.388	0.764	0.0062	0.0081
FCGR2A	Hs01013402_gH	0.449	0.732	0.0114	0.0140
CA4	Hs01088413_m1	0.786	0.579	0.0152	0.0177
PROK2	Hs01587689_m1	0.551	0.683	0.0162	0.0179
PNPLA2	Hs00982042_m1	0.324	0.799	0.0359	0.0378
TLR5	Hs00152825_m1	0.254	0.838	0.0763	0.0763

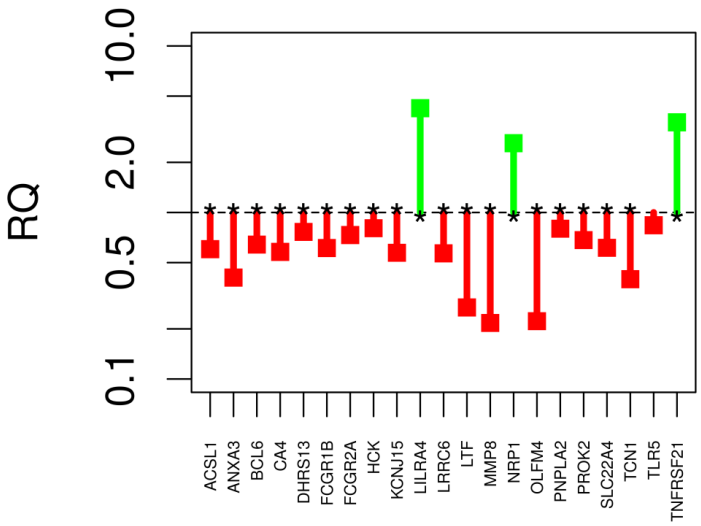

Figure 21. Relative gene expression of genes validated by RT-qPCR. Fold changes (RQ) are shown relative to CLAD group. On the x axis is reported the list of the 21 target genes analysed. On the y axis is reported the results of the relative quantification calculations or folds changes. Relative quantities are graphed on a logarithmic scale. Asterisks indicate differentially expressed genes (FDR<0.05; Student's t-test).

Overall, from these 21 genes selected, 20 were validated by RT-qPCR and 8 DEG with a raw p-value below 0.01 and absolute logarithmic FC above 1 were identified: 3 up-regulated DEG (*TNFRSF21*, *LILRA4* and *NRP1*), and 5 down-regulated DEG (*ANXA3, MMP8, LTF, TCN1* and *OLFM4*) in LTS group, compared to CLAD individuals.

Gene expression results from both platforms were highly correlated; the sense of the change and the magnitude of FC values were very similar between the two technologies (correlation value between microarrays and qPCR techniques of 0.98). The FC values for each gene and technology are detailed in *Supplementary Information section.*

3.2.2.2 microRNA EXPRESSION ANALYSES BLOCK

3.2.2.2.1 Differential microRNA Expression Analysis

One of the samples (corresponding to a CLAD patient) was discarded in quality control analyses; therefore 59 samples were used for the differential expression analysis. After removing miRNAs not belonging to *Homo Sapiens*, 6631 miRNAs were included and 2578 of which were mature miRNAs. FDR p-values were calculated, but no differences were found in miRNA expression between LTS and CLAD groups. Regarding raw p-values, miRNA expression analysis revealed 108 differentially expressed miRNAs between LTS and CLAD subjects with a raw p-value below 0.01. A complete list with the top 50 differentially expressed miRNAs is provided in *Supplementary Information section.*

A volcano plot showing differentially expressed miRNAs with a raw p-value below 0.01 and absolute logarithmic FC above 0.75 was performed (Figure 22). In LTS group, non up-regulated differentially expressed miRNA was observed, whereas the down-regulated differentially expressed miRNAs were: snoRNA U78 and the matures miRNAs hsa-miR-223-5p (MIMAT0000280_st) and hsa-miR-26b-5p (MIMAT0000083_st).

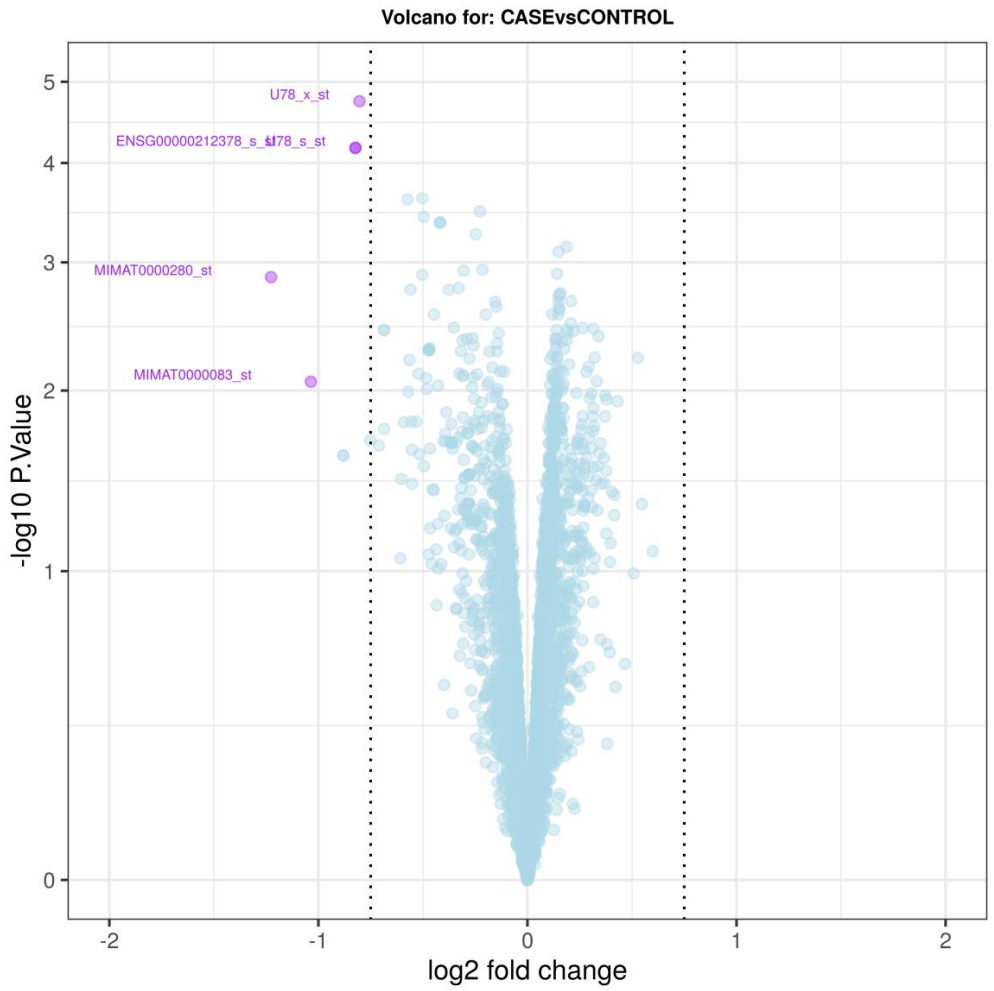

Figure 22. Volcano plot of the differentially expressed miRNAs between LTS compared with CLAD patients. Each dot of the graph corresponds to a miRNA. The fold difference in expression between LTS and CLAD patients is graphed on the x axis (logarithm of the base 2-fold changes), giving an idea of the magnitude of the change. The p-value for each miRNA is graphed on the y axis (negative logarithm to the base 10 of the t-test p-values). The vertical dashed lines correspond to logarithmic fold difference of -0.75 and 0.75. The purple dots represent down-regulated differentially expressed miRNAs whose raw p-value is below 0.01 and absolute logarithmic2 fold change is above 0.75. The blue dots denote miRNAs that do not fit that criteria of differentially expressed miRNAs.

Among the 108 differentially expressed miRNAs between LTS and CLAD patients, 36 were mature miRNAs: 15 mature miRNAs were up-regulated in LTS patients and 21 mature miRNAs were down-regulated in LTS patients. In subsequent analyses, only mature miRNAs were considered.

Two heatmaps comparing LTS and CLAD patients using the differentially expressed mature miRNAs were performed. Hierarchical clustering showed a misclassification of samples (columns). Nevertheless, supervised clustering showed a different expression profile between samples of LTS and CLAD condition (Figure 23).

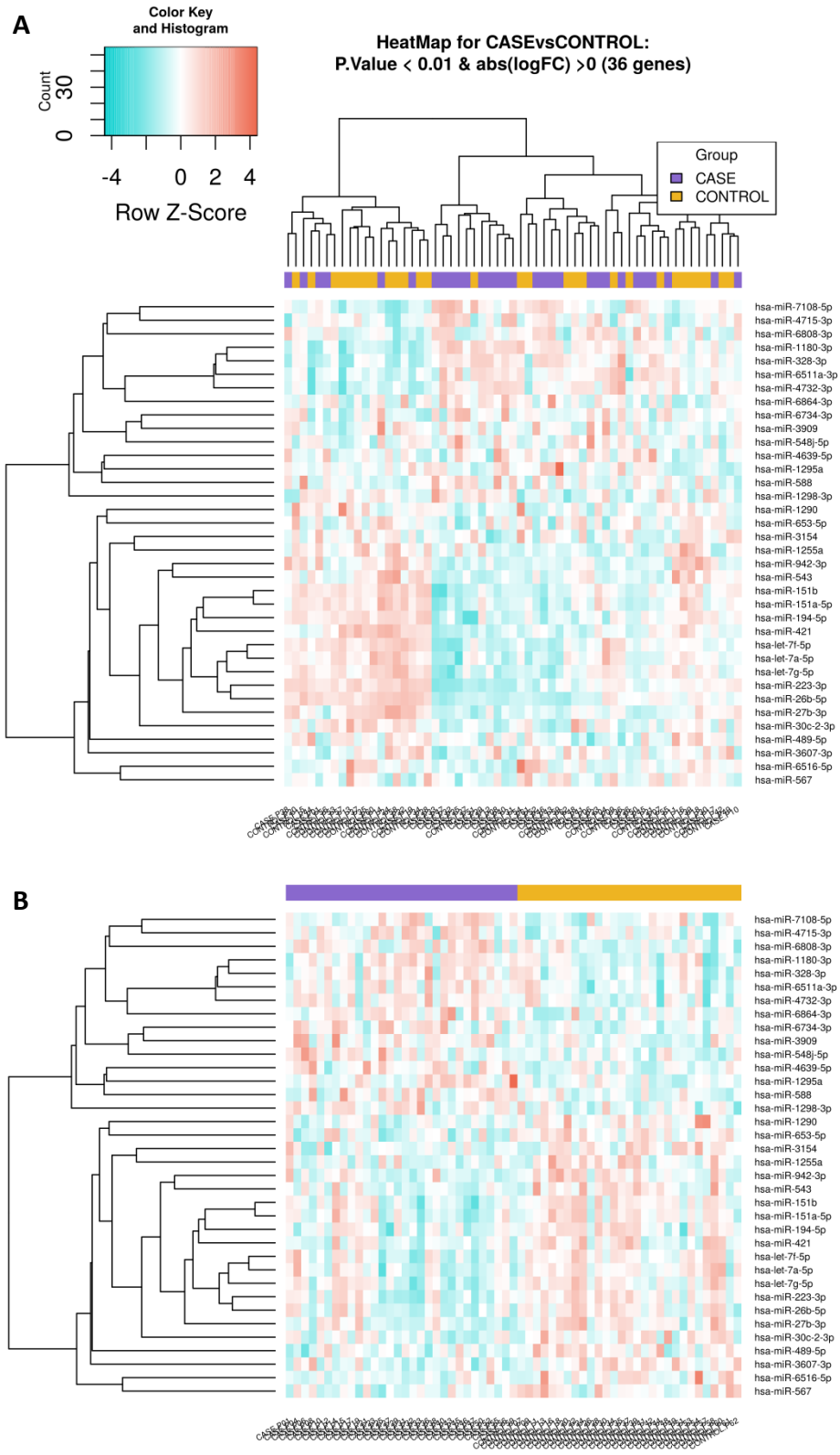

Figure 23. Clustering heatmaps of microarray data showing differential expression of miRNAs between LTS versus CLAD patients (A) Hierarchical clustering of the 2 experimental groups based on their miRNA expression profiles. Each column represents a patient, being purple LTS group and yellow CLAD group, whereas each row represents a miRNA. For each miRNA, red indicates up-regulated expression, and blue indicates down-regulated expression. (B) Supervised clustering of the 2 experimental groups based on the state of the individuals.

3.2.2.2.2 microRNA Classification Model Building

The classification capacity combining different classifier miRNA sets with different classification methods is displayed in Table 12. In this case, the best discriminatory power was provided by the combination of the Diagonal Discriminant Analysis classifier algorithm using 25 miRNAs (AUC of 0.78, misclassification value of 0.29) (Figure 24).

It has been observed that, the higher number of variables (miRNAs), the lower the error. The performance of all the models with the lower number of miRNAs is far from acceptable, since it will misclassify almost the 50% (randomness of classification) of the individuals. The 25 miRNAs included in the classifier model are detailed in Table 13.

Table 12. Performance of the 25 miRNA classification models derived from the combination of the different classifier miRNAs sets with the 5 classification algorithms to discriminate LTS and CLAD patients. The best classification model is marked in bold. SN: sensitivity, SP: specificity, AUC: area under the curve.

Number of miRNAs	Classification algorithms	Misclassification	SN	SP	AUC
8	Diagonal Discriminant Analysis	0.42	0.62	0.57	0.60
	Penalized Logistic Regression	0.44	0.60	0.54	0.59
	Random Forest	0.45	0.57	0.57	0.57
	Lasso	0.48	0.56	0.54	0.53
	Shrunken Centroids Discriminant Analysis	0.42	0.61	0.56	0.59
10	Diagonal Discriminant Analysis	0.39	0.64	0.59	0.63
	Penalized Logistic Regression	0.42	0.63	0.56	0.62
	Random Forest	0.43	0.58	0.59	0.59
	Lasso	0.44	0.59	0.57	0.59
	Shrunken Centroids Discriminant Analysis	0.40	0.63	0.59	0.63
15	Diagonal Discriminant Analysis	0.34	0.67	0.65	0.69
	Penalized Logistic Regression	0.38	0.66	0.60	0.67
	Random Forest	0.38	0.63	0.64	0.66
	Lasso	0.37	0.65	0.62	0.67
	Shrunken Centroids Discriminant Analysis	0.35	0.67	0.65	0.69
20	Diagonal Discriminant Analysis	0.32	0.69	0.69	0.75
	Penalized Logistic Regression	0.34	0.70	0.63	0.71
	Random Forest	0.34	0.66	0.68	0.71
	Lasso	0.34	0.69	0.65	0.72
	Shrunken Centroids Discriminant Analysis	0.32	0.69	0.68	0.74
25	**Diagonal Discriminant Analysis**	**0.29**	**0.70**	**0.72**	**0.78**
	Penalized Logistic Regression	0.32	0.72	0.65	0.74
	Random Forest	0.32	0.67	0.71	0.75
	Lasso	0.32	0.72	0.68	0.76
	Shrunken Centroids Discriminant Analysis	0.30	0.70	0.71	0.77

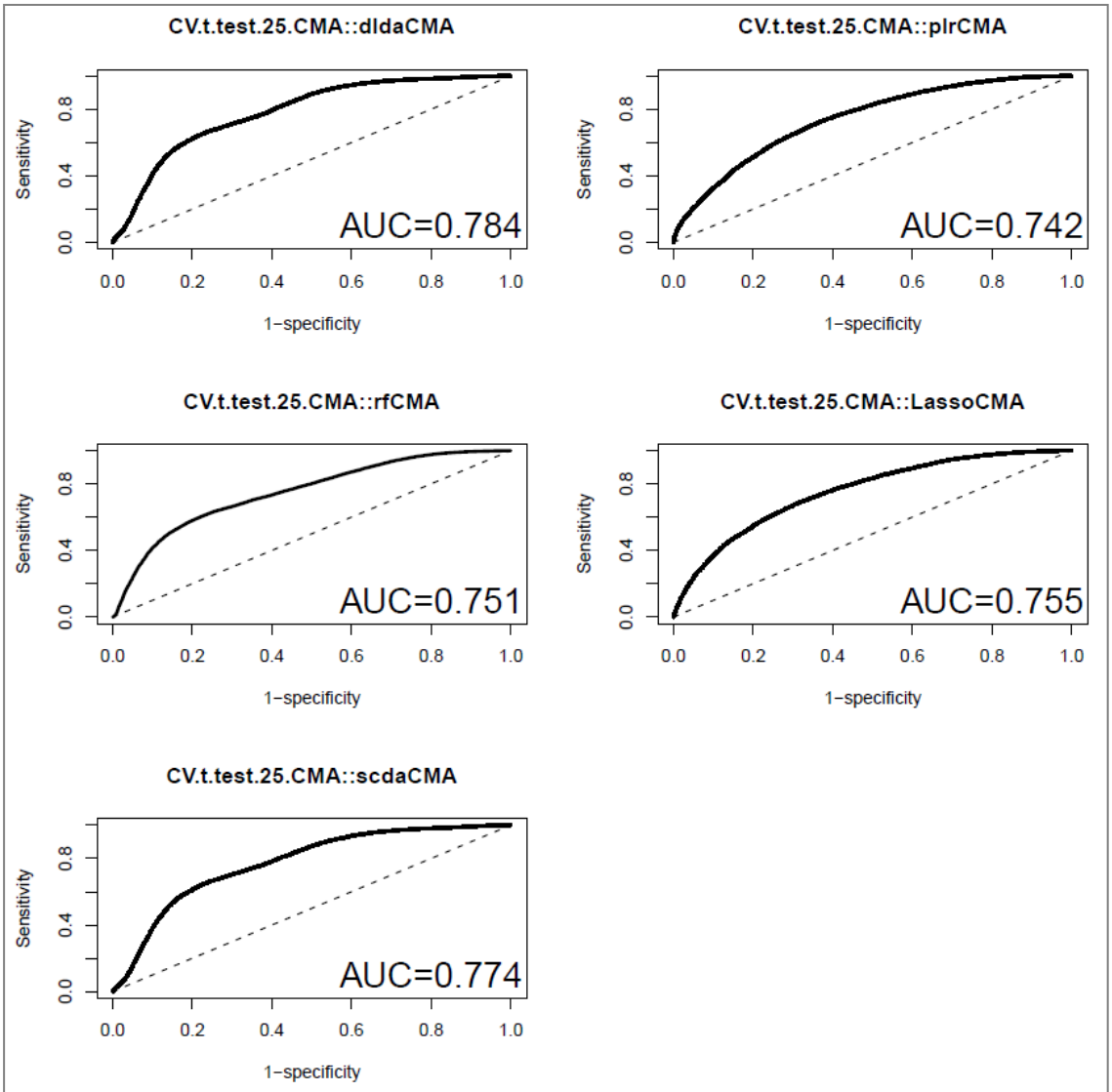

Figure 24. ROC curves showing the accuracy of the miRNA classification models derived from the combination of the 25 classifier miRNAs with the 5 classification algorithms. dlda: Diagonal Discriminant Analysis; plr: Penalized Logistic Regression; rf: Random Forest; Lasso: least absolute shrinkage and selection operator; scda: Shrunken Centroids Discriminant Analysis.

Table 13. List of the 25 mature miRNAs finally used for building the miRNA classification models. miRNAs chosen for subsequent RT-qPCR validation are identified with an *. FDR values come from the differential miRNA expression analysis which included human mature miRNAs, pre-miRNAs, snoRNAs, CDBox RNAs, H/ACA Box RNAs and scaRNAs.

	miRNA ID	Linear FC LTS vs. CLAD	Number of validated gene targets	p-value	FDR
1	*hsa-miR-223-3p	0.427	84	0.0014	0.4977
2	*hsa-miR-942-3p	0.806	51	0.0044	0.5256
3	*hsa-miR-543	0.783	96	0.0035	0.5256
4	*hsa-miR-27b-3p	0.678	384	0.0017	0.5256
5	*hsa-miR-let-7a-5p	0.833	589	0.0042	0.5256
6	*hsa-miR-1290	0.901	59	0.0024	0.5256
7	*hsa-miR-let-7g-5p	0.723	301	0.005	0.5256
8	*hsa-miR-151b	0.733	24	0.0028	0.5256
9	*hsa-miR-421	0.697	224	0.0077	0.5754
10	*hsa-miR-let-7f-5p	0.676	361	0.0061	0.5425
11	*hsa-miR-26b-5p	0.488	1864	0.0087	0.5811
12	*hsa-miR-1180-3p	1.244	60	0.0036	0.5256
13	hsa-miR-4715-3p	1.078	99	0.0092	0.5909
14	*hsa-miR-4732-3p	1.266	64	0.0041	0.5256
15	*hsa-miR-194-5p	0.716	70	0.0098	0.5930
16	hsa-miR-6864-3p	1.078	209	0.006	0.5381
17	*hsa-miR-489-5p	0.909	1	0.0039	0.5256
18	*hsa-miR-4639-5p	1.138	63	0.0036	0.5256
19	*hsa-miR-6808-3p	1.164	34	0.0037	0.5256
20	*hsa-miR-7108-5p	1.259	48	0.0086	0.5811
21	*hsa-miR-151a-5p	0.825	56	0.006	0.5381
22	hsa-miR-6511a-3p	1.226	68	0.0068	0.5754
23	hsa-miR-3607-3p	0.904	92	0.0046	0.5256
24	hsa-miR-653-5p	0.914	65	0.0074	0.5754
25	hsa-miR-567	0.904	163	0.0053	0.5256

3.2.2.2.3 Validation of Microarray microRNA Expression Data by RT-qPCR

Just like the gene validation study, RT-qPCR analyses employing TLDAs were performed on the same set of samples used for microarray experiments to confirm the expression results of a selected target mature miRNAs list.

Selected target miRNAs for RT-qPCR experiments included 19 mature miRNAs that were part of the miRNA classifier (identified with an * in Table 13) (*see Table S-2 in Supplementary Information section)*, 1 mature miRNA (hsa-miR-6734-3p) which had the lower raw p-value of the 2578 mature miRNA included in the differential miRNA expression analysis and that was not included in the miRNA classifier and 1 mature miRNA (hsa-miR-6516-5p) detected in the integrative analysis which had a relevant negative correlation with DEG (Table 14). Thus, 21 target mature miRNAs were analysed by RT-qPCR plus 2 housekeeping genes.

Table 14. List of the two mature miRNAs that did not form part of the classifiers included in the RT-qPCR analyses. FDR values come from the differential miRNA expression analysis which included human mature miRNAs, pre-miRNAs, snoRNAs, CDBox RNAs, H/ACA Box RNAs and scaRNAs.

	miRNA name	Linear FC LTS vs. CLAD	Number of validated gene targets	p-value	FDR
1	hsa-miR-6734-3p	1.115	209	0.0018	0.5256
2	hsa-miR-6516-5p	0.715	329	0.0082	0.5811

Two of the samples were discarded in the RT-qPCR quality control analysis and the sample previously discarded in the microarray miRNA expression analysis, was also not included in RT-qPCR validation experiments; therefore 57 samples (30 LTS and 27 CLAD) were used for the differential expression analysis.

The analysis of the control sample included in every TLDA showed very low inter-assay variability (CV of 0.56%).

The results showed that 13 targets were not amplified during RT-qPCR experiments, so only 8 of the 21 mature miRNAs (38.09%) were included in the differential expression analysis. Based on the raw p-value 4 mature miRNAs were differentially expressed between LTS and CLAD groups: down-regulation of hsa-miR-194-5p, hsa-miR-151b, hsa-miR-26b-5p and hsa-miR-421 were confirmed in LTS patients by RT-qPCR analysis Conversely, hsa-miR-223-3p, hsa-miR-1180-3p, hsa-miR-543 and hsa-let-7g-5p were differentially expressed when the microarray was assessed but not when RT-qPCR was performed. Hence, RT-qPCR confirmed the differential expression of 19.05% of the mature miRNAs selected by microarrays (Table 15 and Figure 25).

Table 15. List of the miRNAs amplified using RT-qPCR ranked by FDR value.

miRNA ID	Taqman Advanced miRNA Assay ID	$\Delta\Delta C_{RT}$	Linear FC	p-value	FDR
hsa-miR-194-5p	477956_mir	0.522	0.696	0.0096	0.0464
hsa-miR-151b	477811_mir	0.396	0.760	0.0103	0.0464
hsa-miR-26b-5p	478418_mir	0.522	0.696	0.0218	0.0654
hsa-miR-421	478088_mir	0.342	0.789	0.0422	0.0950
hsa-miR-223-3p	477983_mir	0.543	0.687	0.0636	0.1117
hsa-miR-1180-3p	477869_mir	-0,145	1.106	0.1095	0.1408
hsa-miR-543	478155_mir	0.441	0.737	0.1947	0.2190
hsa-let-7g-5p	478580_mir	0.146	0.904	0.4373	0.4373

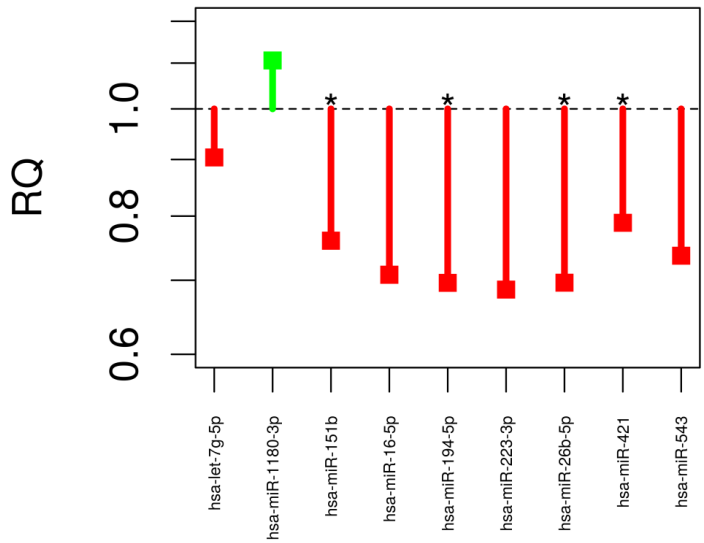

Figure 25. Relative expression of mature miRNA amplified by RT-qPCR. Fold changes (RQ) are shown relative to CLAD group. On the x axis is reported the list of the target miRNA analysed. On the y axis is reported the results of the relative quantification calculations. Relative quantities are graphed on a linear scale. Asterisks indicate differentially expressed miRNAs (raw p-value<0.05; Student's t-test).

Overall, 4 down-regulated differentially expressed miRNAs with a raw p-value below 0.05 and absolute linear FC above 0.6 were identified in LTS group: hsa-miR-151b, hsa-miR-194-5p, hsa-miR-26b-5p and hsa-miR-421.

Mature miRNA expression results from both platforms were highly correlated; the sense of the change and the magnitude of FC values were very similar between the two technologies (correlation value between microarrays and qPCR techniques of 0.95). The FC values for each miRNA and technology are detailed in *Supplementary Information section.*

3.2.2.3 INTEGRATIVE ANALYSES BLOCK

3.2.2.3.1 Correlation Analysis of DEG and Differentially Expressed microRNA Expression Values

The Clustered Image Map (Figure 26) showed intense positive and negative correlation patterns between some miRNA and some gene clusters.

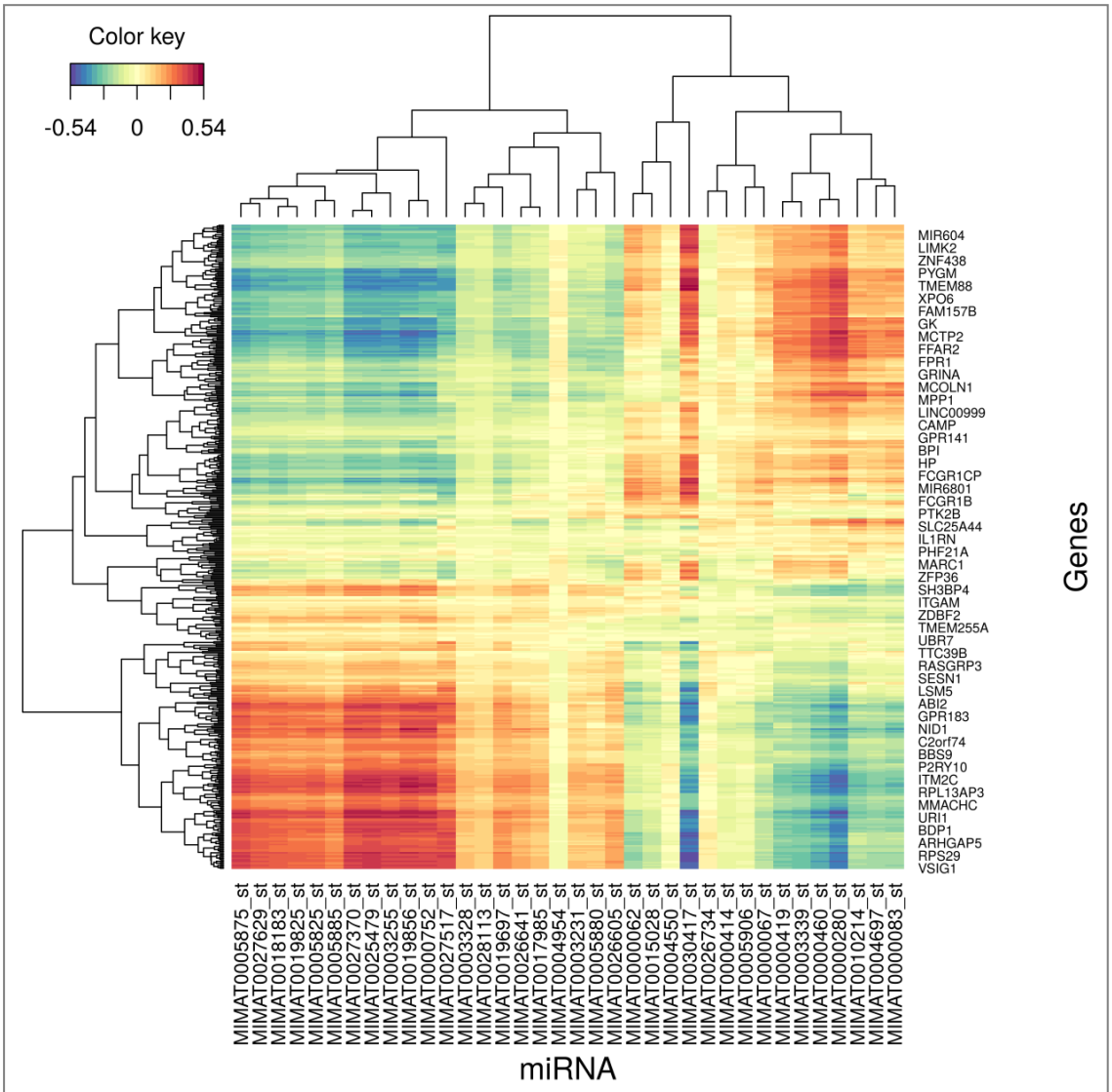

Figure 26. Clustered Image Map (Euclidean distance, Complete linkage) displaying the correlation structure between the elements. Each colored block represents an association between miRNAs and genes, spanning a range of colors from blue (negative correlation) to red (positive correlation).

A relevance network was plotted, showing those elements connected with a rCCA correlation value above 0.5, and depicting the positive or negative correlation by the color of the lines (Figure 27).

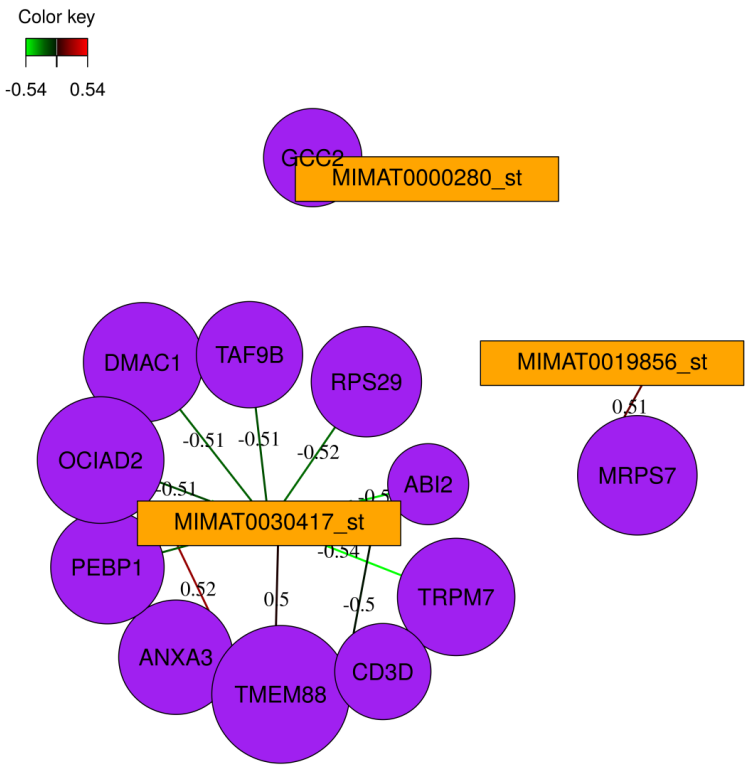

Figure 27. Relevance correlation network between miRNAs and genes with a rCCA correlation value higher than 0.5. The color of the lines indicates the direction of the association between the elements (red marks positive correlation and green marks negative correlation).MIMAT0030417_st, MIMAT0019856_st and MIMAT0000280_st are the probe IDs of hsa-miR-6516-5p, hsa-miR-4732-5p and hsa-miR-223-5p, respectively.

None of the genes included in the correlation network were validated targets for the 3 miRNAs.

3.2.2.3.2 Pathway Enrichment Analysis of the Differentially Expressed Experimentally Validated microRNA Gene Targets

The analysis was performed across the validated *multiMiR* databases for the subset of the 36 mature miRNAs differentially expressed (raw p-value below 0.01). A total of 4791 validated unique gene targets were found for the 36 miRNAs analysed, corresponding to 6929 individual interactions.

The resulting validated gene targets were intersected with the top 458 DEG derived from the gene expression analysis (*see 3.2.2.1 Gene Expression Analysis Results section*) to find the subset of validated genes targets that were differentially expressed. A total of 113 genes, among the 458 DEG, were also found in the list of 4791 validated target genes (intersecting genes); corresponding to 30 miRNAs (Figure 28).

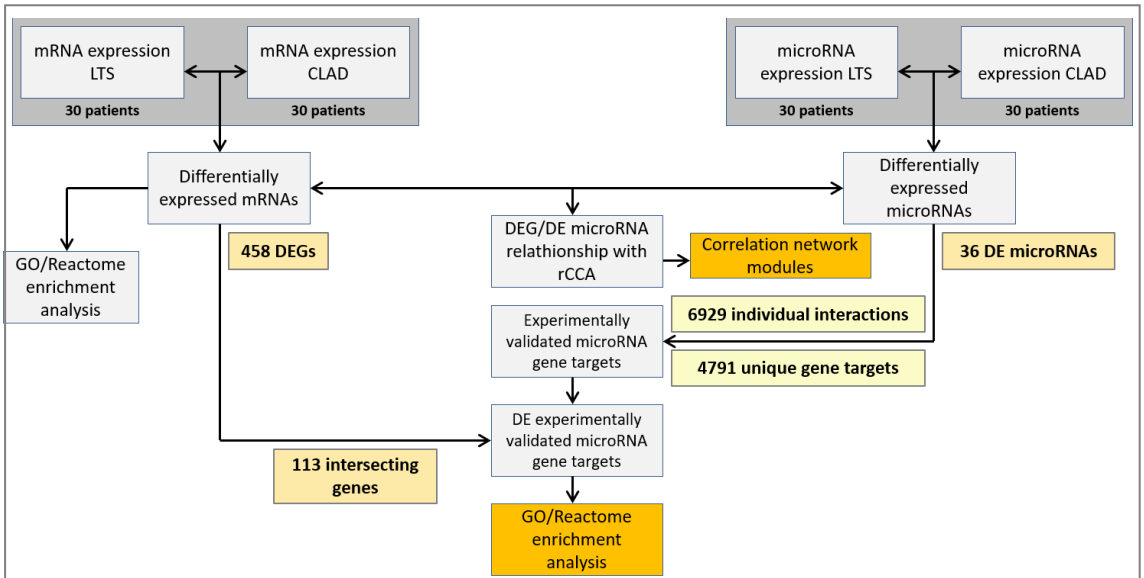

Figure 28. Algorithm for the pathway enrichment analysis of the differentially expressed experimentally validated miRNA gene targets.

The list of 113 differentially expressed validated gene targets was submitted to pathway analysis. The most significant GO biological process terms enriched in the gene list were related to neutrophil mediated processes (Table 16). Pathways significantly enriched in this gene list using Reactome database were related to CD28 costimulation and neutrophil degranulation (Table 17).

Graphically, these results were represented in dot plots of the top enriched pathways (Figure 29).

Table 16. Pathway enrichment analysis representing top 10 GO enriched biological processes among differentially expressed validated target genes between LTS and CLAD patients. Enriched terms are ranked based on the FDR value.

Term	ID	Gene ratio	p-value	FDR
T cell differentiation in thymus	GO:0033077	5/105	4.21e-05	8.42e-02
Homeostasis of number of cells	GO:0048872	7/105	5.50e-04	2.64e-01
Neutrophil degranulation	GO:0043312	10/105	6.26e-04	2.64e-01
Neutrophil activation involved in immune response	GO:0002283	10/105	6.56e-04	2.64e-01
Neutrophil activation	GO:0042119	10/105	7.67e-04	2.64e-01
Neutrophil mediated immunity	GO:0002446	10/105	7.91e-04	2.64e-01
T cell differentiation	GO:0030217	6/105	2.26e-03	3.53e-01
Regulation of erythrocyte differentiation	GO:0045646	3/105	2.42e-03	3.53e-01
Protein autophosphorylation	GO:0046777	6/105	2.81e-03	3.53e-01
Response to starvation	GO:0042594	5/105	4.13e-03	3.53e-01

Table 17. Pathway enrichment analysis representing top 10 Reactome enriched pathways among differentially expressed validated target genes between LTS and CLAD patients. Enriched terms are ranked based on the FDR value.

Term	ID	Gene ratio	p-value	FDR
Costimulation by the CD28 family	R-HSA-388841	4/73	1.37e-03	3.08e-01
CD28 co-stimulation	R-HSA-389356	3/73	1.49e-03	3.08e-01
Mitochondrial biogenesis	R-HSA-1592230	4/73	4.16e-03	4.07e-01
Interleukin-10 signalling	R-HSA-6783783	3/73	4.65e-03	4.07e-01
Neutrophil degranulation	R-HSA-6798695	9/73	5.53e-03	4.07e-01
Cellular hexose transport	R-HSA-189200	2/73	9.09e-03	4.07e-01
CTLA4 inhibitory signalling	R-HSA-389513	2/73	9.09e-03	4.07e-01
CD28 dependent PI3K/Akt signalling	R-HSA-389357	2/73	9.96e-03	4.07e-01
RNA Polymerase I Promoter Escape	R-HSA-73772	2/73	1.81e-02	4.07e-01
RNA Polymerase I Transcription Termination	R-HSA-73863	2/73	2.04e-02	4.07e-01

.

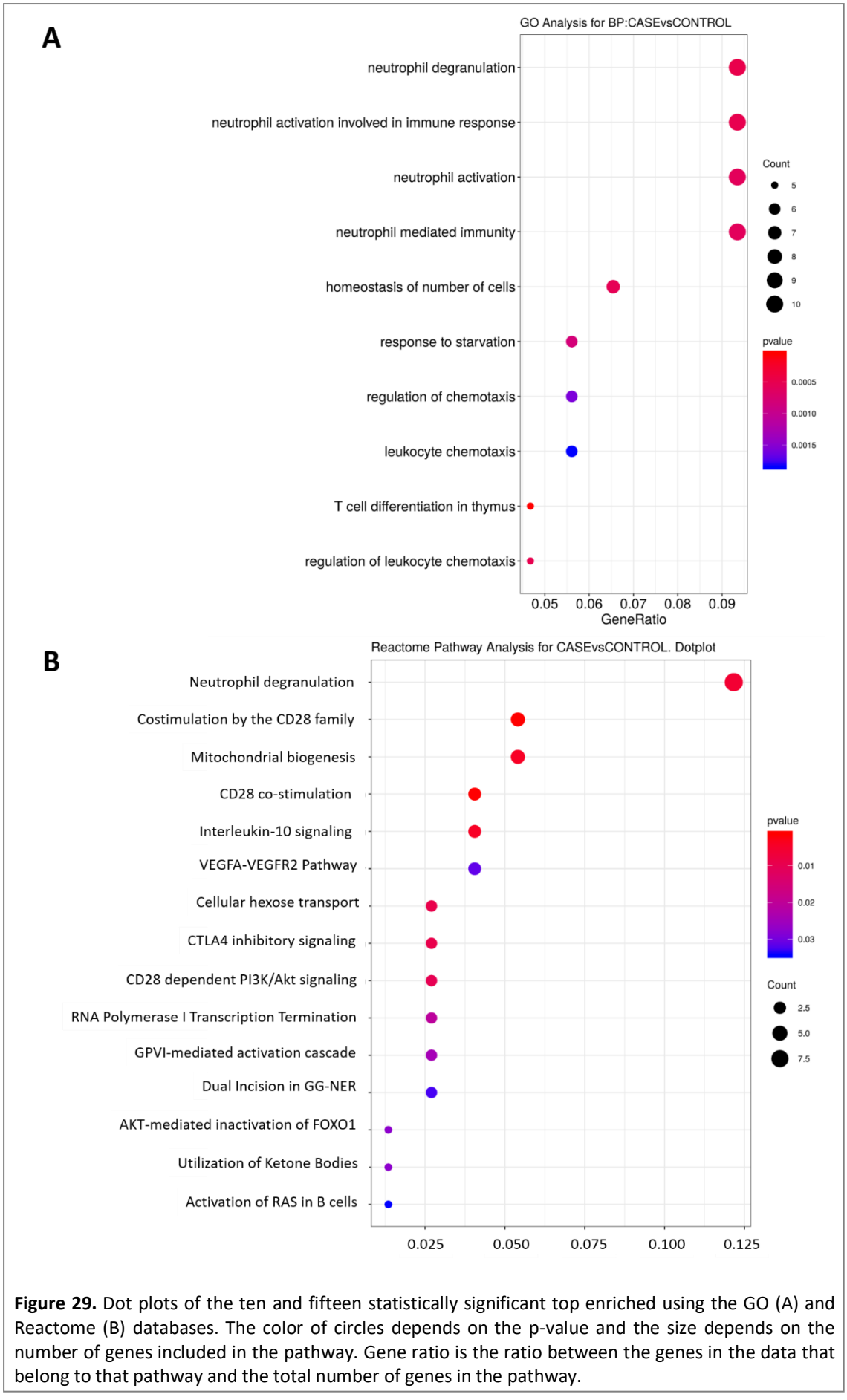

Figure 29. Dot plots of the ten and fifteen statistically significant top enriched using the GO (A) and Reactome (B) databases. The color of circles depends on the p-value and the size depends on the number of genes included in the pathway. Gene ratio is the ratio between the genes in the data that belong to that pathway and the total number of genes in the pathway.

The analysis of biological significance was also performed for hsa-miR-26b-5p, since this miRNA presented the highest number of validated differentially expressed gene targets (53 genes). The most significant GO biological process terms enriched in the hsa-miR-26b-5p differentially expressed validated gene targets are listed in Table 18.

Table 18. Pathway enrichment analysis representing top 5 GO enriched biological processes among the hsa-miR-26b-5p differentially expressed validated target genes between LTS and CLAD patients. Enriched terms are ranked based on the FDR value.

Term	ID	Gene ratio	p-value	FDR
T cell differentiation in thymus	GO:0033077	3/49	0	0.29
B cell activation involved in immune response	GO:0002312	3/49	0	0.29
Animal organ regeneration	GO:0031100	3/49	0	0.29
Dendritic cell chemotaxis	GO:0002407	2/49	0	0.29
Dendritic cell migration	GO:0036336	2/49	0	0.29

3.3 PART III. IMMUNOPHENOTYPE AND MOLECULAR CHARACTERIZATION

3.3.1 IMMUNOPHENOTYPE AND MOLECULAR MATERIAL AND METHODS

3.3.1.1 IMMUNOPHENOTYPING ANALYSES

Immunophenotyping was performed by flow cytometry on fresh peripheral blood samples, obtained by venous puncture in EDTA and heparin Vacutainer™ (BD Biosciences) tubes.

Peripheral white blood cells were stained using five different Duraclone immunophenotype panels computing 6 to 10 cell markers (Beckman Coulter, Peenya, Bangalore, India): Basic, T cell subsets, T cell receptor (TCR) subsets, regulatory T cells (Treg) and B cells, according to the manufacture's protocol. For the intracelullar Helios and Foxp3 staining (included in the Treg panel), PerFix-no centrifuge assay Kit (Beckman Coulter) was used.

The amount of fresh whole blood used for surface staining was 300 μl for the characterization of B lymphocyte subset phenotypes and 100 μl for the characterization of Basic panel and T lymphocyte subset phenotypes (T cell subsets, TCRs and Treg panels).

The identification of the different leucocyte subpopulations was based on the use of antibodies specific for different cell surface and intracellular markers labeled with different fluorochromes (Table 19).

Table 19. Summary of the DuraClone panels used, detailing the cell markers labeled with their respective fluorochromes. FITC: Fluorescein isothiocyanate; PE: R Phycoerythrin; ECD: R Phycoerythrin Texas Red-X; PC5.5: R Phycoerythrin-Cyanine 5.5; PC7: R Phycoerythrin-Cyanine 7; APC: Allophycocyanin; A700: Alexa Fluor 700; A647: Alexa Fluor 647; APC-A750: Allophycocyanin Alexa Fluor 750; PBE: Pacific Blue; KrO: Krome Orange.

	Immunophenotype panel				
Fluorochrome	**Basic**	**TCR**	**T cell**	**Treg**	**B cell**
FITC	CD16	TCR γδ	CD45RA	CD45RA	IgD
PE	CD56	TCR αβ	CD197	CD25	CD21
ECD	CD19	CD45RO	CD28	-	CD19
PC5.5	-	-	CD279	CD39	-
PC7	CD14	-	CD27	CD4	CD27
APC	CD4	CD4	CD4	-	CD24
A700	CD8	CD8	CD8	-	-
A647	-	-	-	Foxp3	-
APC-A750	CD3	CD3	CD3	CD3	CD38
PBE	CD64	-	CD57	Helios	IgM
KrO	CD45	CD45	CD45	CD45	CD45

Furthermore, a customised panel of 4 colours was designed for the characterization of granulocyte subsets. For that purpose, 100 µl of heparinized venous blood was incubated with the fluorochrome-labeled monoclonal antibodies detailed in Table 20 and Brilliant Stain Buffer (BD Horizon™) at room temperature in the dark for 30 min using a negative control without staining. Following incubation, 1.5 ml of the mix of erythrocyte lysing solution (VersaLyse, Beckman Coulter) and fixative solution (IOTest 3, Beckman Coulter) was added to the samples and incubated under the same conditions for 15 min.

Table 20. Details of the granulocyte panel indicating the cell markers labeled with their respective fluorochromes. FITC: Fluorescein isothiocyanate; PE: Phycoerythrin; APC: Allophycocyanin; BV510: Brilliant Violet 510.

	Immunophenotype panel
Fluorochrome	**Granulocyte**
FITC	CD45 (BD Pharmingen™; clone HI30)
PE	CD16b (BD Pharmingen™, clone CLB-gran11.5)
APC	CD11b (BD Biosciences, clone D 12)
BV510	CD62L (BD Horizon™, clone DREG-56)

Stained cells were acquired on LSR Fortessa flow cytometer and data were analysed with DIVA software (BD Biosciences) using specific gating strategies (*Supplementary Information section*).

To ensure data quality, leucocyte subpopulations with less than 100 events were not considered for subsequent analysis. Comparisons between the two groups were performed employing parametric unpaired t-test or nonparametric Mann-Whitney test, according to data distribution. A p-value below 0.05 was considered statistically significant. R software version 3.3.2 (Copyright© 2015 The R Foundation for Statistical Computing) was used for statistical analysis.

3.3.1.2 ANTI-HLA ANTIBODIES DETECTION

Anti-HLA antibodies were detected in serum samples using solid-phase Luminex bead assays (Immucor Medizinische Diagnostik GmbH, Rodermark, Germany), following the validated protocols used for clinical samples by the Histocompatibility Laboratory of Catalonia, Biomedical Diagnostic Center, Hospital Clinic de Barcelona. The fluorescence intensities of the samples were measured on a Luminex 100 System (Luminex Corp., Austin, TX, USA) and data were analysed with MATCH-IT software provided by the manufacturer (Immucor).

All samples were first assessed using screening Lifecodes LifeScreen Deluxe kit. Samples with a positive or doubtful result were further tested to identify antibody specificity using Lifecodes class I (LSA1) and class II (LSA2) single antigen beads (SAB) kits. Samples were run with positive and negative control samples and control beads.

The mean fluorescence intensity (MFI) was normalized by negative control beads and a standard sample provided by the manufacturer was added as a quality negative control. For SAB assays, a MFI cut-off of 3000 was considered positive, representing the clinical threshold used at the Histocompatibility Laboratory of Catalonia.

3.3.1.3 SERUM PROTEIN DETERMINATIONS

Individual sandwich enzyme-linked immunosorbent assay (ELISA) was used to measure the serum levels of MMP8 (dilution 1:10), LTF (dilution 1:100), KL-6 (dilution 1:50), IL-10 (undiluted) and IL-17A (undiluted) using commercially available kits (R&D Systems, Minneapolis, MN, USA; Novus Biologicals, Littleton, CO, USA; Sekisui Medical Co. Ltd. Tokyo, Japan and eBioscience, Inc., San Diego, CA, USA, respectively). The lower limits of detection for each protein are indicated in Table 22 and Table 24

In addition, a panel of Th17 cytokines [IL-17F, interferon-gamma (IFN-γ), IL-33, IL-4, IL-5, IL-6 and TNF-α] were measured in undiluted serum samples using a magnetic bead-base multiplex assay employing the Human Th17 Magnetic Bead Panel (Millipore Milliplex Map Kit, Billerica, MA, USA) on a MAGPIX instrument (Luminex Corp., Austin, TX, USA) according to the manufacturer's protocols. Data analyses were performed with xPONENT 4.2 Software (Luminex Corp., Austin, TX, USA). The lower limits of detection for each protein are indicated in Table 22.

Percentages of detection were determined for all the cytokines and the statistical analyses were restricted to the cytokines with a detection percentage above 60% in order to avoid a confusing interpretation of the results. For statistical analysis, non-detectable values were assigned the lower limit of detection of the corresponding assay.

All samples were measured in duplicate, and mean values were used for the subsequent analysis. For the multiplex assay, samples with a CV above 30% were not taken into account.

Categorical data (percentages of detection) were presented as absolute numbers and proportions and continuous variables (protein levels) were expressed as ng/ml or pg/ml as appropriate, and data were represented as median and interquartile range as they did not follow a normal distribution.

The Chi-square or Fisher's exact tests were used to compare the distributions of categorical variables. The concentrations for each serum protein were compared between the LTS and CLAD groups using the non-parametric Mann-Whitney U test. A p-value below 0.05 was considered statistically significant. Statistical analyses were performed using GraphPad Prism version 6.0 (GraphPad Software Inc., San Diego, CA).

3.3.2 IMMUNOPHENOTYPE AND MOLECULAR RESULTS

3.3.2.1 IMMUNOPHENOTYPING ANALYSES

LTS recipients exhibited increased proportions of $CD14^{high}$ $CD16^{-}$ monocytes, $CD56^{+}$ $CD16^{-}$ NK cells, $CD4^{-}$ $CD8^{-}$ $\alpha\beta$ T cells and $CD62L^{+}$ granulocytes, whereas $CD14^{high}CD16^{+}$ monocytes, $CD56^{+}CD16^{+}$ NK cells and $V\delta1^{+}$ $\gamma\delta$ T cells were significantly elevated in CLAD patients (Table 21 and Figure 30).

No differences were observed in the frequency of other cell subsets. Leucocyte subpopulations measured in the study that did not reach statistical significance are detailed in *Supplementary Information section (Tables from S5 to S12).*

Table 21. Leucocyte subpopulations with significant differences between LTS and CLAD groups. LTS: long term survivors, CLAD: chronic lung allograft dysfunction; NK: natural killer.

Leucocyte Subsets		Percentages (%)		p-value
		LTS	CLAD	
Monocytes	$CD14^{high}$ $CD16^{-}$	86.9	83.5	0.046
	$CD14^{high}$ $CD16^{+}$	5.8	9.3	0.009
NK Cells	$CD56^{+}$ $CD16^{-}$	15.6	6.2	0.02
	$CD56^{+}$ $CD16^{+}$	86.3	94.2	0.004
T cells	$CD4^{-}$ $CD8^{-}$ $\alpha\beta$	1.8	0.8	0.002
	$V\delta1^{+}$ $\gamma\delta$	59.9	71.9	0.027
Granulocytes	$CD62L^{+}$	99.8	98.8	0.007

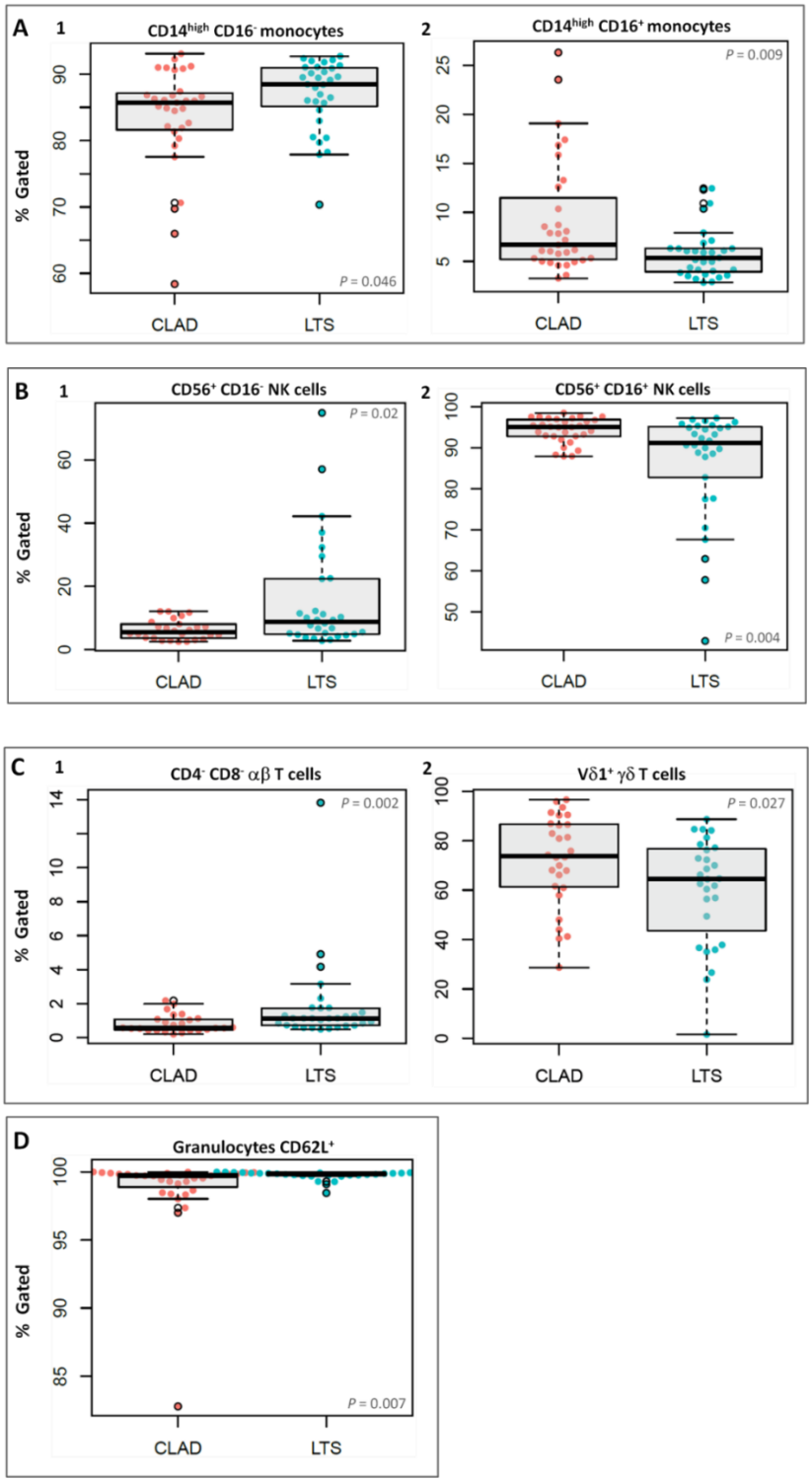

Figure 30. Quantitative differences of leucocyte subpopulations between LTS and CLAD groups. (A) Monocytes, expressed as the percent of $CD14^{high}$ $CD16^{-}$ (1) and $CD14^{high}$ $CD16^{+}$ (2) of the total monocytes. (B) Natural killer cells, expressed as the percent of $CD56^{+}$ $CD16^{-}$ (1) and $CD56^{+}$ $CD16^{+}$ (2) of the total NK cells. (C) $CD4^{-}$ $CD8^{-}$ αβ T cells (1) shown as the percent of the total αβ T cells and $V\delta1^{+}$ T cells (2) shown as the percent of the total γδ T cells. (D) Granulocytes $CD62L^{+}$ expressed as the percent of the total granulocytes. Boxes depict median and IQR; whiskers denote 1.5 x IQR. Two-sided p-values for Mann-Whitney U test comparisons between groups are shown ($P<0.05$).

3.3.2.2 ANTI-HLA ANTIBODIES DETECTION

Anti-HLA antibodies were detected in 2 out of 62 (3.23%) samples in the SAB assay against Class I (2 CLAD patients) and 9 out of 62 (14.52%) against class II (4 LTS and 5 CLAD patients). No significant differences were observed between groups for Class I and Class II. Among the 9 anti class II positive patients, the donor HLA typing only was obtained from 7 of them (2 LTS donor typing missing).

DSA anti class II were observed in 4 CLAD patients (12.90%) and in 2 LTS patients (6.5%), but difference was not statistically significant (p=0.671).

Serum non-donor-specific antibodies (NDSAs) were detectable in patients from both LTS and CLAD groups, although no significative differences were found.

3.3.2.3 SERUM PROTEIN DETERMINATIONS

Except for IL-4, IL-10 and IL-17A, the rest of the cytokines were detectable above 60%. Percentages of detection for each cytokine are shown in Table 22. Percentages of detection were significantly different for IL-6 between LTS and CLAD patients (p=0.037), being higher for CLAD.

The results in cytokine levels are shown in Table 23 and visually represented in Figure 31. No differences were found in the cytokine serum levels between the two groups. Measurement of the mentioned cytokines in serum revealed increases in IL-33 and IL-6 levels in CLAD group, although statistical significance was not reached (0.456 and p=0.078, respectively).

Table 22. Percentage of detection of serum cytokines in the studied groups. Data are presented as the total number of detected samples (% of detection). P-value in bold is below 0.05. All limits of detection were determined by the manufacturer.

Cytokines	Detection limit	Total (n=62)	LTS (n=31)	CLAD (n=31)	p-value
IL-17F	0.009 ng/ml	43 (69.35%)	19 (61.29%)	24 (77.42%)	0.1684
IFN-γ,	1.8 pg/ml	51 (82.26%)	24 (77.42%)	27 (87.10%)	0.5077
IL-33	6.3 pg/ml	39 (62.90%)	18 (58.06%)	21 (67.74%)	0.5996
IL-4	0.009 ng/ml	16 (25.81%)	8 (25.81%)	8 (25.81%)	1.0
IL-5	1.2 pg/ml	42 (67.74%)	20 (64.52)	22 (70.97%)	0.5869
IL-6	1.7 pg/ml	38 (61.29%)	15 (48.39%)	23 (74.19%)	**0.037**
TNF-α	0.9 pg/ml	60 (96.77%)	29 (93.55%)	31 (100%)	0.4918
IL-10	0.05 pg/ml	23 (37.10%)	12 (38.71%)	11 (35.48%)	0.7926
IL-17A	0.01 pg/ml	15 (24.19%)	9 (29.03%)	6 (19.35%)	0.3737

Table 23. Comparison of serum cytokine levels between LTS and CLAD patients. Data are presented as median, interquartile ranges (IQR).

Cytokines	LTS (n=31)	CLAD (n=31)	p-value
IL-17F (ng/ml)	0.02 (0.009-0.115)	0.02 (0.009-0.16)	0.4999
IFN-γ (pg/ml)	11.85 (3.65-110.3)	9.91 (5.028-42.04)	0.7259
IL-33 (pg/ml)	6.3 (6.3-281)	28.32 (6.3-140.3)	0.4561
IL-5 (pg/ml)	1.2 (0.985-3.58)	1.93 (1.2-4.785)	0.41
IL-6 (pg/ml)	1.7 (1.7-6.965)	5.1 (1.7-22.91)	0.0782
TNF-α (pg/ml)	12.47 (8.513-18.83)	14.56 (9.57-18.91)	0.4116

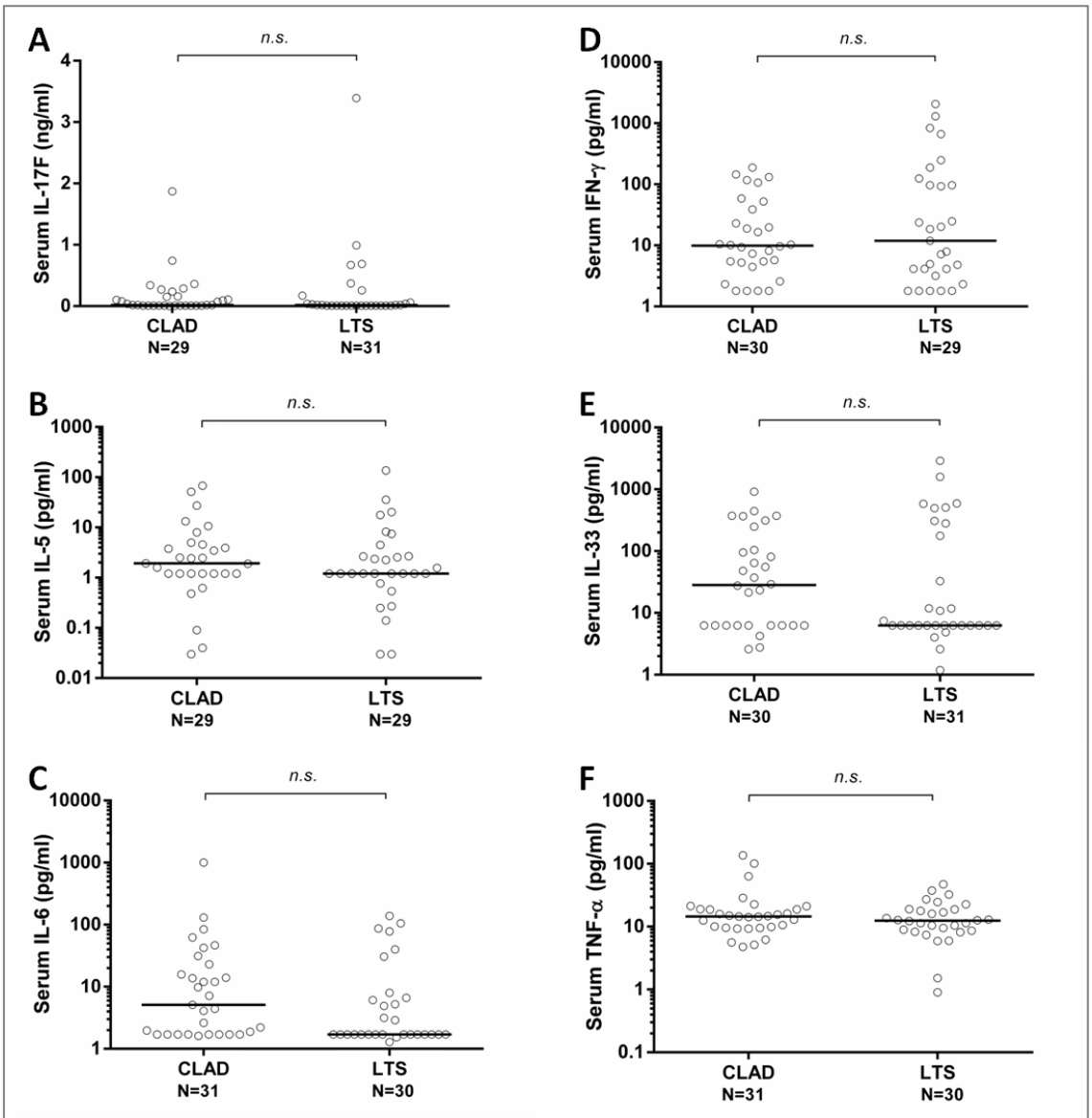

Figure 31. Comparison of IL-17F, IL-5, IL-6, IFN-γ, IL-33 and TNF-α in serum between LTS and CLAD patients. Each dot represents the result from one serum sample. No significant differences in serum cytokine levels were found between the two groups.

Serum levels of MMP8, LTF and KL-6 in the two groups are shown in Table 24 and visually represented in Figure 32. Differences were found in MMP8 and KL-6 serum levels between both groups (p=0.0054 and p=0.0042 respectively).

Table 24. Comparison of serum MMP8, LTF and KL-6 levels between LTS and CLAD patients. Data are presented as median, interquartile ranges (IQR). All limits of detection were determined by the manufacturer.

Protein	Detection limit	LTS (n=31)	CLAD (n=31)	p-value
MMP8 (ng/ml)	0.013 ng/ml	25.20 (13.69-33.99)	49.19 (24.99-81.23)	0.0054
LTF (ng/ml)	0.3 ng/ml	1596 (1227-2323)	1842 (1097-3814)	0.3115
KL-6 (U/ml)	1 U/ml	470.4 (374.7-583.8)	630.5 (482.9-744.5)	0.0042

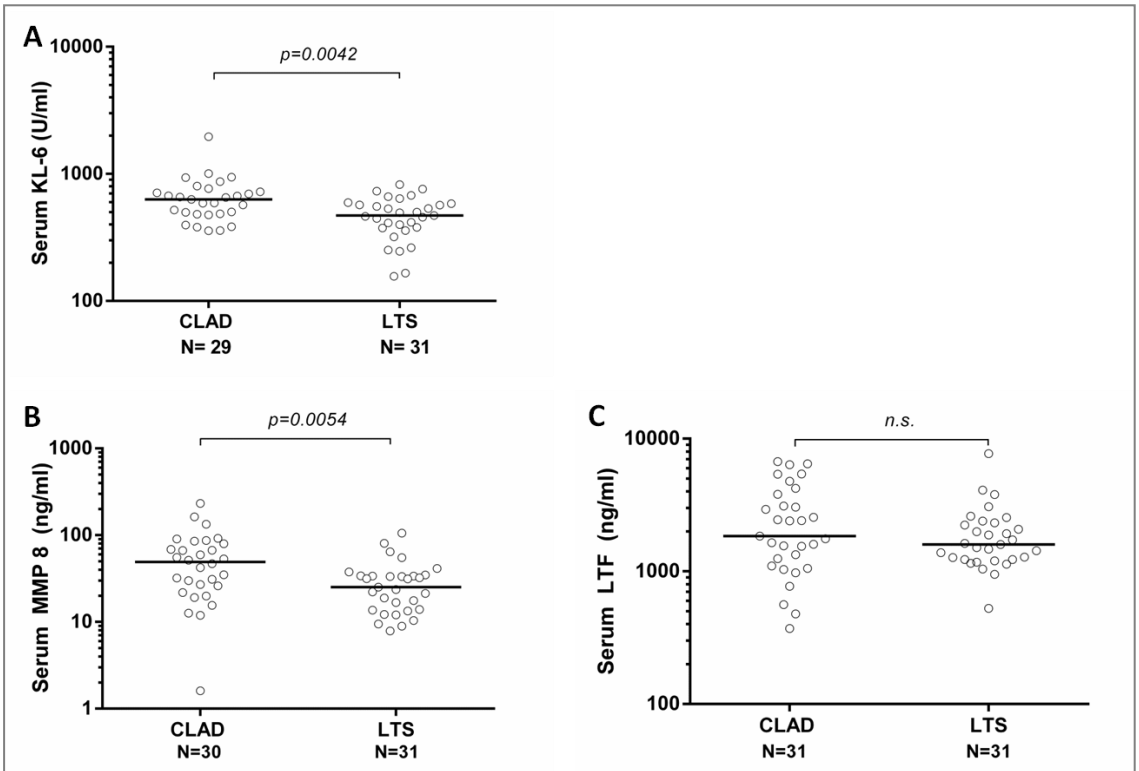

Figure 32. Comparison of serum MMP8, LTF and KL-6 levels between LTS and CLAD patients. Each dot represents the result from one serum sample. No significant differences in serum LTF levels were found between the two groups.

3.4 PART IV. MULTI-PLATFORM BIOMARKER ANALYSIS

After clinical, transcriptomic (mRNA and miRNA) and immunophenotyping data were analysed separately, the next step was to combine the four data blocks and perform a multilevel data integration analysis to assess if the classification ability to discriminate between both groups of patients improve by using a cross-platform approach.

Classic classification algorithms are not usually focused on associating biological information and consequently, any derived discriminative marker used to classify may not mechanistically link the underlying biology to the phenotype. To address this concern, this analysis was performed using a new integrative classification method, which in addition to identify discriminative features of each biological data block, explains the correlation structure between them, assuming that correlation involves similar functional relationships[222,223].

Therefore, the aim of this integrative analysis was to identify a highly correlated multi-biomarker signature discriminating LTS and CLAD patients.

3.4.1 MULTI-PLATFORM BIOMARKER MATERIAL AND METHODS

3.4.1.1 STATISTICAL AND BIOINFORMATICS METHODOLOGY

3.4.1.1.1 Construction of the Training and Validation Data Sets

Only the patients who had data from the four data blocks were included in the integrative analysis (59 patients).

The construction and performance of the multi-platform biomarker classifier was assessed by the holdout method: the dataset was randomly partitioned into two independent groups ("train" and "test" sets). The training set (67% of total samples, 39 patients) was used to train the model, whereas the test set (33% of total samples, 20 patients) was used to evaluate the accuracy of the classifier[224].

3.4.1.1.2 Variable Selection

The most relevant variables selected from each biological block are detailed as following:

- Two clinical variables: immunological events rate and infection rate.
- Twenty-one genes validated by RT-qPCR; 20 of them with a FDR below 0.05 (*ANXA3, FCGR1B, TNFRSF21, NRP1, LILRA4, SLC22A4, HCK, KCNJ15, PNPLA2, CA4, ACSL1, MMP8, FCGR2A, DHRS13, LRRC6, BCL6, PROK2, OLFM4, LTF, TCN1*) and one with a FDR below 0.08 (*TLR5*).
- Four mature miRNAs validated by RT-qPCR with a raw p-value below 0.05 (hsa-miR-194-5p, hsa-miR-151b, hsa-miR-26b-5p and hsa-miR-421).
- Eight leucocyte subpopulations; 7 of them with a raw p-value below 0.05 ($CD14^{high}$ $CD16^{+/-}$ monocytes, $CD56^{+}$ $CD16^{+/-}$ NK cells, , $CD4^{-}$ $CD8^{-}$ $\alpha\beta$ T cells, $V\delta1^{+}$ $\gamma\delta$ T cells , $CD62L^{+}$ granulocytes) and another relevant subpopulation (NK T cells) was also included although statistical significance was not reached (raw p-value= 0.053).

3.4.1.1.3 Data Integration

The integration analyses were performed using the multivariate dimension reduction discriminant analysis method, DIABLO[225] (Data Integration Analysis for Biomarker discovery using a Latent component method for Omics studies) implemented in *mixOmics* R package[221].

DIABLO is a supervised method that uses sparse Generalized Canonical Correlation Analysis (sGCCA), which extends the Partial Least Squares (PLS) regression method for multiple data sets integration. The aim of DIABLO is to identify correlated or co-expressed variables measured on the same samples on different datasets which explain the classification of LT patients[225]. All the statistical analyses were performed using R software version 3.4.4 (Copyright© 2018 The R Foundation for Statistical Computing) and the *mixOmics* R package[221].

To improve the interpretation of the data integration results, a Circos plot and a Clustered Image Map were plotted:

1- The Circos plot[3] represents the connections between variables of different biological blocks, indicating positive or negative correlations. Only the correlations above 0.75 in the multi-platform biomarker signature were plotted.

2- The Clustered Image Map represents the multi-platform biomarker signature expression for each sample, and it is very similar to a classic hierarchical clustering. The value of each variable scaled between +2 and -2 is shown in the center of the graph and, both in the upper (columns) and left (rows) parts, a hierarchical cluster has been made.

The classification performance of the multi-biomarker model was assessed using the test set.

[3] The Circos plot is built based on a similarity matrix, extended to the case of multiple data sets[310].

3.4.2 MULTI-PARAMETER BIOMARKER RESULTS

3.4.2.1 CORRELATION ANALYSIS

Most relationships within and between biological blocks were positive correlations. Nevertheless, correlations between the infection rate, NKT cells, *LILRA4* and *TNFRSF21* genes were negative (Figure 33).

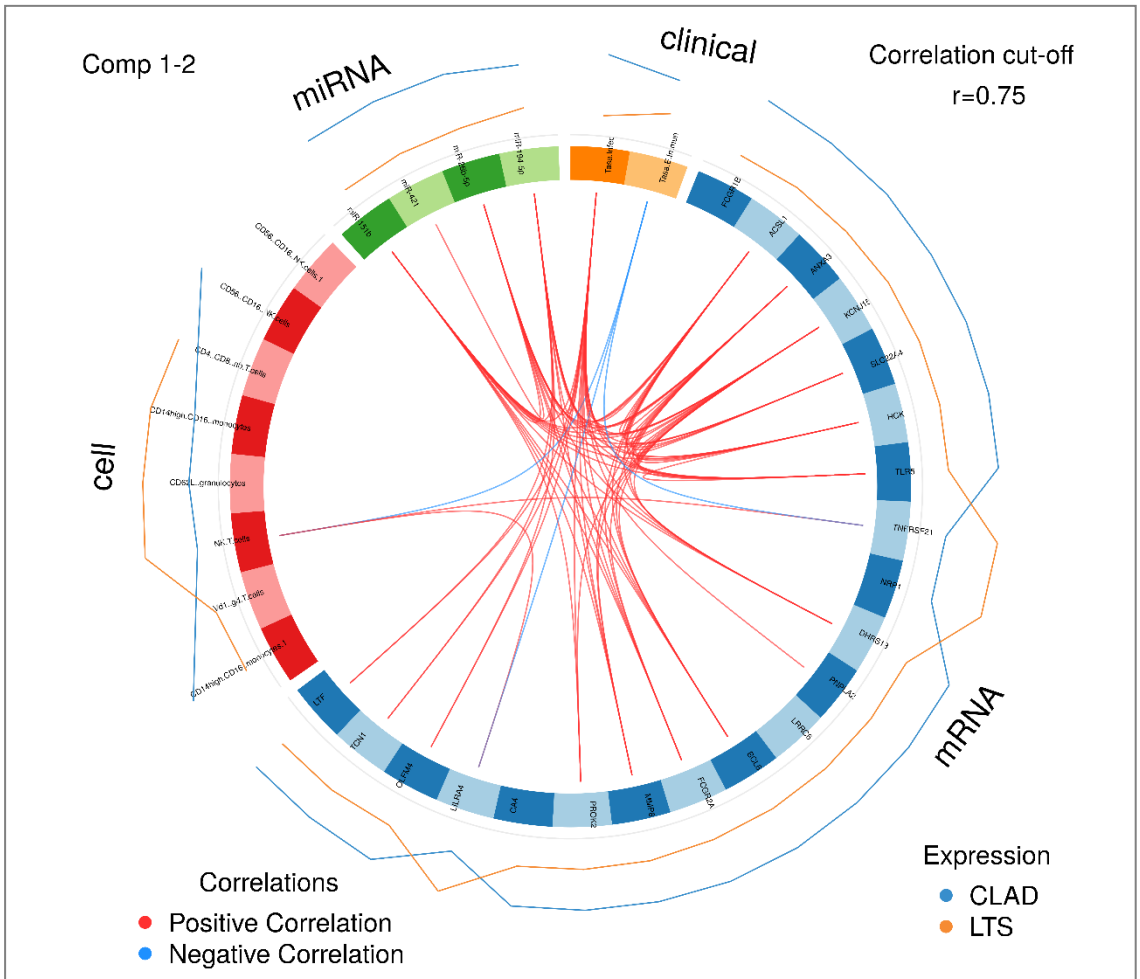

Figure 33. Circos plot depicting the correlation (r>0.75) between selected features (genes, miRNAs, cell populations and clinical variables) pairs as indicated by the red (positive correlation) and blue (negative correlation) links, feature names appear in the quadrants. External lines (blue, LTS; orange, CLAD) reflect expression levels of each feature within each biological level.

The Clustered Image Map displayed a good clustering for samples (rows), except for 2 patients of CLAD group and 3 patients of LTS group, which were classified within the other group (Figure 34).

The grouping of the variables used, according to their expression among the different patients, was observed in the columns of the Clustered Image Map.

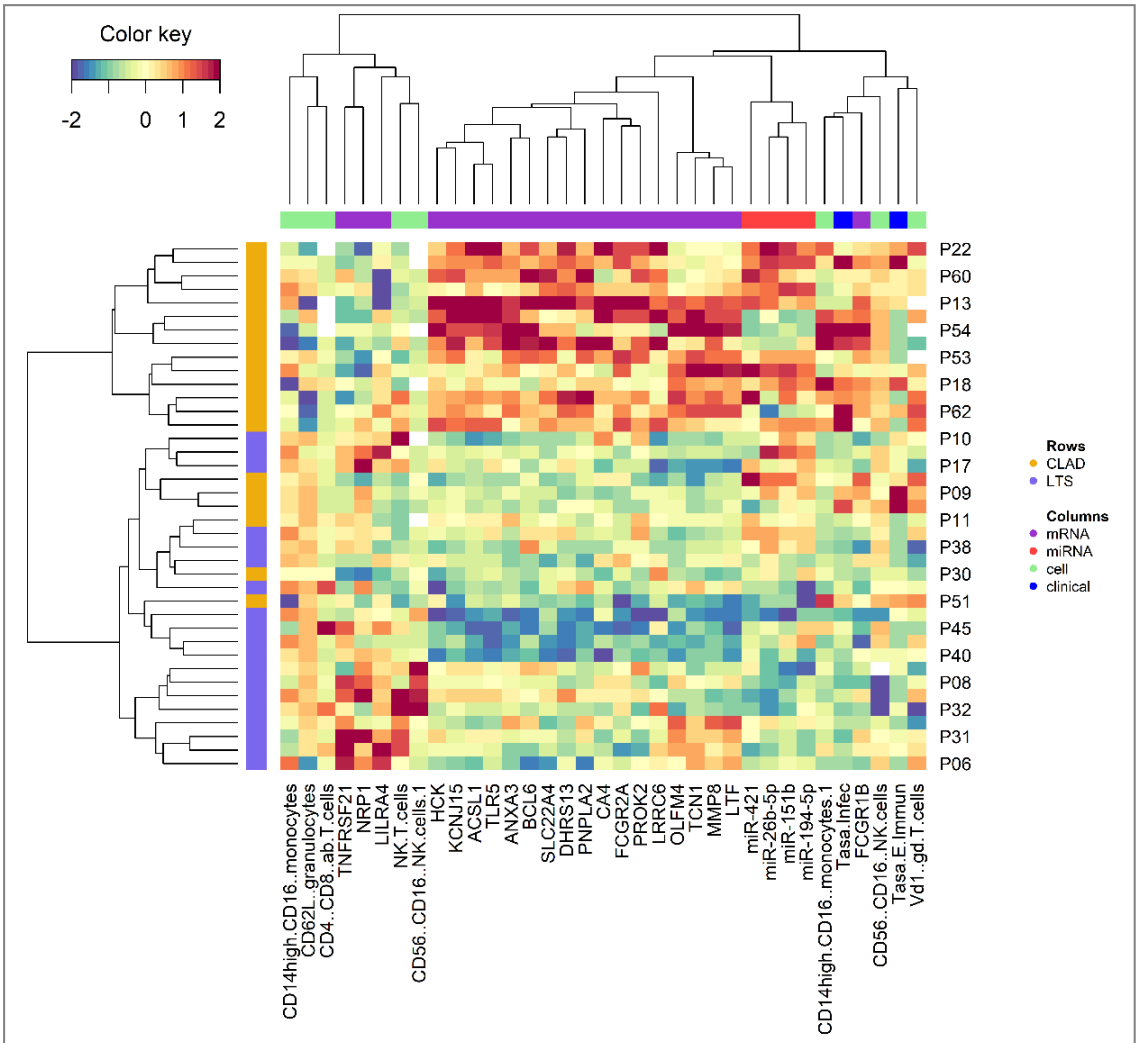

Figure 34. Clustered Image Map (Euclidean distance, Complete linkage) representing the "high dimensional" multi-platform biomarker signature expression for each sample. Samples are represented in rows and selected features (genes, miRNAs, cell populations and clinical variables) in columns. For each variable, red indicates up-regulation and blue indicates down-regulation.

3.4.2.2 PERFORMANCE ASSESSMENT

To assess the classification performance of the multi-platform biomarker model, the test set (20 samples; 11 LTS and 9 CLAD patients) was used.

The confusion table compares the real patient status (LTS, CLAD) with the predicted status. Nine of 11 LTS patients were correctly identified as LTS, and 7 of 9 CLAD participants were correctly identified as CLAD, yielding a positive predictive value (PPV) and negative predictive value (NVP) of 82% and 78%, respectively (Table 25).

Table 25. Confusion matrix and classification summary using the 35-biomarker prediction model with the samples from the test set (n=20). (PPV, 82%, NPV, 78%).

	Predicted as LTS	Predicted as CLAD	Not predicted
Actual LTS	9	0	2
Actual CLAD	1	7	1

Additionally, a ROC graph per biological block was plotted. The AUC of the multi-biomarker classifier using a holdout validation method was 0.859. The performance (AUC based) of the combined model was similar to performances of individual biological blocks, despite little improvements for miRNA and cells (Figure 35).

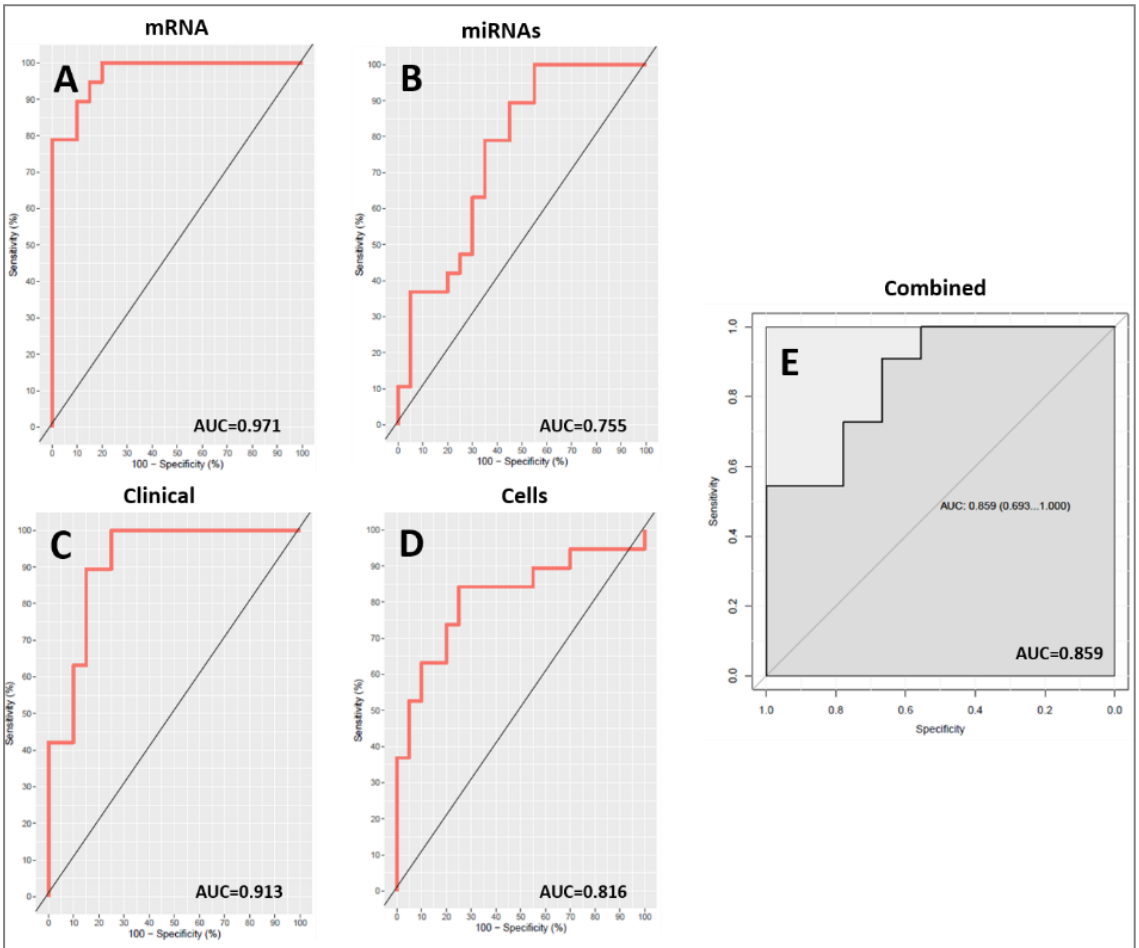

Figure 35. ROC curves corresponding to each biological block (A, mRNA; B, miRNAs; C, clinical variables; D, cell populations) and combined model (E).

3.5 PART V. UPPER RESPIRATORY TRACT BACTERIAL MICROBIOME COMPOSITION

3.5.1 MICROBIOME MATERIAL AND METHODS

3.5.1.1 DNA EXTRACTION, PCR AMPLIFICATION AND SEQUENCING

The microbiome of nasopharyngeal swabs from 26 LTS patients, 25 CLAD patients and 10 healthy (non-transplanted) control subjects (HC) was analysed. DNA was extracted from the nasopharyngeal swab from each individual using a modified "Godon" protocol [226,227]. Briefly, nasopharyngeal swabs were eluted in 250 μl of guanidine thiocyanate (Sigma-Aldrich, St. Louis, MO, USA), 0.1 M Tris (pH 7.5), 40 μl of 10% N-lauroyl sarcosine (Sigma-Aldrich), and 500 μl of 5% N-lauroyl sarcosine.

Microbial cells were mechanically disrupted using zirconia silica beads and RNA was removed by the addition of 4 μl of a 100-mg/ml solution of RNAase A (Qiagen). DNA was purified and recovered by ethanol precipitation and resuspended in 30 μl of a Tris-EDTA buffer solution (Tris 10mM, 1mM EDTA, pH 7) (Invitrogen, Lithuania) and stored at -20°C for further analyses.

To create the amplicon library, the hyper-variable region (V4) of the bacterial and archaeal 16S ribosomal RNA (rRNA) gene was amplified by standard PCR, using 20 pmol/μL of the forward (V4F_515_19) and reverse (V4R_806_20) primers (Table 26) targeting the 16S gene, and 0.75 units of Taq polymerase (Roche). Specific reverse primers contained a unique Golay barcode (a sequence of 12 bases, indicated in bold in Table 26) different for each sample in order to tag specifically each one of the samples[228]. Besides, the 5' ends of both forward and reverse primers were tagged with specific sequences

Table 26. Specific sequences of primers targeting the bacterial V4 16S rRNA gene.

Primers	Specific sequences
Forward	5'-{AATGATACGGCGACCACCGAGATCTACACTATGGTAATTGT}{GTGCCAGCMGCCGCGGTAA}-3'
Reverse	5'-{CAAGCAGAAGACGGCATACGAGAT}**{Golay Barcode}**{GGACTACHVGGGTWTCTAAT}-3'

Three negative and one positive PCR controls were included in the run. PCR was conducted in a TGradient thermocycler (Biometra) at 94°C for 3 min, followed by 35 cycles of 94°C for 45 sec, 56°C for 60 sec, 72°C for 90 sec, and a final cycle of 72°C for 10 min.

Amplicons were purified using the QIAquick® PCR Purification Kit (Qiagen) according to manufacturer's instructions in order to remove primers, nucleotides, enzymes and other impurities and were quantified using a NanoDrop ND-1000 Spectrophotometer (Nucliber). DNA integrity was evaluated by microcapillary gel electrophoresis using an Agilent 2100 Bioanalyzer (Agilent Technologies) with the DNA 12000 kit, and then all samples were pooled in equal concentrations. The pooled amplicons were sequenced using Illumina MiSeq technology at the technical support unit of *Universitat Autònoma de Barcelona* (UAB, Spain) following standard Illumina platform protocols.

3.5.1.2 STATISTICAL AND BIOINFORMATICS METHODOLOGY

3.5.1.2.1 Pre-processing of 16S rRNA Sequence Reads

Raw sequence reads were demultiplexed using the idemp tool[229] with its default parameters. Then, the reads were processed by following the pipeline for the DADA2 R package (version 1.10.1)[230] to obtain counts of amplicon sequence variants (ASVs). Sequence taxonomy was assigned using the DADA2-formatted database of sequences derived from the SILVA database version 132[231]. The resulting ASV counts were stored along with metadata for samples and analysed using the Phyloseq R package (version 1.26.1)[232]. A phylogenetic tree of the organisms present in the dataset was approximated following a workflow[233] which relies on the DECIPHER (version 2.10.2)[234] and phangorn (version 2.5.5)[235] R packages. Only samples with at least 1000 total counts after processing with DADA2 were retained.

ASV counts were normalized per sample using two methods which were analysed in parallel: relative abundance of each taxon within a sample, and centered log ratio values. For the latter, zero counts were first transformed using the "count zero multiplicative" method in the cmultRepl function from the zCompositions R package (version 1.3.2-1)[236], and then the centered log ratios were calculated using the codaSeq.clr function from the CoDaSeq R package (version 0.99.3)[237,238].

3.5.1.2.2 Diversity Measures

The estimate richness function from the Phyloseq package was used to calculate alpha diversity measures, including the Shannon and Simpson indices, which determine the biological diversity of organisms present within a given sample.

For beta diversity, which measures the difference between a given pair of samples based on the values of all taxa in the dataset, a few different approaches were used to obtain distance matrices. The UniFrac function from Phyloseq was used to obtained both weighted and unweighted UniFrac distances, which give weights based on phylogenetic distances between taxa (the weighted distance also gives weights based on relative abundances of taxa, and thus differences between samples are more affected by higher abundance taxa as opposed to rare taxa). In addition, the Aitchison distance was calculated using the aDist function from the robComposition R package (version 2.1.0)[239]. The Aitchison distance is based on the centered log ratio values, and thus is robust to changes in variation of abundances between samples, regardless of the relative number of counts from a given taxon.

3.5.1.2.3 Statistical Analyses

The global effects of metadata variables on the microbiome composition of samples were tested using the adonis function from the vegan R package (version 2.5-5)[240], which runs a permutation multivariate ANOVA by fitting linear models to distance matrices. Each variable was tested using each of the distance matrices calculated in order to test the association of the variable with the differing effects of each beta diversity calculation. The linear model for each variable also included three covariates, which were SampleStatus (LTS, CLAD or HC), as this

was the most relevant and seemingly influential variable, as well as age and gender to account for systematic variation from these factors.

The associations between variables and particular taxa were tested using the lm function from the base R package stats (version 3.5.0)[241]. The function fits a linear model, again using the same covariates as fixed effects in the model. Figures were generated using the ggplot2 R package (version 3.2.1)[242].

3.5.2 MICROBIOME RESULTS

In this study, specimens collected from 26 LTS and 25 CLAD patients were considered. However, 45 samples (23 LTS and 22 CLAD) were finally included in the analysis because 6 of them did not reach the reads cut off. The characteristics of these subjects are summarized in Table 27.

Table 27. Clinical characteristics of LTS and CLAD subjects included in microbiome analysis. For age variable comparison, a Kruskal-Wallis test was performed (data presented as medians with interquartile ranges (IQR)), whereas Chi-square or Fisher's exact tests were used for comparing categorical variables (data presented as frequencies with percentages). HC: Healthy Controls; NA: not applicable.

	LTS (n=23)	CLAD (n=22)	HC (n=10)	p-value
Age, *median (IQR)*	42 (36.0; 61.0)	52.5 (36.0; 58.25)	56.0 (40.0; 60.0)	0.873
Gender (males), *n (%)*	10 (43.48)	12 (54.55)	7 (70.0)	0.365
Underlying disease, *n (%)*				
ILD	3 (13.04)	2 (9.09)	NA	>0.999
COPD	4 (17.39)	8 (36.36)	NA	0.189
CF	11 (47.83)	9 (40.91)	NA	0.641
Non-CF bronchiectasis	1 (4.35)	2 (9.09)	NA	0.608
Pulmonary arterial hypertension	1 (4.35)	0 (0.0)	NA	>0.999
Langerhans cell histiocytosis	1 (4.35)	0 (0.0)	NA	>0.999
LAM	2 (8.69)	1 (4.55)	NA	>0.999
Anti-microbial treatment				
Cotrimoxazole, n (%)	14 (60.87)	20 (90.91)	NA	**0.035**
Azithromycin, n (%)	15 (65.22)	22 (100.0)	NA	**0.002**
Inhaled amphotericin B, n (%)	11 (47.83)	19 (86.36)	NA	**0.011**
Immunosuppressive therapy				
Calcineurin inhibitors, n (%)	23 (100.0)	22 (100.0)	NA	1.0
Antimetabolites, n (%)	19 (82.61)	3 (13.64)	NA	**<0.0001**
mTOR inhibitors, n (%)	1 (4.35)	19 (86.36)	NA	**<0.0001**
Corticosteroids, n (%)	20 (86.96)	21 (95.45)	NA	0.608

In the Figure 36 the distributions of abundances of the most common phyla (A) and genera (B) among the samples of each group (LTS, CLAD and HC) were illustrated. LTS patients followed essentially the same trends as the healthy control group, being the Actinobacteria phylum and *Corynebacterium* genus more dominant in the upper respiratory tract of these patients. Conversely, the phylum Firmicutes and genus *Staphylococcus* were enriched in CLAD group.

Many of the top 10 genera were members of the Firmicutes phylum, including: *Staphylococcus, Streptococcus, Anaerococcus, Dolosigranulum, Peptoniphilus and Finegoldia*.

Corynebacterium and *Lawsonella* were the only genera in the top 10 from the phylum Actinobacteria.

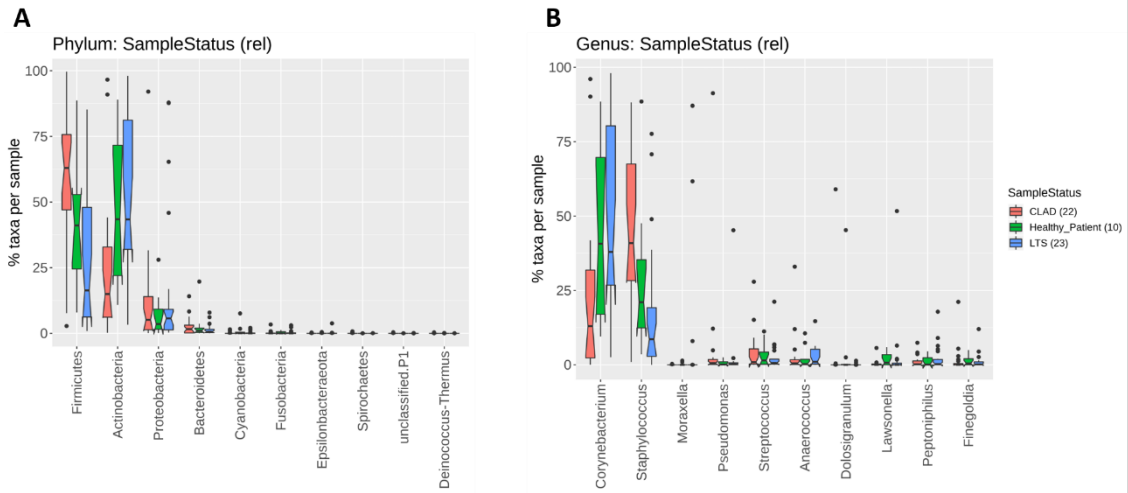

Figure 36. Relative abundance of the 10 most abundant upper respiratory tract phyla (A) and genera (B).

Both LT groups, LTS and CLAD, did not present significant differences concerning alpha diversity (data not shown). However, the upper respiratory tract microbiota showed a significant difference in the overall bacterial composition between both groups. For the two indices computed for beta diversity (Weighted Unifrac and Aitchison method), LTS and CLAD groups were separated. It may not appear to be an obvious separation in the Aitchison Principal Coordinate Analysis (PCoA) plot, but the Adonis function accounts for differences in the variation of all the taxa in each sample. The highest difference was observed for the Aitchison method (Adonis test for weighted index: p-value=0.002 and Adonis test for Aitchison index: p-value=0.001). (Figure 37). Both indices were performed as they gave complementary information: Weighted Unifrac, based on changes in relative abundances of organisms was easier to interpret while Aitchison approach offered a better indication of true variation in abundance between organisms.

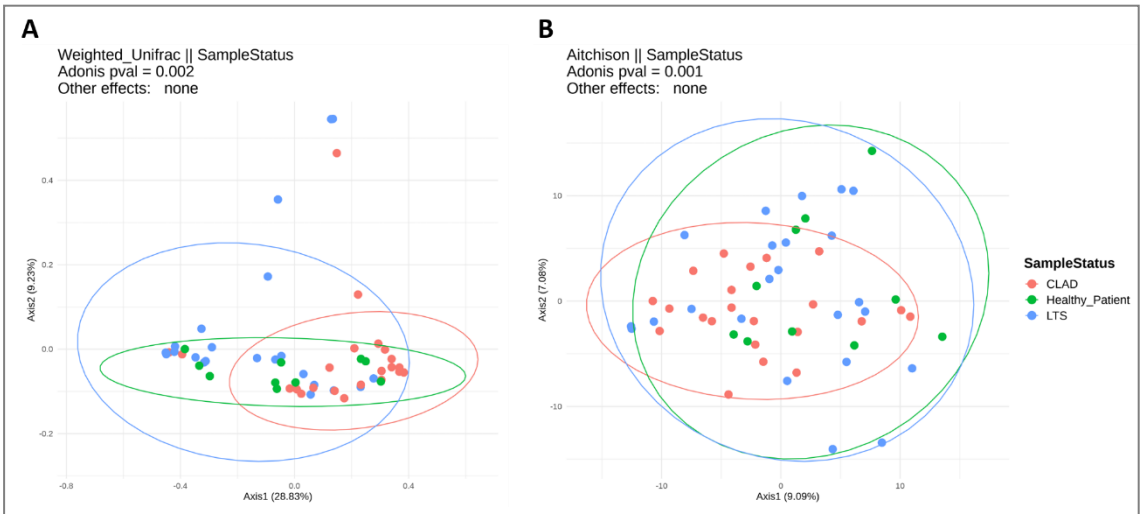

Figure 37. Bacterial diversity clustering by Weighted UniFrac PCoA (A) and Aitchison PCoA (B) of upper respiratory tract microbiota. Each dot represents a sample (red, CLAD; green, healthy patients; blue, LTS), the variance explained by the Principal Coordinates is indicated in parentheses on the axes.

LTS patients showed a statistically significant increase in the Actinobacteria phylum (p-value= 0.009) (Figure 38A), and a decrease in the Firmicutes phylum (p-value=0.019) (Figure 38B) compared to CLAD patients. LTS and HC groups did not present statistical differences.

Regarding genus, LTS and healthy control samples had greater abundance of the genus *Corynebacterium* (p-values of 0.002 and 0.002, respectively) (Figure 38C). Conversely, *Staphylococcus* genus were reduced in LTS group, both with regard to CLAD and healthy control (p-values of 0.031 and 0.016, respectively) (Figure 38D).

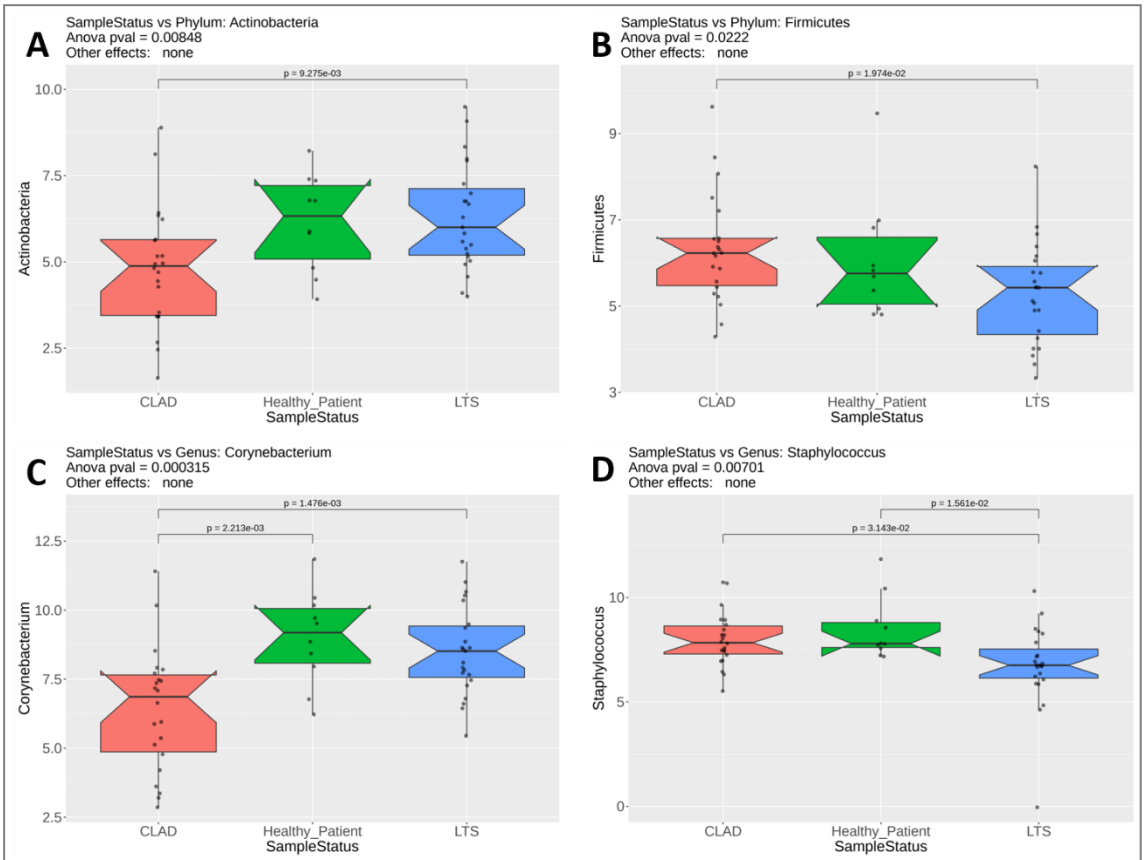

Figure 38. Abundance comparison of Actinobacteria and Firmicutes phyla and Corynebacterium and Staphylococcus genera between LTS, CLAD and healthy control groups.

Moreover, higher abundances of Spirochaetes phylum and *Lactobacillus* genera in CLAD patients and *Acidocella* genera in LTS patients with respect to healthy controls were observed (p-values of 0.030, 0.015 and 0.019, respectively).

As significant differences were observed between groups with respect to treatments (Table 27), in order to verify that all the microbiome findings were not affected by treatment, microbiome composition was analised regarding individuals receiving different treatments.

Microbiome composition was clustered by LT status (LTS, CLAD) regardless of amphotericin (A), azythromycin (B), cotrimoxazole (C) and corticosteroids (D) treatment, based on the Weighted Unifrac distance (Figure 39). The effect of antimetabolites or mTOR inhibitors intake could not be determined, as most of LTS patients were taking antimetabolites while most of CLAD patients were under mTOR inhibitor treatment.

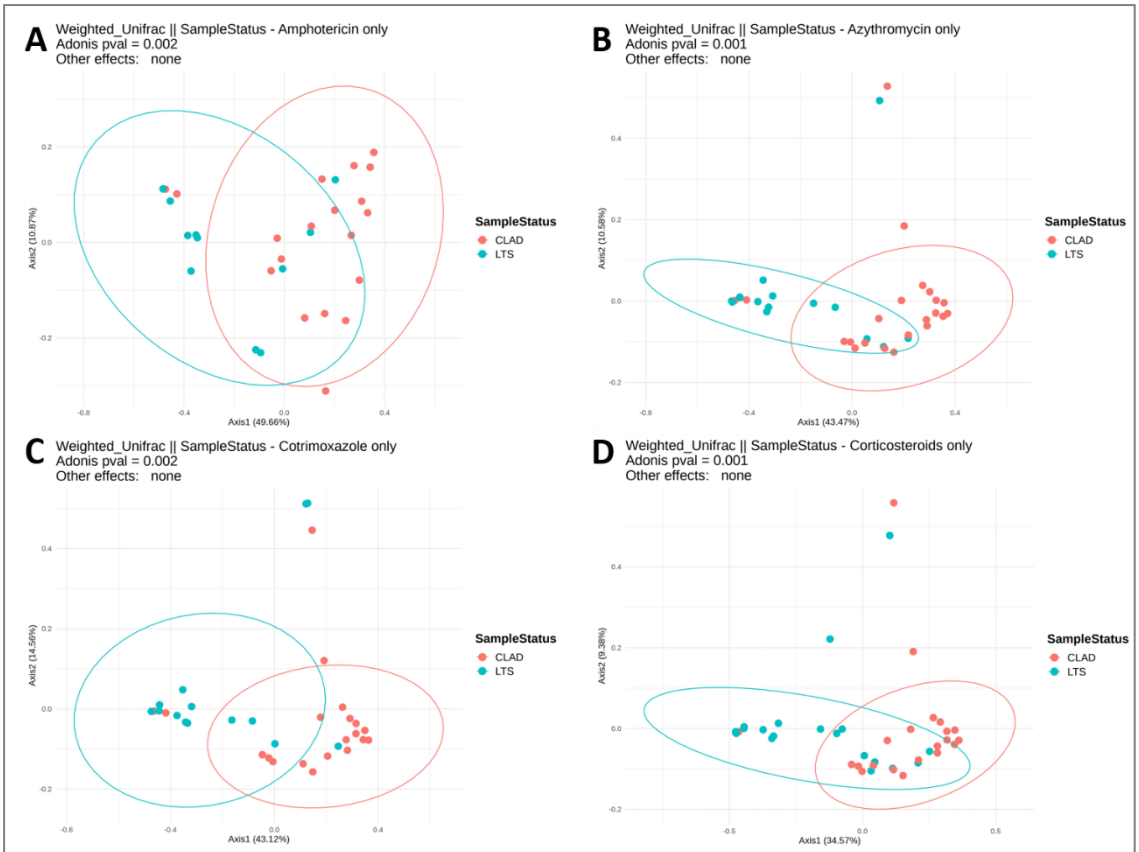

Figure 39. Bacterial diversity clustering by Weighted UniFrac PCoA of upper respiratory tract microbiota in LT patients treated with amphotericin (A), azythromycin (B), cotrimoxazole (C) and corticosteroids (D). Each dot represents a sample (red, CLAD; blue, LTS) and the variance explained by the Principal Coordinates is indicated in parentheses on the axes.

In Figure 40, Figure 41 and Figure 42 the distributions of abundances of the most common phyla (A) and genera (B) among the individuals receiving different treatments (amphotericin, azithromycin and cotrimoxazole, respectively) selected by group were illustrated.

LTS patients presented the same trends as the analyses performed regardless of treatment, being the Actinobacteria phylum and *Corynebacterium* genus more dominant in the upper respiratory tract of these patients (Figure 40, Figure 41 and Figure 42). Conversely, the phylum Firmicutes and genus *Staphylococcus* were also enriched in CLAD group. In conclusion, these findings were consistent and did not depend on these treatments.

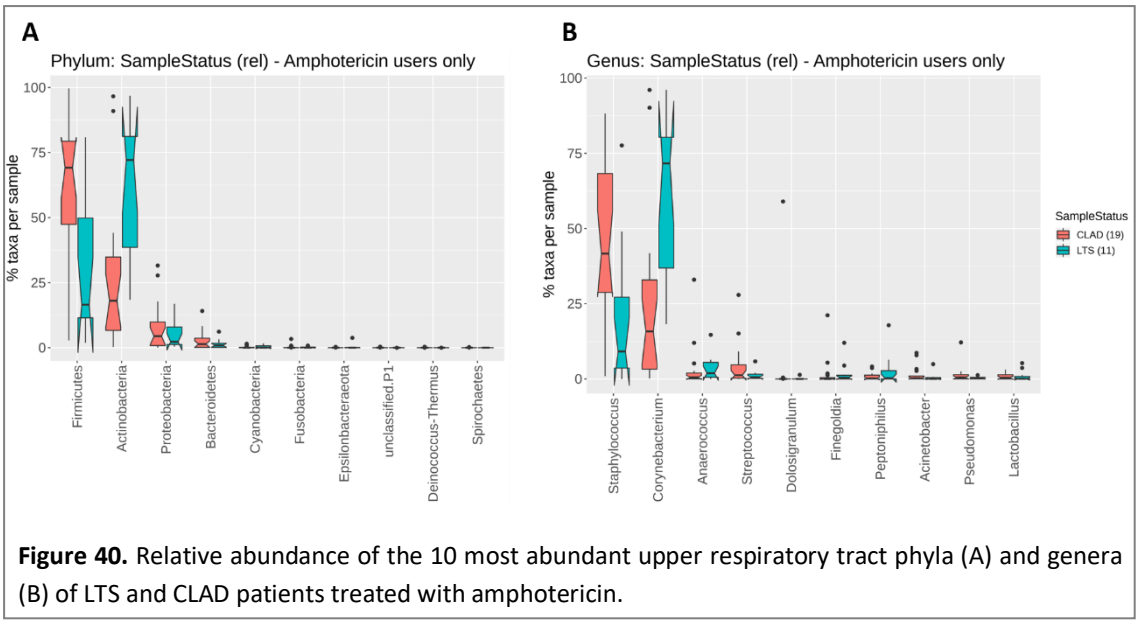

Figure 40. Relative abundance of the 10 most abundant upper respiratory tract phyla (A) and genera (B) of LTS and CLAD patients treated with amphotericin.

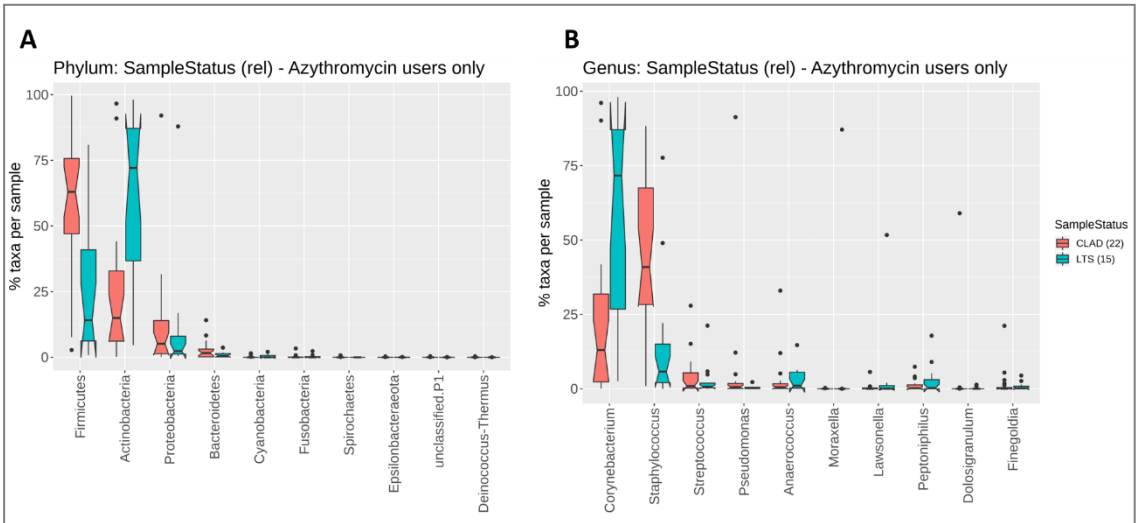

Figure 41. Relative abundance of the 10 most abundant upper respiratory tract phyla (A) and genera (B) of LTS and CLAD patients treated with azythromycin.

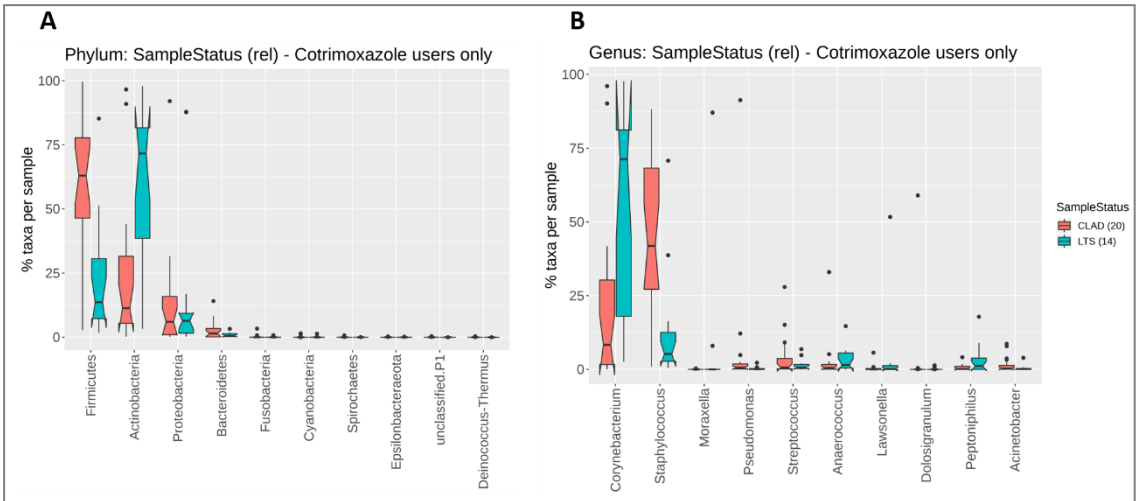

Figure 42. Relative abundance of the 10 most abundant upper respiratory tract phyla (A) and genera (B) of LTS and CLAD patients treated with cotrimoxazole.

4

GENERAL DISCUSSION

Lung transplantation (LT) is the final treatment option for patients with end-stage respiratory diseases[24]. Advances in surgical techniques, organ preservation, immunosuppressive treatment and perioperative management have improved short-term survival. However, despite the beneficial effects of LT on quality of life, long-term survival after LT is hindered mainly by the development of CLAD.

Kidney, liver and heart transplantation present a ten year survival rate of 86.2%[154], 61%[155], and 56%[156], respectively, compared to 34.3% among LT[20]. One plausible explanation for this lower survival rate is that lungs are continuously exposed to the external environment, being the first line of protection from pathogens and noxious agents.

The lifelong immunosuppression of SOT patients poorly influences their long-term survival, leading to severe complications such as nephrotoxicity[162,163], infectious diseases[72], malignancies[164], and metabolic disorders[165]. For this reason, the main goal in organ transplantation is achieving an alloantigen-specific unresponsiveness state in the sustained absence of toxic immunosuppressive therapies.

In most cases, immunosuppression withdrawal leads to transplant rejection. However, a small group of transplant patients has maintained long-term stable graft function despite interrupted treatment (operational tolerance state). This phenomenon is infrequent and varies according to the type of allograft, being more prevalent in kidney and liver transplantation[171–175].

In recent years, the main purpose of organ transplantation has been to characterise the immunological mechanisms involved in tolerance, which remain poorly understood. The intensive research conducted with this small number of kidney[183–188] and liver[189–193] transplant recipients has reported immunophenotypical and transcriptional changes in tolerant patients compared to non-tolerant recipients and healthy individuals. Nevertheless, these studies have revealed that kidney and liver tolerant recipients differed in blood gene expression and immunophenotype patterns, suggesting that the immune mechanisms involved in achieving transplantation tolerance are organ-specific.

In the field of LT, there is only one anecdotal reported case of operational tolerance. The long-term acceptance of the allograft in the absence of ongoing immunosuppression was due to a state of chimerism in the recipient, produced by the HLA-match combining bone marrow and LT from the same living donor[176].

Therefore, LTS patients after LT, included in this study, are the closest group to operationally tolerant kidney or liver transplant individuals. As the recipients of both groups (LTS and CLAD patients) were receiving immunosuppression treatment, the confounding effect of immunosuppression, not assessed in most previous studies performed in other organs, was excluded. Furthermore, to avoid additional differences due to patient characteristics, the recipients were matched by age, sex and underlying disease when feasible.

To date, the association of allograft acceptance with different immune fingerprints has been widely described for kidney and liver transplantation, although this has not been the case with LT. Accordingly, the present thesis was designed to screen the greatest number of clinical and

immunological parameters; the microbiome of the upper respiratory tract and the full transcriptomic expression profile and flow cytometric immunophenotyping of peripheral blood samples were assessed to study the particular characteristics of the patients with normal allograft function after at least ten years from LT.

In addition, the use of peripheral blood samples to perform most studies and nasopharyngeal swabs to carry out microbiome analyses represented a clear benefit for patient safety and for its clinical applicability due to the low invasiveness of these procedures.

The results derived from bioinformatics analyses of gene and miRNA expression provide a better understanding of the mechanisms involved in long-term survival. Moreover, they are highly accurate in the classification of LT patients by employing gene and multi-platform biomarker expression profiling.

The findings obtained have demonstrated the usefulness of clinical data, microbiome discoveries and global transcriptome profile from peripheral blood samples to differentiate between LTS and CLAD patients and to identify some of the potential mechanisms responsible for organ acceptance.

Overall, this study has contributed to the knowledge of long-term survival with normal allograft function in the field of LT.

4.1 PART I. CLINICAL CHARACTERISTICS OF LONG-TERM SURVIVORS WITH NORMAL ALLOGRAFT FUNCTION

Limited evidence about long-term survival after LT of more than ten years considering graft condition has been published and very few studies about long-term survival have been conducted in isolated series of patients from single centers[195–198]. In this study, LTS were identified in five Spanish centers with more than ten years' experience in LT technique at the moment of the study. All selected patients were bilateral to avoid the confounding effect of the native lung.

One of the main limitations of this project was that LTS and CLAD patients did not undergo transplantation at the same time. The longer follow-up time is inherent to the LTS group, and consequently this is why the findings obtained could be due to a favourable patient outcome or to time post-LT. Another major limitation was the heterogeneity of the CLAD group. Although having all the patients with the same CLAD phenotype would have been ideal, the complex matching process did not allow it.

The factors contributing to long-term survival with normal allograft function after LT compared to CLAD patients identified in this study were: donor age (lower in LTS group, data not shown), lower comorbidity and infection rates, the latter mainly due to the lower rate of mild infections and diabetes mellitus, which was more frequent in the follow-up of the CLAD group.

In line with this, Riou[243] *et al* evaluated the impact of diabetes mellitus on survival after LT, observing a worse survival in the patients with diabetes pre-post LT, compared to patients without pre-transplant diabetes. However, they did not find survival differences between

patients who developed diabetes mellitus after LT and non-diabetic LT recipients. Therefore, the results obtained might confirm the impact of diabetes mellitus on survival after LT.

4.2 PART II. TRANSCRIPTOMIC ANALYSES

This study examined the mRNA and miRNA expression profiles of peripheral blood across LTS and CLAD patients. Differences in both mRNA expression and upstream miRNA regulators were found between both groups of patients. Transcriptomic microarray expression analyses revealed 458 DEG and 108 differentially expressed miRNAs, 36 of which were mature miRNAs.

Functional annotation of microarray data showed that the main biological pathways among DEG were referred to neutrophil mediated processes and innate immunity. An interesting result obtained was the up-regulated expression of the gene *RPS26* in LTS recipients. It has been demonstrated that rapamycin represses the expression of the cytoplasmic ribosomal protein *RPS26*[244], so this finding probably reflects the use of Sirolimus in CLAD patients.

An integrative analysis between transcriptomic data was performed following two different approaches. In the first, based on correlations between expression values, a correlation network between three mature miRNAs and twelve genes was identified. The relevance or implications of these new relationships have not yet been described, as none of the target genes included in this correlation network were validated targets for the three miRNAs to date.

The second approach was based on the biological significance of the differentially expressed experimentally validated miRNA gene targets. Of the 36 differentially expressed mature miRNA, 30 miRNAs had experimentally validated target genes enriched in the set of 458 DEG. The bioinformatic evaluation of the 113 differentially expressed experimentally validated miRNA gene targets revealed enrichment for neutrophil mediated processes, as in the case of the functional annotation results of the microarray DEG.

Using a machine learning approach, a reduced number of genes and miRNAs that were able to discriminate LT patients were found. Using these variables, different classification models capable of distinguishing LTS status in the validation sets resulting from the 5-fold cross validation strategy were built.

The combination of the LASSO and diagonal discriminant analysis algorithms with the 25 classifier variables, genes and miRNAS respectively, provided the best discriminatory powers. Concerning genes, the performances of all the models obtained was adequate. However, in the case of miRNAs, the performances of the models with a lower number of miRNAs were far from acceptable. Therefore, these 25 classifier genes are potentially relevant in the discrimination between LTS and CLAD patients, suggesting that they may have a potential clinical applicability.

The gene expression analysis by RT-qPCR successfully validated the most informative genes selected from the classification models, so the reproducibility of the results using different transcriptional platforms was confirmed. Nevertheless, in the miRNA expression analysis by RT-qPCR most targets were not amplified.

A summary of the most relevant miRNAs and genes results found are discussed below.

MicroRNAs (miRNAs) are described as short non-coding RNA molecules that inhibit gene expression post-transcriptionally by binding to the 3' untranslated region (UTR) of target mRNAs, promoting their degradation or inhibiting translation[245]. Since miRNAs regulate hundreds of target genes post-transcriptionally, a single miRNA may be involved in the development of many diseases ("many-to-one" and "one-to-many" relationships), and consequently, their peripheral blood expression may be altered[246]. In the transplant field, miRNAs have recently emerged as diagnostic and prognostic markers and potential therapeutic targets[247].

Considering both statistical criteria and biological changes, four down-regulated miRNAs (hsa-miR-151b, hsa-miR-194-5p, hsa-miR-26b-5p and hsa-miR-421.) were identified in LTS recipients. In the LT field, no studies regarding miRNAs in graft acceptance have been performed although a huge variety of miRNA profiles analysed during lung rejection have been reported[248,249]. However, none of the four miRNAs down-regulated in LTS patients have been previously associated with lung rejection. It is worth noting that none of these studies were performed in whole blood samples.

As regards miR-194, a previous study demonstrated that the serum levels of this miRNA correlated with liver injury after liver transplantation[250]. Specifically, miR-194-5p was presented to suppress type I IFN expression and type I IFN-mediated antiviral response, enhancing viral replication[251]. Furthermore, a recent study reported that miR-194-5p was over-expressed in patients suffering from acute graft-versus-host disease[252].

miR-421 up-regulation was shown to contribute to the progression of multiple cancers such as gastric, pancreatic, hepatocellular, biliary tract and nasopharyngeal cancers[253]. Regarding miR-151b, it was observed that the serum levels of this miRNA were significantly increased in ischemic stroke patients compared to those of healthy controls[254]. However, there are no studies that link these miRNAs with any SOT outcome, so further investigation is needed to elucidate their function in the LT field.

In the integrative analysis, miR-26b-5p presented the highest number of validated DEG targets, which were involved in "T cell differentiation in thymus", "B cell activation" and "DC chemotaxis and migration", suggesting that this miRNA may contribute to these biological processes in LT patients.

In the case of genes, considering both statistical criteria and biological changes, three up-regulated DEG (*TNFRSF21, LILRA4 and NRP1*) and five down-regulated DEG (*ANXA3, MMP8, LTF, TCN1 and OLFM4*) in LTS recipients were identified.

TNFRSF21, also named death receptor 6 (*DR6*) and *CD358*, is a member of the tumour necrosis factor receptor superfamily, which is highly expressed in human plasmacytoid DCs (pDCs)[255]. *TNFRSF21* is involved in NK-κB signaling pathways and plays a regulatory function in the proliferation and survival of T and B cells[256].

Furthermore, *LILRA4*, also named *CD85g* and *ILT7*, is a member of the activating leucocyte immunoglobulin-like receptor (LILRA) family that is abundantly and exclusively expressed by human pDCs[257].

The up-regulation of these two genes in LTS recipients observed in this study probably reflected the presence of circulating pDCs. These tolerogenic DCs can suppress immune responses via several mechanisms, including T cell deletion, the induction of Tregs and anergic T cells, the expression of immunomodulatory molecules and the production of immunosuppressive factors[258].

In recent years, appreciable evidence has supported a role of pDCs in regulating the induction and/or maintenance of solid organ allograft tolerance[259]. Herein, Abe[260] and co-workers demonstrated for the first time that pre-pDCs prolonged murine vascularized heart allograft survival. Later, Ochando[261] *et al* demonstrated that interactions between pDCs and $CD4^+$ T cells in the lymph nodes were required for Treg generation to potentially achieve vascular allograft tolerance.

Finally, in the human liver transplantation field, higher proportions of pDCs precursors had already been observed in the circulation of liver transplant recipients with successful immunosuppression withdrawal compared to those receiving maintenance immunosuppression, suggesting that pDCs might promote liver transplantation tolerance[191].

The third up-regulated DEG, Neuropilin-1 (*NRP1*), is a type I transmembrane glycoprotein exclusively expressed by DCs, NK cells and $Foxp3^+$ Treg cells which plays an important role in establishing the immunological synapse between DCs and T cells[262] and contributes to the function, phenotypic maintenance and survival of Treg cells[263].

In 2012, it was reported that this surface marker served to differentiate between natural-Tregs (developed in the thymus) and induced-Tregs (generated in the periphery), becoming established as a useful tool to identify and isolate viable Tregs in the clinical transplantation field[264].

The contribution of NRP1 to transplant tolerance was first demonstrated in murine studies in which $CD4^+$ $CD25^-$ $NRP1^+$ T cells transferred into heart allograft recipient mice induced long-term graft survival[265]. Regarding human studies, the association of $NRP1^+$ T cells with the acceptance of tissue grafts was also proposed, since the percentage of $NRP1^+$ cells among lymphocytes in kidney transplant biopsies decreased significantly in rejected grafts, when compared to biopsies from non-rejecting individuals[266]

In the present study, the increased expression of NRP1 probably reflected the presence of circulating $CD4^+$ $CD25^-$ $NRP1^+$ T cells since no changes were observed in *Foxp3* microarray expression.

As regards the five down-regulated DEG (*ANXA3, MMP8, LTF, TCN1 and OLFM4*) in LTS, they have all been directly associated with neutrophils. Their protein products are detailed below:

Annexin 3 (*ANXA3*) is associated with neutrophil cytoplasmatic granules and involved in granule fusion processes[267]. ANXA3 has also been identified in the phagosome in bacterial

infection, likely involving its calcium and phospholipid binding ability[268], and revealing its involvement in the innate immune response.

Neutrophils can express the matrix metalloproteinase 8 (*MMP8*) and store it in their granules. The increased levels of this metalloproteinase are associated with the development of BOS, as they contribute to extracellular matrix turnover, epithelial damage, fibrosis, tissue remodelling and inflammation[269].

Lactoferrin (*LTF*) is an iron-binding protein found in the secondary neutrophil granules. This protein plays a direct antimicrobial role, through iron sequestration in biological fluids or its direct interaction with microorganism surfaces, destabilizing its membranes in order to kill them and limit the proliferation and adhesion of microorganisms to the epithelia surfaces[270]. Transcobalamin 1 (*TCN1*), a member of the vitamin B12-binding protein family, is a major constituent of secondary granules in neutrophils and facilitates the transport of cobalamin into cells[271]. Finally, olfactomedin 4 (*OLFM4*) is a constituent of neutrophil-specific granules[272].

In addition to this, a longitudinal study reported high expression of *OLFM4*, *MMP8* and *LTF* during the first week after a kidney transplant. However, these genes were not differentially expressed compared to baseline after the sixth month post-transplant[273].

It has been shown that an elevated expression of these five genes was considered a marker of neutrophil degranulation, suggesting an alteration in the innate immune system, underlying the important role of neutrophils. Since the greater leucocyte population in circulation in BOS patients are neutrophils[116], the higher expression levels of their corresponding markers reflected with high probability the presence of these circulating cells.

Overall, gene profiling revealed a strong association with an up-regulation of genes involved in pDC-mediated processes, and a down-regulation of genes associated with neutrophil pathways in LTS patients.

Concerning protein assessment, differences in *MMP8* expression were confirmed at protein level in serum, whereas LTF protein levels did not differ between LT groups. ELISA experiments do not necessarily reflect RNA expression of blood cells. The aim of these measurements was to find potential new biomarkers and not to replicate of microarrays and RT-qPCR results.

Measurements of the serum levels of KL-6 protein in LT patients with survival time of more than ten years were performed as there were no previous studies evaluating this protein level in this LT population. KL-6 is a high-molecular-weight mucin mainly expressed by type II pneumocytes and to a lesser extent in respiratory bronchiolar epithelial cells which may play a pathological role in fibrosing lung diseases due to its chemotactic, pro-proliferative and anti-apoptotic activity on fibroblasts[122].

In a previous study[122], increased levels of KL-6 were observed in RAS recipients compared to BOS recipients, suggesting that this protein could serve as a potential biomarker to differentiate between BOS and RAS phenotypes. In the present study, serum KL-6 levels were lower in LTS patients compared to the CLAD group, both when considering RAS patients and not (data not shown). Compared to previous results, LTS patients presented higher levels of KL-6 than the stable LT group. This difference can be explained by the post-transplant time, as

the stable samples were taken six months after LT versus more than ten years in the case of LTS patients.

Despite the lack of statistical significance, serum IL-33 and IL-6 levels showed an upward trend in CLAD patients.

The specific role of IL-33 in alloimmunity is controversial; some studies reported that serum up-regulated IL-33 can contribute to chronic allograft dysfunction in kidney transplant patients[274], whereas in a chronic cardiac rejection model[275] study this interleukin prolonged allograft survival. The pro-inflammatory cytokine IL-6, identified as a key player in inflammatory and immunomodulatory pathways, has been associated with kidney[276] and cardiac[277] graft rejection.

In accordance with this, the elevation levels of IL-33 and IL-6 in CLAD patients suggest that these cytokines may play a role in poor graft outcomes

4.3 PART III. IMMUNOPHENOTYPE AND MOLECULAR CHARACTERIZATION

Two different Treg cell populations were found in the peripheral blood of LTS and CLAD patients: $V\delta1^+$ $\gamma\delta$ T cells, significantly elevated in CLAD patients, and $CD4^-$ $CD8^-$ $\alpha\beta$ T cells, significantly elevated in LTS patients.

$\gamma\delta$ T cells are "non-conventional" T cells, representing a small subset of around 1-5% of the total T cell population[278] which participate in both innate and adaptive immunity as cytolytic effector cells and also in immunoregulatory responses.

There are two main $\gamma\delta$ T cell subpopulations in human peripheral blood: Vδ1 and Vδ2. In healthy individuals, the Vδ2 repertoire constitutes the major subtype in peripheral blood (>80% of circulating $\gamma\delta$ T cells), while Vδ1 $\gamma\delta$ T cells prevail in tissues such as skin, intestine, liver and spleen[279,192].

The role of $\gamma\delta$ T cells in clinical organ transplantation remains ambiguous; they may potentially contribute to both allograft acceptance and rejection, since they mediate anti-inflammatory and pro-inflammatory responses[280].

Several animal model studies have shown that $\gamma\delta$ T cells could be involved in liver[281] and cardiac[282,283] allograft rejection. Conversely, other clinical studies have proposed a protective role of $\gamma\delta$ T cells after associating high percentages of circulating $\gamma\delta$ T cells with stable kidney[284] and liver allograft function[189,285,286]. In addition, a prevalence of circulating Vδ1 γδ T cells was found in operationally tolerant liver recipients[189,190], suggesting that this type of regulatory cell was involved in liver transplant tolerance.

Surprisingly, the present results show that Vδ1 γδ T cells prevailed in the peripheral blood of CLAD patients compared with LTS patients. However, caution is required in the interpretation of $\gamma\delta$ T cells findings in clinical organ transplantation as an expansion of Vδ1 γδ T cells (leading to an elevated total number of γδ T cells and to a shift in the ratio between Vδ1 and Vδ2 T cells) was observed following kidney and liver transplantation regardless of the chronic

administration or not of an immunosuppression drug. Therefore, the quantification of γδ T cell subpopulations was unlikely to constitute a useful biomarker of operational solid organ allograft tolerance[287]. Nonetheless, these cells exhibit cytotoxic effects as discussed later.

The double negative $CD4^-$ $CD8^-$ $\alpha\beta^+$ TCR (DN) subset is a Treg cell population present in both animal models and human peripheral blood and constitutes approximately 1-3% of total T cells[288].

Previous studies reported that the DN T cell subpopulation was able to suppress antigen-specific immune responses preventing allograft rejection[289,290] by killing mature or immature DCs and activated alloreactive T cells ($CD8^+$ or $CD4^+$) through the Fas pathway. Similarly, B cells and NK cells can also be killed by DN T cells via a perforin/granzyme-mediated process[291]. Recently, a new mechanism of DN T cell-mediated suppression based on mTOR pathway inhibition in $CD4^+$ T cells has been revealed, demonstrating that cellular therapy using these cells could limit the alloreactive immune response[292].

In agreement with these previous studies, the present results showed an increase of DN T cells in the peripheral blood of LTS patients, concluding that these Treg cells might be beneficial in prolonging allograft survival.

Furthermore, Foxp3 Treg cells have been shown to be critically involved in the induction and maintenance of transplant tolerance in a broad range of studies[181,182]. However, in the present work these cells were not observed in peripheral blood of neither LTS nor CLAD groups. This could be due to the use of immunosuppressant drugs, especially calcineurin inhibitors, in all the patients included in the study. The presence of IL-2 is critical for Treg suppressor function and a reduction of this cytokine, due to calcineurin inhibitors administration, correlated with a decrease number of $Foxp3^+$ T cells[293]. In line with this, a recent study evaluating $Foxp3^+$ Treg cells in long-term lung transplant survivors also showed that $Foxp3^+$ Treg cells were not observed in the blood, but in the BAL fluid, suggesting an accumulation of intragraft $Foxp3^+$ cells in LTS[294].

Regarding monocytes and NK cells, CLAD patients displayed an elevated proportion of both $CD16^+$ cell subpopulations, whereas the LTS group showed a high proportion of $CD16^-$ monocyte and NK cell subpopulations.

The $CD14^{high}$ $CD16^+$ monocyte subset (intermediate monocytes) displays inflammatory function and is associated with antigen presentation and T cell activation[295,296]. The elevation of these circulating cells in CLAD patients suggested a persistence of inflammation within the allograft. On the other hand, $CD14^{high}$ $CD16^-$ monocytes were raised in LTS groups; these cells, known as classical monocytes, trigger phagocytosis in these patients[296].

The high expression level of CD16 in circulating NK cells in the CLAD group makes them efficient mediators of antibody-dependent cell-mediated cytotoxicity (ADCC). In contrast, the expanded $CD56^+$ $CD16^-$ NK subset in the LTS group resulted in decreased cytotoxic activity, as they lack ADCC ability.

The ADCC mechanism is based on the bifunctional format of IgG antibodies. After the antigen-binding fragment (Fab) binds to the surface of the target cell, the NK cell surface Fc receptor

for IgG CD16 interacts with the crystalline fragment (Fc) of the antibody-coated cell[297], inducing NK cell activation which results in both cytotoxicity and cytokine response.

There is increasing evidence that NK cells might play a dual role in mediating either allograft acceptance or rejection in solid organ allografts[298]. In the LT field, NK cells can promote tolerance by eliminating donor APCs and alloreactive T cells and they can also contribute to rejection through cytotoxic effects on allograft tissue recognized as “non-self” or “stressed” and even enhance AMR via ADCC[299].

The findings obtained are consistent with these studies, and furthermore, recent data reported support that alloantibody-mediated NK cell activation via CD16 contributes to rejection in other SOT as in the case of kidney transplant[300,301].

The CD16 marker can also be expressed by γδ T cells, especially by Vδ1 γδ T cells, mediating the ADCC process and promoting a higher cytotoxic potential of these T cells[302]. Furthermore, recent studies have demonstrated that the presence of neutrophils can enhance the killing capacity of activated γδ T cells[303].

On the other hand, L-selectin, also known as CD62L, is an adhesion molecule involved in inflammatory and immune reaction, that mediates leucocyte tethering and rolling[304]. LTS patients showed an elevated percentage of circulating granulocytes with higher CD62L expression, although the magnitude of the change of this population was not clinically relevant.

4.4 PART IV. MULTI-PARAMETER BIOMARKER ANALYSIS

The most relevant clinical, transcriptomic and immunophenotype findings were combined using a new integrative method (DIABLO) to assess if the discrimination ability between the two groups of LT patients improved by using a cross-platform approach. This module approach also sought to improve the biological interpretability of the underlying biological interactions, as the model also explained the correlation structure between the variables included.

The performance of individual biomarker blocks in the multi-biomarker model did not vary considerably in predicting the LT state, and the combined performance was similar. Interestingly, the gene transcript biomarker block performance was the highest in the discrimination of LT patients.

These results suggest that using combinations of different biological markers did not increase their individual discrimination power. This fact is probably due to a previous refining process of the variables included, since in the case of gene for example, they were selected from a pre-internal computational validation strategy. It is likely that, if a greater number of variables had been included in each block, an increase of classification power would have been observed. In any case, the combined performance, with an AUC of 0.86, is more than acceptable.

Positive correlations were the most abundant finding between clinical, mRNA, miRNA and cell populations. However, negative correlations were found between the infection rate and *LILRA4* or *TNFRSF21* genes. These findings again suggested the potential involvement of these

genes in long-term survival after LT. Both genes probably reflected the presence of circulating tolerogenic DCs in LTS patients, which would affect their good outcomes, and this means a reduction in the infection rate.

4.5 PART V. UPPER RESPIRATORY TRACT BACTERIAL MICROBIOME COMPOSITION

To date, this is the first study to assess respiratory tract bacterial microbiome in LTS with normal allograft function after LT compared to both CLAD patients and healthy (non-transplanted) controls.

Although BAL fluid is the preferred sample used in most LT microbiome literature available[78,79,305], in this study nasopharyngeal swabs were used in order to avoid such an invasive procedure in LTS patients without a clinical and ethically justifiable reason.

As regards alpha diversity, neither LT group presented significant differences. There is some controversy about alpha diversity in the LT field; while some authors reported a decrease in microbiome diversity in lung recipients compared to healthy controls[78,80], others have found an increase among LT recipients compared to controls[305].

Considering bacterial beta diversity analysis, the upper respiratory tract microbiota showed a significant difference in the overall bacterial composition between LTS and CLAD patients. Actinobacteria phylum and *Corynebacterium* genera were more prevalent in LTS patients, whereas Firmicutes phylum and *Staphylococcus* genera were enriched in the CLAD group.

Regarding abundance distributions, LTS patients followed essentially the same trends as the healthy control group, with the Actinobacteria phylum and *Corynebacterium* genus being more dominant in the upper respiratory tract of these patients.

Recent literature has indicated that the nasal microbiome of healthy humans was primarily composed of the genera *Corynebacterium* and *Bifidobacterium* (phylum Actinobacteria), *Staphylococcus*, *Streptococcus* and *Dolosigranulum* (phylum Firmicutes), *Moraxella* (phylum Proteobacteria) and the phylum Bacteroidetes[306].

Similarly, numerous studies have characterized the lung flora of healthy adults using BAL samples, with Bacteroides, Firmicutes and Proteobacteria being the most frequent phyla[305,307]. Despite differences in relative abundances, the described phyla in BAL samples were reported to be similar to those observed in upper airway samples (oropharynx, nasal)[307].

In this study, the LTS population presented an increase in the *Corynebacterium* genus compared with CLAD patients, suggesting that LTS patients presented a “healthy” nasopharyngeal flora, since this genus was also predominant in the non-transplant-healthy controls. Conversely, Firmicutes phylum was only elevated in the CLAD group, but not in LTS or healthy control patients.

All the findings were also analysed regarding the treatment received in the experimental groups (amphotericin, azythromycin, cotrimoxazole, and corticosteroid treatments), as this was an important parameter which could alter the results. The results obtained were not altered by the treatment.

Among *Staphylococcus* genera, the *Staphylococcus aureus* pathogen causes most infections. Approximately, 20-30% of the healthy population is persistently colonized by *S. aureus*[308], so the presence of this bacteria in some LTS and healthy patients was an expected finding.

To colonize nasal orifices in healthy subjects, this pathogen must compete with other microorganisms normally present in this region, such as Actinobacteria phylum[308].

Moreover, higher abundances of Spirochaetes phylum and *Lactobacillus* and *Acidocella* genera were observed in LTS and CLAD patients compared to healthy controls. These results suggested a tendency to present higher abundances of these organisms after LT, although their involvement in transplant outcome remains unknown.

Therefore, the microbiome characterization has suggested that LTS patients presented healthy nasopharyngeal flora. Besides, in these patients *Corynebacterium* might prevent infections by potential pathogens such as *Staphylococcus aureus*.

DISCUSSION SUMMARY

In short, the peripheral blood of LTS with normal allograft function patients exhibited an up-regulation of genes involved in pDC-mediated processes, down-regulation of genes associated with neutrophil pathways, an elevation in DN Treg cells and decreased levels of $V\delta1^+$ $\gamma\delta$ T cells and $CD16^+$ monocytes and NK cells. Furthermore, these patients maintain a dominant *Corynebacterium* microbiota in their upper respiratory tracts.

Collectively, the results obtained in the current study reveal that immunophenotypical and transcriptomical expression patterns between LTS and operationally tolerant kidney and liver recipients differ, suggesting that allograft acceptance in kidney, liver and lung transplants is achieved through different immune mechanisms. Unravelling these mechanisms would help to develop specific screening and treatment protocols and result in more personalized medicine.

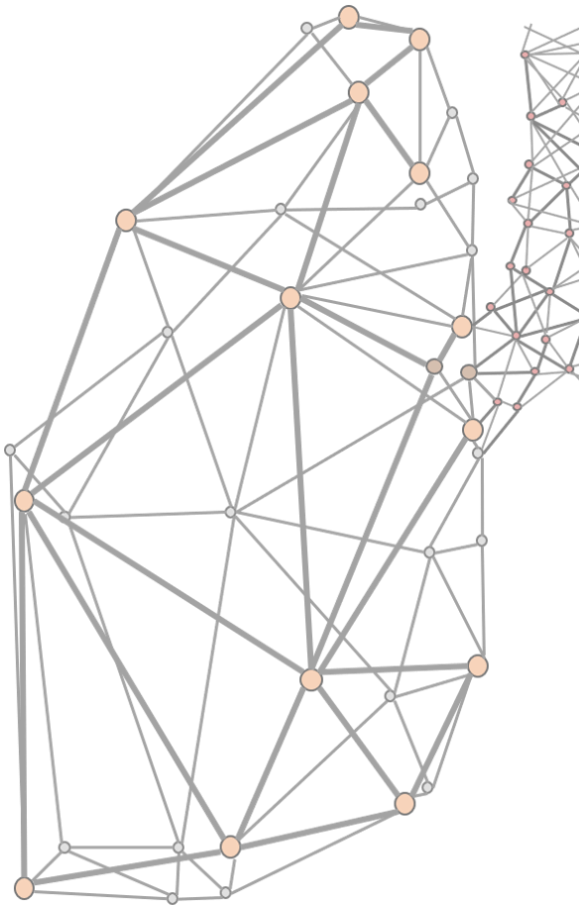

5
CONCLUSIONS

The results obtained in the studies included in this thesis offer valuable insights to gain a better understanding of the potential mechanisms involved in long-term survival after lung transplantation, leading to the following conclusions:

1- Long-term survivors with normal allograft function present a lower frequency of pre-transplant diabetes mellitus, days in waiting list, and lower comorbidity and infection rates after lung transplantation.

2- The expression signature associated with long-term survival after lung transplantation is mainly characterized by enrichment in genes encoding for cell-surface receptors expressed by plasmacytoid dendritic cells and down-regulation of genes associated with neutrophil pathways. Gene classifiers and multi-platform biomarker expression profiling model developed accurately differentiate long-term survivors with normal allograft function from chronic lung allograft dysfunction recipients, although any miRNA set cannot classify patients between both groups.

3- Long-term survivors with normal allograft function exhibit an increased number of double negative regulatory T cells, CD16- monocytes and CD16- NK cells in peripheral blood and lower serum biomarker levels of MMP8 and KL-6 compared to chronic lung allograft dysfunction recipients.

4- Actinobacteria phylum and Corynebacterium genus dominate the upper respiratory tract microbiome of long-term survivors with normal allograft function.

6
FUTURE PERSPECTIVES

The principal aim of this thesis was to characterize LTS with normal allograft function ten years after LT. The results provided here could contribute to a better understanding of the underlying mechanisms of graft acceptance after LT and open up new perspectives for future research.

Several studies have already analysed specific parameters in the peripheral blood of kidney and liver tolerant recipients. The present research is the first to describe the long-term survival with normal allograft function after LT state, the closest phenomenon to kidney or liver operational tolerance, by employing exhaustive transcriptomic and immunophenotypic analyses. Moreover, serum protein analyses and the microbiome composition of the upper respiratory tract have also provided new data about this condition.

Although these results are of potential relevance, the external validation of these findings in other independent cohort of LT recipients with similar clinical group characteristics would be required to confirm the results in leucocyte subpopulations, genes and miRNAs.

Once external validation has been carried out, studies evaluating the predictive nature of transcriptional and immunophenotypical profiles should be performed. The relationship between the mechanisms of *LILRA4*, *TNFRSF21* and *NRP1* genes and their role as potential predictors of long-term survival with normal allograft function after LT need to be further investigated in prospective studies.

In this vein, the genetic findings suggested that pDCs in the peripheral blood of LTS patients could play an important role in long-term survival with normal allograft function. Primarily, the presence of these cells in the peripheral blood of LTS patients must be analysed. After confirming that, the specific role of pDCs would be assessed in the graft acceptance process.

The characterization of LTS patients validated some features described for other organ transplantation fields, such as the potential role of DN T cells in the maintenance of long-term survival with normal allograft function, highlighting the importance of this pool of cells for prolonging allograft survival.

This was not the case for Foxp3 Treg cells which were absent in the peripheral blood of all patients regardless LT condition. In line with this, studies have demonstrated that immunosuppressive drugs can inhibit Foxp3 expression. Consequently, it will be necessary to confirm that the absence of Foxp3 Treg cells is due to the immunosuppressive treatment and assess the intragraft role of these cells.

Considering the exploratory nature of this study, the present findings could be used as a starting point in the unravelling of the mechanisms involved in lung transplant immunology.

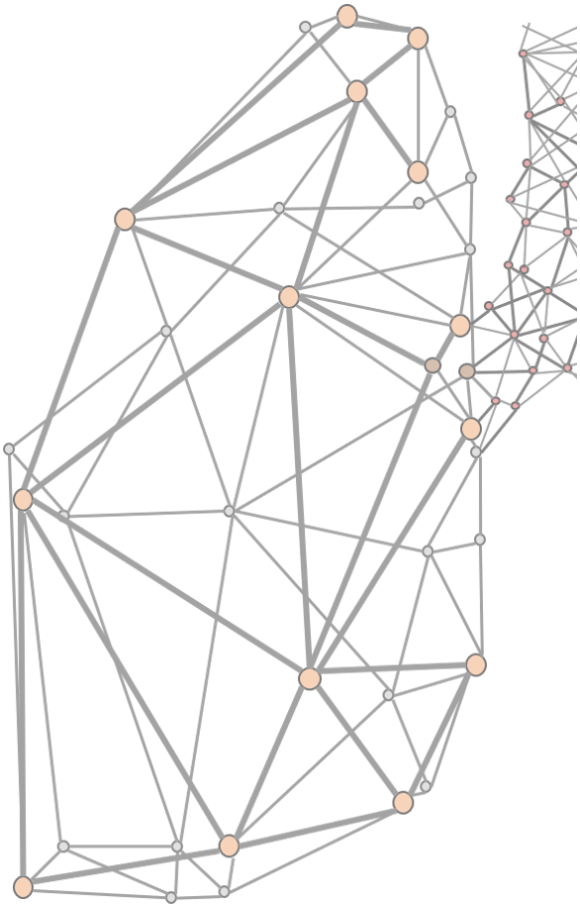

7
REFERENCES

1. Demikhov, V. Transactions of the First All-Union Conference in Thoracic Surgery, Moscow, May 14-21, 1947. In: Problems of Thoracic Surgery [Russian]. Medgiz. (1949).

2. Hardin, C. A., Kitte, C. F. Experiences with transplantation of the lung. *Science (80-.).* **119**, 97–98 (1954).

3. Hardy, J. D., Eraslan, S., Dalton, M. L., Alican, F. & Turner, M. D. Re-implantation and homotransplantation of the lung: laboratory studies and clinical potential. *Ann. Surg.* **157**, 707–718 (1963).

4. Hardy, J. D., Webb, W. R., Dalton, M. L. & Walker, G. R. Lung homotransplantation in man: Report of the Initial Case. *J. Am. Med. Assoc.* **186**, 1065–1074 (1963).

5. Veith F. J., K. S. K. The present status of lung transplantation. *Arch Surg* **109**, 734–740 (1974).

6. Nelems, J. M. *et al.* Human lung transplantation. *Chest* **78**, 569–573 (1980).

7. Veith F. J., Koerner S. K., Siegelman S. S., Torres M., Bardfeld P. A., Attai L. A., Boley S. J., Takaro T., G. M. L. Single lung transplantation in experimental and human emphysema. *Ann. Surg.* **178**, 463–476 (1973).

8. Derom F, Barbier F, Ringoir S, Versieck J, Rolly G, Berzsenyi G, Vermeire P, V. L. Ten-month survival after lung homotransplantation in man. *J Thorac Cardiovasc Surg.* **61**, 835–46 (1971).

9. Borel, J. F., Feurer, C., Gubler, H. U. & Stähelin, H. Biological effects of cyclosporin A: A new antilymphocytic agent. *Agents Actions* **6**, 468–475 (1976).

10. Calne R. Y., White D. J., Evans D. B., Thiru S., Henderson R. G., Hamilton D. V., Rolles K., McMaster P., Duffy T. J., MacDougall B. R., W. R. Cyclosporin A in cadaveric organ transplantation. *Br. Med. J. (Clin. Res. Ed).* **282**, 934–936 (1981).

11. Powles R.L., Barrett A.J., Clink H., Kay H.E., Sloane J., M. T. J. Cyclosporin A for the treatment of graft-versus-host disease in man. *Lancet* **2**, 1327–1331 (1978).

12. Goldberg M., Lima O., Morgan E., Ayabe H.A., Luk S., Ferdman A., Peters W.J., C. J. D. A comparison between cyclosporin A and methylprednisolone plus azathioprine on bronchial healing following canine lung autotransplantation. *J Thorac Cardiovasc Surg.* **85**, 821–826 (1983).

13. Cooper J. D., Ginsberg R. J., G. M. et al. Unilateral lung transplantation for pulmonary fibrosis. *N Engl J Med.* **314**, 1140–1145 (1986).

14. Cooper J.D., Pearson F.G., Patterson G.A., Todd T.R., Ginsberg R.J., Goldberg M., D. W. A. Technique of successful lung transplantation in humans. *J Thorac Cardiovasc Surg.* **93**, 173–181 (1987).

15. Pearson, F. G. Lung transplantation: The Toronto experience. *Eur. J. Cardio-thoracic Surg.* **3**, 6–11 (1989).

16. Dark, J. H. *et al.* Experimental en bloc double-lung transplantation. *Ann. Thorac. Surg.* **42**, 394–398 (1986).

17. Patterson G. A., Cooper J. D., Dark J. H., Jones M. T., the T. L. T. G. Experimental and clinical double lung transplantation. *J. Thorac. Cardiovasc. Surg.* **95**, 70–74 (1988).

18. Pasque, M. K. *et al.* Improved technique for bilateral lung transplantation: Rationale and initial clinical experience. *Ann. Thorac. Surg.* **49**, 785–791 (1990).

19. Kaiser, L. R. *et al.* Bilateral sequential lung transplantation: The procedure of choice for double-lung replacement. *Ann. Thorac. Surg.* **52**, 438–446 (1991).

20. Chambers, D. C. *et al.* The international thoracic organ transplant registry of the international society for heart and lung transplantation: thirty-sixth adult lung and heart–lung transplantation report—2019; focus theme: donor and recipient size match. *J. Hear. Lung Transplant.* **38**, 1042–1055 (2019).

21. Roman A., Bravo C., Tenorio L., Astudillo J., Margarit C., M. F. Single lung transplant for idiopathic pulmonary fibrosis: normocapnea after prolonged hypercapnea. Vall d'Hebron Transplant Group. *Transpl. Proc.* **24**, 21 (1992).

22. *NEWSLETTER TRANSPLANT.International figures on organ, tissue & haematopoietic stem cell donation & transplantation activities. Documents produced by The Council of Europe European Committee (partial agreement) on organ transplantation (CP-P-TO).* (2019).

23. *Registre de trasplantament pulmonar de Catalunya 1990-2018. Informe estadístic. Organització Catalana de Trasplantaments (OCATT)*. (2019).

24. Hartert, M. *et al.* Lung Transplantation: A Treatment Option in End-Stage Lung Disease. *Dtsch. Arztebl. Int.* **111**, 107–116 (2014).

25. Yusen, R. D. *et al.* The Registry of the International Society for Heart and Lung Transplantation: Thirty-second Official Adult Lung and Heart-Lung Transplantation Report - 2015; Focus Theme: Early Graft Failure. *J. Hear. Lung Transplant.* **34**, 1264–1277 (2015).

26. Mahajan, A. K. *et al.* The Diagnosis and Management of Airway Complications Following Lung Transplantation. *Chest* **152**, 627–638 (2017).

27. Kroegel C., Hekmat K., Möser A., Happe J., Walther R., R. A. [Airway complications following lung transplantation – clinic, diagnosis, and interventional management]. *Pneumologie* **65**, 293–307 (2011).

28. Banerjee S. K., Santhanakrishnan K., Shapiro L., Dunning J., Tsui S., P. J. Successful stenting of anastomotic stenosis of the left pulmonary artery after single lung transplantation. *Eur Respir Rev* **20**, 59–62 (2011).

29. Chaaya G., V. P. Pulmonary vein thrombosis: a recent systematic review. *Cureus* **9**, 1–13 (2017).

30. Sano Y., Oto T., Toyooka S., Yamane M., Okazaki M., D. H. [Phrenic nerve paralysis following lung transplantation]. *Kyobu Geka* **60**, 993–997 (2007).

31. Mogayzel P. J. Jr, Colombani P. M., Crawford T. O., Y. S. C. Bilateral diaphragm paralysis following lung transplantation and cardiac surgery in a 17-year-old. *J. Hear. Lung Transplant.* **21**, 710–712 (2002).

32. Ferrer, J. *et al.* Acute and chronic pleural complications in lung transplantation. *J. Hear. Lung Transplant.* **22**, 1217–1225 (2003).

33. Lee, J. C., Christie, J. D. & Keshavjee, S. Primary graft dysfunction : definition, risk factors, short- and long-term outcomes. *Semin Respir Crit Care Med.* **31**, 161–171 (2010).

34. Daud, S. A. *et al.* Impact of immediate primary lung allograft dysfunction on bronchiolitis obliterans syndrome. *Am. J. Respir. Crit. Care Med.* **175**, 507–513 (2007).

35. Huang H. J., Yusen R. D., Meyers B. F., Walter M. J., Mohanakumar T., Patterson G. A., Trulock E. P., H. R. R. Late primary graft dysfunction after lung transplantation and bronchiolitis obliterans syndrome. *Am J Transpl.* **8**, 2454–2462 (2008).

36. Bando K., Paradis I. L., Similo S., Konishi H., Komatsu K., Zullo T. G., Yousem S. A., Close J. M., Zeevi A., Duquesnoy R. J., et al. Obliterative bronchiolitis after lung and heart-lung transplantation. An analysis of risk factors and management. *J Thorac Cardiovasc Surg.* **110**, 4–13 (1995).

37. Girgis R. E., Tu I., Berry G. J., Reichenspurner H., Valentine V. G., Conte J. V., Ting A., Johnstone I, Miller J, Robbins R. C., Reitz B. A., T. J. Risk factors for the development of obliterative bronchiolitis after lung transplantation. *J Hear. Lung Transplant.* **15**, 1200–1208 (1996).

38. Hachem, R. R. *et al.* The significance of a single episode of minimal acute rejection after lung transplantation. *Transplantation* **80**, 1406–1413 (2005).

39. Snydear, L. D. & Palmer, S. M. Immune mechanisms of lung allograft rejection. *Semin. Respir. Crit. Care Med.* **27**, 534–543 (2006).

40. Martinu, T., Chen, D. F. & Palmer, S. M. Acute rejection and humoral sensitization in lung transplant recipients. *Proc. Am. Thorac. Soc.* **6**, 54–65 (2009).

41. Clelland, C. *et al.* Bronchoalveolar lavage and transbronchial lung biopsy during acute rejection and infection in heart-lung transplant patients: studies of cell counts, lymphocyte phenotypes, and expression of HLA-DR and interleukin-2 receptor. *Am. Rev. Respir. Dis.* **147**, 1386–1392 (1993).

42. Hachem, R. R. Lung allograft rejection: diagnosis and management. *Curr. Opin. Organ Transplant.* **14**, 477–482 (2009).

43. McManigle, W., Pavlisko, E. & Martinu, T. Acute cellular and antibody-mediated allograft rejection. *Semin. Respir. Crit. Care Med.* **34**, 320–335 (2013).

44. Lowery, E. M. *et al.* Low vitamin D levels are associated with increased rejection and infections after lung transplantation. *J. Hear. Lung Transplant.* **31**, 700–707 (2012).

45. Zheng, H. X. *et al.* Interleukin-10 production genotype protects against acute persistent rejection after lung transplantation. *J. Hear. Lung Transplant.* **23**, 541–546 (2004).

46. Zheng, H. X. *et al.* The impact of pharmacogenomic factors on acute persistent rejection in adult lung transplant patients. *Transpl. Immunol.* **14**, 37–42 (2005).

47. Palmer, S. M. *et al.* Innate immunity influences long-term outcomes after human lung transplant. *Am. J. Respir. Crit. Care Med.* **171**, 780–785 (2005).

48. Palmer, S. M. *et al.* Genetic regulation of rejection and survival following human lung transplantation by the innate immune receptor CD14. *Am. J. Transplant.* **7**, 693–699 (2007).

49. Brugiére, O. *et al.* Lung transplantation in patients with pretransplantation donor-specific antibodies detected by luminex assay. *Transplantation* **95**, 761–765 (2013).

50. Palmer, S. M. *et al.* Development of an antibody specific to major histocompatibility antigens detectable by flow cytometry after lung transplant is associated with bronchiolitis obliterans syndrome. *Transplantation* **74**, 799–804 (2002).

51. Jaramillo, A. *et al.* Activation of human airway epithelial cells by non-HLA antibodies developed after lung transplantation: A potential etiological factor for bronchiolitis obliterans syndrome. *Transplantation* **71**, 966–976 (2001).

52. Kulkarni H. S., Bemiss B. C., H. R. R. Antibody-mediated rejection in lung transplantation. *Curr Transpl. Rep* **2**, 316–323 (2015).

53. Masson, E. *et al.* Hyperacute rejection after lung transplantation caused by uUndetected low-titer anti-HLA antibodies. *J. Hear. Lung Transplant.* **26**, 642–645 (2007).

54. Martinu T., Pavlisko E. N., Chen D. F., P. S. M. Acute Allograft Rejection: Cellular and Humoral Processes. *Clin Chest Med* **32**, 295–310 (2011).

55. Cecka, J. M., Kucheryavaya, A. Y., Reinsmoen, N. L. & Leffell, M. S. Calculated PRA: initial results show benefits for sensitized patients and a reduction in positive crossmatches. *Am. J. Transplant.* **11**, 719–724 (2011).

56. Levine, D. J. *et al.* Antibody-mediated rejection of the lung: A consensus report of the International Society for Heart and Lung Transplantation. *J. Hear. Lung Transplant.* **35**, 397–406 (2016).

57. Benzimra, M., Calligaro, G. L. & Glanville, A. R. Acute rejection. *J. Thorac. Dis.* **9**, 5440–5457 (2017).

58. Blume, O. R., Yost, S. E. & Kaplan, B. Antibody-mediated rejection: pathogenesis, prevention, treatment, and outcomes. *J. Transplant.* **2012**, 201754 (2012).

59. Hammond, M. E. H. & Kfoury, A. G. Antibody-mediated rejection in the cardiac allograft: diagnosis, treatment and future considerations. *Curr. Opin. Cardiol.* **32**, 326–335 (2017).

60. Moll, S. & Pascual, M. Humoral rejection of organ allografts. *Am. J. Transplant.* **5**, 2611–2618 (2005).

61. Witt, C. A. *et al.* Acute antibody-mediated rejection after lung transplantation. *J. Hear. Lung Transplant.* **32**, 1034–1040 (2013).

62. Glanville, A. R. Antibody-mediated rejection in lung transplantation: myth or reality? *J. Hear. Lung Transplant.* **29**, 395–400 (2010).

63. Roden, A. C. *et al.* Diagnosis of acute cellular rejection and antibody-mediated rejection on lung transplant biopsies: A perspective from members of the pulmonary pathology society. *Arch. Pathol. Lab. Med.* **141**, 437–444 (2017).

64. Magro C. M., Deng A., Pope-Harman A., Waldman W. J., Bernard Collins A., Adams P. W., Kelsey M, R. P. Humorally mediated posttransplantation septal capillary injury syndrome as a common form of pulmonary allograft rejection: a hypothesis. *Transplantation* **74**, 1273–1280 (2002).

65. Roux, A. *et al.* Donor-specific HLA antibody-mediated complement activation is a significant indicator of antibody-mediated rejection and poor long-term graft outcome during lung transplantation: a single center cohort study. *Transpl. Int.* **31**, 761–772 (2018).

66. Westall, G. P. *et al.* C3d and C4d deposition early after lung transplantation. *J. Hear. Lung Transplant.* **27**, 722–728 (2008).

67. Speich, R. & van der Bij, W. Epidemiology and Management of Infections after Lung Transplantation. *Clin. Infect. Dis.* **33**, S58–S65 (2001).

68. Czebe K., Antus B., Varga M., C. E. Pulmonary infections after lung transplantation. *Orv. Hetil.* **149**, 99–109 (2008).

69. Kotloff, R. M., Ahya, V. N. & Crawford, S. W. Pulmonary complications of solid organ and hematopoietic stem cell transplantation. *Am. J. Respir. Crit. Care Med.* **170**, 22–48 (2004).

70. Remund, K. F., Best, M. & Egan, J. J. Infections relevant to lung transplantation. *Proc. Am. Thorac. Soc.* **6**, 94–100 (2009).

71. Valentine V. G., Gupta M. R., Walker J. E. Jr, Seoane L., Bonvillain R. W., Lombard G. A., Weill D., D. G. S. Effect of etiology and timing of respiratory tract infections on development of bronchiolitis obliterans syndrome. *J. Hear. Lung Transplant.* **28**, 163–169 (2009).

72. Fishman, J. A. Infections in solid-organ transplant recipients. *N. Engl. J. Med.* **357**, 2601–2614 (2007).

73. Nosotti, M., Tarsia, P. & Morlacchi, L. C. Infections after lung transplantation. *J. Thorac. Dis.* **10**, 3849–3868 (2018).

74. Nakajima, T., Palchevsky, V., Perkins, D. L., Belperio, J. A. & Finn, P. W. Lung transplantation: infection, inflammation, and the microbiome. *Semin. Immunopathol.* **33**, 135–156 (2011).

75. Gregson, A. L. *et al.* Interaction between pseudomonas and CXC chemokines increases risk of bronchiolitis obliterans syndrome and death in lung transplantation. *Am. J. Respir. Crit. Care Med.* **187**, 518–526 (2013).

76. Weigt, S. S. *et al.* Colonization with small conidia aspergillus species is associated with bronchiolitis obliterans syndrome: a two- center validation study. *Am. J. Transplant.* **13**, 919–927 (2013).

77. Gregson A. L., Wang X., Injean P., Weigt S. S., Shino M., Sayah D., DerHovanessian A., Lynch J. P., Ross D. J., Saggar R., Ardehali A., Li G., Elashoff R., B. J. A. Staphylococcus via an interaction with the ELR+ CXC chemokine ENA-78 is associated with BOS. *Am. J. Transplant.* **15**, 792–799 (2015).

78. Charlson, E. S. *et al.* Lung-enriched organisms and aberrant bacterial and fungal respiratory microbiota after lung transplant. *Am. J. Respir. Crit. Care Med.* **186**, 536–545 (2012).

79. Dickson R. P., Erb-Downward J. R., Britt Z. E., Walker N., Lama V. N., H. G. B. The lung microbiota is distinct following lung transplantation and is associated with bronchiolitis obliterans syndrome. *Am. J. Respir. Crit. Care Med.* **187:A2209**, (2013).

80. Willner, D. L. *et al.* Reestablishment of recipient-associated microbiota in the lung allograft is linked to reduced risk of bronchiolitis obliterans syndrome. *Am. J. Respir. Crit. Care Med.* **187**, 640–647 (2013).

81. Vermeire, P. *et al.* Respiratory function after lung homotransplantation with a ten-month survival in man. *Am. Rev. Respir. Dis.* **106**, 515–527 (1972).

82. Burke, C. M. *et al.* Post-transplant obliterative bronchiolitis and other late lung sequelae in human heart-lung transplantation. *Chest* **86**, 824–829 (1984).

83. Cooper J. D. , Billingham M. , Egan T. , Hertz M. I. , Higenbottam T. , Lynch J. , Mauer J. , Paradis I. , Patterson G. A. , Smith C., et al. A working formulation for the standardization of nomenclature and for clinical staging of chronic dysfunction in lung allografts. International Society for Heart and Lung Transplantation. *J Hear. Lung Transpl.* **12**, 713–6 (1993).

84. Verleden, G. M. *et al.* Chronic lung allograft dysfunction: Definition, diagnostic criteria, and approaches to treatment—A consensus report from the Pulmonary Council of the ISHLT. *J. Hear. Lung Transplant.* **38**, 493–503 (2019).

85. Glanville, A. R. Bronchoscopic monitoring after lung transplantation. *Semin. Respir. Crit. Care Med.* **31**, 208–221 (2010).

86. Vos, R., Verleden, S. E. & Verleden, G. M. Chronic lung allograft dysfunction: Evolving practice. *Curr. Opin. Organ Transplant.* **20**, 483–491 (2015).

87. Verleden, G. M., Raghu, G., Meyer, K. C., Glanville, A. R. & Corris, P. A new classification system for chronic lung allograft dysfunction. *J. Hear. Lung Transplant.* **33**, 127–133 (2014).

88. Verleden, S. E. *et al.* Restrictive chronic lung allograft dysfunction: Where are we now? *J. Hear. Lung Transplant.* **34**, 625–630 (2015).

89. Sato, M. *et al.* Restrictive allograft syndrome (RAS): A novel form of chronic lung allograft dysfunction. *J. Hear. Lung Transplant.* **30**, 735–742 (2011).

90. Sato, M. Chronic lung allograft dysfunction after lung transplantation: the moving target. *Gen. Thorac. Cardiovasc. Surg.* **61**, 67–78 (2013).

91. Sato, M. *et al.* Time-dependent changes in the risk of death in pure bronchiolitis obliterans syndrome (BOS). *J. Hear. Lung Transplant.* **32**, 484–491 (2013).

92. Sato, M., Hwang, D. M., Waddell, T. K., Singer, L. G. & Keshavjee, S. Progression pattern of restrictive allograft syndrome after lung transplantation. *J. Hear. Lung Transplant.* **32**, 23–30 (2013).

93. Peltz M. , Edwards L. B. , Jessen M. E. , Torres F., M. D. M. HLA mismatches influence lung transplant recipient survival, bronchiolitis obliterans and rejection: implications for donor lung allocation. *J Hear. Lung Transplant.* **30**, 426–434 (2011).

94. Burton, C. M. *et al.* Acute cellular rejection is a risk factor for bronchiolitis obliterans syndrome independent of post-transplant baseline FEV1. *J. Hear. Lung Transplant.* **28**, 888–893 (2009).

95. Glanville, A. R. *et al.* Severity of lymphocytic bronchiolitis predicts long-term outcome after lung transplantation. *Am. J. Respir. Crit. Care Med.* **177**, 1033–1040 (2008).

96. Haque, M. A. *et al.* Evidence for immune responses to a self-antigen in lung transplantation: role of type V collagen-specific T cells in the pathogenesis of lung allograft rejection. *J. Immunol.* **169**, 1542–1549 (2002).

97. Weber, D. J. & Wilkes, D. S. The role of autoimmunity in obliterative bronchiolitis after lung transplantation. *Am. J. Physiol. - Lung Cell. Mol. Physiol.* **304**, 307–311 (2013).

98. Neurohr, C. *et al.* Prognostic value of bronchoalveolar lavage neutrophilia in stable lung transplant recipients. *J. Hear. Lung Transplant.* **28**, 468–474 (2009).

99. Kauke, T. *et al.* Bronchiolitis obliterans syndrome due to donor-specific HLA-antibodies. *Tissue Antigens* **86**, 178–185 (2015).

100. Gutierrez, C. *et al.* The effect of recipient's age on lung transplant outcome. *Am. J. Transplant.* **7**, 1271–1277 (2007).

101. Fiser, S. M. *et al.* Ischemia-reperfusion injury after lung transplantation increases risk of late bronchiolitis obliterans syndrome. *Ann. Thorac. Surg.* **73**, 1041–1048 (2002).

102. Davis, R. D. *et al.* Improved lung allograft function after fundoplication in patients with gastroesophageal reflux disease undergoing lung transplantation. *J. Thorac. Cardiovasc. Surg.* **125**, 533–542 (2003).

103. Cantu, E. *et al.* Early fundoplication prevents chronic allograft dysfunction in patients with gastroesophageal reflux disease. *Ann. Thorac. Surg.* **78**, 1142–1151 (2004).

104. Ruttmann, E. *et al.* Combined CMV prophylaxis improves outcome and reduces the risk for Bronchiolitis obliterans syndrome (BOS) after lung transplantation. *Transplantation* **81**, 1415–1420 (2006).

105. Snyder, L. D. *et al.* Cytomegalovirus pneumonitis is a risk for bronchiolitis obliterans syndrome in lung transplantation. *Am. J. Respir. Crit. Care Med.* **181**, 1391–1396 (2010).

106. Billings, J. L., Hertz, M. I., Savik, K. & Wendt, C. H. Respiratory viruses and chronic rejection in lung transplant recipients. *J. Hear. Lung Transplant.* **21**, 559–566 (2002).

107. Kumar, D. *et al.* Clinical impact of community-acquired respiratory viruses on bronchiolitis obliterans after lung transplant. *Am. J. Transplant.* **5**, 2031–2036 (2005).

108. Botha, P. *et al.* Pseudomonas aeruginosa colonization of the allograft after lung transplantation and the risk of bronchiolitis obliterans syndrome. *Transplantation* **85**, 771–774 (2008).

109. Weigt, S. S. *et al.* Aspergillus colonization of the lung allograft is a risk factor for bronchiolitis obliterans syndrome. *Am. J. Transplant.* **9**, 1903–1911 (2009).

110. Nawrot, T. S. *et al.* The impact of traffic air pollution on bronchiolitis obliterans syndrome and mortality after lung transplantation. *Thorax* **66**, 748–754 (2011).

111. Bhinder, S. *et al.* Air pollution and the development of posttransplant chronic lung allograft dysfunction. *Am. J. Transplant.* **14**, 2749–2757 (2014).

112. Palmer, S. M. *et al.* The role of innate immunity in acute allograft rejection after lung transplantation. *Am. J. Respir. Crit. Care Med.* **168**, 628–632 (2003).

113. Boehler, A. & Estenne, M. Post-transplant bronchiolitis obliterans. *Eur. Respir. J.* **22**, 1007–1018 (2003).

114. Palmer, S. M. *et al.* Innate immunity influences long-term outcomes after human lung transplant. *Am. J. Respir. Crit. Care Med.* **171**, 780–785 (2005).

115. Stewart, S. *et al.* Revision of the 1996 working formulation for the standardization of nomenclature in the diagnosis of lung rejection. *J. Hear. Lung Transplant.* **26**, 1229–1242 (2007).

116. Elssner A., V. C. The role of neutrophils in the pathogenesis of obliterative bronchiolitis after lung transplantation. *Transpl Infect Dis* **3**, 168–176 (2001).

117. Cagnone, M. *et al.* A pilot study to investigate the balance between proteases and α1-antitrypsin in bronchoalveolar lavage fluid of lung transplant recipients. *High-Throughput* **8**, 1–15 (2019).

118. Royer, P. J. *et al.* Chronic lung allograft dysfunction: A systematic review of mechanisms. *Transplantation* **100**, 1803–1814 (2016).

119. Ofek, E. *et al.* Restrictive allograft syndrome post lung transplantation is characterized by pleuroparenchymal fibroelastosis. *Mod. Pathol.* **26**, 350–356 (2013).

120. Verleden S. E., Ruttens D., Vandermeulen E., Vaneylen A., Dupont L. J., Van Raemdonck D. E., Verleden G. M., Vanaudenaerde B. M., V. R. Bronchiolitis obliterans syndrome and restrictive allograft syndrome: do risk factors differ? *Transplantation* **95**, 1167–1172 (2013).

121. Glanville, A. R. *et al.* Chronic lung allograft dysfunction: Definition and update of restrictive allograft syndrome—A consensus report from the Pulmonary Council of the ISHLT. *J. Hear. Lung Transplant.* **38**, 483–492 (2019).

122. Berastegui, C. *et al.* Use of serum KL-6 level for detecting patients with restrictive allograft syndrome after lung transplantation. *PLoS One* **15**, 1–14 (2020).

123. Budding, K. Chronic lung allograft dysfunction after lung transplantation. Novel insights into immunological mechanisms. (2016).

124. Verleden, G. M. *et al.* Current views on chronic rejection after lung transplantation. *Transpl. Int.* **28**, 1131–1139 (2015).

125. Hayes, D. A review of bronchiolitis obliterans syndrome and therapeutic strategies. *J. Cardiothorac. Surg.* **6**, 92 (2011).

126. Estenne, M. *et al.* Bronchiolitis obliterans syndrome 2001: An update of the diagnostic criteria. *J. Hear. Lung Transplant.* **21**, 297–310 (2002).

127. Sato, M. *et al.* Revisiting the pathologic finding of diffuse alveolar damage after lung transplantation. *J. Hear. Lung Transplant.* **31**, 354–363 (2012).

128. Bankier A. A., Van Muylem A., Knoop C., Estenne M., G. P. A. Bronchiolitis obliterans syndrome in heart-lung transplant recipients: diagnosis with expiratory CT. *Radiology* **218**, 533–539 (2001).

129. Verleden, S. E. *et al.* The site and nature of airway obstruction after lung transplantation. *Am. J. Respir. Crit. Care Med.* **189**, 292–300 (2014).

130. Meyer, K. C. *et al.* An international ISHLT/ATS/ERS clinical practice guideline: Diagnosis and management of bronchiolitis obliterans syndrome. *Eur. Respir. J.* **44**, 1479–1503 (2014).

131. Gerhardt, S. G. *et al.* Maintenance azithromycin therapy for bronchiolitis obliterans syndrome: Results of a pilot study. *Am. J. Respir. Crit. Care Med.* **168**, 121–125 (2003).

132. Vos, R. *et al.* Long-term azithromycin therapy for bronchiolitis obliterans syndrome : Divide and conquer ? *J. Hear. Lung Transplant.* **29**, 1358–1368 (2010).

133. Vos, R. *et al.* Azithromycin in posttransplant bronchiolitis obliterans syndrome. *Chest* **139**, 1246 (2011).

134. Federica, M. *et al.* Clinical and immunological evaluation of 12-month azithromycin therapy in chronic lung allograft rejection. *Clin. Transplant.* **25**, 381–389 (2011).

135. Vos, R. *et al.* A randomised controlled trial of azithromycin to prevent chronic rejection after lung transplantation. *Eur. Respir. J.* **37**, 164–172 (2011).

136. Vos, R. *et al.* Anti-inflammatory and immunomodulatory properties of azithromycin involved in treatment and prevention of chronic lung allograft rejection. *Transplantation* **94**, 101–109 (2012).

137. Corris, P. A. *et al.* A randomised controlled trial of azithromycin therapy in bronchiolitis obliterans syndrome (BOS) post lung transplantation. *Thorax* **70**, 442–450 (2015).

138. Suwara, M. I. *et al.* Mechanistic differences between phenotypes of chronic lung allograft dysfunction after lung transplantation. *Transpl. Int.* **27**, 857–867 (2014).

139. Verleden, G. M. *et al.* Are we near to an effective drug treatment for bronchiolitis obliterans? *Expert Opin. Pharmacother.* **15**, 2117–2120 (2014).

140. Fisher, A. J. *et al.* The safety and efficacy of total lymphoid irradiation in progressive bronchiolitis obliterans syndrome after lung transplantation. *Am. J. Transplant.* **5**, 537–543 (2005).

141. Jaksch, P. *et al.* A prospective interventional study on the use of extracorporeal photopheresis in patients with bronchiolitis obliterans syndrome after lung transplantation. *J. Hear. Lung Transplant.* **31**, 950–957 (2012).

142. Shino, M. Y. *et al.* CXCR3 ligands are associated with the continuum of diffuse alveolar damage to chronic lung allograft dysfunction. *Am. J. Respir. Crit. Care Med.* **188**, 1117–1125 (2013).

143. Paraskeva, M. *et al.* Acute fibrinoid organizing pneumonia after lung transplantation. *Am. J. Respir. Crit. Care Med.* **187**, 1360–1368 (2013).

144. Meyer, K. C., Bierach J., Kanne J., R. Torrealba J. R., and D. O. N. C. Acute fibrinous and organising pneumonia following lung transplantation is associated with severe allograft dysfunction and poor outcome: a case series. *pneumonia* **6**, 67–76 (2015).

145. Costa A. N., Carraro R. M., Nascimento E. C., Junior J. E., Campos S. V., de Camargo P. C., Teixeira R. H., Samano M. N., Fernandes L. M., Abdalla L. G., D. M. Acute fibrinoid organizing pneumonia in lung transplant: The most feared allograft dysfunction. *Transplantation* **100**, e11–e12 (2016).

146. Dubbeldam, A. *et al.* Restrictive allograft syndrome after lung transplantation: new radiological insights. *Eur. Radiol.* **27**, 2810–2817 (2017).

147. Verleden, S. E. *et al.* Functional and computed tomographic evolution and survival of restrictive allograft syndrome after lung transplantation. *J. Hear. Lung Transplant.* **33**, 270–277 (2014).

148. Ho, S. *et al.* The mechanism of action of cyclosporin A and FK506. *Clin. Immunol. Immunopathol.* **80**, S40–S45 (1996).

149. Hahn, B. H. & King, J. K. *Treatment of Autoimmune Disease: Established Therapies*. *The Autoimmune Diseases: Fifth Edition* (Elsevier Inc., 2013). doi:10.1016/B978-0-12-384929-8.00080-0

150. Mele, T.S., Halloran, P. F. The use of mycophenolate mofetil in transplant recipients. *Immunopharmacology* **47**, 215–245 (2000).

151. Dowling, R. J. O., Topisirovic, I., Fonseca, B. D. & Sonenberg, N. Dissecting the role of mTOR: Lessons from mTOR inhibitors. *Biochim. Biophys. Acta - Proteins Proteomics* **1804**, 433–439 (2010).

152. Smith, L. Corticosteroids in Solid Organ Transplantation: Update and Review of the Literature. *J. Pharm. Pract.* **16**, 380–387 (2003).

153. Barnes, P. J., Karin, M. Nuclear factor-kappaB: a pivotal transcription factor in chronic inflammatory diseases. *N. Engl. J. Med.* **336**, 1066–1071 (1997).

154. Ojo, A. O. *et al.* Comparison of the long-term outcomes of kidney transplantation: USA versus Spain. *Nephrol. Dial. Transplant.* **28**, 213–220 (2013).

155. Adam, R. *et al.* 2018 Annual Report of the European Liver Transplant Registry (ELTR) – 50-year evolution of liver transplantation. *Transpl. Int.* **31**, 1293–1317 (2018).

156. Khush, K. K. *et al.* The International Thoracic Organ Transplant Registry of the International Society for Heart and Lung Transplantation: Thirty-sixth adult heart transplantation report — 2019; focus theme: Donor and recipient size match. *J. Hear. Lung Transplant.* **38**, 1056–1066 (2019).

157. Gruessner, A. C. & Gruessner, R. W. G. Long-term outcome after pancreas transplantation: a registry analysis. *Curr. Opin. Organ Transplant.* **21**, 377–385 (2016).

158. Grant, D. *et al.* Intestinal transplant registry report: Global activity and trends. *Am. J. Transplant.* **15**, 210–219 (2015).

159. Burton, C. M. *et al.* Long-term survival after lung transplantation depends on development and severity of bronchiolitis obliterans syndrome. *J. Hear. Lung Transplant.* **26**, 681–686 (2007).

160. Copeland, C. A. F. *et al.* Survival after bronchiolitis obliterans syndrome among bilateral lung transplant recipients. *Am. J. Respir. Crit. Care Med.* **182**, 784–789 (2010).

161. Kulkarni, H. S. *et al.* Bronchiolitis obliterans syndrome–free survival after lung transplantation: An International Society for Heart and Lung Transplantation Thoracic Transplant Registry analysis. *J. Hear. Lung Transplant.* **38**, 5–16 (2019).

162. Ojo, A. O. *et al.* Chronic renal failure after transplantation of a nonrenal organ. *N. Engl. J. Med.* **349**, 931–940 (2003).

163. Post, D. J., Douglas, D. D. & Mulligan, D. C. Immunosuppression in liver transplantation. *Liver Transplant.* **11**, 1307–1314 (2005).

164. Dantal, J. *et al.* Effect of long-term immunosuppression in kidney-graft recipients on cancer incidence: randomised comparison of two cyclosporin regimens. *Lancet* **351**, 623–628 (1998).

165. Bamgbola, O. Metabolic consequences of modern immunosuppressive agents in solid organ transplantation. *Ther. Adv. Endocrinol. Metab.* **7**, 110–127 (2016).

166. Lechler, R. I., Garden, O. A. & Turka, L. A. The complementary roles of deletion and regulation in transplantation tolerance. *Nat. Rev. Immunol.* **3**, 147–158 (2003).

167. Billingham, R. E., Brent, L., Medawar, P. B. 'Actively acquired tolerance' of foreign cells. *Nature* **172**, 603–606 (1953).

168. Kingsley, C. I., Nadig, S. N. & Wood, K. J. Transplantation tolerance: lessons from experimental rodent models. *Transpl. Int.* **20**, 828–841 (2007).

169. Jovanovic, V., Lair, D., Soulillou, J. P. & Brouard, S. Transfer of tolerance to heart and kidney allografts in the rat model. *Transpl. Int.* **21**, 199–206 (2008).

170. Chandrasekharan, D., Issa, F. & Wood, K. J. Achieving operational tolerance in transplantation: How can lessons from the clinic inform research directions? *Transpl. Int.* **26**, 576–589 (2013).

171. Orlando, G., Soker, S. & Wood, K. Operational tolerance after liver transplantation. *J. Hepatol.* **50**, 1247–1257 (2009).

172. Salisbury, E. M., Game, D. S. & Lechler, R. I. Transplantation tolerance. *Pediatr. Nephrol.* **29**, 2263–2272 (2014).

173. Roussey-Kesler, G. *et al.* Clinical operational tolerance after kidney transplantation. *Am. J. Transplant.* **6**, 736–746 (2006).

174. Ashton-Chess, J., Giral, M., Brouard, S. & Soulillou, J. P. Spontaneous operational tolerance after immunosuppressive drug withdrawal in clinical renal allotransplantation. *Transplantation* **84**, 1215–1219 (2007).

175. Brouard, S. *et al.* The natural history of clinical operational tolerance after kidney transplantation through twenty-seven cases. *Am. J. Transplant.* **12**, 3296–3307 (2012).

176. Svendsen, U. G. *et al.* Transplantation of a lobe of lung from mother to child following previous transplantation with maternal bone marrow. *Eur. Respir. J.* **8**, 334–337 (1995).

177. Comerci, G. D., Williams, T. M. & Kellie, S. Immune tolerance after total lymphoid irradiation for heart transplantation: immunosuppressant-free survival for 8 years. *J. Hear. Lung Transplant.* **28**, 743–745 (2009).

178. Aguirre O., Houlihan B., Fishbein T., K. A. Immunomonitoring of operational tolerance in intestinal transplantation. *Am. J. Transplant.* **17**, suppl 3 (2017).

179. Biomarkers Definitions Working G. Biomarkers and surrogate endpoints: preferred definitions and conceptual framework. *Clin. Pharmacol. Ther.* **69**, 89–95 (2001).

180. Horwitz, P. A. *et al.* Detection of cardiac allograft rejection and response to immunosuppressive therapy with peripheral blood gene expression. *Circulation* **110**, 3815–3821 (2004).

181. Louis, S. *et al.* Contrasting CD25hiCD4+T cells/FOXP3 patterns in chronic rejection and operational drug-free tolerance. *Transplantation* **81**, 398–407 (2006).

182. Pons, A. *et al.* FoxP3 in peripheral blood is associated with operational tolerance in liver transplant patients during immunosuppression withdrawal. *Clin. Transplant.* **86**, 1370–1378 (2008).

183. Sagoo, P. *et al.* Development of a cross-platform biomarker signature to detect renal transplant tolerance in humans. *J. Clin. Invest.* **120**, 1848–1861 (2010).

184. Newell, K. *et al.* Identification of a B cell signature associated with renal transplant tolerance in humans. *J. Clin. Invest.* **120**, 1836–1847 (2010).

185. Lozano, J. J. *et al.* Comparison of transcriptional and blood cell-phenotypic markers between operationally tolerant liver and kidney recipients. *Am. J. Transplant.* **11**, 1916–1926 (2011).

186. Moreso, F. *et al.* Gene expression signature of tolerance and lymphocyte subsets in stable renal transplants: Results of a cross-sectional study. *Transpl. Immunol.* **31**, 11–16 (2014).

187. Baron, D. *et al.* A common gene signature across multiple studies relate biomarkers and functional regulation in tolerance to renal allograft. *Kidney Int.* **87**, 984–995 (2015).

188. Rebollo-Mesa, I. *et al.* Biomarkers of tolerance in kidney transplantation: are we predicting tolerance or response to immunosuppressive treatment? *Am. J. Transplant.* **16**, 3443–3457 (2016).

189. Li, Y. *et al.* Analyses of peripheral blood mononuclear cells in operational tolerance after pediatric living donor liver transplantation. *Am. J. Transplant.* **4**, 2118–2125 (2004).

190. Martínez-Llordella, M. *et al.* Multiparameter immune profiling of operational tolerance in liver transplantation. *Am. J. Transplant.* **7**, 309–319 (2007).

191. Mazariegos, G. V. *et al.* Dendritic cell subset ratio in peripheral blood correlates with successful withdrawal of immunosuppression in liver transplant patients. *Am. J. Transplant.* **3**, 689–696 (2003).

192. Martínez-Llordella, M. *et al.* Using transcriptional profiling to develop a diagnostic test of operational tolerance in liver transplant recipients. *J. Clin. Invest.* **118**, 2845–2857 (2008).

193. Li, L. *et al.* A common peripheral blood gene set for diagnosis of operational tolerance in pediatric and adult liver transplantation. *Am. J. Transplant.* **12**, 1218–1228 (2012).

194. Heidt S., Wood K. J., P. D. Biomarkers of operational tolerance in solid organ transplantation. *Expert Opin Med Diagn* **6**, 281–293 (2012).

195. De Perrot, M. *et al.* Twenty-year experience of lung transplantation at a single center: influence of recipient diagnosis on long-term survival. *J. Thorac. Cardiovasc. Surg.* **127**, 1493–1501 (2004).

196. Sithamparanathan, S. *et al.* Observational study of lung transplant recipients surviving 20 years. *Respir. Med.* **117**, 103–108 (2016).

197. Fakhro, M. *et al.* 25-year follow-up after lung transplantation at Lund University Hospital in Sweden: superior results obtained for patients with cystic fibrosis. *Interact. Cardiovasc. Thorac. Surg.* **23**, 65–73 (2016).

198. Blitzer, D. *et al.* Long term survival after lung transplantation: a single center experience. *J. Card. Surg.* **35**, 273–278 (2019).

199. Clariom™ D solutions for human, mouse, and rat. Datasheet. Available at: https://tools.thermofisher.com/content/sfs/brochures/EMI07313-2_DS_Clariom-D_solutions_HMR.pdf.

200. Gentleman R., Carey V., Huber W., Irizarry R., D. S. Bioinformatics and Computational Biology Solutions using R and Bioconductor. in *Springer* (2005).

201. Irizarry, R. A. *et al.* Exploration, normalization, and summaries of high density oligonucleotide array probe level data. *Biostatistics* **4**, 249–264 (2003).

202. Smyth, G. K. Linear models and empirical bayes methods for assessing differential expression in microarray experiments. *Stat. Appl. Genet. Mol. Biol.* **3**, (2004).

203. Benjamini, Yoav ; Hochberg, Y. Controlling the False Discovery Rate: a Practical and Powerful Approach to Multiple Testing. *J. R. Stat. Soc. Ser. B* **57**, 289–300 (1995).

204. Fabregat, A. *et al.* The Reactome Pathway Knowledgebase. *Nucleic Acids Res.* **46**, D649–D655 (2018).

205. Jirapech-Umpai, T. & Aitken, S. Feature selection and classification for microarray data analysis: evolutionary methods for identifying predictive genes. *BMC Bioinformatics* **6**, 1–11 (2005).

206. Díaz-Uriarte, R. & Alvarez de Andrés, S. Gene selection and classification of microarray data using random forest. *BMC Bioinformatics* **7**, 1–13 (2006).

207. Baker, S. G. & Kramer, B. S. Identifying genes that contribute most to good classification in microarrays. *BMC Bioinformatics* **7**, 1–7 (2006).

208. Foster, K. R., Koprowski, R. & Skufca, J. D. Machine learning, medical diagnosis, and biomedical engineering research - commentary. *Biomed. Eng. Online* **13**, 1–9 (2014).

209. Pérez-Ortiz M., Cruz-Ramírez M., Fernández-Caballero J. C., H.-M. C. Hybrid multi-objective machine learning classification in liver transplantation. *Hybrid Artif. Intell. Syst.* **7208**, 397–408 (2012).

210. Yue, W., Wang, Z., Chen, H., Payne, A. & Liu, X. Machine learning with applications in breast cancer diagnosis and prognosis. *Designs* **2**, 1–17 (2018).

211. Vihinen, M. How to evaluate performance of prediction methods? Measures and their interpretation in variation effect analysis. *BMC Genomics* **13 Suppl 4**, S2 (2012).

212. Azuaje F. *Bioinformatics and Biomarker Discovery: 'Omic' Data Analysis for Personalized Medicine.* (2010).

213. Shalev-Shwartz S., B.-D. S. *Understanding machine learning :from theory to algorithms*. (2014).

214. Slawski M., Boulesteix A. L., B. C. CMA: Synthesis of microarray-based classification. R package version 1.28.1. (2009).

215. Fawcett, T. An introduction to ROC analysis. *Pattern Recognit. Lett.* **27**, 861–874 (2006).

216. Vandesompele, J. *et al.* Accurate normalization of real-time quantitative RT-PCR data by geometric averaging of multiple internal control genes. *Genome Biol.* **3**, 1–12 (2002).

217. Livak, K. J. & Schmittgen, T. D. Analysis of relative gene expression data using real-time quantitative PCR and the 2-ΔΔCT method. *Methods* **25**, 402–408 (2001).

218. GeneChip® miRNA 4.0 Array. Datasheet. Available at: https://assets.thermofisher.com/TFS-Assets/LSG/brochures/miRNA_4-0_and_4-1_datasheet.pdf.

219. Cannell, I. G., Kong, Y. W. & Bushell, M. How do microRNAs regulate gene expression? *Biochem. Soc. Trans.* **36**, 1224–1231 (2008).

220. Ru, Y. *et al.* The multiMiR R package and database: integration of microRNA-target interactions along with their disease and drug associations. *Nucleic Acids Res.* **42**, e133 (2014).

221. Rohart, F., Gautier, B., Singh, A. & Lê Cao, K. A. mixOmics: An R package for omics feature selection and multiple data integration. *PLoS Comput. Biol.* **13**, 1–19 (2017).

222. Lee, H. K., Hsu, A. K., Sajdak, J., Qin, J. & Pavlidis, P. Coexpresion analysis of human genes across many microarray data sets. *Genome Res.* **14**, 1085–1094 (2004).

223. Singh, A. Blood biomarker panels of the late phase asthmatic response. (The University of British Columbia (Vancouver), 2016).

224. Kohavi, R. Wrappers for performance enhancement and oblivious decision graphs. (Standford University, Stanford, CA, USA, 1996).

225. Singh, A., Gautier, B., Shannon, C. P., Vacher, M., Rohart, F., Tebbutt, S. J., Lê Cao, K. DIABLO: from multi-omics assays to biomarker discovery, an integrative approach. *bioRxiv. Cold Spring Harb. Labs Journals* (2017).

226. Godon, J. J., Zumstein, E., Dabert, P., Habouzit, F. & Moletta, R. Molecular microbial diversity of an anaerobic digestor as determined by small-subunit rDNA sequence analysis. *Appl. Environ. Microbiol.* **63**, 2802–2813 (1997).

227. Santiago, A. *et al.* Alteration of the serum microbiome composition in cirrhotic patients with ascites. *Sci. Rep.* **6**, 1–9 (2016).

228. Caporaso, J. G. *et al.* Ultra-high-throughput microbial community analysis on the Illumina HiSeq and MiSeq platforms. *ISME J.* **6**, 1621–1624 (2012).

229. Wu, Y. Barcode demultiplex for Illumina I1, R1, R2 fastq.gz files. (2014).

230. Callahan, B. J. *et al.* DADA2: High-resolution sample inference from Illumina amplicon data. *Nat. Methods* **13**, 581–583 (2016).

231. Callahan, B. Silva taxonomic training data formatted for DADA2 (Silva version 132) [Data Set]. (2018).

232. McMurdie, P. J. & Holmes, S. Phyloseq: An R Package for Reproducible Interactive Analysis and Graphics of Microbiome Census Data. *PLoS One* **8**, (2013).

233. Callahan, B. J., Sankaran, K., Fukuyama, J. A. McMurdie, P. J., Holmes, S. P. Bioconductor Workflow for Microbiome Data Analysis: from raw reads to community analyses [version 2; peer review: 3 approved]. *F1000Research* **5**, (2016).

234. Wright, E. S. Using DECIPHER v2.0 to analyze big biological sequence data in R. *R J.* **8**, 352–359 (2016).

235. Schliep, K. P. phangorn: phylogenetic analysis in R. *Bioinformatics* **27**, 592–593 (2011).

236. Palarea-Albaladejo, J. & Martín-Fernández, J. A. ZCompositions - R package for multivariate imputation of left-censored data under a compositional approach. *Chemom. Intell. Lab. Syst.* **143**, 85–96 (2015).

237. Gloor, G. B., Wu, J. R., Pawlowsky-Glahn, V. & Egozcue, J. J. It's all relative: analyzing microbiome data as compositions. *Ann. Epidemiol.* **26**, 322–329 (2016).

238. Gloor, G. B. & Reid, G. Compositional analysis: a valid approach to analyze microbiome high-throughput sequencing data. *Can. J. Microbiol.* **62**, 692–703 (2016).

239. Templ, M., Hron, K. & Filzmoser, P. *robCompositions: an R-package for robust statistical analysis of compositional data*. *Compositional Data Analysis: Theory and Applications* (2011). doi:10.1002/9781119976462.ch25

240. Oksanen J., Blanchet, F. G., Friendly, M., Kindt, R., Legendre, P., McGlinn, D., Minchin, P. R., O'Hara, R. B., Simpson, G. L., Solymos, P., Stevens, M. H. H., Szoecs, E., and Wagner, H. vegan: Community Ecology Package. R package version 2.5-5. (2019).

241. R Core Team. R: A language and environment for statistical computing. R Foundation for Statistical Computing. (2018).

242. Wickham, H. *ggplot2: elegant graphics for data analysis*. (2016).

243. Riou, M. *et al.* Impact of diabetes mellitus on survival and hospitalization after lung transplantation. *Eur. Respir. J.* **48**, PA4645 (2016).

244. Cardenas, M. E., Cutler, N. S., Lorenz, M. C., Di Como, C. J. & Heitman, J. The TOR signaling cascade regulates gene expression in response to nutrients. *Genes Dev.* **13**, 3271–3279 (1999).

245. Ha, M. & Kim, V. N. Regulation of microRNA biogenesis. *Nat. Rev. Mol. Cell Biol.* **15**, 509–524 (2014).

246. Yuan, D. *et al.* Enrichment analysis identifies functional microRNA-disease associations in humans. *PLoS One* **10**, 1–16 (2015).

247. Mas, V. R., Dumur, C. I., Scian, M. J., Gehrau, R. C. & Maluf, D. G. MicroRNAs as biomarkers in solid organ transplantation. *American Journal of Transplantation* **13**, 11–19 (2013).

248. Ladak, S. S., Ward, C. & Ali, S. The potential role of microRNAs in lung allograft rejection. *J. Hear. Lung Transplant.* **35**, 550–559 (2016).

249. Xu, Z. *et al.* Role of circulating microRNAs in the immunopathogenesis of rejection after pediatric lung transplantation. *Transplantation* **101**, 2461–2468 (2017).

250. Farid, W. R. R., Pan, Q., Van der Meer, A. J. P., de Ruiter, P. E., Ramakrishnaiah, V., de Jonge, J., Kwekkeboom, J., Janssen, H. L. A. & Metselaar, H. J., Tilanus, H. W., Kazemier, G., Van der Laan, L. J. W. Hepatocyte-derived microRNAs as serum biomarkers of hepatic injury and rejection after liver transplantation. *Liver Transplant.* **18**, 290–297 (2012).

251. Wang, K. *et al.* miR-194 inhibits innate antiviral immunity by targeting FGF2 in influenza H1N1 virus infection. *Front. Microbiol.* **8**, 1–10 (2017).

252. Gimondi, S. *et al.* Circulating miRNA panel for prediction of acute graft-versus-host disease in lymphoma patients undergoing matched unrelated hematopoietic stem cell transplantation. *Exp. Hematol.* **44**, 624–634 (2016).

253. Chen, L., Tang, Y., Wang, J., Yan, Z. & Xu, R. miR-421 induces cell proliferation and apoptosis resistance in human nasopharyngeal carcinoma via downregulation of FOXO4. *Biochem. Biophys. Res. Commun.* **435**, 745–750 (2013).

254. Cheng, X. *et al.* Exploring the potential value of miR-148b-3p, miR-151b and miR-27b-3p as biomarkers in acute ischemic stroke. *Biosci. Rep.* **38**, 1–8 (2018).

255. Li, J. *et al.* Death receptor 6 is a novel plasmacytoid dendritic cell-specific receptor and modulates type I interferon production. *Protein Cell* **7**, 291–294 (2016).

256. Klíma, M., Broučková, A., Koc, M. & Anděra, L. T-cell activation triggers death receptor-6 expression in a NF-κB and NF-AT dependent manner. *Mol. Immunol.* **48**, 1439–1447 (2011).

257. Cao, W. *et al.* Plasmacytoid dendritic cell-specific receptor ILT7-FcεRIγ inhibits Toll-like receptor-induced interferon production. *J. Exp. Med.* **203**, 1399–1405 (2006).

258. Li, H. & Shi, B. Tolerogenic dendritic cells and their applications in transplantation. *Cell. Mol. Immunol.* **12**, 24–30 (2015).

259. Rogers, N. M., Isenberg, J. S. & Thomson, A. W. Plasmacytoid dendritic cells: no longer an enigma and now key to transplant tolerance? *Am. J. Transplant.* **13**, 1125–1133 (2013).

260. Abe, M., Wang, Z., De Creus, A. & Thomson, A. W. Plasmacytoid dendritic cell precursors induce allogeneic T-cell hyporesponsiveness and prolong heart graft survival. *Am. J. Transplant.* **5**, 1808–1819 (2005).

261. Ochando, J. C. *et al.* Alloantigen-presenting plasmacytoid dendritic cells mediate tolerance to vascularized grafts. *Nat. Immunol.* **7**, 652–662 (2006).

262. Campos-Mora, M., Morales, R. A., Gajardo, T., Catalán, D. & Pino-Lagos, K. Neuropilin-1 in transplantation tolerance. *Front. Immunol.* **4**, 1–9 (2013).

263. Campos-Mora, M. *et al.* CD4+Foxp3+T regulatory cells promote transplantation tolerance by modulating effector CD4+ T cells in a neuropilin-1-dependent manner. *Front. Immunol.* **10**, 1–15 (2019).

264. Yadav, M. *et al.* Neuropilin-1 distinguishes natural and inducible regulatory T cells among regulatory T cell subsets in vivo. *J. Exp. Med.* **209**, 1713–1722 (2012).

265. Yuan, Q. *et al.* CD4+CD25-Nrp1+ T cells synergize with rapamycin to prevent murine cardiac allorejection in immunocompetent recipients. *PLoS One* **8**, 1–8 (2013).

266. Zhou, H. *et al.* Expression of Neuropilin-1 in kidney graft biopsies: what is the significance? *Transplant. Proc.* **39**, 81–83 (2007).

267. Le Cabec, V. & Maridonneau-Parini, I. Annexin 3 is associated with cytoplasmic granules in neutrophils and monocytes and translocates to the plasma membrane in activated cells. *Biochem. J.* **303**, 481–487 (1994).

268. Song, F. *et al.* The frontline of immune response in peripheral blood. *PLoS One* **12**, 1–22 (2017).

269. Heijink, I. H. *et al.* Metalloproteinase profiling in lung transplant recipients with good outcome and bronchiolitis obliterans syndrome. *Transplantation* **99**, 1946–1952 (2015).

270. Legrand, D., Elass, E., Carpentier, M. & Mazurier, J. Interactions of lactoferrin with cells involved in immune function. *Biochem. Cell Biol.* **84**, 282–290 (2006).

271. TCN1 transcobalamin 1 [Homo sapiens (human)] National Center for Biotechnology Information. (2020).

272. Clemmensen, S. N. *et al.* Olfactomedin 4 defines a subset of human neutrophils. *J. Leukoc. Biol.* **91**, 495–500 (2012).

273. Dorr, C. *et al.* Differentially Expressed Gene Transcripts Using RNA Sequencing from the Blood of Immunosuppressed Kidney Allograft Recipients. *PLoS One* **10**, 1–14 (2015).

274. Xu, Z. *et al.* Interleukin-33 levels are elevated in chronic allograft dysfunction of kidney transplant recipients and promotes epithelial to mesenchymal transition of human kidney (HK-2) cells. *Gene* **644**, 113–121 (2018).

275. Brunner, S. M. *et al.* Interleukin-33 prolongs allograft survival during chronic cardiac rejection. *Transpl. Int.* **24**, 1027–1039 (2011).

276. Jordan, S. C. *et al.* Interleukin-6, a cytokine critical to mediation of inflammation, autoimmunity and allograft rejection: therapeutic implications of IL-6 receptor blockade. *Transplantation* **101**, 32–44 (2017).

277. Booth, A. J. *et al.* IL-6 promotes cardiac graft rejection mediated by CD4+ Cells. *J. Immunol.* **187**, 5764–5771 (2011).

278. Hinz, T. *et al.* Identification of the complete expressed human TCR V(γ) repertoire by flow cytometry. *Int. Immunol.* **9**, 1065–1072 (1997).

279. O'Brien, R. L. *et al.* γδ T-cell receptors: functional correlations. *Immunol. Rev.* **215**, 77–88 (2007).

280. Sullivan, L. C. *et al.* The complex existence of γδ T cells following transplantation: the good, the bad and the simply confusing. *Clin. Transl. Immunol.* **8**, 1–10 (2019).

281. Malone, F., Carper, K., Reyes, J. & Li, W. γδT cells are involved in liver transplant tolerance. *Transplant. Proc.* **41**, 233–235 (2009).

282. DeFina, R. A. *et al.* Analysis of immunoglobulin and T-cell receptor gene deficiency in graft rejection by gene expression profiles. *Transplantation* **77**, 580–586 (2004).

283. Kimura, N. *et al.* Potential role of γδ T cell-derived IL-17 in acute cardiac allograft rejection. *Ann. Thorac. Surg.* **94**, 542–548 (2012).

284. Malan Borel, I. *et al.* γδ T cells and interleukin-6 levels could provide information regarding the progression of human renal allograft. *Scand. J. Immunol.* **58**, 99–105 (2003).

285. Koshiba, T. *et al.* Clinical, immunological, and pathological aspects of operational tolerance after pediatric living-donor liver transplantation. *Transpl. Immunol.* **17**, 94–97 (2007).

286. Yu, X. *et al.* Characteristics of Vδ1+ and Vδ2+ γδ T cell subsets in acute liver allograft rejection. *Transpl. Immunol.* **29**, 118–122 (2013).

287. Puig-Pey, I. *et al.* Characterization of γδ T cell subsets in organ transplantation. *Transpl. Int.* **23**, 1045–1055 (2010).

288. Hillhouse, E. E., Delisle, J. S. & Lesage, S. Immunoregulatory CD4- CD8- T cells as a potential therapeutic tool for transplantation, autoimmunity, and cancer. *Front. Immunol.* **4**, 1–10 (2013).

289. Young, K. J., Yang, L., James Phillips, M. & Zhang, L. Donor-lymphocyte infusion induces transplantation tolerance by activating systemic and graft-infiltrating double-negative regulatory T cells. *Blood* **100**, 3408–3414 (2002).

290. Lee, B. P.-L. *et al.* Expression profiling of murine double-negative regulatory T cells suggest mechanisms for prolonged cardiac allograft survival. *J. Immunol.* **174**, 4535–4544 (2005).

291. Juvet, S. C. & Zhang, L. Double negative regulatory T cells in transplantation and autoimmunity: recent progress and future directions. *J. Mol. Cell Biol.* **4**, 48–58 (2012).

292. Haug, T. *et al.* Human double-negative regulatory T-cells induce a metabolic and functional switch in effector T-cells by suppressing mTOR activity. *Front. Immunol.* **10**, 1–14 (2019).

293. Zeiser, R. *et al.* Inhibition of CD4+ CD25+ regulatory T-cell function by calcineurin-dependent interleukin-2 production. *Blood* **108**, 390–400 (2006).

294. O'Sullivan, B. J., Hopkins, P., Trotter, M., Fiene, A., Tan, M., Sinclair, K., C. D. Accumulation of Intragraft CD15s+Tregs in Long-term Lung Transplant Survivors. *J. Hear. Lung Transplant.* **37**, S209 (2018).

295. Wong, K. L. *et al.* Gene expression profiling reveals the defining features of the classical, intermediate,and nonclassical human monocyte subsets. *Blood* **118**, 16–31 (2011).

296. Yang, J., Zhang, L., Yu, C., Yang, X. F. & Wang, H. Monocyte and macrophage differentiation: circulation inflammatory monocyte as biomarker for inflammatory diseases. *Biomark. Res.* **2**, 1–9 (2014).

297. Seidel, U. J. E., Schlegel, P. & Lang, P. Natural killer cell mediated antibody-dependent cellular cytotoxicity in tumor immunotherapy with therapeutic antibodies. *Front. Immunol.* **4**, 1–8 (2013).

298. Benichou, G., Yamada, Y., Aoyama, A., M. J. C. Natural killer cells in rejection and tolerance of solid organ allografts. *Curr Opin Organ Transpl.* **16**, (2011).

299. Calabrese, D. R., Lanier, L. L. & Greenland, J. R. Natural killer cells in lung transplantation. *Thorax* **74**, 397–404 (2019).

300. López-Botet, M. *et al.* Dual role of natural killer cells on graft rejection and control of cytomegalovirus infection in renal transplantation. *Front. Immunol.* **8**, 1–11 (2017).

301. Parkes, M. D., Halloran, P. F. & Hidalgo, L. G. Evidence for CD16a-mediated NK cell stimulation in antibody-mediated kidney transplant rejection. *Transplantation* **101**, e102–e111 (2017).

302. Lawand, M., Déchanet-Merville, J. & Dieu-Nosjean, M. C. Key features of gamma-delta T-cell subsets in human diseases and their immunotherapeutic implications. *Front. Immunol.* **8**, 1–9 (2017).

303. Oberg, H., Wesch, D., Kalyan, S. & Kabelitz, D. Regulatory interactions between neutrophils, tumor cells and T cells. *Front. Immunol.* **10**, 1–15 (2019).

304. Ivetic, A., Green, H. L. H. & Hart, S. J. L-selectin: a major regulator of leukocyte adhesion, migration and signaling. *Front. Immunol.* **10**, 1–22 (2019).

305. Borewicz, K., Pragman, A. A., Kim, H. B., Hertz, M., Wendt, C., Isaacson, R. E. Longitudinal analysis of the lung microbiome in lung transplantation. *FEMS Microbiol Lett* **339**, 57–65 (2013).

306. Kumpitsch, C., Koskinen, K., Schöpf, V. & Moissl-Eichinger, C. The microbiome of the upper respiratory tract in health and disease. *BMC Biol.* **17**, 1–20 (2019).

307. Dickson, R. P., Erb-Downward, J. R. & Huffnagle, G. B. The role of the bacterial microbiome in lung disease. *Expert Rev. Respir. Med.* **7**, 245–257 (2013).

308. Frank, D. N. *et al.* The human nasal microbiota and Staphylococcus aureus carriage. *PLoS One* **5**, (2010).

309. González, I., Déjean, S., Martin, P. G., Baccini, A. CCA: An R package to extend canonical correlation analysis. *J. Stat. Softw.* **23**, 1–14 (2008).

310. González, I., Cao, K. A. L., Davis, M. J. & Déjean, S. Visualising associations between paired 'omics' data sets. *BioData Min.* **5**, 1–23 (2012).

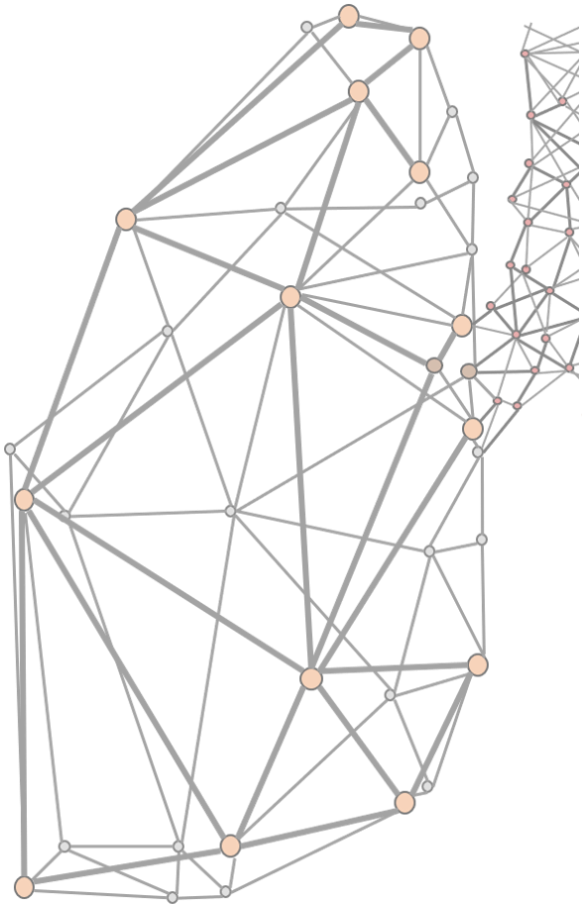

8

SUPPLEMENTARY INFORMATION

List of clinical variables recorded.

- Pre-transplant diagnosis
- Academic degree and working status
- Family support
- Pre-transplant characteristics and functional status
- HLA mismatch
- Characteristics of the transplantation procedure
- PGD
- Need of reintervention
- Complications during Intensive Care Unit stay
- Intensive Care Unit length of stay
- Characteristics at the first protocol bronchoscopy (macroscopic, microscopic, cytological and microbiologic)
- Episodes of infections (bacterial, viral o fungal) and their characteristics
- Episodes of biopsy-proven AR or other immunological complication
- Presence of anti-HLA donor specific antibodies
- Other comorbidities (arterial hypertension, dyslipidemia, diabetes mellitus, osteoporosis, anemia, renal dysfunction, malignancies)
- Duration of intubation
- Immunosuppression protocol
- Respiratory functional tests (first spirometry post-LT, best spirometry post-LT, last spirometry)
- Presence and time to CLAD development
- Laboratory data (hemoglobin, leucocytes, urea, creatine, glomerular filtration rate and cholesterol)
- Time and cause of death.

The results of the analyses of some of the characteristics indicated above have not been shown in the present thesis.

Table S- 1. List of the top 50 differentially expressed genes between LTS and CLAD patients.

Rank position	Gene Symbol	Entrez Gene ID	Gene name	Linear FC LTS vs. CLAD	FDR
1	*ANXA3*	306	Annexin A3	0.514	0.0003
2	*FCGR1B*	2210	Fc fragment of IgG receptor Ib	0.488	0.0008
3	*LILRA4*	23547	Leucocyte immunoglobulin like receptor A4	1.544	0.0025
4	*TNFRSF21*	27242	TNF receptor superfamily member 21	1.387	0.0025
5	*KCNJ2-AS1*	400617	KCNJ2 antisense RNA 1	0.654	0.0025
6	*ACSL1*	2180	Acyl-CoA synthetase long chain family member 1	0.563	0.0025
7	*LRRC6*	23639	Leucine rich repeat containing 6	0.630	0.0025
8	*NRP1*	8829	Neuropilin 1	1.493	0.0032
9	*KCNJ15*	3772	Potassium voltage-gated channel subfamily J member 15	0.565	0.0032
10	*FCGR1CP*	100132417	Fc fragment of IgG receptor Ic, pseudogene	0.568	0.0035
11	*DHRS13*	147015	Dehydrogenase/reductase 13	0.685	0.0035
12	*MGAM2*	93432	Maltase-glucoamylase 2 (putative)	0.522	0.0035
13	*MMP8*	4317	Matrix metallopeptidase 8	0.270	0.0039
14	*BCL6*	604	B cell CLL/lymphoma 6	0.636	0.0046
15	*SLC22A4*	6583	Solute carrier family 22 member 4	0.674	0.0053
16	*DYSF*	8291	Dysferlin	0.578	0.0091
17	*GPR183*	1880	G protein-coupled receptor 183	1.729	0.0091
18	*PROK2*	60675	Prokineticin 2	0.658	0.0112
19	*PNPLA2*	57104	Patatin like phospholipase domain containing 2	0.768	0.0120
20	*PLD4*	122618	phospholipase D family member 4	1.353	0.0159
21	*TLR5*	7100	Toll like receptor 5	0.717	0.0168
22	*ITM2C*	81618	Integral membrane protein 2C	1.499	0.0168
23	*MIR3161*	100423000	MicroRNA 3161	0.655	0.0169
24	*HRH2*	3274	Histamine receptor H2	0.706	0.0169
25	*FCGR2A*	2212	Fc fragment of IgG receptor IIa	0.747	0.0169
26	*LTF*	4057	Lactotransferrin	0.364	0.0169
27	*FCER1A*	2205	Fc fragment of IgE receptor Ia	1.793	0.0169
28	*SLED1*	643036	Proteoglycan 3, pro eosinophil major basic protein 2 pseudogene	0.635	0.0169
29	*KCNJ2*	3759	Potassium inwardly rectifying channel subfamily J member 2	0.617	0.0169
30	*RPS26*	6231	Ribosomal protein S26	2.517	0.0169
31	*MAPK14*	1432	Mitogen-activated protein kinase 14	0.673	0.0169
32	*LIMK2*	3985	LIM domain kinase 2	0.685	0.0169
33	*HCK*	3055	HCK proto-oncogene, Src family tyrosine kinase	0.773	0.0169
34	*DSC2*	1824	Desmocollin 2	0.620	0.0169
35	*SLC2A3*	6515	Solute carrier family 2 member 3	0.678	0.0170
36	*OLR1*	4973	Oxidized low density lipoprotein receptor 1	0.469	0.0175
37	*SH3BP4*	23677	SH3 domain binding protein 4	1.247	0.0184
38	*TGM2*	7052	Transglutaminase 2	0.795	0.0184
39	*CHIT1*	1118	Chitinase 1	0.564	0.0184

Rank position	Gene Symbol	Entrez Gene ID	Gene name	Linear FC LTS vs. CLAD	FDR
40	*FAM41C*	284593	Family with sequence similarity 41 member C	0.689	0.0184
41	*SBNO2*	22904	Strawberry notch homolog 2	0.721	0.0187
42	*SIRPD*	128646	Signal regulatory protein delta	0.753	0.0187
43	*FAM19A1*	407738	TAFA chemokine like family member 1	1.438	0.0187
44	*RPS26P11*	441502	Ribosomal protein S26 pseudogene 11	2.219	0.0188
45	*ALOX5*	240	Arachidonate 5-lipoxygenase	0.726	0.0199
46	*FCGR1A*	2209	Fc fragment of IgG receptor Ia	0.550	0.0205
47	*PFKFB3*	5209	6-phosphofructo-2-kinase/ fructose-2,6-biphosphatase 3	0.716	0.0211
48	*MCEMP1*	199675	Mast cell expressed membrane protein 1	0.605	0.0211
49	*CEACAM6*	4680	CEA cell adhesion molecule 6	0.574	0.0211
50	*GK*	2710	Glycerol kinase	0.652	0.0211

Table S- 2. List of the top 50 differentially expressed miRNAs between LTS and CLAD patients. Analysis included human mature miRNAs, pre-miRNAs, snoRNAs, CDBox RNAs, H/ACA Box RNAs and scaRNAs.

Rank position	miRNA ID	Accession	Linear FC LTS vs. CLAD	p-value	FDR
1	U78	U78	0.573	1.81E-05	1.20E-01
2	ENSG00000212378	ENSG00000212378	0.565	6.73E-05	1.49E-01
3	U78	U78	0.565	6.73E-05	1.49E-01
4	U17b	U17b	0.706	2.41E-04	2.80E-01
5	U75	U75	0.672	2.47E-04	2.80E-01
6	ENSG00000252199	ENSG00000252199	0.854	3.27E-04	2.80E-01
7	U75	U75	0.709	3.71E-04	2.80E-01
8	ACA7B	ACA7B	0.748	4.23E-04	2.80E-01
9	ACA7	ACA7	0.748	4.23E-04	2.80E-01
10	ENSG00000206913	ENSG00000206913	0.748	4.23E-04	2.80E-01
11	U46	U46	0.843	5.48E-04	3.31E-01
12	hsa-mir-548o-2	MI0016746	1.139	7.20E-04	3.98E-01
13	hsa-mir-3142	MI0014166	1.109	8.01E-04	4.09E-01
14	hsa-mir-1973	MI0009983	0,862	1.16E-03	4.98E-01
15	ACA48	ACA48	0,809	1.19E-03	4.98E-01
16	HBI-6	HBI-6	1.103	1.26E-03	4.98E-01
17	U30	U30	0.705	1.29E-03	4.98E-01
18	hsa-miR-223-3p	MIMAT0000280	0.427	1.35E-03	4.98E-01
19	HBII-180C	HBII-180C	0.796	1.67E-03	5.26E-01
20	hsa-miR-27b-3p	MIMAT0000419	0.678	1.73E-03	5.26E-01
21	HBII-251	HBII-251	0.771	1.73E-03	5.26E-01
22	hsa-miR-6734-3p	MIMAT0027370	1.115	1.84E-03	5.26E-01
23	ENSG00000264346	ENSG00000264346	1.114	1.90E-03	5.26E-01
24	ENSG00000200536	ENSG00000200536	1.109	1.96E-03	5.26E-01
25	ENSG00000252438	ENSG00000252438	1.156	2.16E-03	5.26E-01
26	ENSG00000253042	ENSG00000253042	0.899	2.18E-03	5.26E-01
27	ENSG00000221345	ENSG00000221345	1.109	2.20E-03	5.26E-01
28	hsa-miR-1290	MIMAT0005880	0.901	2.38E-03	5.26E-01
29	ENSG00000239098	ENSG00000239098	1.109	2.44E-03	5.26E-01
30	hsa-mir-4461	MI0016807	1.113	2.52E-03	5.26E-01
31	ENSG00000238925	ENSG00000238925	1.087	2.76E-03	5.26E-01
32	U58C	U58C	0.871	2.76E-03	5.26E-01
33	hsa-miR-151b	MIMAT0010214	0.733	2.76E-03	5.26E-01
34	hsa-mir-548h-3	MI0006413	1.107	2.76E-03	5.26E-01
35	hsa-mir-8064	MI0025900	1.155	3.24E-03	5.26E-01
36	hsa-miR-543	MIMAT0004954	0.783	3.51E-03	5.26E-01
37	hsa-mir-3937	MI0016593	1.202	3.52E-03	5.26E-01
38	hsa-miR-1180-3p	MIMAT0005825	1.244	3.58E-03	5.26E-01
39	hsa-miR-4639-5p	MIMAT0019697	1.138	3.64E-03	5.26E-01
40	ACA44	ACA44	0.622	3.66E-03	5.26E-01
41	ENSG00000252840	ENSG00000252840	0.622	3.66E-03	5.26E-01
42	hsa-mir-1287	MI0006349	1.102	3.66E-03	5.26E-01
43	hsa-miR-6808-3p	MIMAT0027517	1.164	3.73E-03	5.26E-01
44	ENSG00000212579	ENSG00000212579	1.142	3.85E-03	5.26E-01
45	hsa-miR-489-5p	MIMAT0026605	0.909	3.87E-03	5.26E-01
46	hsa-miR-4732-3p	MIMAT0019856	1.266	4.08E-03	5.26E-01
47	hsa-let-7a-5p	MIMAT0000062	0.833	4.24E-03	5.26E-01
48	ENSG00000252236	ENSG00000252236	1.100	4.24E-03	5.26E-01
49	hsa-miR-548j-5p	MIMAT0005875	1.097	4.27E-03	5.26E-01
50	U31	U31	0.818	4.28E-03	5.26E-01

Table S- 3. Comparison of the gene expression results obtained by microarrays and RT-qPCR technologies. In order to compare the FC values of both technologies, a transformation of the negative linear FC values (-1/FC) was performed.

Gene Symbol	qPCR Linear FC	qPCR FDR	Microarray Linear FC	Microarray FDR
TNFRSF21	3.478	0	1.387	0.0025
LILRA4	4.231	0	1.544	0.0025
NRP1	2.606	1E-05	1.493	0.0032
ANXA3	-2.463	4E-05	-1.946	0.0003
MMP8	-4.608	0.0003	-3.698	0.0039
FCGR1B	-1.634	0.0004	-2.051	0.0008
LTF	-3.717	0.0007	-2.744	0.0169
TCN1	-2.519	0.0008	-2.334	0.0336
OLFM4	-4.505	0.0022	-2.421	0.0612
ACSL1	-1.661	0.0022	-1.776	0.0025
KCNJ15	-1.745	0.0022	-1.769	0.0032
LRRC6	-1.761	0.0026	-1.588	0.0025
BCL6	-1.56	0.0039	-1.572	0.0046
SLC22A4	-1.631	0.0041	-1.483	0.0053
HCK	-1.244	0.0060	-1.293	0.0169
DHRS13	-1.309	0.0081	-1.459	0.0035
FCGR2A	-1.366	0.0140	-1.339	0.0169
CA4	-1.727	0.0177	-1.353	0.0336
PROK2	-1.464	0.0179	-1.519	0.0112
PNPLA2	-1.252	0.0378	-1.302	0.012
TLR5	-1.193	0.0763	-1.394	0.0168

Table S- 4. Comparison of the miRNA expression results obtained by microarrays and RT-qPCR technologies. Microarray FDR values come from the differential miRNA expression analysis which included human mature miRNAs, pre-miRNAs, snoRNA, CDBox RNAs, H/ACA Box RNAs and scaRNAs.

miRNA ID	qPCR Linear FC	qPCR FDR	Microarray Linear FC	Microarray FDR
hsa-miR-194-5p	-1.436	0.0464	-1.396	0.5930
hsa-miR-151b	-1.316	0.0464	-1.364	0.5256
hsa-miR-26b-5p	-1.436	0.0654	-2.05	0.5811
hsa-miR-421	-1.268	0.0950	-1.434	0.5754
hsa-miR-223-3p	-1.457	0.1117	-2.34	0.4977
hsa-miR-1180-3p	1.106	0.1408	1.244	0.5256
hsa-miR-543	-1.357	0.2190	-1.276	0.5256
hsa-let-7g-5p	-1.106	0.4373	-1.383	0.5256

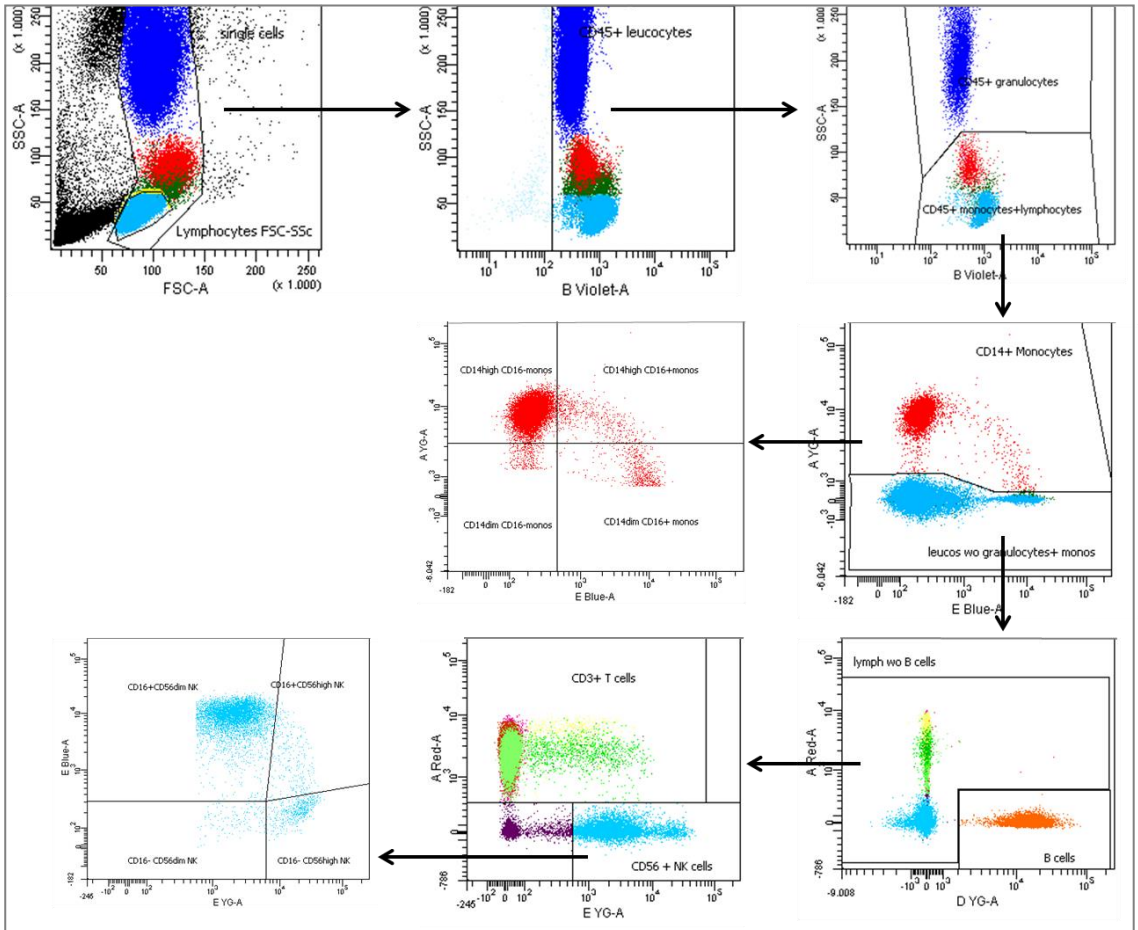

Figure S- 1. Gating strategy for CD14^{high} CD16$^{+/-}$ monocytes and CD56^{+} CD16$^{+/-}$ NK cells in flow cytometry. PBMCs were gated on leucocytes by CD45 staining. Within the CD45^{+} leucocyte population, CD45^{+} monocytes and lymphocytes were identified. CD14^{high} CD16$^{+/-}$ monocytes were gated from the CD14^{+} monocyte population. Within lymphocytes without B cells (gated from the leucocytes without granulocytes and monocytes), NK cells were identified as CD3^{-} CD56^{+} cells and CD56^{+} CD16$^{+/-}$ NK subpopulations were gated from them. Representative data from one patient is shown.

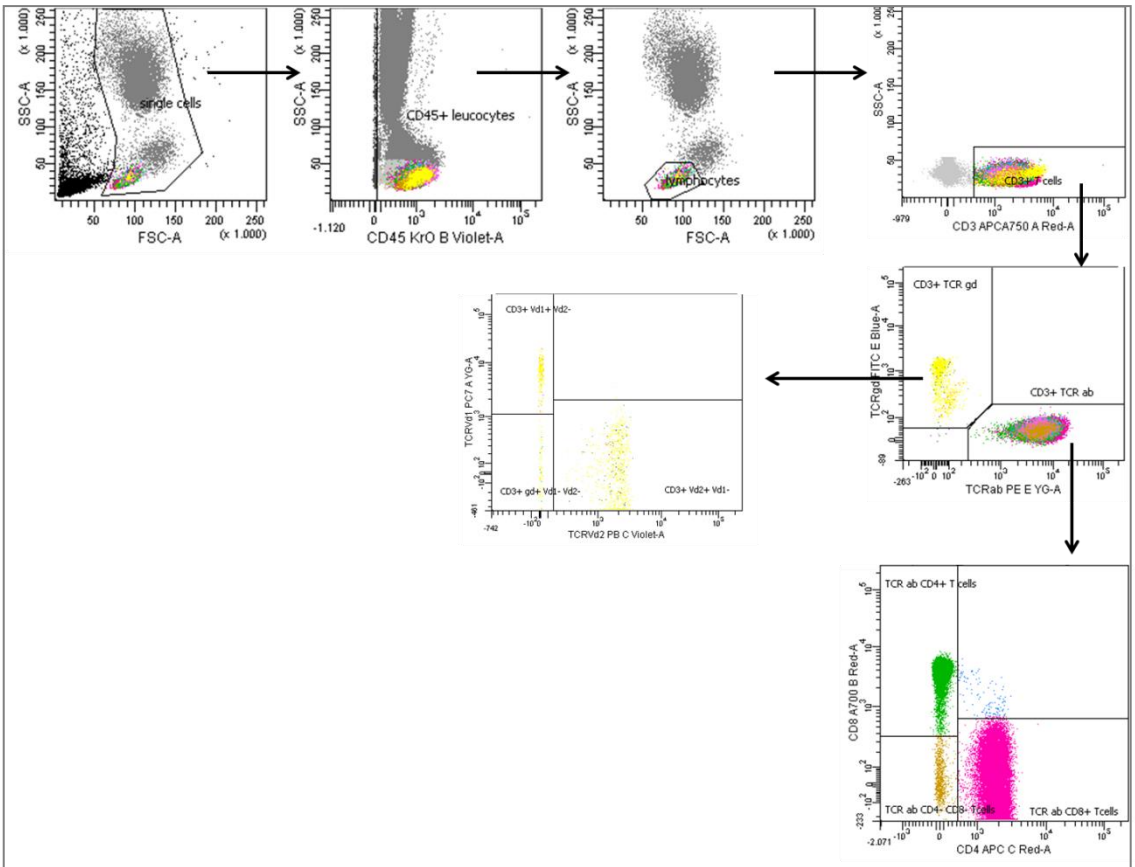

Figure S- 2. Gating strategy for DN and Vδ1$^+$ γδ TCR T cells in flow cytometry. PBMCs were gated on leucocytes by CD45 staining Within the CD45$^+$ leucocyte population, T cells were identified as CD45$^+$ CD3$^+$ population. Within the T cell population, αβ and γδ TCR T cells were identified. Vδ1$^+$ γδ T cells were identified as CD3$^+$ Vδ1$^+$ Vδ2$^-$ from the γδ$^+$ TCR T population whereas DN T cells were identified as CD4$^-$ CD8$^-$ αβ$^+$ TCR from the αβ$^+$ TCR T cell population. Representative data from one patient is shown.

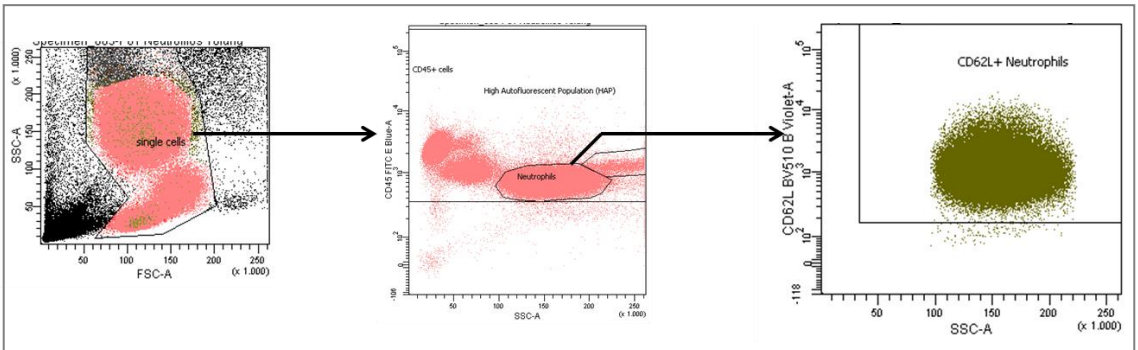

Figure S- 3. Gating strategy for CD62L$^+$ granulocytes in flow cytometry. PBMCs were gated on leucocytes by CD45 staining. CD62L$^+$ granulocytes were identified from CD45$^+$ granulocyte population. Representative data from one patient is shown.

Table S- 5. Percentages of leucocyte subpopulations between LTS and CLAD patients. Comparisons between the two groups were performed employing parametric unpaired t-test or nonparametric Mann-Whitney test, according to data distribution. Variables compared using t-test are presented as mean with SD whereas variables compared using Mann-Whitney test are presented as median with interquartile range. * Immunophenotype of NKT subsets is indicated in Table S- 6.

Cell subpopulation (Basic Panel)	CLAD	LTS	p-value
granulocytes (out of total leucocytes)	61.1 (13.9)	56.1 (11.6)	0.131
Monocytes and lymphocytes (out of total leucocytes)	38.9 (13.9)	43.9 (11.6)	0.133
monocytes (out of total leucocytes)	9.03 (3.02)	8.95 (2.86)	0.911
$CD14^{+}$ $CD16^{+}$ monocytes (out of total monocytes)	12.4 [9.52;16.8]	9.57 [7.13;12.1]	0.025
$CD14^{+}$ $CD16^{-}$ monocytes (out of total monocytes)	87.6 [83.2;90.5]	90.4 [87.9;92.9]	0.025
$CD14^{high}$ $CD16^{-}$ monocytes (out of total monocytes)	85.7 [81.6;87.1]	88.5 [85.1;91.0]	0.046
$CD14^{high}$ $CD16^{+}$ monocytes (out of total monocytes)	6.69 [5.22;11.5]	5.38 [3.94;6.31]	0.009
$CD14^{dim}$ $CD16^{-}$ monocytes (out of total monocytes)	2.01 [1.45;2.58]	1.95 [1.54;2.70]	0.953
$CD14^{dim}$ $CD16^{+}$ monocytes (out of total monocytes)	4.33 [3.16;5.39]	3.79 [2.98;6.02]	0.977
lymphocytes (out of total leucocytes)	28.4 (11.8)	33.2 (10.1)	0.091
B cells (out of total lymphocytes)	4.39 [2.38;7.28]	4.98 [2.67;7.22]	0.678
NK cells (out of total lymphocytes)	8.73 [5.75;17.1]	8.88 [4.62;16.2]	0.531
NK $CD56^{high}$ (out of total NK cells)	8.55 [5.54;12.4]	8.47 [4.71;16.6]	0.608
NK $CD56^{dim}$ (out of total NK cells)	92.6 [88.3;95.7]	91.5 [81.0;95.2]	0.234
$CD56^{+}$ $CD16^{+}$ NK (out of total NK cells)	95.0 [92.8;96.9]	91.2 [84.1;95.1]	0.004
$CD56^{+}$ $CD16^{-}$ NK (out of total NK cells)	5.45 [3.63;7.81]	8.82 [4.95;19.8]	0.020
$CD56^{dim}$ $CD16^{+}$ NK (out of total NK cells)	89.3 [84.5;93.2]	88.3 [77.5;93.1]	0.186
$CD56^{high}$ $CD16^{+}$ NK (out of total NK cells)	4.53 [3.22;8.14]	3.92 [2.15;7.28]	0.298
$CD56^{dim}$ $CD16^{-}$ NK (out of total NK cells)	3.18 [1.39;4.03]	2.65 [1.78;5.09]	0.721
$CD56^{high}$ $CD16^{-}$ NK (out of total NK cells)	3.64 [2.53;4.72]	4.74 [2.89;9.33]	0.052
T cells (out of total lymphocytes)	79.4 [72.7;87.7]	81.1 [75.2;89.2]	0.379
$CD4^{+}$ T cells (out of total T cells)	51.4 (14.1)	54.2 (12.9)	0.419
$CD8^{+}$ T cells (out of total T cells)	42.9 (11.8)	38.6 (10.4)	0.131
NKT cells (out of total T cells)	8.55 [4.14;11.7]	8.99 [7.15;19.2]	0.101
NKT subset 1 (out of total NKT)	73.9 [61.3;79.2]	73.7 [60.2;78.9]	0.637
NKT subset 2 (out of total NKT)	17.7 [8.58;28.1]	13.7 [8.09;26.0]	0.852
NKT subset 3 (out of total NKT)	15.0 [4.92;24.6]	11.7 [8.23;17.5]	0.629
NKT (out of total lymphocytes)	5.23 [3.17;9.06]	7.34 [5.20;14.3]	0.053
NKT subset 1 (out of total lymphocytes)	4.55 [2.34;6.10]	5.12 [3.54;8.65]	0.161
NKT subset 2(out of total lymphocytes)	0.76 [0.39;1.84]	1.26 [0.55;2.41]	0.302
NKT subset 3 (out of total lymphocytes)	0.62 [0.35;1.41]	0.94 [0.53;2.42]	0.242

Table S- 6. Proposed immunophenotype of NKT subpopulations.

NKT population	Markers used
NKT subset 1	$CD3^{+}$ $CD56^{+}$ $CD4^{-}$ $CD8^{-}$
NKT subset 2	$CD3^{+}$ $CD56^{+}$ $CD4^{-}$ $CD8^{+}$
NKT subset 3	$CD3^{+}$ $CD56^{+}$ $CD4^{+}$ $CD8^{-}$

Table S- 7. Percentages of B cell subpopulations between LTS and CLAD patients. Comparisons between the two groups were performed employing parametric unpaired t-test or nonparametric Mann-Whitney test, according to data distribution. Variables compared using t-test are presented as mean with SD whereas variables compared using Mann-Whitney test are presented as median with interquartile range. * Immunophenotype of B cell subsets is indicated in **Table S- 8**.

Cell subpopulation (B cells Panel)	CLAD	LTS	p-value
Leucocytes (out of total single cells)	99.9 [99.8;99.9]	99.8 [99.2;99.9]	0.039
Lymphocytes (out of total leucocytes)	26.6 (12.0)	30.9 (9.31)	0.128
B cells (out of total lymphocytes)	3.77 [2.03;6.24]	4.43 [2.19;6.15]	0.678
Naive and $CD27^-$ B cells (out of total B cells)	65.5 [49.5;73.0]	63.8 [44.2;76.6]	0.638
Memory B cells (out of total B cells)	41.6 (18.0)	42.0 (20.7)	0.945
Naïve and transitional B cells (out of total B cells)	54.8 (16.4)	53.3 (21.9)	0.766
Mature naïve B cells (out of total B cells)	13.4 [10.5;26.9]	16.0 [11.0;20.8]	0.759
Transitional T1/T2 B cells (out of total B cells)	-	-	-
Mature B cells (out of total B cells)	19.7 (6.01)	22.2 (7.92)	0.215
ASC and SwM B cells (out of total B cells)	24.3 [18.8;31.5]	22.5 [11.9;35.7]	0.498
SwM B cells (out of total B cells)	15.2 (6.13)	15.1 (9.57)	0.956
Plasmablast cells (out of total B cells)	5.73 [4.06;6.63]	8.67 [4.32;12.4]	0.133
B10 cells (out of total B cells)	18.1 [15.4;26.8]	17.2 [9.74;31.9]	0.594
Unswitched memory B cells (out of total B cells)	15.4 [11.8;19.3]	11.4 [8.81;20.9]	0.346
IgD^- $CD27^-$ B cells (out of total B cells)	7.38 [5.83;10.7]	7.48 [5.63;9.30]	0.569
IgD^- B cells (out of total B cells)	32.0 [25.9;40.8]	33.7 [17.5;45.9]	0.602
DN B cells (out of total B cells)	6.42 [4.69;8.33]	5.95 [4.88;7.68]	0.716
IgM only B cells (out of total B cells)	5.02 [3.48;6.41]	5.93 [3.58;11.5]	0.477
$CD21^{-/low}$ $CD38^{low}$ B cells (out of total B cells)	10.2 [7.69;16.3]	10.3 [7.73;14.7]	0.563

Table S- 8. Proposed immunophenotype of B cell subpopulations.

B cell population	B cell markers used
Naive and DN B cells	$CD19^+$ $CD27^-$
Memory B cells	$CD19^+$ $CD27^+$
Naïve and transitional B cells	$CD19^+$ IgD^+ $CD27^-$
Mature naïve B cells	$CD19^+$ IgD^+ $CD27^-$ $CD38^+$ $CD24^+$
Transitional T1/T2 B cells	$CD19^+$ IgD^+ $CD27^-$ $CD38^{high}$ $CD24^{high}$
Mature B cells	$CD19^+$ IgD^+ $CD38^{low/+}$ $CD24^+$
Antibody-secreting cells (ASC) and “switched” memory (SwM) B cells	$CD19^+$ IgD^- $CD27^+$
Switched memory (SwM) cells	$CD19^+$ IgD^- $CD27^+$ IgM^- $CD38^-$
Plasmablast cells	$CD19^+$ IgD^- $CD27^+$ IgM^- $CD38^{high}$
B10 cells	$CD19^+$ IgD^- $CD27^+$ IgD^- $CD24^+$
Unswitched memory B cells	$CD19^+$ IgD^+ $CD27^+$
Double negative (DN) B cells	$CD19^+$ IgD^- $CD27^-$ IgM^-
IgM only B cells	$CD19^+$ IgD^- $CD27^+$ IgM^+

Table S- 9. Percentages of T cell subpopulations between LTS and CLAD patients. Comparisons between the two groups were performed employing parametric unpaired t-test or nonparametric Mann-Whitney test, according to data distribution. Variables compared using t-test are presented as mean with SD whereas variables compared using Mann-Whitney test are presented as median with interquartile range.

Cell subpopulation (T cells Panel)	CLAD	LTS	p-value
Lymphocytes (out of total leucocytes)	26.5 (10.6)	30.2 (8.02)	0.126
T cells (out of total lymphocytes)	79.1 [72.5;87.0]	80.5 [73.9;87.5]	0.531
$CD4^+$ T cells (out of total T cells)	51.7 (13.9)	54.3 (13.1)	0.453
$CD4^+$ $CD57^+$ T cells (out of total $CD4^+$ T cells)	9.95 [3.75;15.1]	5.14 [2.25;12.0]	0.131
$CD4^+$ $CD27^-$ $CD28^+$ T cells (out of total $CD4^+$ T cells)	9.16 [5.72;11.1]	7.99 [5.07;11.6]	0.598
$CD4^+$ $CD27^+$ $CD28^+$ T cells (out of total $CD4^+$ T cells)	85.9 [76.0;91.9]	86.8 [77.7;92.8]	0.598
$CD4^+$ $CD27^-$ $CD28^-$ T cells (out of total $CD4^+$ T cells)	10.9 [5.43;16.0]	8.22 [4.32;18.2]	0.745
$CD4^+$ $CD27^+$ $CD28^-$ T cells (out of total $CD4^+$ T cells)	0.54 (0.07)	0.62 (0.21)	0.515
$CD4^+$ $CD27^+$ T cells (out of total $CD4^+$ T cells)	86.1 [76.1;91.9]	86.8 [77.9;92.8]	0.607
$CD4^+$ $CD27^-$ T cells (out of total $CD4^+$ T cells)	13.9 [8.07;23.9]	13.2 [7.19;22.1]	0.607
$CD4^+$ $CD28^+$ T cells (out of total $CD4^+$ T cells)	95.7 [87.2;99.7]	95.9 [89.9;99.9]	0.678
$CD4^+$ $CD28^-$ T cells (out of total $CD4^+$ T cells)	11.0 [5.61;16.2]	8.14 [4.05;18.7]	0.584
$CD4^+$ $CD28^-$ $CD279^+$ T cells (out of total $CD4^+$ T cells)	5.91 [2.72;14.0]	4.43 [3.31;9.77]	0.822
$CD4^+$ $CD28^+$ $CD279^+$ T cells (out of total $CD4^+$ T cells)	24.9 [18.2;35.0]	26.2 [18.7;30.1]	0.578
$CD4^+$ $CD28^-$ $CD279^+$ T cells (out of total $CD4^+$ T cells)	5.54 [3.39;9.27]	3.97 [1.43;5.62]	0.188
$CD4^+$ $CD28^+$ $CD279^-$ T cells (out of total $CD4^+$ T cells)	63.8 [57.0;75.5]	68.5 [61.4;75.0]	0.269
$CD4^+$ $CD279^+$ T cells (out of total $CD4^+$ T cells)	32.7 [23.1;39.4]	30.3 [21.5;35.6]	0.288
$CD4^+$ $CD279^-$ T cells (out of total $CD4^+$ T cells)	67.3 [60.6;76.9]	69.7 [64.4;78.5]	0.288
$CD4^+$ $CD197^+$ $CD45RA^-$ T cells (out of total $CD4^+$ T cells)	48.1 (14.0)	47.8 (15.6)	0.926
$CD4^+$ $CD197^+$ $CD45RA^+$ T cells (out of total $CD4^+$ T cells)	31.0 [18.4;43.1]	33.3 [25.0;38.6]	0.718
$CD4^+$ $CD197^-$ $CD45RA^-$ T cells (out of total $CD4^+$ T cells)	11.4 [7.53;15.3]	9.19 [5.42;14.4]	0.157
$CD4^+$ $CD197^-$ $CD45RA^+$ T cells (out of total $CD4^+$ T cells)	9.71 [3.33;12.1]	6.06 [2.98;11.9]	0.536
$CD4^+$ $CD197^+$ T cells (out of total $CD4^+$ T cells)	83.9 [74.5;90.3]	87.4 [75.6;92.2]	0.426
$CD4^+$ $CD197^-$ T cells (out of total $CD4^+$ T cells)	16.1 [9.71;25.5]	12.6 [7.76;24.4]	0.426
$CD4^+$ $CD45RA^+$ T cells (out of total $CD4^+$ T cells)	42.0 [27.3;48.1]	37.3 [31.4;46.9]	0.741
$CD4^+$ $CD45RA^-$ T cells (out of total $CD4^+$ T cells)	58.0 [51.9;72.7]	62.7 [53.1;68.6]	0.741
$CD8^+$ T cells (out of total T cells)	42.2 (11.6)	37.7 (10.7)	0.119
$CD8^+$ $CD57^+$ T cells (out of total $CD8^+$ T cells)	26.9 (15.6)	24.1 (17.2)	0.507
$CD8^+$ $CD27^-$ $CD28^+$ T cells (out of total $CD8^+$ T cells)	3.47 [3.03;6.68]	4.72 [3.16;7.62]	0.290
$CD8^+$ $CD27^+$ $CD28^+$ T cells (out of total $CD8^+$ T cells)	36.9 [28.0;59.0]	49.1 [30.7;75.1]	0.301
$CD8^+$ $CD27^-$ $CD28^-$ T cells (out of total $CD8^+$ T cells)	51.5 [30.3;58.0]	35.5 [8.16;49.1]	0.204
$CD8^+$ $CD27^+$ $CD28^-$ T cells (out of total $CD8^+$ T cells)	7.35 [5.23;9.68]	5.91 [5.00;10.4]	0.647
$CD8^+$ $CD27^+$ T cells (out of total $CD8^+$ T cells)	45.2 [38.1;67.0]	59.8 [42.7;83.7]	0.328
$CD8^+$ $CD27^-$ T cells (out of total $CD8^+$ T cells)	54.8 [33.0;61.9]	40.2 [16.3;57.3]	0.328
$CD8^+$ $CD28^+$ T cells (out of total $CD8^+$ T cells)	42.3 [33.2;65.5]	53.6 [40.2;80.0]	0.251
$CD8^+$ $CD28^-$ T cells (out of total $CD8^+$ T cells)	57.7 [34.5;66.8]	46.4 [20.0;59.8]	0.251

Cell subpopulation (T cells Panel)	CLAD	LTS	p-value
$CD8^+$ $CD28^-$ $CD279^+$ T cells (out of total $CD8^+$ T cells)	8.82 [5.92;21.2]	5.93 [4.52;14.5]	0.097
$CD8^+$ $CD28^+$ $CD279^+$ T cells (out of total $CD8^+$ T cells)	11.5 [9.79;18.6]	15.2 [10.4;21.5]	0.371
$CD8^+$ $CD28^-$ $CD279^-$ T cells (out of total $CD8^+$ T cells)	39.3 [20.6;48.0]	31.0 [12.0;42.9]	0.335
$CD8^+$ $CD28^+$ $CD279^-$ T cells (out of total $CD8^+$ T cells)	30.2 [21.6;47.4]	36.6 [24.7;52.4]	0.394
$CD8^+$ $CD279^+$ T cells (out of total $CD8^+$ T cells)	25.7 [18.2;38.2]	26.7 [17.3;36.3]	0.949
$CD8^+$ $CD279^-$ T cells (out of total $CD8^+$ T cells)	74.3 [61.8;81.8]	73.3 [63.7;82.7]	0.949
$CD8^+$ $CD197^+$ $CD45RA^-$ T cells (out of total $CD8^+$ T cells)	9.79 [7.63;14.3]	11.1 [7.99;15.8]	0.453
$CD8^+$ $CD197^+$ $CD45RA^+$ T cells (out of total $CD8^+$ T cells)	25.2 [14.7;41.3]	29.9 [14.8;45.2]	0.644
$CD8^+$ $CD197^-$ $CD45RA^-$ T cells (out of total $CD8^+$ T cells)	14.2 [9.83;23.7]	14.3 [8.94;21.2]	0.912
$CD8^+$ $CD197^-$ $CD45RA^+$ T cells (out of total $CD8^+$ T cells)	43.0 (22.0)	40.5 (24.5)	0.670
$CD8^+$ $CD197^+$ T cells (out of total $CD8^+$ T cells)	35.9 [23.5;55.2]	49.9 [20.7;63.3]	0.522
$CD8^+$ $CD197^-$ T cells (out of total $CD8^+$ T cells)	64.1 [44.8;76.5]	50.1 [36.7;79.3]	0.522
$CD8^+$ $CD45RA^+$ T cells (out of total $CD8^+$ T cells)	72.2 (12.2)	72.3 (15.6)	0.968
$CD8^+$ $CD45RA^-$ T cells (out of total $CD8^+$ T cells)	27.8 (12.2)	28.6 (15.0)	0.828

Table S- 10. Percentages of TCR T cell subpopulations between LTS and CLAD patients. Comparisons between the two groups were performed employing parametric unpaired t-test or nonparametric Mann-Whitney test, according to data distribution. Variables compared using t-test are presented as mean with SD whereas variables compared using Mann-Whitney test are presented as median with interquartile range.

Cell subpopulation (TCR T cells Panel)	CLAD	LTS	p-value
Lymphocytes (out of total leucocytes)	27.9 (11.2)	32.1 (9.21)	0.107
T cells (out of total lymphocytes)	79.3[68.2;85.2]	79.0[73.4;84.3]	0.477
$CD4^+$ T cells (out of total T cells)	51.3 (14.0)	54.3 (12.9)	0.386
$CD4^+$ HLA DR^+ T cells (out of total $CD4^+$ T cells)	12.0[7.25;18.9]	9.71[6.57;16.9]	0.356
$CD8^+$ T cells (out of total T cells)	43.4 (11.9)	39.2 (10.5)	0.148
$CD8^+$ HLA DR^+ (out of total $CD8^+$ T cells)	42.6 (18.1)	39.4 (20.6)	0.511
$\alpha\beta^+$ TCR T cells (out of total T cells)	96.1[94.3;98.2]	95.9[92.1;97.8]	0.559
$\alpha\beta^+$ TCR $CD8^+$ T cells (out of total $\alpha\beta^+$ TCR T cells)	53.9 (13.5)	57.6 (11.3)	0.247
$\alpha\beta^+$ TCR $CD4^+$ T cells (out of total $\alpha\beta^+$ TCR T cells)	44.4 (13.4)	39.9 (11.2)	0.161
$\alpha\beta^+$ TCR $CD4^-$ $CD8^-$ T cells (out of total $\alpha\beta^+$ TCR T cells)	0.58[0.45;1.08]	1.13[0.72;1.67]	0.002
$\gamma\delta^+$ TCR T cells (out of total T cells)	3.91[1.91;5.73]	4.12[2.22;7.99]	0.404
$V\delta1^+$ $V\delta2^-$ $\gamma\delta^+$ TCR T cells (out of total $\gamma\delta^+$ TCR T cells)	73.8[61.4;86.7]	64.5[46.5;76.5]	0.027
$V\delta1^+$ $V\delta2^-$ $\gamma\delta^+$ TCR $CD4^-$ $CD8^+$ T cells (out of total $V\delta1^+$ $V\delta2^-$ $\gamma\delta^+$ TCR T cells)	47.6 (23.2)	40.1 (16.3)	0.202
$V\delta1^+$ $V\delta2^-$ $\gamma\delta^+$ TCR $CD4^+$ $CD8^-$ T cells (out of total $V\delta1^+$ $V\delta2^-$ $\gamma\delta^+$ TCR T cells)	-	-	-
$V\delta1^+$ $V\delta2^-$ $\gamma\delta^+$ TCR $CD4^-$ $CD8^-$ T cells (out of total $V\delta1^+$ $V\delta2^-$ $\gamma\delta^+$ TCR T cells)	59.9 (19.8)	63.6 (16.9)	0.475
$V\delta1^-$ $V\delta2^+$ $\gamma\delta^+$ TCR T cells (out of total $\gamma\delta^+$ TCR T cells)	16.1[10.3;26.9]	17.0[7.34;33.1]	0.968
$V\delta1^-$ $V\delta2^+$ $\gamma\delta^+$ TCR $CD4^-$ $CD8^+$ T cells (out of total $V\delta1^-$ $V\delta2^+$ $\gamma\delta^+$ TCR T cells)	-	-	-
$V\delta1^-$ $V\delta2^+$ $\gamma\delta^+$ TCR $CD4^+$ $CD8^-$ T cells (out of total $V\delta1^-$ $V\delta2^+$ $\gamma\delta^+$ TCR T cells)	-	-	-
$V\delta1^-$ $V\delta2^+$ $\gamma\delta^+$ TCR $CD4^-$ $CD8^-$ T cells (out of total $V\delta1^-$ $V\delta2^+$ $\gamma\delta^+$ TCR T cells)	84.3[77.6;88.3]	87.1[81.9;90.2]	0.383
$V\delta1^-$ $V\delta2^-$ $\gamma\delta^+$ TCR T cells (out of total $\gamma\delta^+$ TCR T cells)	16.4[9.52;40.6]	19.7[15.1;29.7]	0.479
$V\delta1^-$ $V\delta2^-$ $\gamma\delta^+$ TCR $CD4^-$ $CD8^+$ T cells (out of total $V\delta1^-$ $V\delta2^-$ $\gamma\delta^+$ TCR T cells)	57.2 (30.6)	45.7 (22.0)	0.345
$V\delta1^-$ $V\delta2^-$ $\gamma\delta^+$ TCR $CD4^+$ $CD8^-$ T cells (out of total $V\delta1^-$ $V\delta2^-$ $\gamma\delta^+$ TCR T cells)	-	-	-
$V\delta1^-$ $V\delta2^-$ $\gamma\delta^+$ TCR $CD4^-$ $CD8^-$ T cells (out of total $V\delta1^-$ $V\delta2^-$ $\gamma\delta^+$ TCR T cells)	75.1 (20.7)	67.4 (17.9)	0.299
$\gamma\delta^+$ TCR $CD8^+$ T cells (out of total $\gamma\delta^+$ TCR T cells)	43.6 (18.8)	36.8 (17.4)	0.184
$\gamma\delta^+$ TCR $CD4^+$ T cells (out of total $\gamma\delta^+$ TCR T cells)	-	-	-
$\gamma\delta^+$ TCR $CD4^-$ $CD8^-$ T cells (out of total $\gamma\delta^+$ TCR T cells)	62.9[56.5;77.0]	72.4[50.6;77.4]	0.632

Table S- 11. Percentages of T cell subpopulations between LTS and CLAD patients. Comparisons between the two groups were performed employing parametric unpaired t-test or nonparametric Mann-Whitney test, according to data distribution. Variables compared using t-test are presented as mean with SD whereas variables compared using Mann-Whitney test are presented as median with interquartile range.

Cell subpopulation (Regulatory T Cells Panel)	CLAD	LTS	p-value
Lymphocytes (out of total single cells)	39.3 (14.0)	40.7 (12.6)	0.684
T cells (out of total lymphocytes)	77.8 [71.5;86.2]	80.3 [72.6;87.2]	0.575
$CD4^+$ $CD25^+$ T cells (out of total T cells)	18.8 [14.1;25.5]	15.1 [9.04;21.3]	0.129
$CD4^+$ $CD25^{low}$ T cells (out of total T cells)	18.5 (8.81)	14.9 (8.96)	0.123
$CD4^+$ $CD25^{high}$ T cells (out of total T cells)	1.70 [1.02;2.25]	1.33 [0.76;1.88]	0.316
$CD4^+$ $CD25^{low}$ T cells (out of total $CD4^+$ $CD25^+$ T cells)	91.2 [87.2;94.1]	90.2 [83.8;93.9]	0.514
$CD4^+$ $CD25^{high}$ T cells (out of total $CD4^+$ $CD25^+$ T cells)	8.95 [6.14;12.5]	9.25 [5.32;16.8]	0.613
$CD4^+$ $CD25^+$ $Foxp3^+$ T cells (out of total T cells)	1.00 [0.70;1.39]	0.91 [0.68;1.30]	0.646
$CD4^+$ $CD25^+$ $Foxp3^{low}$ $CD45RA^+$ T cells (out of total $CD25^+$ $Foxp3^+$ T cells)	-	-	-
$CD4^+$ $CD25^+$ $Foxp3^{low}$ $CD45RA^-$ T cells (out of total $CD25^+$ $Foxp3^+$ T cells)	75.0 (14.9)	70.7 (14.6)	0.297
$CD4^+$ $CD25^+$ $Foxp3^{high}$ $CD45RA^-$ T cells (out of total $CD25^+$ $Foxp3^+$ T cells)	35.6 (12.1)	34.7 (15.5)	0.886
$CD4^+$ $CD25^+$ $Foxp3^+$ $Helios^+$ T cells (out of total $CD25^+$ $Foxp3^+$ T cells)	80.1 [72.0;87.5]	79.8 [72.3;84.5]	0.592
$CD4^+$ $CD25^+$ $Foxp3^+$ $Helios^-$ T cells (out of total $CD25^+$ $Foxp3^+$ T cells)	38.8 [26.2;56.3]	29.2 [24.6;36.7]	0.480
$CD4^+$ $CD25^+$ $Foxp3^+$ $CD39^-$ T cells (out of total $CD25^+$ $Foxp3^+$ T cells)	56.2 (23.4)	51.8 (18.4)	0.495
$CD4^+$ $CD25^+$ $Foxp3^+$ $CD39^+$ T cells (out of total $CD25^+$ $Foxp3^+$ T cells)	55.1 (21.4)	59.5 (15.6)	0.451
$CD4^+$ T cells (out of total T cells)	52.9 (13.7)	51.9 (13.6)	0.790
$CD4^+$ $Foxp3^+$ T cells (out of total T cells)	1.20 [1.01;2.26]	1.18 [0.85;2.02]	0.425
$CD4^+$ $Foxp3^+$ (out of total $CD4^+$ T cells)	2.94 [2.00;4.64]	2.34 [1.74;3.93]	0.407
$CD4^+$ $CD25^{low}$ T cells (out of total T cells)	17.7 [12.1;25.5]	14.0 [8.21;21.6]	0.146
$CD4^+$ $CD25^{high}$ T cells (out of total T cells)	1.69 [1.03;2.25]	1.34 [0.76;1.91]	0.301
$CD4^+$ $CD25^+$ $Foxp3^+$ T cells (out of total T cells)	0.99 [0.70;1.39]	0.85 [0.66;1.33]	0.450
$CD4^+$ $Foxp3^{low}$ $CD45RA^+$ T cells (out of total $CD4^+$ $Foxp3^+$ T cells)	19.3 (17.0)	26.4 (13.0)	0.532
$CD4^+$ $Foxp3^{low}$ $CD45RA^-$ T cells (out of total $CD4^+$ $Foxp3^+$ T cells)	72.4 [59.7;94.9]	69.5 [57.8;79.8]	0.290
$CD4^+$ $Foxp3^{high}$ $CD45RA^-$ T cells (out of total $CD4^+$ $Foxp3^+$ T cells)	30.5 [18.6;37.6]	23.4 [19.9;28.7]	0.538
$CD4^+$ $Foxp3^+$ $CD39^-$ T cells (out of total $CD4^+$ $Foxp3^+$ T cells)	52.2 [33.3;84.6]	55.7 [43.8;80.8]	0.566
$CD4^+$ $Foxp3^+$ $CD39^+$ T cells (out of total $CD4^+$ $Foxp3^+$ T cells)	47.2 (22.0)	49.8 (22.3)	0.697
$CD4^+$ $Foxp3^+$ $Helios^+$ T cells (out of total $CD4^+$ $Foxp3^+$ T cells)	63.3 (22.0)	68.1 (22.6)	0.782
$CD4^+$ $Foxp3^+$ $Helios^-$ T cells (out of total $CD4^+$ $Foxp3^+$ T cells)	32.5 [27.5;50.9]	39.6 [26.1;60.3]	0.927
$CD4^+$ $CD25^+$ $Foxp3^+$ T cells (out of total lymphocytes)	0.74 [0.55;1.16]	0.68 [0.49;1.03]	0.671
$CD4^+$ $Foxp3^+$ T cells (out of total lymphocytes)	1.02 [0.83;1.69]	0.80 [0.69;1.60]	0.380
$CD4^+$ $CD25^+$ $Foxp3^+$ T cells (out of total $CD4^+$ T cells)	1.78 [1.19;2.73]	1.53 [1.12;2.61]	0.633
$CD4^+$ $Foxp3^+$ T cells (out of total $CD4^+$ T cells)	2.94 [2.00;4.64]	2.34 [1.74;3.93]	0.407

Table S- 12. Percentages of granulocyte subpopulations between LTS and CLAD patients. Comparisons between the two groups were performed employing parametric unpaired t-test or nonparametric Mann-Whitney test, according to data distribution. Variables compared using t-test are presented as mean with SD whereas variables compared using Mann-Whitney test are presented as median with interquartile range. HAP= High Autofluorescent Population.

Cell subpopulation (Granulocyte Panel)	CLAD	LTS	p-value
$CD45^+$ $CD16^+$ leucocytes (out of total $CD45^+$ leucocytes)	0.66 [0.17;57.2]	0.22 [0.09;51.8]	0.088
$CD45^+$ $CD16^+$ $CD62L^+$ leucocytes (out of total $CD45^+$ leucocytes)	0.56 [0.17;56.6]	0.22 [0.09;51.5]	0.095
$CD45^+$ $CD16^+$ $CD11b^+$ leucocytes (out of total $CD45^+$ leucocytes)	0.50 [0.15;57.2]	0.23 [0.11;52.7]	0.206
Granulocytes (out of total $CD45^+$ leucocytes)	58.8 (15.0)	53.6 (10.7)	0.124
$CD16^+$ granulocytes (out of total granulocytes)	96.2 [0.17;99.2]	0.48 [0.15;98.2]	0.360
$CD62L^+$ granulocytes (out of total granulocytes)	99.7 [98.9;99.8]	99.9 [99.7;99.9]	0.007
$CD11b^+$ granulocytes (out of total granulocytes)	100.0 [99.9;100.0]	100.0 [100.0;100.0]	0.894
HAP (out of total $CD45^+$ leucocytes)	1.76 [1.23;3.54]	2.13 [1.24;3.69]	0.578
$CD16^+$ HAP (out of total HAP)	20.8 [8.09;40.6]	29.8 [14.9;46.2]	0.521
$CD11b^+$ HAP (out of total HAP)	97.8 [96.9;98.9]	98.7 [95.6;99.3]	0.468
$CD62L^+$ HAP (out of total HAP)	99.3 [98.3;99.7]	99.7 [99.1;99.9]	0.110
Single cells without HAP (out of total single cells)	94.5 [91.1;96.1]	94.7 [92.6;96.4]	0.751
$CD45^+$ leucocytes without HAP (out of total single cells without HAP)	99.8 [99.4;99.9]	99.7 [99.6;99.8]	0.321
$CD45^+$ $CD16^+$ leucocytes without HAP (out of total $CD45^+$ leucocytes without HAP)	26.9 [0.19;60.0]	0.50 [0.16;52.4]	0.412
$CD45^+$ $CD16^+$ $CD11b^+$ leucocytes without HAP (out of total $CD45^+$ leucocytes without HAP)	33.8 [0.18;60.0]	0.44 [0.16;52.6]	0.383
$CD45^+$ $CD16^+$ $CD62L^+$ leucocytes without HAP (out of total $CD45^+$ leucocytes without HAP)	26.8 [0.19;59.5]	0.50 [0.16;52.2]	0.424